Armando Pombeiro
Coordinator

CELEBRATION OF THE PERIODIC TABLE OF THE ELEMENTS AT THE ACADEMY OF SCIENCES OF LISBON. A CHEMISTRY SYMPOSIUM

October 3rd, 10th and 17th, 2019

ACADEMIA DAS CIÊNCIAS
DE LISBOA

FICHA TÉCNICA

TÍTULO
CELEBRATION OF THE PERIODIC TABLE OF THE ELEMENTS AT THE ACADEMY OF SCIENCES OF LISBON. A CHEMISTRY SYMPOSIUM

COORDINATOR
ARMANDO POMBEIRO

EDITOR
ACADEMIA DAS CIÊNCIAS DE LISBOA

EDIÇÃO
DIANA SARAIVA DE CARVALHO

ISBN
978-972-623-394-7

ORGANIZAÇÃO

Academia das Ciências de Lisboa
R. Academia das Ciências, 19
1249-122 LISBOA
Telefone: 213219730
Correio Electrónico: geral@acad-ciencias.pt
Internet: www.acad-ciencias.pt

Table of contents

CELEBRATION OF THE PERIODIC TABLE OF THE ELEMENTS AT THE ACADEMY OF SCIENCES OF LISBON. A CHEMISTRY SYMPOSIUM. PREFACE

Armando J. L. Pombeiro

Centro de Química Estrutural, Instituto Superior Técnico, Universidade de Lisboa, Av. Rovisco Pais, 1049-001 Lisboa, Portugal

The celebration of the sesquicentennial of the proposal by **Dmitrii Mendeleev** of a periodic system (expressed by what became to be known as Periodic Table) of the elements is well justified by the relevance of such an event which has contributed in an unparalleled way for the systematization of Chemistry and Science in general.

The observation of periodic trends, based on atomic weights, of chemical and physical properties of the elements and their compounds, inspired Mendeleev to propose a periodic system of the elements based on a "Periodic Law" of the elements (Figure 1).

We know nowadays that the observed periodicity of properties of the elements upon listing along their atomic number (instead of atomic weight) relates to the corresponding periodic recurrence of their outer shells electronic configuration. The usefulness of this relationship is well patented by the widespread use of the omnipresent Periodic Table of the elements.

In Mendeleev´s first version (1869, published in the 1st volume of the journal of the then recently founded Russian Chemical Society and in the 1st edition of his book "**The Principles of Chemistry**"), the groups of the elements were arranged horizontally, whereas in the second one (1870), they are vertically, an arrangement that is followed in the Periodic Table used nowadays.

The vertical alignment is shown in the gigantic **wall Periodic Table** in Saint Petersburg, that is based on the periodic system published in the 1906 edition (the last one during Mendeleev's life) of "The Principles of Chemistry" (Figure 1). It is a mosaic workshop by the Academy of Art, to celebrate the centennial anniversary of his birth (1834). Red elements are those known until then, whereas the blue ones were discovered later [*C&EN*, March 1995, p.84].

This wall Periodic Table, together with a Mendeleev's **statue** stand in front of the "Palata Mer i Vesov" ("Chamber of Measures and Weights") of which he was Director, and the shine of Mendeleev´s nose results from the traditional students´ touches to pray for good examination marks.

Mendeleev received his education in Saint Petersburg, Russia, and it was also therein that he developed most of his professional career, namely gaining a professorship at the Technological Institute (1864) and later at the nowadays Saint Petersburg State University where he achieved

tenure (1867), published his book “The Principles of Chemistry” (volume 1 in 1869) and proposed the “Periodic Law” and the periodic chartering of the elements (see below the Museum called after his name).

Figure 1. Mendeleev’s wall Periodic Table and statue in Saint Petersburg, in front of the “Palata Mer i Vesov” (“Chamber of Measures and Weights”) of which he was Director (photos by courtesy of Prof. Vadim Kukushkin).

This celebration also provides an opportunity to reflect about paternity and evolution of ideas in science. Although without intending to dip into this area, it is noteworthy to mention that the discovery of the Periodic Table and of the Periodic Law, as it has occurred with other

breakthroughs in science, was a continued process to which a number of scientists have contributed and it would be appropriate to evoke herein a few other representative **pioneers**.

Just to mention the 1860 decade, in which Mendeleev presented his proposal, a relevant pioneer was the French mineralogist **Alexandre-Émile Béguyer de Chancourtois** who arranged (in 1862, *i.e.*, 7 years before Mendeleev's publication) the chemical elements according to the atomic weight in a helical mode on the surface of a cylinder. However, in view of the high dimension of the chart, it could not be included in the journal (*Comptes Rendues de l´ Académie des Sciences*), although being available in the off-prints of the paper. This difficulty, associated to the fact that the publication appeared in a geological context, hampered the spread of the proposal which remained virtually unknown within the scientific community. Other important pioneers of the Periodic Table in the 1860s include the British **John Newlands** who published in 1865 (*Chemical News*) the "Law of Octaves" (by analogy with the music octaves) with an horizontal representation of the groups of elements, and the German **Lothar Meyer** of the Wroclaw University who proposed (1864) a classification of the elements, revised in 1870 with marked similarities to that of Mendeleev. Information on these pioneers' contributions can be found in an interview with Peter Wothers (University of Cambridge): http://www.periodicvideos.com/videos/first_periodic_table.htm

But such contributions towards the establishment of a chemical periodicity of the elements do not decrease Mendeleev´s merit and vision. His system not only succeeded in the arrangement of the elements in a coherent way (for the knowledge of that time), but also provided accurate predictions of missing elements (by filling gaps in the table) and of properties of their compounds, apart from correcting the atomic weights of some known elements, aspects that he properly highlighted. He associated the system to a law of nature and defended its viability along his life. Moreover, it is understandable that discoveries in science can occur simultaneously and independently in more than one place (*e.g.*, scientists can reach comparable conclusions and propose innovative interpretations and directions, based on similar sources) and that they can be recognized differently.

Numerous initiatives have been undertaken in the world and much has been said in this celebratory year of 2019. We should refrain from repeating herein but the following points are illustrative.

On this occasion, many Universities have made available different modes of visualizing the Periodic Table of the Elements. Among them, the **Periodic Table of videos** (http://www.periodicvideos.com/) deserves to be highlighted. It is a didactic web series coordinated scientifically by Martin Polyakoff of the University of Nottingham (videos recorded

by the video journalist Brady Haran), where each of the 118 elements is described by the corresponding video.

A Periodic Table prepared freely as a collaborative **patchwork by members of the Universidade Nova de Lisboa,** under the coordination of our *Confrade* José Moura and Prof. Ana Ricardo, was on display in the Chapter Room of the Academy of Sciences of Lisbon on the occasion of the celebrations (Figure 2).

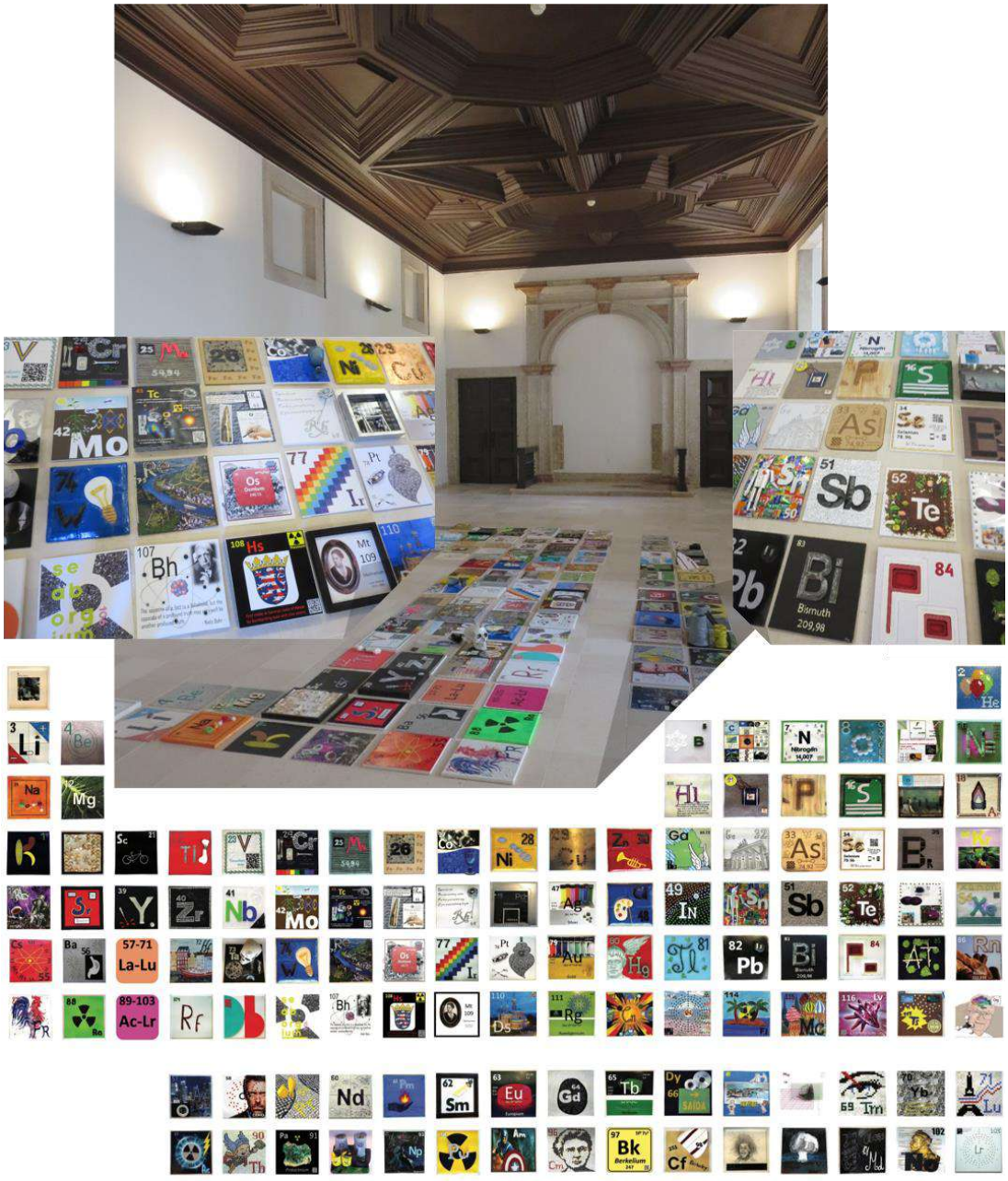

Figure 2. Periodic Table of the Universidade Nova de Lisboa (bottom figure by courtesy of Prof. José Moura) which was on display at the Academy of Sciences of Lisbon on the occasion of the celebratory symposium (overall views and detailed parts).

However, the Academy celebrations of the sesquicentennial of the Mendeleev periodic system proposal focused mainly on a **Celebratory Symposium** (with members of its Chemistry section) to illustrate the significance of elements of the Periodic Table in Chemical sciences, and I had the privilege to be in charge of its organization.

The scheduled program was combined with a visit of three Foreign Members of the Academy and according also to the convenience of the national Members of the Chemistry section of the Academy who joined the initiative. It consisted of three main sessions (held on October 3rd, 10th and 17th, 2019), with the following scientific program:

A - Catalysis and the Periodic Table

- Pierre Brausntein, *University of Strasbourg, France*

"Hybrid Ligands for Metal Complexes, Catalysts and Nanomaterials"

- Pierre Dixneuf, *University of Rennes, France*

"Ruthenium Catalysts: Their Empire for Green and Sustainable Chemistry" (renamed in the publication as "*"From a 175 year old Ruthenium to its Empire on Green Catalysis and Sustainable Chemistry")

- Luis Oro, *University of Zaragoza, Spain*

"Mechanistic Studies on Rhodium and Iridium Homogeneous Catalysts"

- Armando Pombeiro, *Instituto Superior Técnico, Universidade de Lisboa*

"Selected Metal Catalysts Spanned over the Periodic Table Towards Alkane Functionalization"

B - Metal Centres in Supramolecular and Biological Structures

- João Rocha, *Universidade de Aveiro*

"Nanoporous Materials: Functional Silicates and Metal Organic Frameworks"

- José Moura, *Universidade Nova de Lisboa*

"Design of Artificial Enzymes Using the Metals of the Periodic Table"

C - Carbon: an Essential Element

- José Figueiredo, *Universidade do Porto*

"The Versatility of Carbon: Custom-Made Nanostructures"

- José Cavaleiro, *Universidade de Aveiro*

"Carbon as a Natural Element, Chemistry and Life" (postponed to another session)

- António Varandas, *Universidade de Coimbra*

"Cost-effective Dual-strategy for Molecular Reaction Dynamics and the Challenging Carbon Clusters" (renamed in the publication as "*Ab initio* potentials: From CBS Extrapolation to Globalness to Riddles in the Chemistry of Small Carbon Clusters)

These contributions in Chemistry instantiate the importance of the properties of different types of chemical compounds with relevant elements, in association to their positions in the Periodic Table. They include, for instance: molecular compounds with either precious or non-precious metals in catalytic processes towards sustainable synthesis of added value organic compounds; nanomaterials and metal organic frameworks (MOFs) in supramolecular and biological structures with various applications; and carbon as a key element in nanostructures and in biology. Extended abstracts of all these contributions are gathered in this collection.

A different area, concerning Mathematics and the Periodic Table, was addressed in another Academy session organized by the Section of Mathematics (*Confrade* José Rodrigues).

Moreover, the Celebratory Symposium of the Academy of Sciences of Lisbon is complemented with an historical account on the **discovery of Mendeleev´s Periodic Law and Periodic Table**, by **Igor S. Dmitriev**, the Director of the **Mendeleev Museum** of the Saint Petersburg State University, and our *Confrade* **Vadim Yu. Kukushkin** of the same University, where Mendeleev created his periodic system. In fact, this museum (Figure 3) comprises the apartment where Mendeleev lived at the University (what reflects a treatment, a recognition and an approach to support scientists that are quite different from those followed nowadays, specially in western countries), a scientific archive with his manuscripts, personal belongings (including his desk and other furniture) and a library. It is hosted on the ground floor of the former "Twelve Collegia" which were commissioned by Peter the Great to host his Government but later became the headquarters of the University.

This complementary contribution, entitled "**Sublime Generalization: Discovery of The Periodic Law**", follows immediately this Preface, appearing at the beginning of this collection, as a vivid evocation of the Mendeleev Periodic Table discovery.

Figure 3. Entrance to the Mendeleev Museum at Saint Petersburg State University (Universitetskaya emb., 7-9) (photos taken on the occasion of the "Frontiers of Organometallic Chemistry" symposium, Sept. 2012).

I take the opportunity to **acknowledge** all the *Confrades* and Colleagues who have contributed to the above symposium and historical description of Mendeleev's periodic table and/or to this collection (their names are indicated above), Prof. M. Fátima Guedes da Silva (Instituto Superior Técnico) for the kind editorial assistance in the preparation of the files for publication, and the President and Secretary General of the Academy (*Confrades* Carlos Salema and Salomé Pais, respectively) for their invitation to coordinate the symposium and the publication of this collection, as well as for the support provided.

SUBLIME GENERALIZATION: DISCOVERY OF THE PERIODIC LAW

Igor S. Dmitriev*[1] and Vadim Yu. Kukushkin[2]

[1]*The Herzen State Pedagogical University, 48 Moika Nab., 191186 Saint Petersburg, Russian Federation; e-mail: isdmitriev@gmail.com*

[2]*Saint Petersburg State University, Universitetskaya Nab. 7/9, 199034 Saint Petersburg, Russian Federation; e-mail: v.kukushkin@spbu.ru*

Igor Sergeevich Dmitriev was born in 1948 in Leningrad (now Saint Petersburg), Russian Federation. He studied chemistry at Leningrad (then Saint Petersburg) State University, where he obtained his Diploma with distinction in 1971 and doctoral degree in 1993. From 1971 to 2019 he worked at the D. Mendeleev Museum and Archives (Saint Petersburg State University), form 1993 as director. In addition, he was appointed in 2004 full professor of history of science at the Faculty of Philosophy, Saint Petersburg State University, where he taught until 2018. In 2020, he was appointed professor at The Herzen State Pedagogical University, Saint Petersburg. He was visiting professor at Tokyo Technological Institute, (Japan) in 2007. He is member of the editorial boards of *Russian Journal of General Chemistry* (Russia), *Voprosy istorii estestvoznaniia i tekhniki* [Studies in the History of Science and Technology] (Russia), and *Nature* (Russia). Author of 75 research publications, including 12 monographs.

Vadim Yurievich Kukushkin was born in 1956 in Leningrad (now Saint Petersburg), Russian Federation. He studied chemistry at Lensovet Technological Institute (Technical University), where he obtained his Diploma with distinction in 1979 and doctoral degree in 1982. Following two years at the industrially oriented Mekhanobr Institute (Leningrad), he joined the faculty at Saint Petersburg State University (1984). He obtained his post-habilitation DSc degree in 1992, was appointed full Professor in 1996 and became head of the Department of Physical Organic Chemistry in 2007. He is a full member of the Russian Academy of Sciences (elected 2019), foreign member of the Academy of Sciences of Lisbon (Portugal; elected 2011), member of the European Academy of Sciences (elected 2020), invited chair professor at the National Taiwan University of Science and Technology (since 2007). He is vice-president (elected 2016) of the Russian Chemical Society and the chairman (since 2012) of the Saint Petersburg branch of this society, member of the Councils of the Russian Foundation for Basic Research (2008–2016), Grant Commission of the Government of the Russian Federation (since 2012), and the Russian Science Foundation (since 2014; coordinator in chemistry since 2017). Prof. Kukushkin is a recipient of numerous prizes for his achievements in science and teaching. His research interests include platinum group metal chemistry, ligand reactivity, noncovalent interactions, organic synthesis involving metal complexes, and catalysis. He is an author of ca. 400 original papers, patents, reviews, as well as two books and a number of book chapters.

In October 1867, Dmitrii Ivanovich Mendeleev (1834–1907) (**Photo 1** [1]; for 3D-virtual tour at The D. I. Mendeleev Museum and Archives see Ref. [2]) began teaching his year-long course in inorganic chemistry, which the thirty-three-year professor of Saint Petersburg University (**Photos 2–3**) delivered to freshmen at the Faculty of Physics and Mathematics. He would continue teaching this course every year until he left the University in 1890. During this period his teaching load averaged five hours of lectures per week.

Photo 1. Dmitrii I. Mendeleev in 1869.

Photo 2. Building of Saint Petersburg University in 19th Century (watercolor by M.B. Belyavskii).

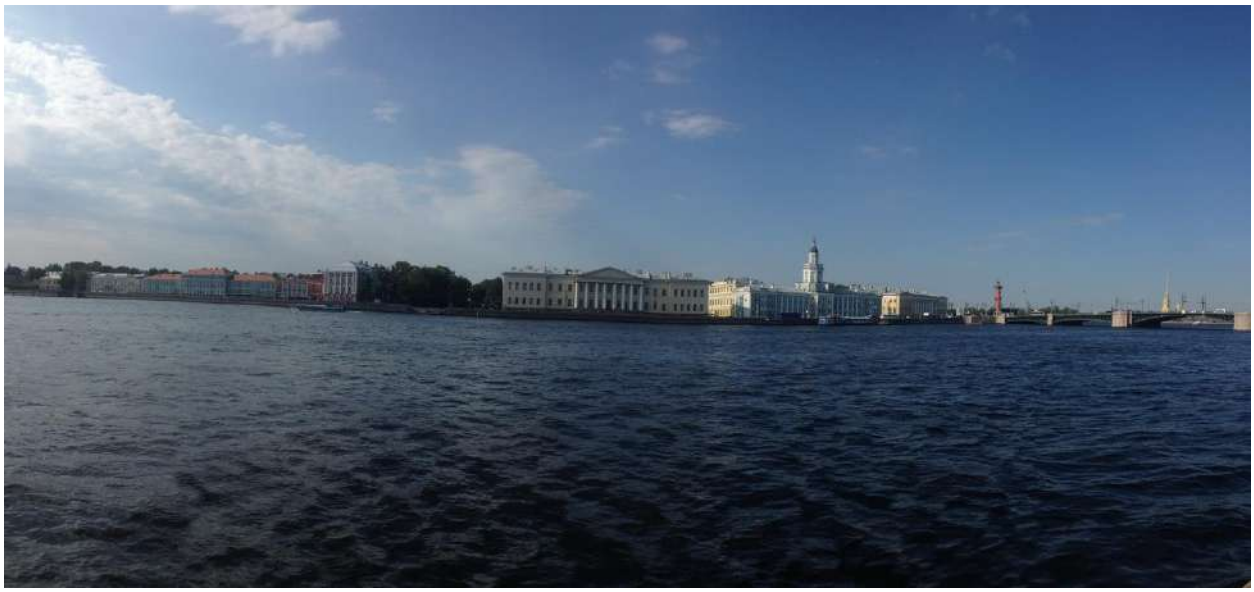

Photo 3. Panorama of Vasilyevsky Island with Saint Petersburg State University (former Saint Petersburg University) campus on the left from the park (taken 2019).

As Mendeleev himself put it, he was unable to find a textbook appropriate to such an intensive course, and thus decided to write his own, what would become the *Principles of Chemistry* (*Osnovy Khimii).* There was, however, another reason that motivated him to write the textbook. The reason was money.

Unlike a scientific monograph, a textbook can be republished many times, each time to the author's financial benefit. *Principles* became an important source of additional income for Mendeleev. Furthermore, the University granted him a sizeable cash allowance for the publication of the first issue of the textbook. For subsequent editions, as a rule, the University did not give monetary rewards (that is, only the first impulse was encouraged), but it was possible to receive royalties from the publisher. At that time, textbooks were initially published as a series of separate issues, which after making corrections and additions were later republished as a complete set, either under one cover or in several volumes.

The first issue of *Principles* appeared in the early summer of 1868. Mendeleev immediately set to work on the second issue, which was published in March 1869. These two issues made up the first part of his textbook [3]. It was during the work on the second issue of the first part of *Principles* that Mendeleev discovered the periodic law.

Notably, in the first issue of *Principles* Mendeleev did not introduce elements, atoms, or any theory of chemical combination. The issue mostly covers basic definitions, plans for chemical experiments, and general information on chemical phenomena. It is in Chapter 15 ("Carbon") of the second issue that Mendeleev first draws a clear distinction between the concepts "element" and "simple body". It was a historical turning point leading up to the discovery of the periodic law. Before turning to classification, one must understand what is there to classify.

Mendeleev understood that it were not simple bodies that had to be classified, but chemical elements. The concept of an element corresponded to the smallest chemically indivisible weight amount of matter of a certain type entering the particles (molecules) of bodies. Thus, an element in the understanding of Mendeleev was an "abstract concept", "matter contained in a simple body and capable of passing into all bodies resulting from this body without a change in weight." An element, according to Mendeleev, potentially contains in itself all the possible forms, properties and states that it is able to reveal under certain conditions. The possibility (or impossibility) of the formation of certain compounds, allotropic modifications, metallic or other states, etc., is all included (encapsulated) in the concept of "element". In other words, a simple body turns out to be, in the language of Aristotle, the *entelechy* of the element, that is, the realization of what existed potentially (Phys. III.1; Metaph. IX.8) in the chemical element.

Mendeleev's first article on the periodic law began with the following words: "The systematic distribution of elements has been subjected in our science to various vicissitudes". This was true. But Mendeleev kept silent about one thing: the problem of the "systematic distribution of elements" for the contemporary scientific community was considered utterly marginal, not worthy of attention for a serious scientist. Mendeleev decided to develop his system of classification of elements in spite of this widespread derision.

The most active phase of his work on the first two issues of his textbook and the classification of elements fell on 1867–1869. Mendeleev split the workload between his estate in Boblovo (Tver' province) and his University-owned apartment in Saint Petersburg (**Photo 4**, left). Since he suffered from hemorrhoids, he often had to work while standing at the bureau (**Photo 4**, right). It was while working at this desk that he discovered the periodic law.

Photo 4. Left: Mendeleev's home office; right: the bureau at which Mendeleev worked.

"First Attempt"

We will begin with the testimony of Mendeleev himself: "The first attempt made in this respect was the following: I selected the bodies with the lowest atomic weights and arranged them in order of magnitude of their atomic weight. It turned out that there exists a sort of periodical repetition of properties of simple bodies, and even in atomicities (valencies) elements follow each other in the order of the arithmetic sequence of the magnitude of their atomic weights:

Li = 7	Be = 9.4	B = 11	C = 12	N = 14	O = 16	F = 19
Na = 23	Mg = 24	Al = 27.4	Si = 28	P = 31	S = 32	Cl = 35.5
K = 39	Ca = 40	–	Ti = 50	V = 51	→	

... The following suggestion immediately springs to mind: perhaps the properties of the elements are displayed in their atomic weights, and could one then base a system on these?" [4; page 17].

Already when considering these light elements (with atomic weights from 1 to 40), Mendeleev arrived at important assumptions:

1. “Are the properties of elements in their atomic weight expressed, is it possible to create the system on it?” [4; page 18];

2. When the elements are ordered by their atomic weights, a “sort of period of properties” is observed. Thus, even if Mendeleev had not yet proposed the final formulation of the periodic law, he had already grasped its essence, the main point — the periodic nature of change in the properties of elements following the increase in their atomic weights. All his further efforts were aimed at testing this proposition, which at that point remained merely a hypothesis. The word “hypothesis” is, however, missing in the text of his first article on the classification of chemical elements. Instead, Mendeleev uses the word “law”:

“I propose that the law *(zakon)* I have established does not contradict the general direction of the natural sciences, and that until now its proof has not appeared, although there were already hints of it. From now on, it seems to me, a new interest will develop in the determination of atomic weights, in the discovery of new simple substances, and in the seeking out of new analogies between them” [4; page 21].

However, what exactly Mendeleev called “law” requires a more specific definition, and we will return to this further.

3. It is possible to build a system of elements from structural units of the following form:

Alkali Metals –	**Intermediate Elements –** “exhibiting less expressed chemical character” [4; page 22]	**Halogens**

(1)

By “chemical character” Mendeleev meant all properties of a simple body corresponding to a given element. Elements “exhibiting less expressed chemical character” comprised those with less pronounced “metallic” character than the alkali metals but less “non-metallic” than the halogens.

In other words, Mendeleev decided to build a system of elements by stacking fragments of type (1) in such a way that the atomic weights increase from top to bottom and from left to right.

This was a powerful insight, but Mendeleev's design was not easy to implement due to a number of difficulties:

– not all elements were known at that time (1869);

– for known elements, not all atomic weights were correctly defined, and it remained unclear which ones were to be trusted;

– the number of elements in different parts of type (1) was unequal: there were only five elements between Li and F, as well as between Na and Cl, while the interval between K = 39 and Br = 80 had to accommodate at least 12 elements known at the time: Ca = 40; Ti = 50; V = 51; Cr = 52; Mn = 55; Fe = 56; Co = Ni = 58.8; Cu = 63; Zn = 65; As = 75; Se = 79):

Li	Be	B	C	N	O	F											
Na	Mg	Al	Si	P	S	Cl											
K	Ca	–	Ti	V	Cr	Mn	Fe	Co	Ni	Cu	Zn	–	–	As	Se	Br	
Rb	Sr	–	Zr	Nb	Mo	–	Rh	Ru	Pd	Ag	Cd	U	Sn	Sb	Te	I	(2)

– the intervals (Li—F) and (Na—Cl) differed from the rest not only in the number of elements contained in them, but also, and more importantly, in their chemical character, as well as in the rate and rhythm of changes in the properties of simple bodies and corresponding compounds when moving from an alkali metal to halogen (for example, such elements as V, Cr, Mn, whose chemistry was significantly different from the chemistry of direct analogues of phosphorus, sulfur, and chlorine, i.e. As, Se, and Br, turned out to be among the K—Br series);

– there were two types of analogies between elements, which had to be somehow reflected in the system. This last difficulty should be considered in more detail.

Variant (2) did not suit Mendeleev, and it is easy to see why. In the first two lines, the analogous elements are located underneath one another, highlighting their natural order. In the third line however, As, a direct analogue of phosphorus, Se, a direct analogue of sulfur, and Br, a direct analogue of chlorine, were pushed to the side, sidestepped by other elements. Mendeleev decided "to break" the long lines:

Li	Be	B	C	N	O	F				
Na	Mg	Al	Si	P	S	Cl				
K	Ca	–	Ti	V	Cr	Mn	Fe	Co	Ni	
Cu	Zn	_	_	As	Se	Br				
Rb	Sr	–	Zr	Nb	Mo	–	Rh	Ru	Pd	
Ag	Cd	U	Sn	Sb	Te	I				(3)

This, however, did not resolve the difficulties. Some elements (for example, Fe, Co, Ni) ended up "suspended" outside the system. Worse yet, although arsenic was brought to same column with phosphorus, selenium with sulfur and bromine with chlorine, in these columns the elements that were direct analogues were blended with "aliens": between phosphorus and arsenic appeared vanadium, between sulfur and selenium – chromium, between chlorine, and bromine manganese… Was there anything in common between vanadium and phosphorus? At first glance, the two elements seemed nothing alike. But only at first glance. And Mendeleev knew that.

"Some Difficulty"

He knew that vanadium and phosphorus (as well as chromium and sulfur, or chlorine and manganese) were not entirely "alien" to each other. There was some similarity between them, but it manifested itself only in higher compounds. For example, the highest degree of oxidation of both chlorine and manganese is 7 (later they will be in the seventh group), and the corresponding higher compounds of these elements (Cl_2O_7

and Mn_2O_7; $KClO_4$ and $KMnO_4$ etc.) exhibit similar properties. The same can be said about the P—V and S—Cr pairs.

Mendeleev was aware of this prior to 1869, as were many other chemists before him, but the question remained: was this similarity of higher compounds, say, higher oxygen compounds, due to the similarity of the elements themselves, which were in a special, "limiting" state, or due to there being so much oxygen in these compounds that it equalized ("camouflaged") differences in the nature of the generic elements? This was one of the hardest questions facing Mendeleev, and it took him a long time, at least a year, to answer it.

Thus, the variant (3) of the system of elements, which quite satisfied such predecessors of Mendeleev as William Odling and Lothar Meyer, and which suits us today, to Mendeleev in early 1869 was completely unacceptable. The main reason he rejected this variant was the lack of clear and strict criteria for incorporating into one column elements of different classes (*razryad*), as they were then called, or, in modern terminology, the main-group (i.e. *ns*- and *np*-elements) and transition elements (i.e. (n – 1)*d*-elements).

With the criteria for unifying the elements of both "classes" into one group not yet clear, although even in his first article on the periodic law Mendeleev already wrote that, for example, "in manganese there is some similarity with chlorine, as in chrome with sulfur" [4; page 26]. Mendeleev was having "some difficulty", as he carefully put it later [5; page 78]. And besides that such "difficulty" arose at all, Mendeleev must have had at his disposal such a form (or structure) of a system of elements that would become the source of said difficulty. Such a form could only be a system of type (3). But in the absence of criteria for unifying dissimilar elements into one group, he could not use this form of the table, so it seemed to him more natural to separate elements of different classes.

That was his decision. In this way, after closely approaching the variant of the system that would later be known as the "short form: (or "natural system"), Mendeleev refused to place transitional elements among the elements of the main subgroups, arguing that should manganese be positioned in the column between chlorine and bromine, chromium between sulfur and selenium, vanadium between phosphorus and arsenic, etc., "the naturalness of the relations of members of the same... row [i.e., members of the same

main subgroup, as we would say today. – *I. S. D., V. Yu. K.*] would be broken" [4; page 26].

The task of unifying elements of different "classes", set by Mendeleev, may seem relatively simple, but only at first glance. After all, one had to precisely regroup more than sixty elements, to do so in such a way so as to keep their arrangement by increasing their atomic weights, and in no way obscure the periodic nature of changes in the properties of elements. Otherwise, the system lost its integrity and value. The task was complicated by the fact that Mendeleev initially attributed Cu, Ag, Zn and Cd to the elements of the first class, i.e. to the elements of the main subgroups, in modern terms.

Since the short form of the system (with "broken" periods) did not seem to fit, Mendeleev tried his luck with another form that would later become the "long" (or "long-period") version:

Li	Be											B	C	N	O	F
Na	Mg											Al	Si	P	S	Cl
K	Ca	–	Ti	V	Cr	Mn	Fe	Co	Ni	Cu	Zn	–	–	As	Se	Br
etc.																

Alas, this allocation of elements did not satisfy Mendeleev either, since he was confused by the emptiness (gaps) in the first two lines. The empty space inside the natural system seemed to suggest the existence of elements not yet discovered, whereas there was no reason to suspect the existence of unknown elements between Be and B and between Mg and Al.

As a result, Mendeleev, surmounting many obstacles, created a version of the system that he called with uncharacteristic modesty "An Attempt at a System of Elements, Based on Their Atomic Weight and Chemical Affinity" (hereinafter abbreviated as "Attempt"). The handwritten leaflet with the "Attempt" (**Photo 5**) is dated by hand: February 17th, 1869 (hereinafter all dates are given according to the Julian Calendar). The first public announcement of the discovery of the periodic law was made by Nikolai Menshutkin, a friend of Mendeleev (**Photo 6**).

Mendeleev handed "Attempted System" over to him for publication in the *Journal* and for communication at the upcoming meeting of the society. Menshutkin fulfilled Mendeleev's request and on March 6th, 1869 made on his behalf a presentation on the periodic law.

Photo 5. Final manuscript of "An Attempt at a System of Elements" (February 17th, 1869).

Photo 6. Nikolay A. Menshutkin (1842–1907), Secretary of the Russian Chemical Society and editor of *The Journal of the Russian Chemical Society*.

Thus, Mendeleev found an optimal way to publicize his work, i. e., through a communication by Menshutkin, the editor of the *Journal*, on behalf of the author of the forthcoming publication, thus avoiding the risk of excessive polemics. Meanwhile, Mendeleev went on March 1st, 1869, to Tver Governorate, where he planned to inspect artel (i. e., cooperative) cheese factories [6; page 105]. The works of Menshutkin were primarily focused on studies of the kinetics of chemical transformations of organic compounds. While studying the decomposition of tertiary amyl acetate upon heating, Menshutkin observed (1882) that one of the reaction products (acetic acid) accelerates the process; this is now a classic example of auto-catalysis. He also discovered the effect of solvent on kinetics (1887–1890), as well as the effect of dilution and chemical structure on the rate of a reaction. In 1890, he discovered the alkylation reaction of tertiary amines by alkyl halides to give quaternary ammonium salts (the Menshutkin reaction).

"Two Laws of Dmitry Mendeleev"

Let us now return to a question raised above regarding the word "law". As noted by Michael Gordin [7; page 31], and before him by Stefan Zamecki [8; page 124]. Mendeleev's "law" refers not to a periodic dependence of properties of elements on their increasing atomic weight, but to a completely different statement, namely: "All the comparisons which I made in this direction bring me to the conclusion that *the magnitude of atomic weight determines the nature of the element.*" [4; page 21]. But this is not at all a statement of the periodic law. Moreover, in an article published in August 1869 on the variation of atomic volumes over the periodic system, Mendeleev shied away from the word "law" and called it a "regularity (*pravil'nost'*)". According to Gordin, only "by November 1870, [Mendeleev] was utterly convinced of both the "naturalness" and the law-like character of his periodic law [7; page 31]." Neither Gordin, nor Zamecki went beyond mentioning this interesting fact. It does, however, point to an important feature in the development of Mendeleev's ideas regarding the classification of elements. On February 17th, 1869 (or, more precisely, by this day) Mendeleev discovered not one, but two laws. The first law was that the atomic weight of elements determines their properties; the second specified the nature of the change in the properties of elements as their atomic weights increased. The discovery of the first law was a logical consequence of

Mendeleev's ideas about the effect of body weight on its physical and chemical properties. Chemical phenomena, Mendeleev emphasized, following in the footsteps of Claude Louis Berthollet, are determined not only by the quantity of chemical energy (the strength of chemical affinity), but also by the mass of interacting bodies [9]. If one considers this idea at the atomic level, it can be said that the atom of a given element is characterized not only by a certain amount of chemical energy, but also by a certain mass (weight); and the chemical energy of the atom (and therefore its properties) depend on the atomic mass (weight):

Chemical energy of the atom = f(*A*), where *A* is the atomic weight.

Mendeleev had no fundamental difficulties with this direction of ideas, and therefore the assertion that "atomic weight determines the properties of an element" he described as a law of nature. With the second law, the law of periodicity, everything was different. Due to the unresolved problem of unifying elements of different classes, Mendeleev preferred to describe the phenomenon he discovered not as a "law", but as "regularity".

Academician Nikolay N. Zinin and Adjunct Aleksander M. Butlerov at a meeting on November 24th, 1870, of the Physics and Mathematics Department of the Saint Petersburg Academy of Sciences presented the Mendeleev's article "On the Place of Cerium in the System of Elements". In that paper, Mendeleev gives a table entitled simply and briefly – "System of elements", which became the prototype of the short form of the system known today, and which Mendeleev called in another article "The Natural System of Chemical Elements" (1870) [5] (**Photo 7**).

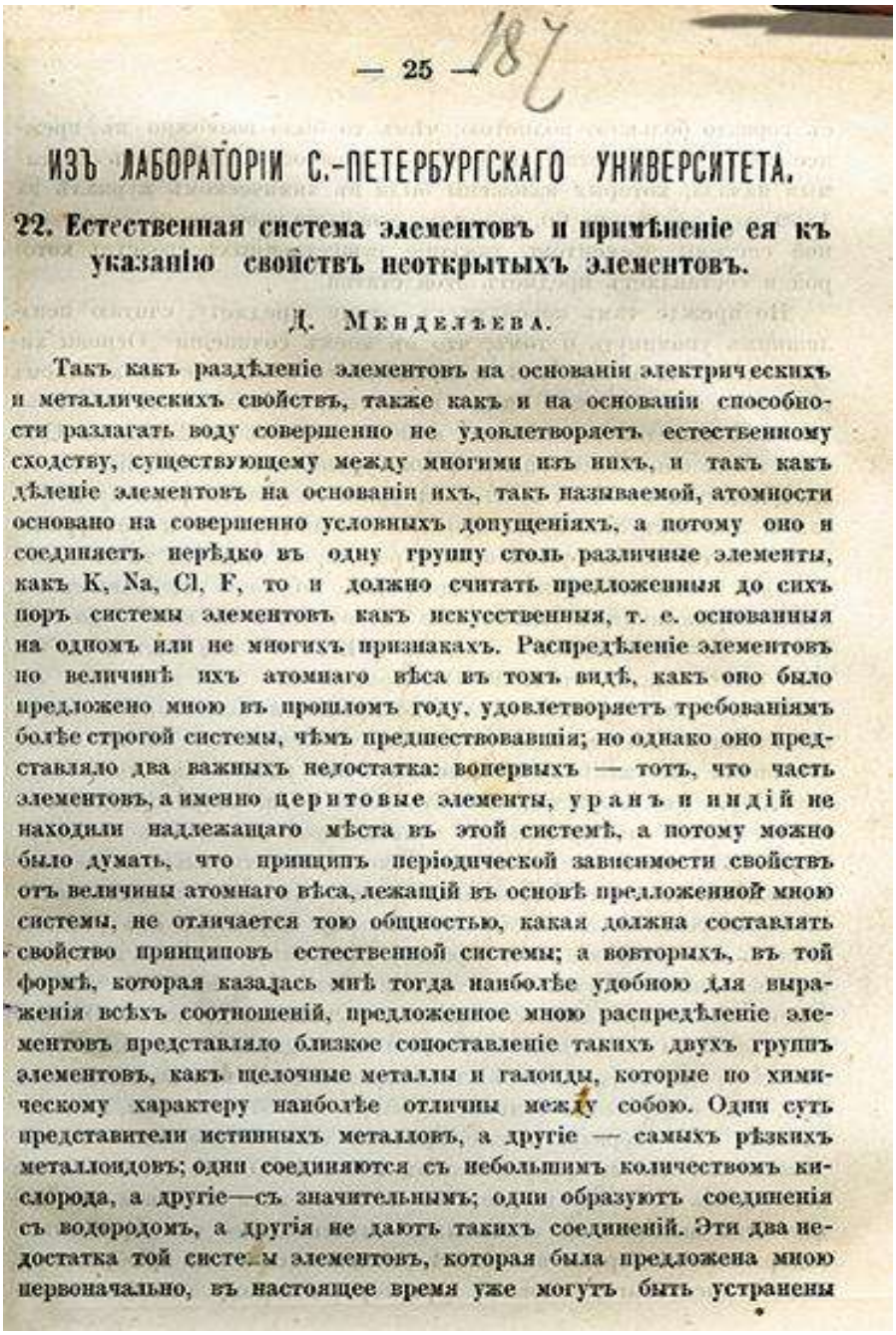

— 25 — 187

ИЗЪ ЛАБОРАТОРІИ С.-ПЕТЕРБУРГСКАГО УНИВЕРСИТЕТА.

22. Естественная система элементовъ и примѣненіе ея къ указанію свойствъ неоткрытыхъ элементовъ.

Д. Менделѣева.

Такъ какъ раздѣленіе элементовъ на основаніи электрическихъ и металлическихъ свойствъ, также какъ и на основаніи способности разлагать воду совершенно не удовлетворяетъ естественному сходству, существующему между многими изъ нихъ, и такъ какъ дѣленіе элементовъ на основаніи ихъ, такъ называемой, атомности основано на совершенно условныхъ допущеніяхъ, а потому оно и соединяетъ нерѣдко въ одну группу столь различные элементы, какъ K, Na, Cl, F, то и должно считать предложенныя до сихъ поръ системы элементовъ какъ искусственныя, т. е. основанныя на одномъ или не многихъ признакахъ. Распредѣленіе элементовъ по величинѣ ихъ атомнаго вѣса въ томъ видѣ, какъ оно было предложено мною въ прошломъ году, удовлетворяетъ требованіямъ болѣе строгой системы, чѣмъ предшествовавшія; но однако оно представляло два важныхъ недостатка: вопервыхъ — тотъ, что часть элементовъ, а именно церитовые элементы, уранъ и индій не находили надлежащаго мѣста въ этой системѣ, а потому можно было думать, что принципъ періодической зависимости свойствъ отъ величины атомнаго вѣса, лежащій въ основѣ предложенной мною системы, не отличается тою общностью, какая должна составлять свойство принциповъ естественной системы; а вовторыхъ, въ той формѣ, которая казалась мнѣ тогда наиболѣе удобною для выраженія всѣхъ соотношеній, предложенное мною распредѣленіе элементовъ представляло близкое сопоставленіе такихъ двухъ группъ элементовъ, какъ щелочные металлы и галоиды, которые по химическому характеру наиболѣе отличны между собою. Одни суть представители истинныхъ металловъ, а другіе — самыхъ рѣзкихъ металлоидовъ; одни соединяются съ небольшимъ количествомъ кислорода, а другіе—съ значительнымъ; одни образуютъ соединенія съ водородомъ, а другія не даютъ такихъ соединеній. Эти два недостатка той систе..ы элементовъ, которая была предложена мною первоначально, въ настоящее время уже могутъ быть устранены

Photo 7. The first page of the article by Mendeleev "A Natural System of the Chemical Elements" (November 29th, 1870) [5] with a detailed elaboration on the essence of the periodic law. Regarding this article, Mendeleev wrote that he decided to publish it "in order to establish the periodicity of the elements. It was a risk but the right (and successful) one" [10; page 54].

Although Mendeleev worked on it concurrently with the article "On the Place of Cerium…" (**Photo 8**), the graphic expression of the periodic law presented in the "Natural System" was substantially improved from the initial version. It was included by Mendeleev in the second part of the first edition of the "Principles of Chemistry" (1871),

and the name of the author was indicated in the title: “The Natural System of Elements of D. Mendeleev” (**Photos 9–10**).

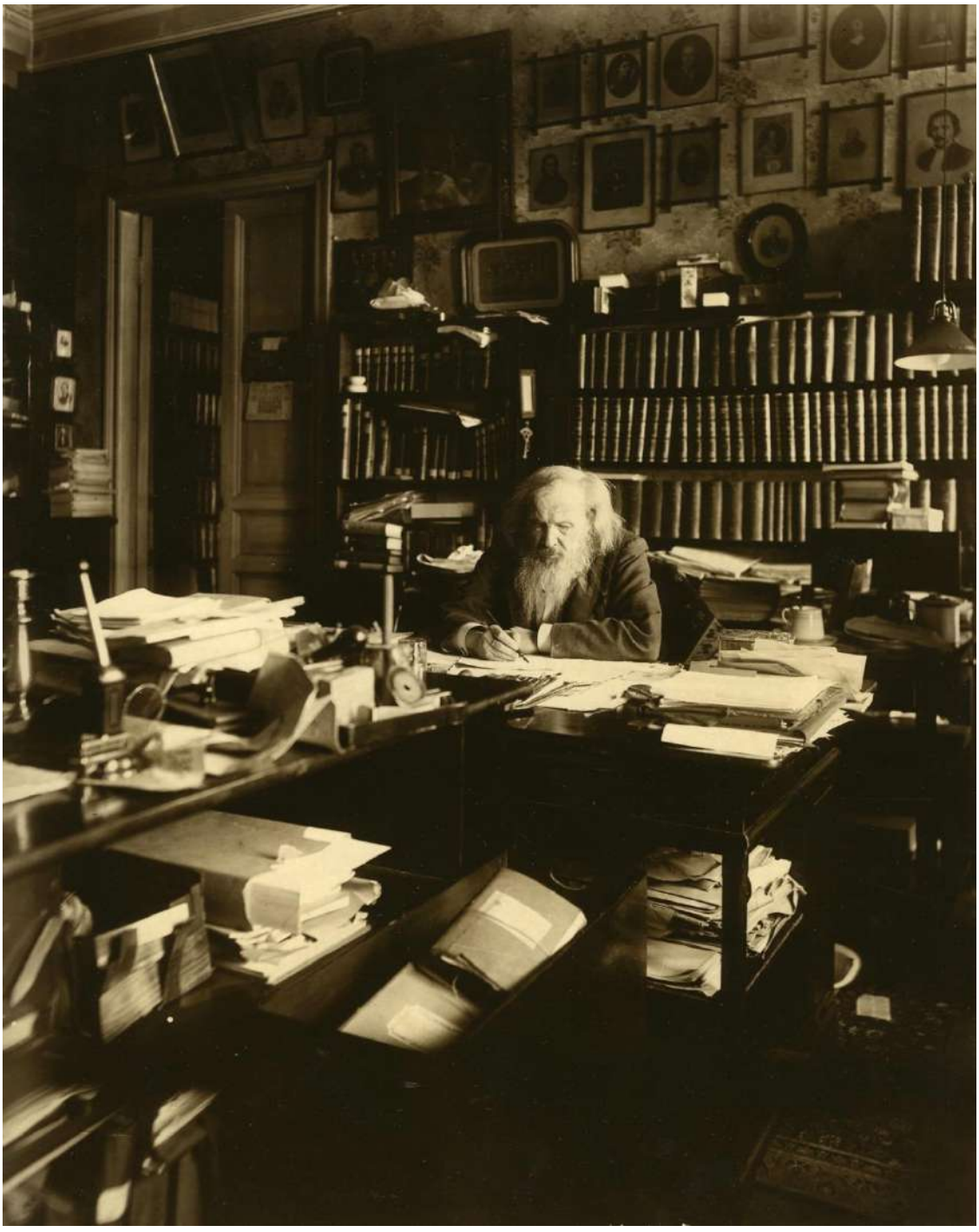

Photo 8. D. Mendeleev at his office at The Chamber of Weights and Measures, Saint Petersburg (1904).

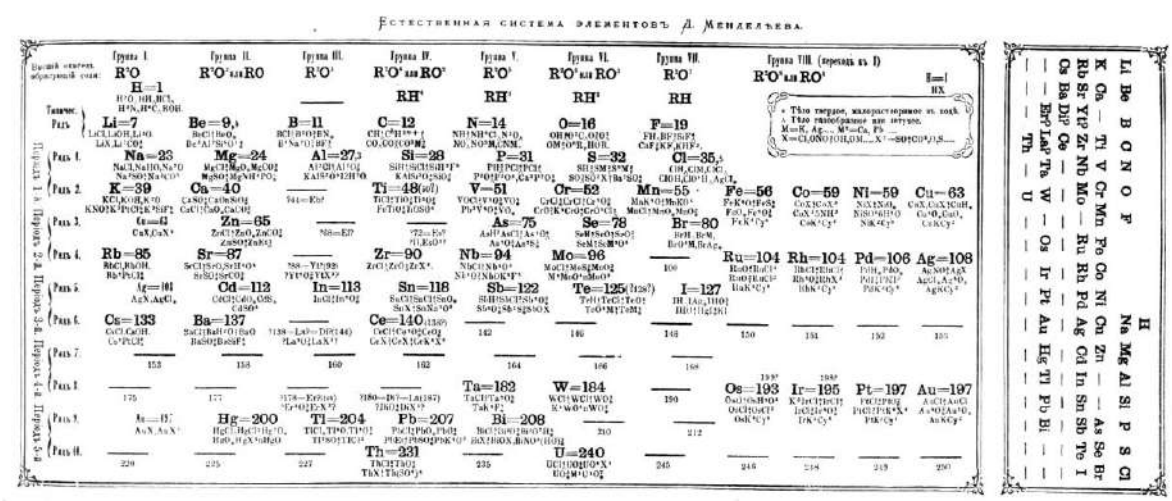

Photo 9. Natural system of the elements of D. Mendeleev (November 1870) from his textbook "Principles of Chemistry" (1st edition, part 2; 1871).

Photo 10. World's oldest periodic table displayed at the lecture theater of the Mendeleev Center of Saint Petersburg State University. Left panel: "D.I. Mendeleev's Periodic Law, 1869"; right panel: "The Table Made as Directed by the Author in 1878."

References and Notes

[1] The originals of photographs 1–2 and 5–9 belong to the open collection of D. Mendeleev Museum and Archives (Saint Petersburg State University) and their copies were made by I. S. Dmitriev. Photographs 3–4 were taken by V. Yu. Kukushkin and I. S. Dmitriev, respectively, and they comprise parts of their private photo collections.

[2] Virtual 3D-tour at The D. I. Mendeleev Museum and Archives: https://english.spbu.ru/images/vtour/mendeleev/index.html

[3] D. I. Mendeleev, Principles of Chemistry [1st Edition]. SPb.: "Obshchestvennaya pol'za". Part I, Issue 1 (1868), IV, 400 p.; Issue 2 (1869), pp. 401–816; Part II, Issue 3 (1870), 392 p.; issues 4/5 (1871), pp. 393–952.

[4] (*a*) D. Mendeleev, Sootnoshenie svoistv s atomnym vesom elementov [On the Relationship of the Properties of the Elements to Their Atomic Weights]; (*b*) D. Mendeleev. Periodicheskii zakon. Osnovnuye stat'i [Periodic Law. Basic Papers], Ed. B. M. Kedrov. Moscow: Izdatelstvo AN SSSR, 1958, pp. 10–31 and p. 18. Original: *Zhurnal Russkogo Khimicheskogo Obshchestva* [*Journal of the Russian Chemical Society*], **1869**, *1*, 60–79.

[5] D. Mendeleev, Estestvennaya sistema elementov I primenenie ee k ukazaniyu svojstv neotkrytyh elementov [Natural System of the Elements and its Use in Predicting the Properties of Undiscovered Elements], in D. Mendeleev. Periodicheskii zakon. Osnovnuye stat'i [Periodic Law. Basic papers], Ed. B. M. Kedrov. Moscow: Izdatelstvo AN SSSR, 1958, pp. 69–101 and p. 78.

[6] I. S. Dmitriev, Chelovek Epokhi Peremen (Ocherki o D. I. Mendeleeve i ego Vremeni) [Man of the Time of Change (Essays on D. I. Mendeleev and his Epoch)]. Saint Petersburg: Khimizdat, 2004; 576 pp. [in Russian].

[7] M. D. Gordin, A Well-Ordered Thing: Dmitrii Mendeleev and the Shadow of the Periodic Table. New York: Basic Book, 2004, 518 pp.

[8] S. Zamecki, Mendeleev's First Periodic Table in its Methodological Aspect, *Organon*, **1995**, *25*, 105–126 (p. 124).

[9] Notably in the *Principles of Chemistry*, Mendeleev puts a strong emphasis on the views of Berthollet, and specifically on the description of the so-called Indefinite Compounds such as solutions, alloys, isomorphous mixtures, and silicate compounds. At that time, in the 1860s, these views went against prevailing traditions (as noted by P. Grapí and M. Izquirdo, "The textbook tradition... contributed to marginalize Berthollet's system" in P. Grapí and M. Izquirdo, Berthollet's Concept of a Chemical Change in Context, *Ambix*, **1997**, *44*, 113–130 (p. 119)).

[10] Arkhiv D. I. Mendeleeva. T. 1. Avtobiograficheskie materialy. Sbornik dokumentov / Sost. M. D. Mendeleeva i T. S. Kudryavceva. Pod obshchej red. S. A. Shchukareva i S. N. Valka. [The Archive of D. I. Mendeleev. T. 1. Autobiographical Materials. Collection of Documents / Compilation by M. D. Mendeleeva and T. S. Kudryavtseva. Ed. S. A. Schukareva and S. N. Valka] Leningrad: Izdatel'stvo Leningradskogo Universiteta

Celebratory Symposium

A — Catalysis and the Periodic Table

HYBRID LIGANDS FOR METAL COMPLEXES, CATALYSTS AND NANOMATERIALS

Pierre Braunstein

University of Strasbourg — CNRS. Institute of Chemistry, 4 rue Blaise Pascal, 67081 Strasbourg (France). braunstein@unistra.fr

Pierre Braunstein received his PhD in Inorganic Chemistry from the University Louis Pasteur (ULP) Strasbourg (France) and then spent a year at University College London, with Profs. R. S. Nyholm and R. J. H. Clark, as a Royal Society/CNRS post-doctoral fellow. After earning his State Doctorate from ULP, he was awarded an Alexander-von-Humboldt post-doctoral fellowship to spend a year at the Technical University Munich with Prof. E. O. Fischer (Nobel Laureate).

He rose through the ranks at the CNRS, became Research Director Exceptional Class and is now Emeritus Research Director and «professeur conventionné» of the University of Strasbourg. He also holds various positions in China: at Qingdao University of Science and Technology, Zhejiang University, Soochow University and Yangzhou University.

His broad research interests lie in the inorganic and organometallic chemistry of the transition and main group elements, where he has (co)authored ca. 600 scientific publications and review articles. They cover the synthesis and coordination/organometallic chemistry of heterofunctional ligands, the study of hemilabile metal-ligand systems, of strongly dipolar quinonoid zwitterions, of low oxidation state metal-metal bonded (hetero)dinuclear and cluster complexes and of magnetic coordination clusters. Focused on fundamental aspects, his research has also led to numerous applications, ranging from homogeneous catalysis, e.g. ethylene oligomerization, to cluster-derived nanoparticles for heterogeneous catalysis and nanosciences.

He has received numerous awards and honors from France, China, Germany, India, Italy, Japan, Portugal, Singapore, Spain, The Netherlands and the United Kingdom. He is a member i.a. of the French Academy of Sciences, of the German National Academy of Sciences Leopoldina and Foreign Corresponding Member of the Academy of Sciences of Lisbon (Portugal) and Zaragoza (Spain). Since 2015, he is Head of the Chemistry Division of the European Academy of Sciences.

Introduction

To celebrate the 150th Anniversary of the publication of *The Principles of Chemistry* by Mendeleev, UNESCO has declared 2019 the International Year of the Periodic Table. Numerous publications have recalled the history of its development and events have been organized on this occasion around the world. For example, the Academy

of Sciences of Lisbon contributed to this celebration through a Symposium held on October 3, 2019,[1] and the French *Académie des Sciences* also dedicated an afternoon to this celebration on November 19, 2019.[2] The classification of the elements certainly represents one of the most fruitful achievements in modern science and the Periodic Table occupies an iconic position in chemistry, knowing no linguistic or geographical border since the language of chemistry is international. Its current form is reproduced in almost every undergraduate inorganic textbook and displayed in chemistry classrooms and lecture theatres.

Through the publication of his book "*The Principles of Chemistry*" in 1869, Dmitri Ivanovitch Mendeleev offered a classification of the 63 elements known that allowed him not only to rationalize several properties and explain similarities between elements but also to predict the existence of elements that remained to be discovered. Although Mendeleev has been rightly given the major credit for this achievement, he recognised the major role played over an 80-year timespan by scientists such as Lavoisier, Dalton, Berzelius, Prout, Döbereiner, Dumas, Cannizzaro, von Pettenkofer, Gmelin, Odling, Béguyer de Chancourtois, Newlands and Meyer. The predictive power of Mendeleev's classification was beautifully demonstrated when François Lecoq de Boisbaudran discovered gallium in 1875, the existence of which had been predicted by Mendeleev 6 years earlier (under the name eka-aluminum), when Lars Fredrik Nilson discovered scandium in 1879 (the eka-boron of Mendeleev) and Clemens Winkler discovered germanium in 1886 (eka-silikon). In 1875 Mendeleev published in the *Comptes Rendus de l'Académie des sciences* a version of his classification that prefigures the Periodic Table as we know it today, with 118 elements organized in 7 periods and 18 columns.[3]

The year 2019 also marks the 100th anniversary of the death of the Nobel laureate Alfred Werner (12 Dec. 1866 - 15 Nov. 1919), the founder of Coordination Chemistry. He was the first to propose correct structures for coordination compounds containing complex ions, in which a central transition metal atom is surrounded by neutral or anionic ligands, such as NH_3, H_2O or Cl^-, respectively. Since these pioneering days, the design of new functional ligands and complexes has become a major endeavour in chemistry, only limited by the chemists' imagination and triggered by fast developments in synthetic organic methodologies and increasing (catalytic) use of metals, that provide access to new molecules or solids endowed with remarkable chemical or physical

properties.[4] Furthermore, the growing research effort directed toward the study of the structural, catalytic and physical properties of coordination/organometallic metal complexes is rewarded by their ever-increasing diversity of applications and performances. In the following, we shall provide an extended abstract of the lecture given on the occasion of the Celebration of the 150th Anniversary of the Periodic Table by the Academy of Sciences of Lisbon on October 3, 2019.

Hemilability: a Powerful Concept Relevant to Homogeneous Catalysis

Catalysis is gaining increasing significance, both in academia and in industry, because it allows chemical transformations to be performed with lower activation energies, higher selectivity and atom economy, thus reducing energy costs and waste production. Catalysis is a major component of the guiding principles of green or sustainable chemistry.[5-7] To achieve a better fine-tuning of the stereoelectronic properties of the metal centres involved in stoichiometric or catalytic transformations, a huge diversity of functional ligands has been designed to control their coordination sphere. In particular, various hybrid ligands, which contain chemically different donor groups, such as hard and soft donors, have been developed. After coordination to one or more metal centres, their potential ability to undergo dynamic behaviour resulting from partial de-coordination of the weaker link is directly relevant to key steps in homogeneous catalysis processes (Scheme 1). This phenomenon, which is readily monitored by variable-temperature NMR spectroscopy, temporarily liberates a coordination site that can be used by a substrate molecule, which upon coordination to the active metal site, will be transformed and the liberation of the product will be assisted by chelation of the hybrid ligand.[8,9] This dynamic feature characterizes a ligand/metal couple and has been coined hemilability *ca*. 40 years ago,[10] although the phenomenon itself had been observed earlier.[11]

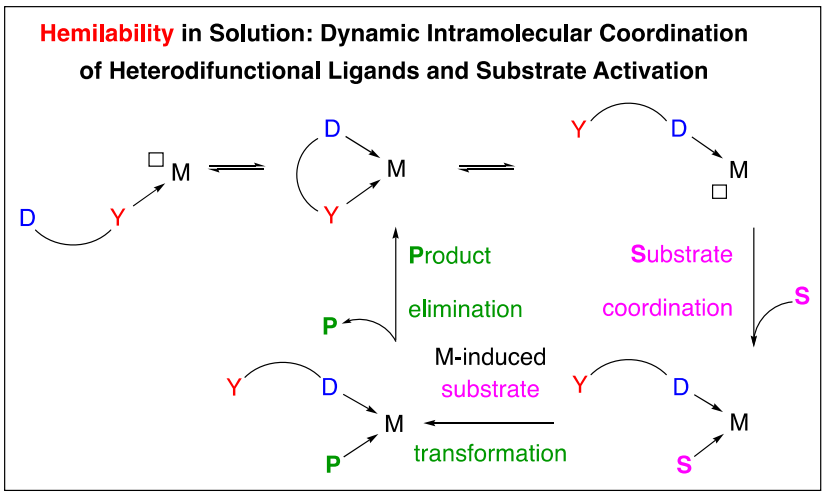

Scheme 1. Relevance of hemilability of a coordinated hybrid ligand to catalytic steps.

Activation and Transformation of CO_2

Using hybrid phosphine ligands containing an ester-enolate group,[12] we unexpectedly discovered a Pd(II) complex that is capable of reversibly binding CO_2 at room temperature and under atmospheric pressure (Scheme 2).[13]

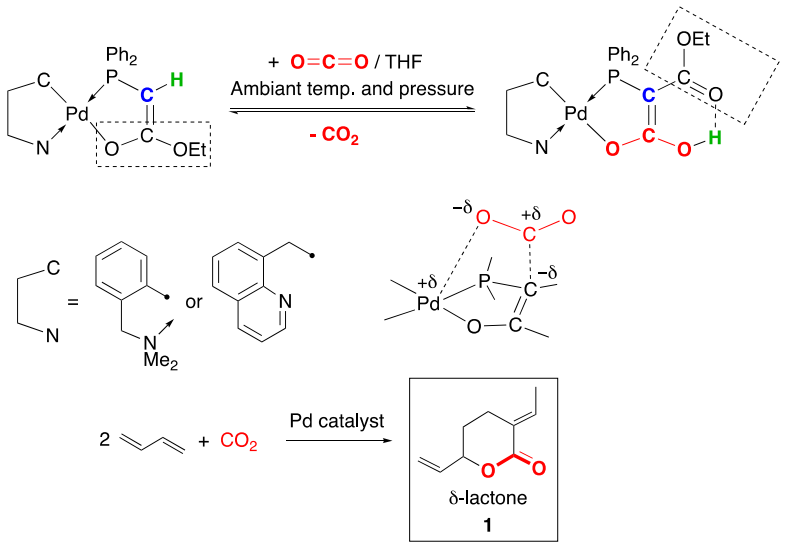

Scheme 2. Activation and valorisation of CO_2

In this process, the P-donor arm remains coordinated to Pd throughout whereas the O-Pd bond opens and liberates a site for one of the oxygen atoms of the CO_2 molecule after nucleophilic attack of the enolate carbon atom to the carbon atom of CO_2 has led to C-C bond formation. Migration of the PCH proton results in a stabilizing H-bonding interaction in a six-membered ring. The reverse steps occur when nitrogen is

bubbled through a solution of the complex under ambient conditions, which causes the liberation of the CO_2 molecule. In both forward and backward reactions, the oxygen-palladium bond formed and broken is in trans position to the σ–bonded carbon atom of the cyclometallated spectator ligand, which has a strong trans-effect and trans-influence. These CO_2 carriers provided the first examples where reversible CO_2 fixation by a transition-metal complex has been fully characterized by X-ray diffraction and shown to occur by carbon-carbon bond formation.[14] Interestingly, no fixation of CO_2 was observed when the ester-enolate group was replaced by a keto-enolate (OEt replaced by Ph), illustrating the importance of the nucleophilicity of the enolate carbon centre that undergoes nucleophilic attack on the carbon atom of CO_2 while the electrophilic centres (Pd(II) and H^+) stabilize the oxygen atoms of CO_2. Thus, each atom of this triatomic molecule is involved in the process, which can be viewed as a trifunctional activation of CO_2. These palladium complexes were used to catalyse the telomerisation of CO_2 with butadiene to afford the δ–lactone **1** (Scheme 2).[15] This work also showed that CO_2 activation by a metal complex was necessary for catalytic activity but may not always be sufficient. After catalyst optimisation, we achieved a 49% yield and 96% selectivity in δ–lactone. Selectivity is the major issue since unreacted butadiene can be readily recycled whereas the formation of other CO_2-containing products, *e.g.* acids and esters, requires subsequent separation steps. It is interesting to note that more than 30 years later, this chemistry remains of prime interest and while the catalyst performances have not been significantly improved,[16] applications of the product appear promising.[17]

The properties and reactivity of alkyl carbonates remain of high academic and industrial interest because they are important, versatile and biodegradable chemical intermediates with moderate toxicity and environmental impact.[18] They may be used *e.g.* for the alkylation of various organic substrates. We reported a rare case of a Lewis acid catalysed formation of anisole or ethoxybenzene by decarboxylation of methyl or ethyl phenyl carbonate, respectively.[19] An Al(III) compound, such as $AlCl_3$ or $Al(OAr)_3$, was used as catalyst in a [Al]/[methyl phenyl carbonate] molar ratio of 0.0036. Facilitating this difficult decarboxylation step is important and O-alkylation of phenol can then be readily achieved in 2 steps using first an alkyl chloroformate and then catalytic decarboxylation of the organic carbonate (Scheme 3).

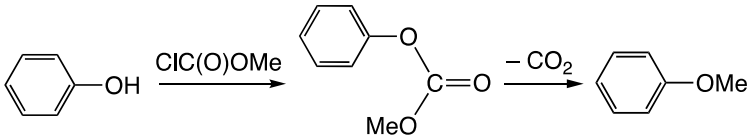

Scheme 3. O-Alkylation of phenol by reaction of methyl chloroformate followed by catalytic decarboxylation of methyl phenyl carbonate affording anisole.

Phosphino-enolates and Functional N-Heterocyclic Carbenes

It is noteworthy that phosphino-enolates of the type seen above behave as 3 electron donor P,O-type chelating ligands with numerous metals and, together with closely related P,N-type chelates, lead to an impressive scope of very diverse catalytic applications,[12] ranging from CO_2 activation (see above) when coordinated to Pd(II), ethylene oligomerization with Ni(II) (SHOP-type industrial process),[20,21,22] transfer-hydrogenation with Ru(II) (with related 3 electron donor anionic phosphinooxazoline chelates)[23] to alkane activation with Rh(I).[24] These examples serve to illustrate the remarkable impact of hybrid ligands in homogeneous catalysis.[8,9,12]

Triggered in particular by the similarities between phosphine and N-heterocyclic carbene (NHC) donors – notwithstanding their differences – the field of NHC ligands is enjoying exponential growth and an increasing number of hybrid ligands are reported that associate NHC with other types of donor functions (Scheme 4). NHC ligands offer advantages over phosphines, such as a lower oxygen-sensitivity and formation of generally more robust bonds to metals. Recent examples illustrate the very interesting and often unique features and properties that functional NHC ligands confer to their metal complexes.[25-34]

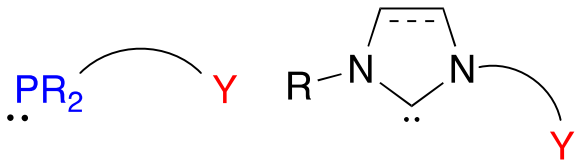

Scheme 4.

Metal Carbonyl Clusters: Well-Defined Precursors to Nanoparticles

Although the notion of metal-metal bonds in molecules was inexistent in the days of Alfred Werner, the field of metal clusters is now well established in chemistry and thousands of molecules containing metal-metal bonds between similar (homometallic) or different (heterometallic) metal centres have been prepared and characterized, usually by X-ray diffraction, the « ultimate » method.[35] Metal clusters are fascinating objects, and both experimentalists and theoreticians worldwide aim at unravelling and understanding their often aesthetically most pleasing structures, their bonding features, the occurrence within their core of metallophilic interactions at distances inferior to the sum of the van der Waals radii,[36] their stoichiometric and catalytic properties in chemistry,[37] including in the gas phase,[38] and their physical, electronic, magnetic and optical properties of relevance to physics and material sciences.

Starting from well-defined carbonyl clusters where the metals are in a low oxidation state, thermal activation allows easy removal of the ligands to afford metal nanoparticles, without drastic rearrangements of the metal core that would occur if redox reactions were involved in the process. The central question was to investigate whether their size and composition, in case of heterometallic systems, could keep the "memory" of the metal core composition of their molecular precursor or whether phase segregation would occur (Figure 1).

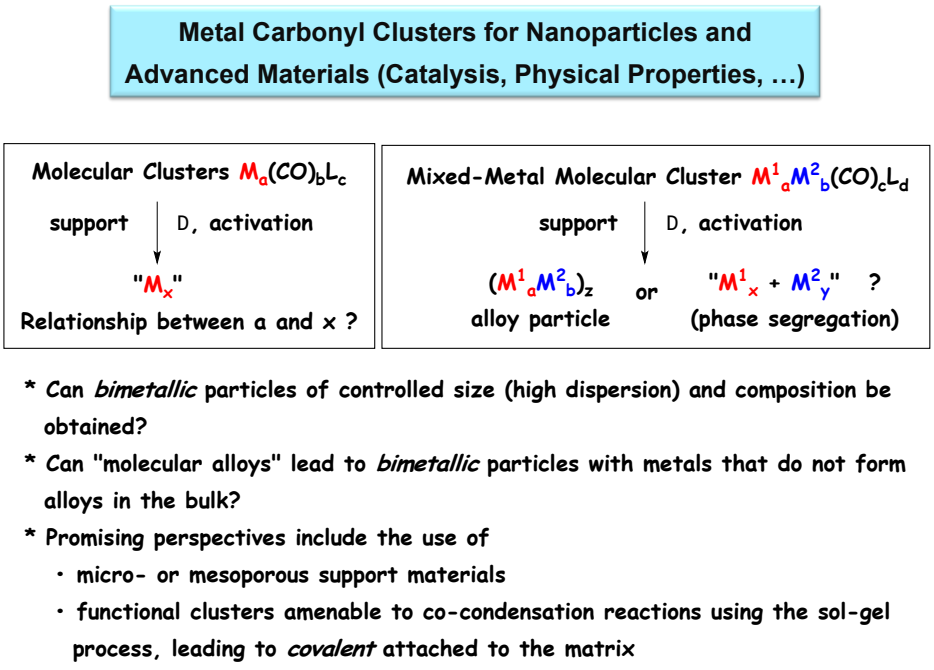

Figure 1. Molecular clusters as precursors to well-defined nanoparticles

This approach led us to report in 1982 the first application of heterometallic clusters as molecular precursors to heterogeneous catalysts in the form of alloy nanoparticles.[39] We investigated the carbonylation of organic nitro derivatives into isocyanates, catalysed by nanoparticles derived from the planar, centrosymmetric bimetallic cluster $[Mo_2Pd_2Cp_2(CO)_6(PPh_3)_2]$ (Figure 2).

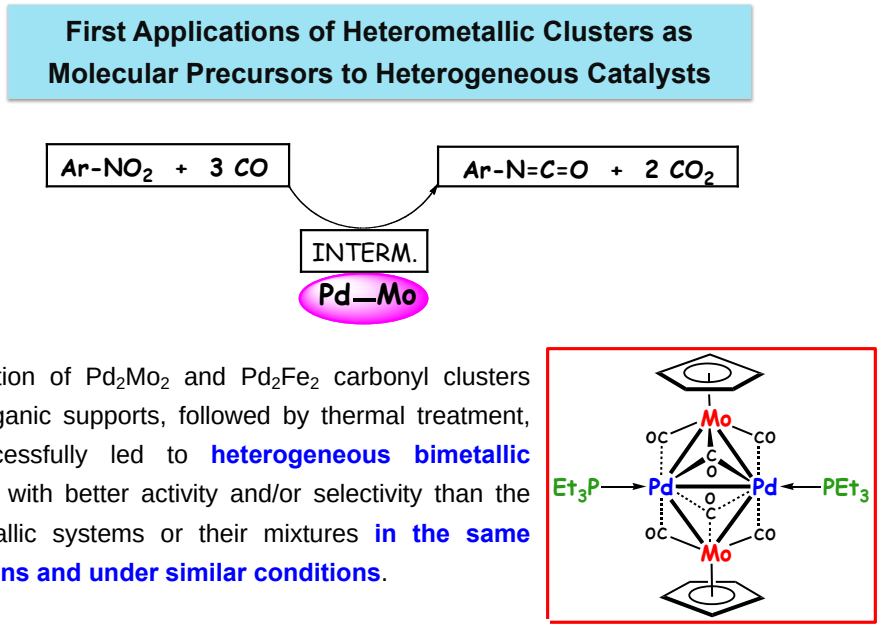

P. Braunstein, R. Bender, J. Kervennal, *Organometallics* **1982**, *1*, 1236.
J. Kervennal, J.-M. Gognion, P. Braunstein, FR 2 515 640 - U.S. 4.478.757 (1982) - Eur. Pat. Appl. EP 78729 A1 (1983) (PCUK)
General review on Heterometallics and Catalysis: P. Buchwalter, J. Rosé, P. Braunstein, *Chem. Rev.* **2015**, *115*, 28-126.

Figure 2. This Mo_2Pd_2 cluster was the first mixed-metal cluster containing palladium and used as a precursor to catalytic bimetallic nanoparticles.

Gratifyingly, these nanoparticles very not only very active but their selectivity for phenyl isocyanate (71−80%) was higher than that of conventional catalysts prepared by mixing the individual components (62−67%). These studies were extended to the use of Fe−Pd clusters impregnated on silica or alumina as precursors to heterogeneous bimetallic catalysts for the conversion of *o*-nitrophenol to benzoxazol-2-one.[40] All the particles obtained by thermal decomposition of the clusters $[FePd_2(CO)_4(\mu\text{-dppm})_2]$ or $[Fe_2Pd_2(CO)_5(NO)_2(\mu\text{-dppm})_2]$ (dppm = $Ph_2PCH_2PPh_2$ (bis(diphenylphosphino)methane) were shown by analytical electron microscopy to have a diameter of 20-50 Å and to be all bimetallic.[41] In contrast, no small bimetallic particles were detected in conventional catalysts prepared by co-impregnation of palladium and iron salts. The preparation of heterogeneous, bimetallic catalysts from well-defined, mixed-metal clusters has become a very successful field of research.[37]

If impregnation of clusters on inorganic oxides, followed by thermal activation under controlled atmosphere, to avoid oxidation of the highly reactive metallic nanoparticles obtained, is a straightforward approach, it also appeared attractive to chemically anchor the clusters to the host matrix, with the hope to better control the distribution of the particles in the solid. Bifunctional ligands may be used for that purpose and we explored and compared complementary approaches to this aim.[4] Starting from the versatile short-bite diphosphine ligand $Ph_2PNHPPh_2$ (bis(diphenylphosphino)amine, dppa),[42] we prepared the alkoxysilyl-functionalized diphosphine ligands $(Ph_2P)_2N(CH_2)_3Si(OMe)_3$, $(Ph_2P)_2N(CH_2)_4SiMe_2(OMe)$ and $(Ph_2P)_2N(CH_2)_3Si(OEt)_3$ which were used to decorate the pore walls of nanoporous alumina membranes.[43,44] The ligand alkoxysilyl end-group allows covalent attachment to the inorganic matrix by formation of strong Si–O bonds. This procedure was also applied to the functionalization of an ordered mesoporous silica of the type SBA-15 and the anchoring of the tetrahedral cluster $[Co_4(CO)_{10}(\mu\text{-dppa})]$ (Figure 3).[45] This cluster was selected because interesting magnetic properties were expected for the resulting cobalt nanoparticles. The bridging dppa ligand not only stabilizes the cluster but also selectively orients the substitution of the alkoxysilyl-functionalized diphosphine to the opposite edge of the tetrahedron.

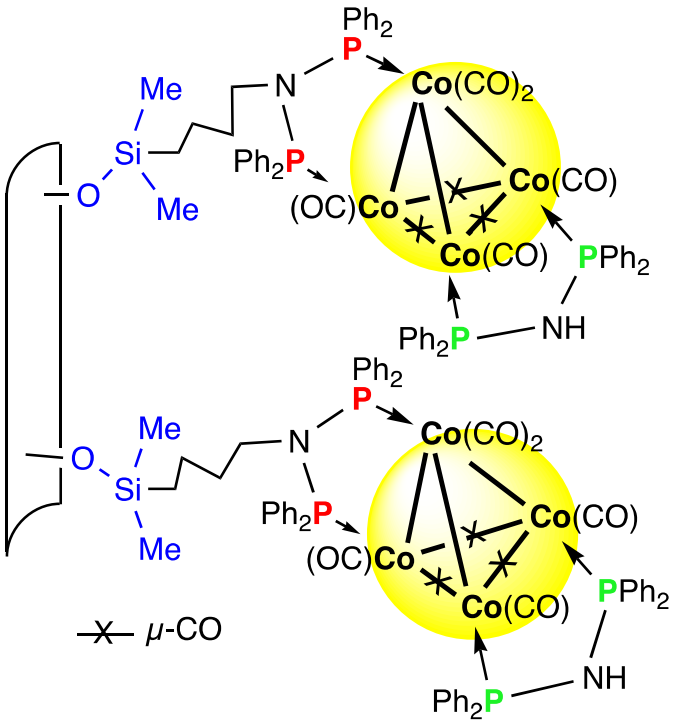

Figure 3. Anchoring of a Co_4 carbonyl cluster onto mesoporous silica.

Subsequent thermal treatment of the functionalized mesoporous silica under H_2 led unexpectedly to pure nanocrystalline, orthorhombic Co_2P particles.[45,46] Their spatial repartition, size, and shape were more regular than when a silica xerogel, obtained by the sol–gel process, was used. Interestingly, the narrow size distribution of the particles of *ca*. 6 nm corresponds to the pore size diameter of SBA-15, consistent with a controlled confinement exerted by the matrix on particle formation. The preparation of transition-metal phosphides is attracting much interest owing to their various properties and it generally requires the direct combination of the elements at higher temperatures, although molecular precursors are being increasingly used.

Heterometallic clusters were also used as precursors to nanoparticles, such as $[RuCo_3(CO)_{12}]^-$ which is isoelectronic to $[Co_4(CO)_{12}]$.[47,48] Starting from the cluster $[Mo_2Pd_2Cp_2(CO)_6(PPh_3)_2]$ depicted in Figure 2, its impregnation in two different silica matrices, amorphous xerogels and ordered SBA-15, followed by thermal activation led to the identification of a new lacunar ternary compound Pd_xMo_yP, isostructural with Mo_3P. Interestingly, the nanoparticles were more uniformly distributed in the SBA-15 framework than in the amorphous xerogels and presented a narrower size distribution.[49]

Clearly, there are several advantages associated with stepwise approaches leading to the anchoring of well-characterized metal clusters in mesoporous materials. They facilitate the subsequent controlled generation of metal nanoparticles, which can be homo- or hetero-metallic depending on the nature of the molecular precursor. Mixed-metal clusters can be viewed as ligand-stabilized “molecular alloys” and convenient precursors to alloy nanoparticles. The study of their catalytic and electronic properties is attracting increasing attention.[37]

Conclusion

Molecular chemistry is a fast expanding and unlimited field of research that deals with all the elements of the Periodic Table. In this presentation, we wished to illustrate, by selecting recent and less recent but still relevant examples from our research activities, how specific ligands associated with mono- or polynuclear metal centres can bring about novel and sometimes unexpected properties. Serendipity is an important and exciting component of fundamental research and, as quoted by Louis Pasteur, « In the fields of observation, chance favors only the prepared mind ».

Acknowledgement

I am most grateful to all the coworkers and collaborators whose names are cited in the references and to the past and present members of our Laboratory for their contributions, dedication, and enthusiasm. I warmly thank all the funding organisations for their support of our various research programmes.

References

1. https://www.youtube.com/watch?v=qgdOqeGZEEI.
2. https://www.academie-sciences.fr/fr/Colloques-conferences-et-debats/variations-autour-du-tableau-periodique.html.
3. D. Mendeleev, Remarques à propos de la découverte du gallium, *C. R. Hebd. Séances Acad. Sci.*, 1875, 969-972.
4. P. Braunstein, Functional ligands and complexes for new structures, homogeneous catalysts and nanomaterials, *J. Organomet. Chem.*, 2004, **689**, 3953-3967.
5. P. T. Anastas and J. C. Warner, *Green Chemistry: Theory and Practice*, Oxford University Press, New York, 1998.
6. I. T. Horvath and P. T. Anastas, Innovations and green chemistry, *Chem Rev*, 2007, **107**, 2169-2173.
7. P. Anastas and N. Eghbali, Green Chemistry: Principles and Practice, *Chem. Soc. Rev.*, 2010, **39**, 301-312.
8. P. Braunstein and F. Naud, Hemilability of hybrid ligands and the coordination chemistry of oxazoline-based systems, *Angew. Chem. Int. Ed.*, 2001, **40**, 680-699.
9. W. H. Zhang, S. W. Chien and T. S. A. Hor, Recent advances in metal catalysts with hybrid ligands, *Coord. Chem. Rev.*, 2011, **255**, 1991-2024.
10. J. C. Jeffrey and T. B. Rauchfuss, Metal complexes of hemilabile ligands. Reactivity and structure of dichlorobis(*o*-(diphenylphosphino)anisole)ruthenium(II), *Inorg. Chem.*, 1979, **18**, 2658-2666.
11. P. Braunstein, D. Matt, F. Mathey and D. Thavard, Functional Phosphines. New Synthesis of Diphenylphosphinoacetonitrile and Ethyl Diphenylphosphinoacetate; Some of Their Complexes with Iron(0), Gold(I), Nickel(II), Palladium(II), Platinum(II), Rhodium(III), and Iridium(III). Stereodynamic Behavior of [Rh($Ph_2PCH_2CO_2Et$)($Ph_2PCH_2CO_2Et$)Cl_3], *J. Chem. Res. (S)*, 1978, 232-233; (*M*) 1978, 3041-3063.
12. P. Braunstein, Bonding and organic and inorganic reactivity of metal-coordinated phosphinoenolates and related functional phosphine-derived anions, *Chem. Rev.*, 2006, **106**, 134-159.
13. P. Braunstein, D. Matt, Y. Dusausoy, J. Fischer, A. Mitschler and L. Ricard, Coordination Properties of (Diphenylphosphino)acetonitrile, Ethyl (Diphenylphosphino)acetate, and

Corresponding Carbanions. Characterization of a New Facile Reversible CO_2 Insertion into Pd(II) Complexes, *J. Am. Chem. Soc.*, 1981, **103**, 5115-5125.

14. P. Braunstein, D. Matt and D. Nobel, Reactions of Carbon Dioxide with Carbon Carbon Bond Formation Catalyzed by Transition-Metal Complexes, *Chem. Rev.*, 1988, **88**, 747-764.

15. P. Braunstein, D. Matt and D. Nobel, Carbon Dioxide Activation and Catalytic Lactone Synthesis by Telomerization of Butadiene and CO_2, *J. Am. Chem. Soc.*, 1988, **110**, 3207-3212.

16. M. Sharif, R. Jackstell, S. Dastgir, B. Al-Shihi and M. Beller, Efficient and selective Palladium-catalyzed Telomerization of 1,3-Butadiene with Carbon Dioxide, *ChemCatChem*, 2017, **9**, 542-546.

17. R. Nakano, S. Ito and K. Nozaki, Copolymerization of carbon dioxide and butadiene via a lactone intermediate, *Nat. Chem.*, 2014, **6**, 325-331.

18. S. Huang, B. Yan, S. Wang and X. Ma, Recent advances in dialkyl carbonates synthesis and applications, *Chem. Soc. Rev.*, 2015, **44**, 3079-3116.

19. P. Braunstein, M. Lakkis and D. Matt, Synthesis of Anisole by Lewis Acid-Catalyzed Decarboxylation of Methyl Phenyl Carbonate, *J. Mol. Catal.*, 1987, **42**, 353-355.

20. W. Keim, Oligomerization of Ethylene to α-Olefins: Discovery and Development of the Shell Higher Olefin Process (SHOP), *Angew. Chem. Int. Ed.*, 2013, **52**, 12492-12496.

21. P. Braunstein, Y. Chauvin, S. Mercier, L. Saussine, A. DeCian and J. Fischer, Intramolecular O-H⋯O-Ni and N-H⋯O-Ni Hydrogen-Bonding in Nickel Diphenylphosphinoenolate Phenyl Complexes: Role in Catalytic Ethene Oligomerization. Crystal-Structure of [NiPh{Ph_2PCH⋯C(⋯O)(*o*-C_6H_4NHPh))(PPh_3)], *J. Chem. Soc., Chem. Commun.*, 1994, 2203-2204.

22. P. Braunstein, Y. Chauvin, S. Mercier and L. Saussine, Influence of intramolecular N-H⋯O-Ni hydrogen bonding in nickel(II) diphenylphosphinoenolate phenyl complexes on the catalytic oligomerization of ethylene, *C. R. Chimie*, 2005, **8**, 31-38.

23. P. Braunstein, F. Naud and S. J. Rettig, A new class of anionic phosphinooxazoline ligands in palladium and ruthenium complexes: catalytic properties for the transfer hydrogenation of acetophenone, *New J. Chem.*, 2001, **25**, 32-39.

24. P. Braunstein, Y. Chauvin, J. Nähring, A. DeCian, J. Fischer, A. Tiripicchio and F. Ugozzoli, Rhodium(I) and iridium(I) complexes with ß-keto phosphine or phosphino enolate ligands. Catalytic transfer dehydrogenation of cyclooctane, *Organometallics*, 1996, **15**, 5551-5567.

25. C. Fliedel and P. Braunstein, Recent advances in S-functionalized N-heterocyclic carbene ligands: From the synthesis of azolium salts and metal complexes to applications, *J. Organomet. Chem.*, 2014, **751**, 286-300.

26. F. He, A. A. Danopoulos and P. Braunstein, Trifunctional pNHC, Imine, Pyridine Pincer-Type Iridium(III) Complexes: Synthetic, Structural, and Reactivity Studies, *Organometallics*, 2016, **35**, 198-206.

27. T. Simler, P. Braunstein and A. A. Danopoulos, Cobalt PNC^{NHC} 'Pincers': Ligand Dearomatisation, Formation of Dinuclear and N_2 Complexes and Promotion of C-H Activation, *Chem. Commun.*, 2016, **52**, 2717-2720.

28. V. Charra, P. de Frémont and P. Braunstein, Multidentate N-Heterocyclic Carbene Complexes of the 3d Metals: Synthesis, Structure, Reactivity and Catalysis, *Coord. Chem. Rev.*, 2017, **341**, 53-176.

29. S. Hameury, P. de Frémont and P. Braunstein, Metal Complexes with Oxygen-Functionalized NHC Ligands: Synthesis and Applications, *Chem. Soc. Rev.*, 2017, **46**, 632-733.

30. P. Ai, K. Yu. Monakhov, J. van Leusen, P. Kögerler, C. Gourlaouen, M. Tromp, R. Welter, A. A. Danopoulos and P. Braunstein, Linear $Cu^{I}_2Pd^0$, $Cu^{I}Pd^0_2$, and $Ag^{I}_2Pd^0$ Metal Chains Supported by Rigid N,N′-Diphosphanyl N-Heterocyclic Carbene Ligands and Metallophilic Interactions, *Chem. Eur. J.*, 2018, **24**, 8697-8697.

31. T. Simler, S. Choua, A. A. Danopoulos and P. Braunstein, Reactivity of a Dearomatised Pincer $Co^{II}Br$ Complex with PNC^{NHC} Donors: Alkylation and Si-H Bond Activation via Metal-Ligand Cooperation, *Dalton Trans.*, 2018, **47**, 7888-7895.

32. A. A. Danopoulos, A. Massard, G. Frison and P. Braunstein, Iron and Cobalt Metallotropism in Remote-Substituted NHC Ligands: Metalation to Abnormal NHC Complexes or NHC Ring Opening, *Angew. Chem. Int. Ed.*, 2018, **57**, 14550-14554.

33. A. A. Danopoulos, T. Simler and P. Braunstein, N-Heterocyclic Carbene Complexes of Copper, Nickel, and Cobalt, *Chem. Rev.*, 2019, **119**, 3730-3961.

34. K. J. Evans and S. M. Mansell, Functionalised N-Heterocyclic Carbene Ligands in Bimetallic Architectures, *Chem. Eur. J.*, 2020, **26**, in press.

35. P. Braunstein, L. A. Oro and P. R. Raithby, *Metal Clusters in Chemistry*, Wiley-VCH, Weinheim, 1999.

36. S. Sculfort and P. Braunstein, Intramolecular d^{10}-d^{10} interactions in heterometallic clusters of the transition metals, *Chem. Soc. Rev.*, 2011, **40**, 2741-2760.

37. P. Buchwalter, J. Rosé and P. Braunstein, Multimetallic Catalysis Based on Heterometallic Complexes and Clusters, *Chem. Rev.*, 2015, **115**, 28-126.

38. S. Zhou, X. Sun, L. Yue, M. Schlangen and H. Schwarz, Tuning the Reactivities of the Heteronuclear $[Al_nV_{3-n}O_{7-n}]^+$ (n = 1, 2) Cluster Oxides towards Methane by Varying the Composition of the Metal Centers, *Chem. Eur. J.*, 2019, **25**, 2967-2971.

39. P. Braunstein, R. Bender and J. Kervennal, Selective Carbonylation of Nitrobenzene over a Mixed Pd-Mo Cluster Derived Catalyst, *Organometallics*, 1982, **1**, 1236-1238.

40. P. Braunstein, J. Kervennal and J. L. Richert, Reductive Carbonylation of Ortho-Nitrophenol with a Fe-Pd Cluster-Derived Heterogeneous Catalyst; CO Migration in $[FePdPt(CO)_4(Ph_2PCH_2PPh_2)_2]$, *Angew. Chem. Int. Ed. Engl.*, 1985, **24**, 768-770.

41. P. Braunstein, R. Devenish, P. Gallezot, B. T. Heaton, C. J. Humphreys, J. Kervennal, S. Mulley and M. Ries, Silica-Supported Fe-Pd Bimetallic Particles: Formation from Mixed-Metal Clusters and Catalytic Activity, *Angew. Chem. Int. Ed. Engl.*, 1988, **27**, 927-929.

42. C. Fliedel, A. Ghisolfi and P. Braunstein, Functional Short-Bite Ligands: Synthesis, Coordination Chemistry, and Applications of N-Functionalized Bis(diaryl/dialkylphosphino)amine-type Ligands, *Chem. Rev.*, 2016, **116**, 9237-9304.

43. I. Bachert, P. Braunstein and R. Hasselbring, Alkoxysilyl-functionalized mixed-metal carbonyl clusters, *New J. Chem.*, 1996, **20**, 993-995.

44. P. Braunstein, H.-P. Kormann, W. Meyer-Zaika, R. Pugin and G. Schmid, Strategies for the anchoring of metal complexes, clusters, and colloids inside nanoporous alumina membranes, *Chem. Eur. J.*, 2000, **6**, 4637-4646.

45. F. Schweyer-Tihay, P. Braunstein, C. Estournès, J. L. Guille, B. Lebeau, J. L. Paillaud, M. Richard-Plouet and J. Rosé, Synthesis and characterization of supported Co_2P nanoparticles by grafting of molecular clusters into mesoporous silica matrixes, *Chem. Mater.*, 2003, **15**, 57-62.

46. P. Buchwalter, J. Rosé, B. Lebeau, O. Ersen, M. Girleanu, P. Rabu, P. Braunstein and J.-L. Paillaud, Characterization of cobalt phosphide nanoparticles derived from molecular clusters in mesoporous silica, *J. Nanopart. Res.*, 2013, **15**, 2132.

47. F. Schweyer, P. Braunstein, C. Estournès, J. Guille, H. Kessler, J.-L. Paillaud and J. Rosé, Metallic nanoparticles from heterometallic Co-Ru carbonyl clusters in mesoporous silica xerogels and MCM-41-type materials, *Chem. Commun.*, 2000, 1271-1272.

48. F. Schweyer-Tihay, C. Estournès, P. Braunstein, J. Guille, J. L. Paillaud, M. Richard-Plouet and J. Rosé, On the nature of metallic nanoparticles obtained from molecular Co_3Ru-carbonyl clusters in mesoporous silica matrices, *PCCP*, 2006, **8**, 4018-4028.

49. S. Grosshans-Vielès, P. Croizat, J. L. Paillaud, P. Braunstein, O. Ersen, J. Rosé, B. Lebeau, P. Rabu and C. Estournès, Molecular clusters in mesoporous materials as precursors to nanoparticles of a new lacunar ternary compound Pd_xMo_yP, *J. Cluster Sci.*, 2008, **19**, 73-88.

FROM A 175 YEAR OLD RUTHENIUM TO ITS EMPIRE ON GREEN CATALYSIS AND SUSTAINABLE CHEMISTRY

Pierre H. Dixneuf

Institut des Sciences Chimiques, UMR 6226 CNRS-Université de Rennes, campus de Beaulieu 35042 Rennes, France, Pierre.dixneuf@univ-rennes1.fr

Pierre H. Dixneuf after his doctorate es Sciences with Prof René Dabard on ferrocene chemistry did a post-doctorate research with Prof. Michael F. Lappert in Brighton UK on the initial steps of N-Heterocyclic Carbene-Metal complexes. Professor at the University of Rennes since 1978 his research interests included bimetallic systems and organometallic chemistry toward carbon rich complexes and in 1985 he initiated the Rennes center for Homogeneous Catalysis. He developed catalytic processes promoted with ruthenium catalysts for the transformations of alkynes and incorporation of CO_2, ruthenium-vinylidenes and -allenylidenes in catalysis, enantioselective catalysis to amines, alkene metathesis catalysts from Ru(II)allenylidenes and for transformation of plant oils. He is now contributing since 2007 to C–H bond activation/functionalization using Ru(II) catalysts especially operating in water and to the catalytic Cu(I) catalyzed sp^3C-H bond functionalization.

He has co-authored 470 publications and reviews, co-edited 7 books, received several international prizes : A. v Humboldt prize for Research 1990, Le Bel SFC award and Grignard-Wittig Prize (GDCh) in 2000, Institut universitaire de France membership in 2000, French Académie des Sciences IFP prize and Sacconi medal (Italy) in 2006, Spanish and Chinese Society of Chemistry awards in 2014, election as a member of the European Academy of Sciences in 2016 and of the Portugal Academy of Sciences in 2017. Former CNRS deputy Director of chemistry in Paris (1996-1999), he is currently a Research Professor at the University of Rennes, France, where he founded the CNRS-UR1 research Institut de chimie de Rennes in 2000 and was university vice-president for research (2001-2004).

Platinum metal complexes, derivatives of Ru, Os, Rh, Ir, Pd, Pt metals, have been revealed as efficient catalysts to perform combinations of simple molecules to produce useful compounds with low waste and via green processes for sustainable development [1]. The Ruthenium element was the last Platinum group metals to be discovered in 1844 by Karl Klaus from platinum ore residue [2]. The ruthenium salts were later easily transformed into a variety of simple ruthenium(II) and Ru(0) complexes which showed efficiency as catalysts for several simple reactions and it was preferably used as the less expensive of the platinum group metals [3].

During the last 2 decades more sophisticated ruthenium complexes were designed in attempts to perform reactions of interest for industry. Now more efforts are made to contribute to clean processes and green catalysis and the transformations of renewables by molecular ruthenium catalysts attract innovations for the development of sustainable chemistry [3].

Several useful catalytic reactions discovered in Rennes with Ru(II) and Rh(I) catalysts have contributed to Green and Sustainable Chemistry such as the alkene metathesis applied to the natural products terpenes, the synthesis of linear aminoacids precursors of polyamides, the sp^2 C-H bond functionalisation of (hetero)arenes with Ru(II) and of biphenylphosphines with Rh(I) catalysts.

Ruthenium catalyzed Alkene metathesis and terpenes transformations

Almost three decades ago it was shown by R. H. Grubbs that alkylidene-ruthenium catalysts could perform efficiently the alkene metathesis reaction, the exchange of carbon groups on olefin double C=C bond, under mild conditions to lead to many useful transformations, even to produce ROMP polymers. This discovery contributed for one part for the Nobel Prize shared in 2005 by Chauvin, Grubbs and Schrock for their contributions to catalyzed alkene metathesis reactions. This discovery led chemists to design more efficient $Ru=CR_2$ catalysts to apply them for new transformations of olefins.

Strong efforts have been done to transform natural products such as terpenes via alkene metathesis with alkylidene-ruthenium catalysts [4,5]. By cross metathesis C. Bruneau has succesfully transformed a variety of terpenes that are natural products often used as natural fragrances or in cosmetics. He has shown that by selecting alkylidene-ruthenium catalysts of type $RuCl_2(=CH(o\text{-}C_6H_4OiPr))$(NHCarbene) the cross metathesis of terpenes such as citronellal or citronellol took place with acrylate and methacrylate with high stereoselectivity (Scheme 1) [6].

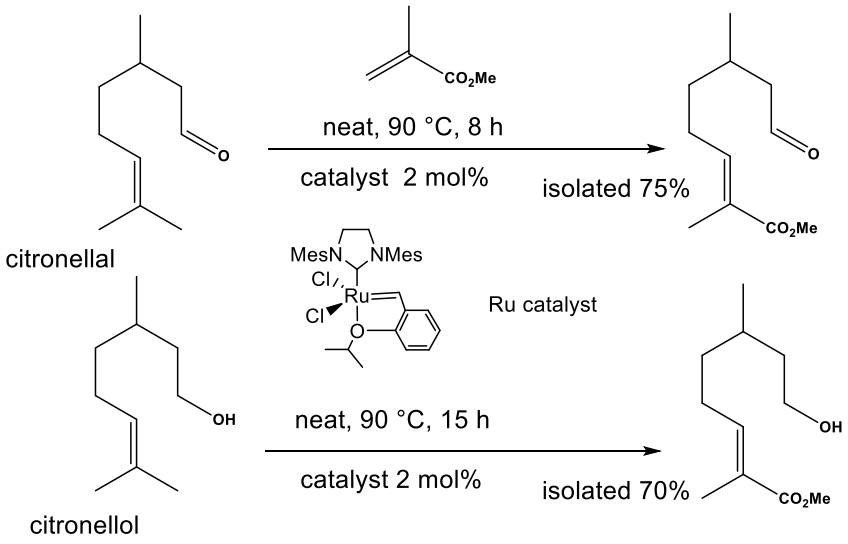

Scheme 1. Ruthenium-alkylidene catalyzed stereoselective alkene metathesis of terpenes

This was a contribution to green chemistry as the reaction can be performed without solvent with methacrylate but also in non toxic dialkycarbonate and it involves only one step whereas to reach the same products before three steps for oxidation of one methyl and esterification were required. Functionalization of (-)-β-pinene and (-)-limonene *via* cross metathesis with symmetrical internal olefins can also be achieved using the same type of catalysts [7].

Ruthenium catalyzed Alkene metathesis and linear aminoacids synthesis

Polyamides and copolyamides are well known industrial precursors for a variety of materials resistant to chemicals or heat and for cloth fibers or sport equipments. It was thus attractive to prepare such linear polyamides precursors from renewable materials. Thus efforts were made in Rennes in cooperation with Arkema company to prepare linear aminoacids by cross metathesis of plant oil unsaturated esters derivatives with acrylonitrile or of methyl acrylate with long chain unsaturated nitrile (Scheme 2) [8].

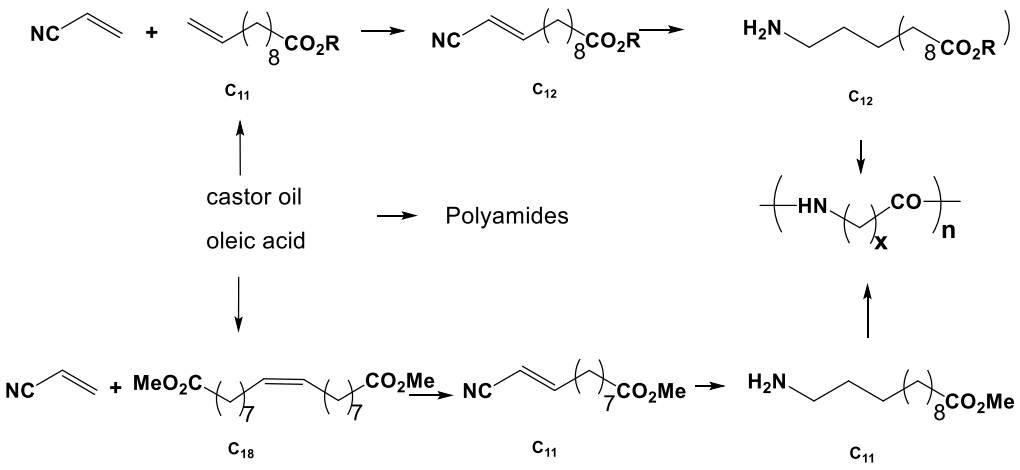

Scheme 2. Principle of plant oils derivatives as precursors of polyamides via cross metathesis.

Cross metathesis of acrylonitrile and C11 unsaturated ester with the Hoveyda II catalyst $RuCl_2(=CH(o\text{-}C_6H_4OiPr))(NHCarbene)$ containing a saturated NHC carbene proceeds easily at 100°C with a TON of 3000. (Scheme 3). Just after cross metathesis the products of the reaction are transfered to an autoclave and under 20 bar of hydrogen in the presence of a base the ruthenium residue arising from the Hoveyda catalyst efficiently allows the hydrogenation of both the C=C and CN bonds to produce the linear aminoacid [9].

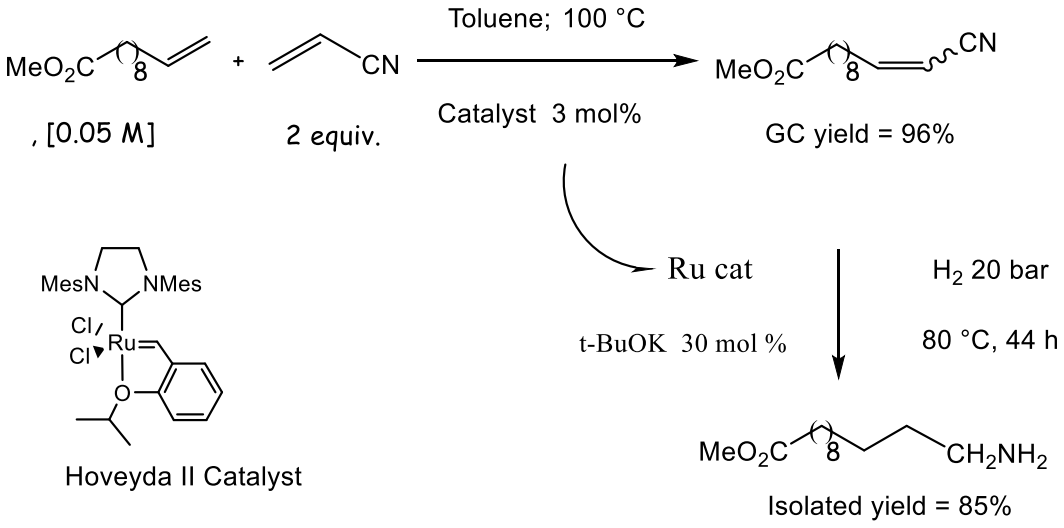

Scheme 3. Synthesis of linear saturated amino-ester by tandem Cross Metathesis/Hydrogenation

A better approach could be found with the cross metathesis of methyl acrylate with 10-undecenenitrile readily obtained by amination of the corresponding unsaturated carboxylic acid arising from plant oil. The same ruthenium catalyst offered a better efficiency of the cross metathesis with a TON of 17200, showing that the position of the

nitrile close to the double bond disfavors the reaction when acrylonitrile is used (TON 3000 only) (Scheme 4) [10].

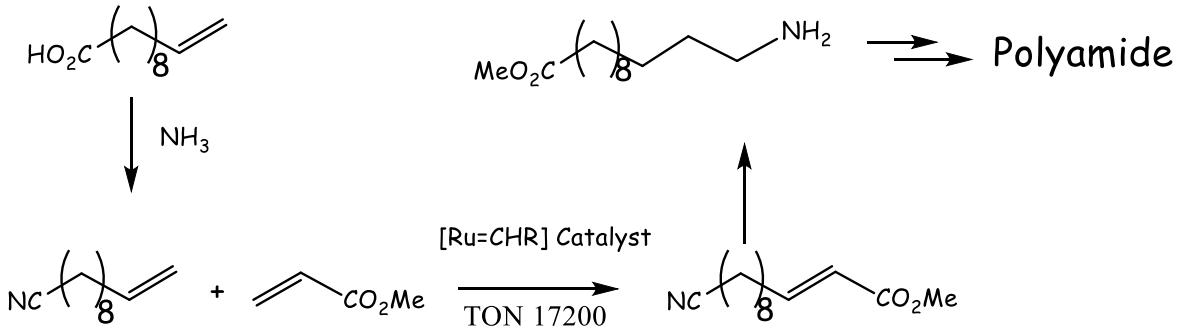

Scheme 4. Synthesis of linear saturated amino-ester from 10-undecenenitrile and methyl acrylate

Ruthenium(II) catalyzed (hetero)arene sp^2 C-H bond activation

One of the most important reactions for the construction of useful molecules for pharmacy and even molecular materials is based on the catalytic C_1-C_2 cross-coupling reaction between a simple organometallic RMgX, RLi, RZnX, $ArB(OH)_2$, $RSnX_3$, $RSiX_3$, etc with an arylhalide mostly catalyzed with Ni(0) or Pd(0) catalysts and known as the Tamao-Kumada, Negishi, Miyaura-Suzuki, Stille and Hiyama reactions. Their usefulness has led the nobel prize of chemistry 2010 to be awarded to Negishi, Heck and Suzuki. Since two decades there is a strong motivation among synthesis promoters to build the same C_1-C_2 bond directly form a C_1-H and (aryl)C_2-Br bonds. However the sp^2 C-H bond is very stable and new ways to functionalize it had to be found.

We have thus considered to use ruthenium(II) catalysts to favour the C-H bond deprotonation as a way to make an activated C-Ru(II) bond [11]. We have shown that ruthenium(II) catalysts associated to a carboxylate partner are able to promote the regioselective sp^2 C-H bond activation of functional arenes and heterocycles to selectively lead to cross-couplings with hetero(aryl) halides. F. Pozgan showed that phenyl pyridine with Ru(II) catalyst are ortho arylated in the presence of aryl chlorides but with 2 equiv. of KOAc per Ru(II) site, whereas the presence of a phosphine or a NHCarbene ligand has not a strong influence, which supported the initial deprotonation. He could prepared a variety of di(hetero)arylated compounds or tridentate heterocycles [12]. A. Jutand studied the kinetic of this reaction at 27°C and found that the first product

to be formed is the cyclometalated intermediate **A** resulting from ortho C-H bond deprotonation by KOAc via an autocatalytic process (Scheme 5). This initial deprotonation is an easy process with respect to the following oxidative addition of arylhalide which requires more energy [13].

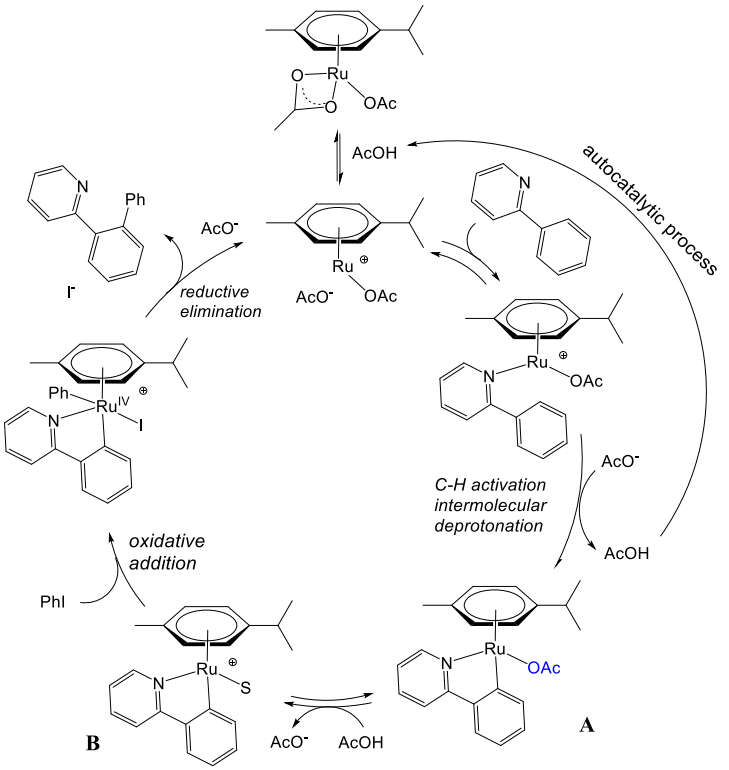

Scheme 5. Kinetic study of Ru(II) catalyzed ortho functionalization of arene C-H bond

This mechanism via C-H bond deprotonation can also be operative in water as most ruthenium(II) catalysts are stable in water. It is possible now to perform such processes in a greener way: in water as renewable solvent without surfactant and with higher catalyst activity. Many C-H bond functionalizations take place in water but in the presence of pivalate and K_2CO_3 with arylchorides which are more soluble in water [14]. C-H bond functionalization in water can take place even directed by imines to produce tridentate ligands [15].

The trispyridine benzene only could be easily prepared in NMP solvent at 150°C from phenyl pyridine by F. Pozgan using a $LnRu(OAc)_2$ catalyst (Scheme 6) [12] but only

recently he succeeded to reach the synthesis of hexapyridylbenzene with Ru(II)/KOPiv/PPh_3 catalyst in water but under microwave irradiation (Scheme 6) [16]. Catalytic sp^2 C-H bond activation/functionalization in water can be directed to produce a variety of Hexaheteroarylbenzenes, as potential ligands for photocatalysis.

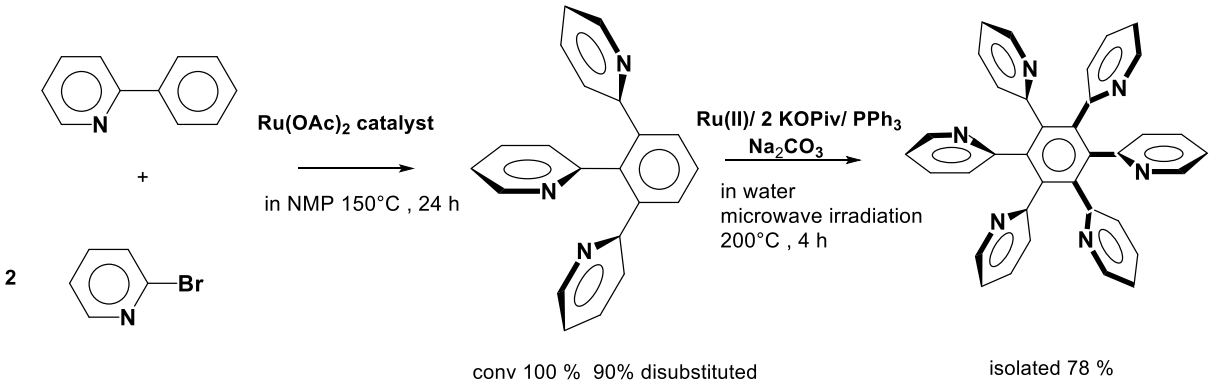

Scheme 6. Ru(II) catalyzed polyheteroarylation of phenyl pyridine

Ruthenium(II) catalyzed phosphine oxide sp^2 C-H bond functionalization

The nature of the ligands linked to a metal center is crucial to reach efficiency of the related catalyst. Thus it is a challenge to quickly modify the ligands to reach better catalyst activity. Phosphine ligands have been shown to be very useful in metal complexes however the functionalization of aryl phosphine is inhibited by the difficulty to produce a 4-membered cyclometalate by deprotonation of ortho C-H bonds with formation of M-C bond. By contrast their phosphorous oxides should allow the formation of 5-membered cyclometalate more easily. Indeed we have shown that ruthenium(II) catalysts are able to assist the deprotonation of the ortho C-H bond of phosphine oxides and in the presence of a functional alkene its C=C bond can insert into the metallacycle Ru-C(ortho) bond and an alkyl group is generated on protonation (Scheme 7) [17]. Thus we have produced alkylation of a variety of phosphine oxides at ortho position of the phosphorous. We were able to show that the ruthenium(II) is maintained and that the use of an oxidant such as Cu(II) is not required. This approach allows the synthesis of phosphines with a pendant functional group attached at the ortho carbon atom. It has the potential to easily modify chiral diphosphines currently used for enantioselective catalysis.

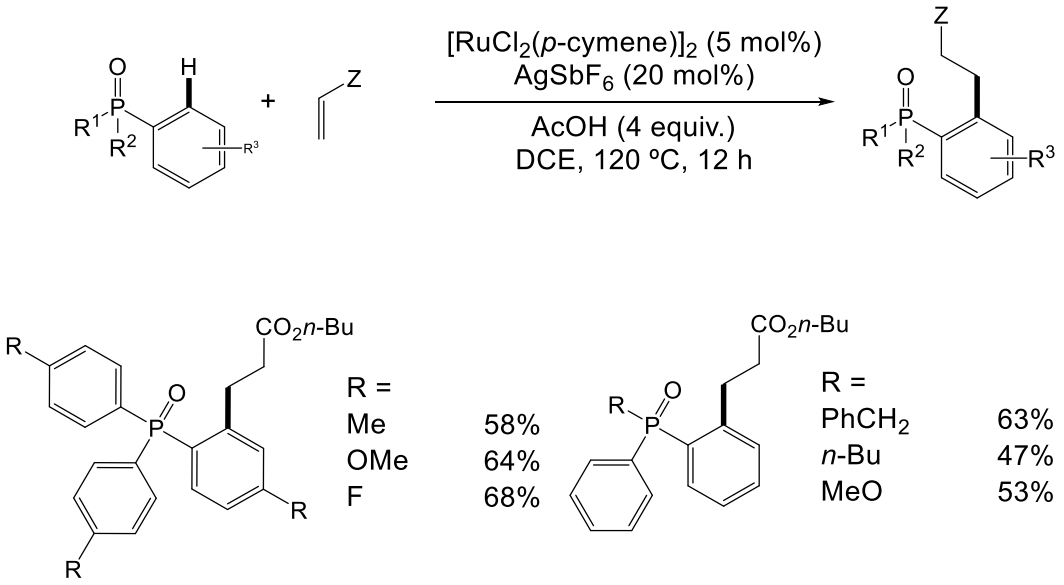

Scheme 7. Ru(II) catalyzed alkylation of ortho C-H bonds of phosphine oxide aryl groups

Rhodium(I) catalyzed sp^2C-H bond functionalization at *ortho'* position of biphenylphosphines

Rhodium(I) catalysts by contrast can alkylate the *ortho'* biaryl C-H bonds of biaryl phosphines by formal insertion of alkene C=C bond into biaryl ortho' C-H bonds to produce functional alkylated and dialkylated phosphines, whereas the Ru(II) catalysts are mostly inert for this regioselective functionalization (Scheme 8) [18]. Thus the diphenyl phosphines Johnphos containing PCy_2 or PPh_2 groups, with acrylate and 2 mol% of $Rh(OAc)(COD)_2$ catalyst in acidic media (PivOH) in toluene can give regioselectively the ortho' alkylated phosphines in good yields. It is noteworthy that alkylation can take place with acrylate containing the chiral *L*-Menthol or with eicosyl acrylate leading respectively to optically active phosphine and to phosphine containing the long alkyl chain $CH_2CH_2CO_2(CH_2)_{19}CH_3$.

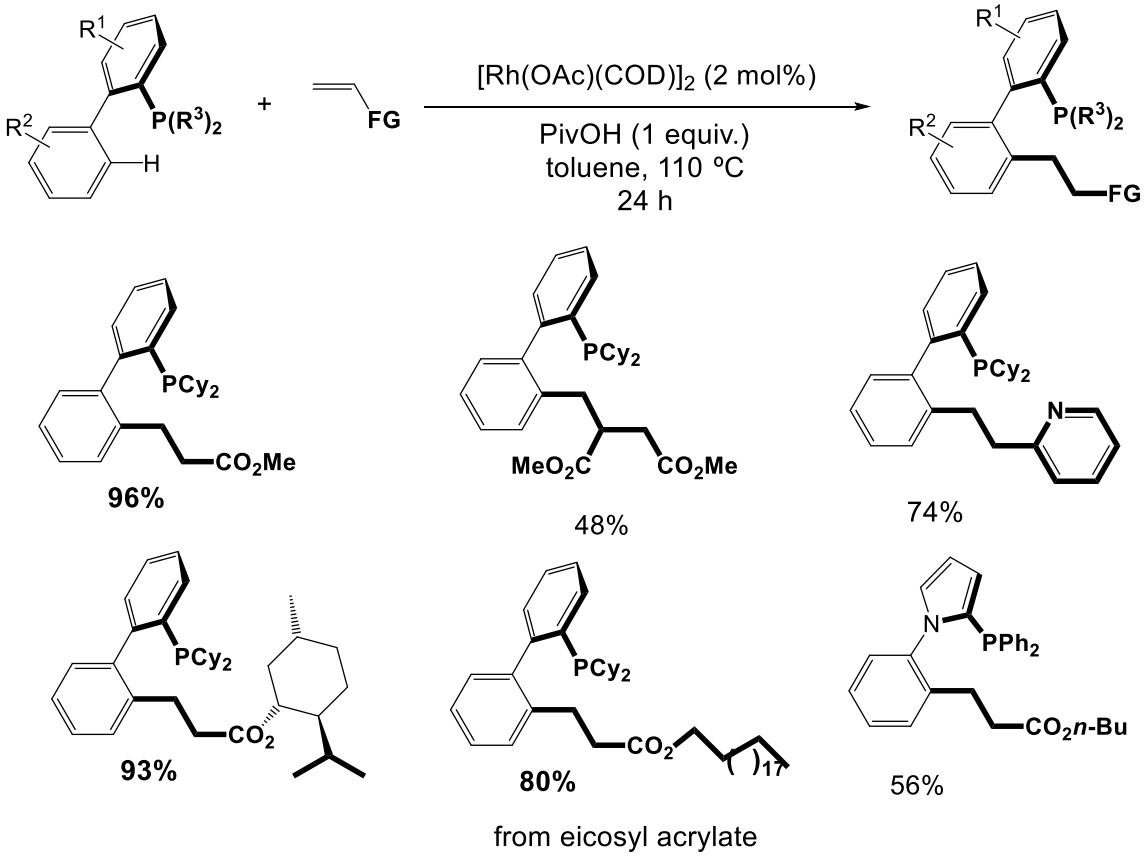

Scheme 8. Rh(I) catalyzed alkylation of ortho' C-H bonds of biaryl phosphines

These JohnPhos type phosphines can thus be dialkylated at both ortho' C-H diaryl group either with identical or with two different functional alkyl groups.

The mechanism for this *ortho'* C-H bond alkylation was proposed to occur as shown on Scheme 9 [18]. As the reaction takes place under deprotonation conditions a first cyclometalate **C** is formed with the help of the pivalate. Then the insertion of the acrylate into the *ortho'*C-Rh bond leads to intermediate **D** which on protonation with PivOH leads to the alkylated phosphine and the Rh(I) catalyst.

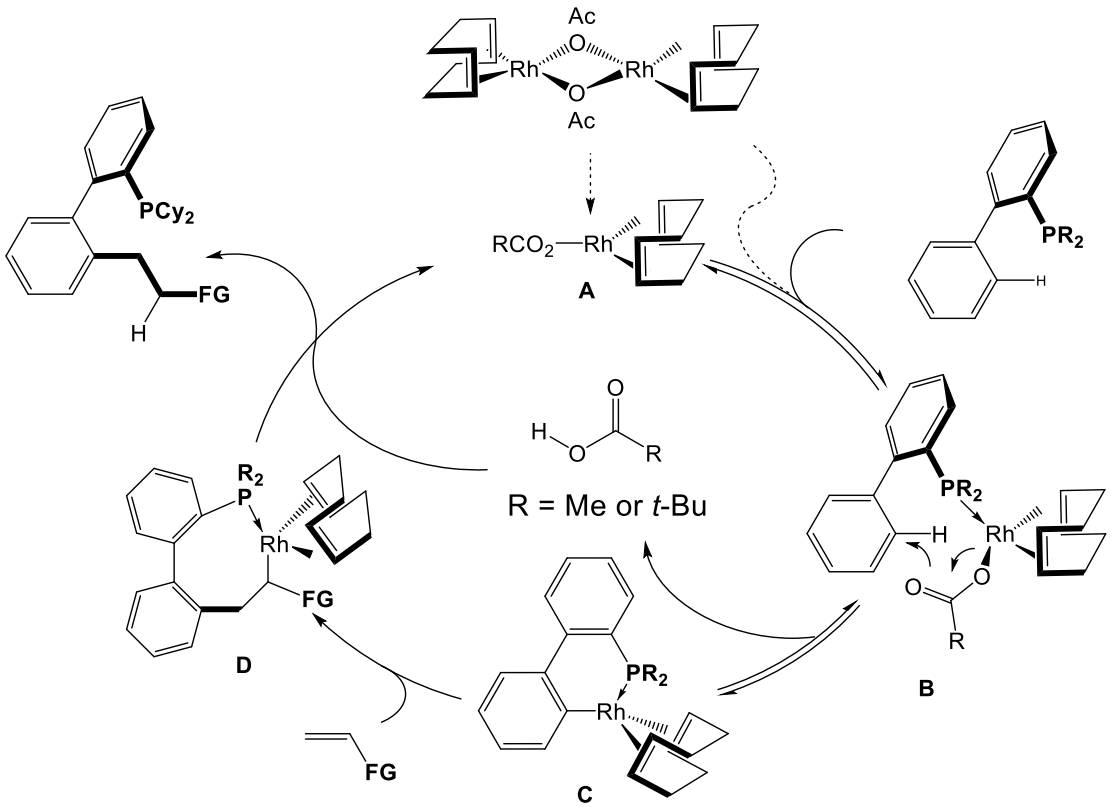

Scheme 9. Mechanism of Rh(I) catalyzed alkylation of ortho' C-H bonds of biaryl phosphines

The advantage of fast modification of JohnPhos phosphine ligand was demonstrated by the use of the just prepared bifunctional dialkylated Phosphine **L_1** which offers the efficient carboxylation of arylbromides with CO_2 with the help of a Pd catalyst and a photoredox system as previously shown by R. Martin and N. Iwasawa [19]. The use of long chain containing phosphine L_1 with $Pd(OAc)_2$ allows the direct access to a variety of (hetero)aryl carboxylic acids in better yields without the use of carbonate according to Scheme 10 [18].

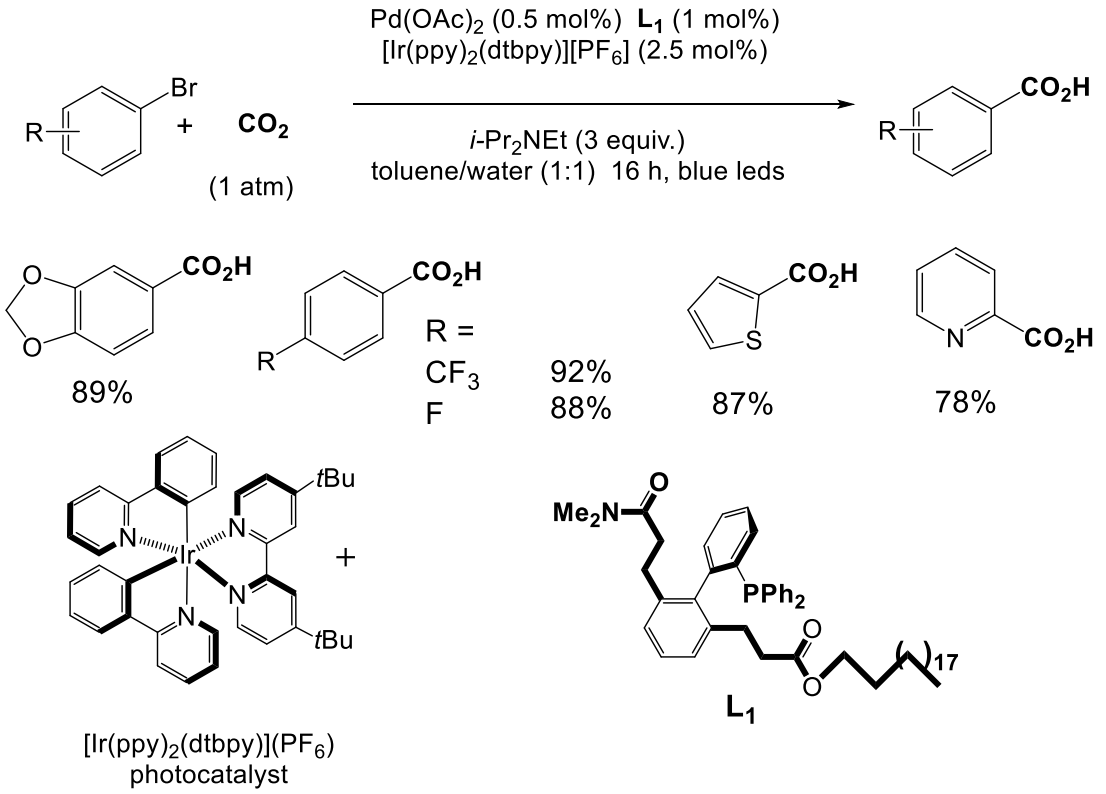

Scheme 10. Carboxylation of arylbromides with CO_2 and $Pd(OAc)_2$ catalyst with long chain phosphine.

The reaction involves first the insertion of CO_2 into the formed XPd-Ar bond to give the carboxylate XPd-OCOAr and then 2 electrons are brought successively by the reduced photocatalyst. Under blue light irradiation the excited Ir(III) photocatalyst is reduced by the NR_3 amine and twice the resulting Ir(II) species allows an electron transfer to the XPd-OCOAr moiety to generate the carboxylate and the Pd(0) catalyst [20]. .

Conclusion

Besides its contribution to alkene metathesis applied to renewable materials,ruthenium(II) catalysts have demonstrated a high efficiency to promote the C-H bond functionalizations of previously inert C-H bonds. The cleavage of C-H bond via deprotonation process requires very mild conditions, and takes place even in water without surfactants. However Ruthenium(II) systems are not able to regioselectively activate some C-H bonds and then especially the rhodium(I) catalyst can contribute to directly functionalize phosphines providing unexpected activity on association to the suitable metal complexes. All the catalytic reactions presented here from renewables

transformations or by direct cross coupling C-C bond formation from C-H bonds contribute to the development of green and sustainable chemistry,

References

[1] P. H. Dixneuf, J. F. Soulé Eds., "Organometallics for Green Catalysis ", *Topics in Organometallic Chemistry*, Springer, volume 63, **2019.** ISSN 1436-6002 ISSN 1616-8534;

doi.org/10.1007/978-3-030-10955-4.

[2] D. E. Lewis, The Minor Impurity in Spent Ores of the "Siberian Metal": Ruthenium Turns 175 *Chem. Eur. J.* **2019**, 25, 11394–11401.

[3] C. Bruneau and P. H. Dixneuf Eds , Ruthenium in Catalysis. *Topics in Organometallic Chemistry series*, Springer, **2014**, DOI 10.1007/978-3-319-08482-4;ISBN978-3-319-08482-4.
[4] C. Bruneau, C. Fischmeister, D. Mandelli, W. A. Carvalho, E. N. dos Santos, P. H. Dixneuf, L. Sarmento Fernandes. Transformations of terpenes and terpenoids *via* carbon-carbon double bond metathesis. *Catal. Sci. Technol.* **2018**, *8*, 3989-4004.

[5] E. Borré, T. H. Dinh, F. Caijo, C. Crévisy and M. Mauduit. Terpenic Compounds as Renewable Sources of Raw Materials for Cross-Metathesis, *Synthesis*, **2011**, *13*, 2125-2130.

[6] H. Bilel, N. Hamdi, F. Zagrouba, C. Fischmeister, C.Bruneau, Cross-metathesis transformations of terpenoids in dialkyl carbonate solvent *Green Chem.* **2011**, *13*, 1448-1452.

[7] L. Sarmento Fernandes, D. Mandelli, W. A. Carvalho, C. Fischmeister, C. Bruneau,

Functionalization of (-)-β-pinene and (-)-limonene *via* cross metathesis with symmetrical internal olefins. *Catal. Commun.* **2020**, *135*, 105893.

[8] P. H. Dixneuf , C. Bruneau, C. Fischmeister. Alkene metathesis catalysis: a key for transformations of unsaturated plant oils and renewable derivatives. *Oil & Gas Sci. Technol.– Rev.* IFP Energies nouvelles **2016,** *71*, 19. DOI: 10.2516/ogst/2015033.

[9] X. Miao, C. Fischmeister, C. Bruneau, P. H. Dixneuf, J.-L. Dubois and J.-L. Couturier. Tandem catalytic acrylonitrile cross-metathesis and hydrogenation of nitriles with ruthenium catalysts: direct access to linear alpha, omega-aminoesters from renewables. *ChemSusChem*, **2012**, 5, 1410 – 1414.

[10] X. Miao, C. Fischmeister, P. H. Dixneuf, C. Bruneau, J.-L. Dubois and J.-L. Couturier. Polyamide precursors from renewable 10-undecenenitrile and methyl acrylate via olefin cross-metathesis. *Green Chem.*, **2012**, *14*, 2179–2183.

[11] P. B. Arockiam, C. Bruneau, P. H. Dixneuf, Ruthenium(II) Catalyzed C-H Bond Activation and Functionalization; *Chem. Rev.* **2012,** *112*, 5879.

[12] F. Pozgan, P. H. Dixneuf Ruthenium(II) Acetate Catalyst for Direct Functionalisation of sp^2-CH Bonds with Aryl Chlorides and Access to Tris- Heterocyclic Molecules, Adv. Synth. Catal. **2009**, 351, 1737- 1743

[13] E. Ferrer Flegeau, C. Bruneau, P. H. Dixneuf, A. Jutand, Autocatalysis for C-H Bond Activation by Ruthenium(II) Complexes in Catalytic Arylation of Functional Arenes *J. Am. Chem. Soc.* **2011,** *133*, 10161- 10170.

[14] P. B. Arockiam, C. Fischmeister, C. Bruneau, P. H. Dixneuf C-H Bond Functionalization in Water Catalyzed by Carboxylato-Ruthenium(II) Systems. *Angew. Chem. Int. Ed.* **2010**, *49*, 6629 –6632.

[15] Bin . Li , P. H. Dixneuf, sp^2C-H Bond activation in water and catalytic cross-coupling reactions. *Chem. Soc. Rev.* **2013**, ***42*, 5744.**

[16] M. Drev, U. Groselj, B. Ledinek, F. Perdih, J. Svete, B. Stefane, F. Pozgan. Ruthenium(II)-Catalyzed Microwave-Promoted Multiple C−H Activation in Synthesis of Hexa(heteroaryl)benzenes in Water. *Org. Lett.* **2018,** *20,* 5268.

[17] C. S. Wang, P. H. Dixneuf, J. F. Soulé, Ruthenium-Catalyzed C-H Bond Alkylation of Arylphosphine Oxides with Alkenes: A Straightforward Access to Bifunctional Phosphorous Ligands with a Pendent Carboxylate *ChemCatChem,* **2017**, *9*, 3117-3120.

[18] Z. Zhang, T. Roisnel, P. H. Dixneuf, J. F. Soulé. Rh(I)-Catalyzed P(III)-Directed C–H Bond Alkylation: Design of Multifunctional Phosphines for Carboxylation of Aryl Bromides with Carbon Dioxide. *Angew. Chem. Int. Ed.* **2019,** *58*, 14110–14114.

[19] K. Shimomaki, K. Murata, R. Martin, N. Iwasawa, Visible-Light-Driven Carboxylation of Aryl Halides by the Combined Use of Palladium and Photoredox Catalysts. *J. Am. Chem. Soc.* **2017**, *139*, 9467-9470.

[20] C. S. Wang, P. H. Dixneuf, J. F. Soulé, Photoredox Catalysis for Building C−C Bonds from C(sp^2)-H Bonds. *Chem. Rev.* **2018,** *118,* 7532-7585.

MECHANISTIC STUDIES ON RHODIUM AND IRIDIUM HOMOGENEOUS CATALYSTS

Luis A. Oro

Departamento de Química Inorgánica, Instituto de Síntesis Química y Catálisis Homogénea, Universidad de Zaragoza-CSIC, 50010-Zaragoza, España

Luis A. Oro obtained his Ph. D. from the University of Zaragoza in 1970. He was postdoctoral fellow at Cambridge University from 1972 to 1973. He has served on the faculties of the Universities of Zaragoza, Madrid Complutense, and Santander. He became full professor of Inorganic Chemistry in Zaragoza in 1982 and served as head and founder of the Homogeneous Catalysis Institute (2004-2013).

His main research interests are in organometallic chemistry and homogeneous catalysis of platinum group metals. He has co-authored well over 650 scientific papers and several books. His research has been recognized with numerous awards including Humboldt Forschungspreise, Sacconi Medal, National Research Prize for Chemistry, Lourenço-Madinaveitia Award, Lord Lewis Prize from the Royal Society of Chemistry and Honoris Causa Doctorates from the Universities of Rennes, Rovira i Virgili, San Jorge and Madrid Complutense.

He has been President of the European Chemical Society (EuChemS) (2008-11). He has also served in high-level positions in the Spanish public administration with responsibilities for science, as well as being vice-president of the European Science Foundation.

The catalysis field began in the nineteenth century with the work on heterogeneous platinum group metals. This background influences the first homogeneous platinum metal catalysts, where rhodium and iridium have been key elements on the understanding of homogeneous catalysts.[1-2]

Precise determination of the mechanism of a catalytic process is essential in order to control the selectivity outcome. In particular, we have studied the mechanism and activity of a set of rhodium and iridium complexes with N-heterocyclic carbene (NHC) ligands in some specific homogeneous reactions. The high steric hindrance and powerful electron-donor capacity of the bulky NHC´s used, along with ancillary N-donor ligands, seems to be determinant to get selective transformations and to facilitate useful information about the reaction mechanisms.[3]

H/D exchange reactions are valuable transformations for the preparation of isotopically labelled compounds that have found practical applications on mechanistic investigations, spectroscopic analysis, or the monitoring of drug metabolism.[4] In particular, we have studied the catalytic activity of a set of rhodium and iridium complexes with N-heterocyclic carbene (NHC) ligands as catalysts in deuterium labeling of α–olefins, choosing styrene as model for the evaluation of catalytic activity and selectivity.[5] The [RhClH(κ^2-O,N-C_9H_6NO)(IPr)] catalyst, bearing a 8-quinolinolate ligand and an electron-donor and bulky N-heterocyclic carbene as 1,3-bis-(2,6-diisopropylphenyl)imidazol-2-carbene (IPr), showed very high selectivity for the β-vinylic positions (Figure 1).

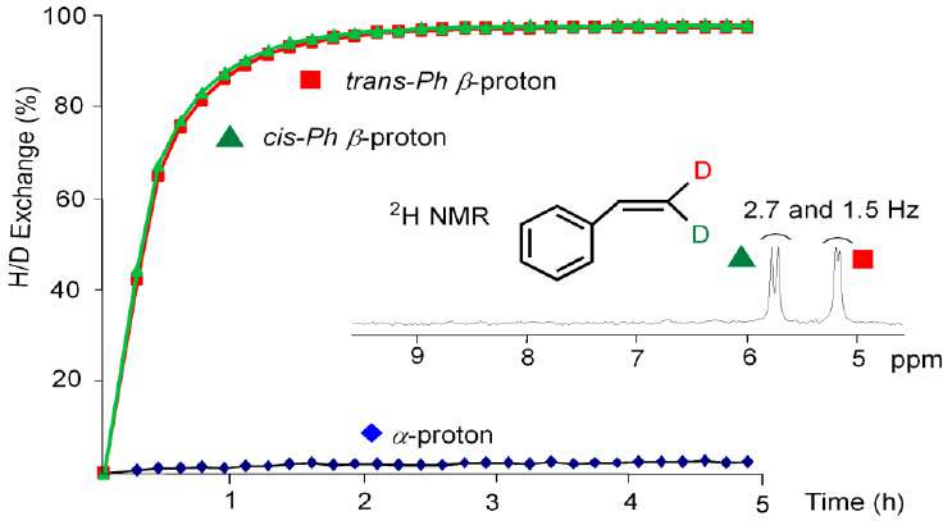

Figure 1. H/D exchange in styrene catalyzed by [RhClH(κ^2-O,N-C_9H_6NO)(IPr)] at 25ºC.

The bulky 1,3-bis-(2,6-diisopropylphenyl)imidazol-2-carbene (IPr) ligand is responsible of the controlled steric induction for selective H/D exchange because the required rotation around the C1-C2 axis of the alkyl ligand is required to exchange the proton and deuterium positions as shown in Figure 2. The first step could be deuteration of the hydride ligand in [RhClH(κ^2-O,N-C_9H_6NO)(IPr)] catalyst by CD_3OD to produce **a**. NMR observations suggest that only the deuterium atom from the O-D group are responsible for the exchange. The disposition of the chelating quinolinate ligand directs the coordination of the alkene to the equatorial position. Two orientations (**b** and **c**) are

possible for olefin coordination and the Markovnikov insertion is kinetically favored, and according with DFT calculations the liner alkyl species **d** is more stable than the branched alkyl derivative **f**, but the steric hindrance imposed by the bis-isopropylphenyl substituents of IPr restricts the C1-C2 rotation due to repulsion with the phenyl group of the alkyl ligand. Subsequent *β*–elimination reforms the starting olefin but with a deuterium atom at the *β*–position in either a *cis* o *trans* disposition, thereby explaining the similar rate observed for H/D exchange for both *cis* and *trans* protons.

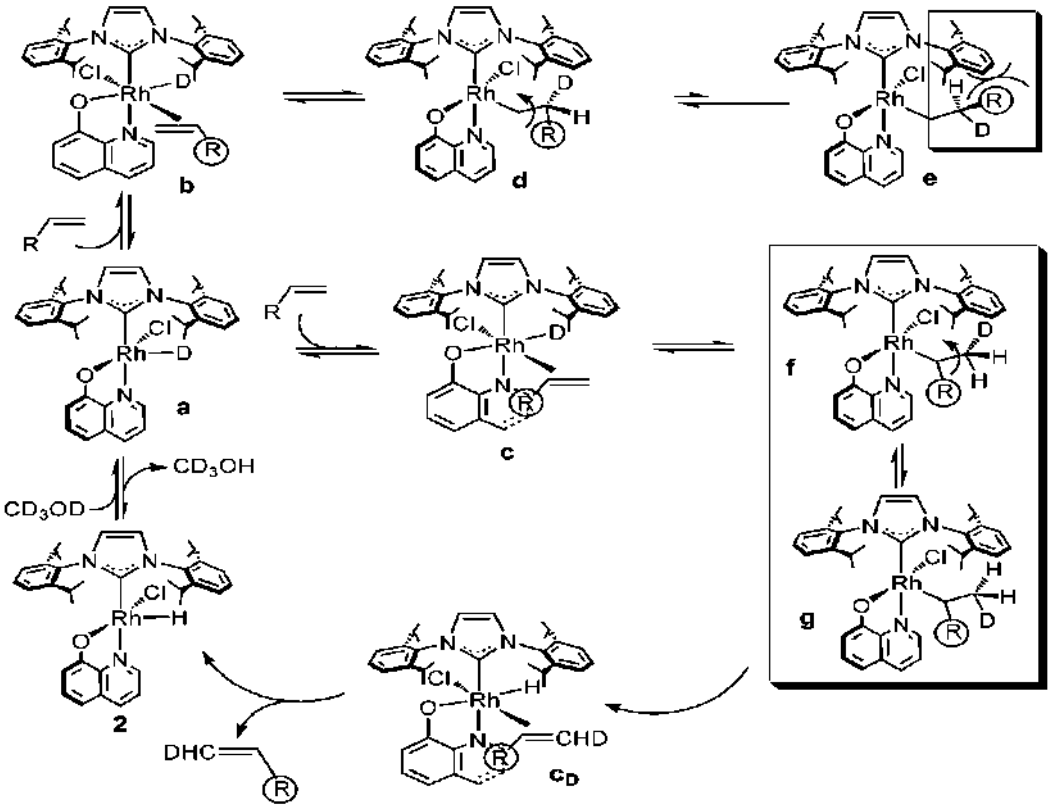

Figure 2. IPr-controlled steric induction for selective H/D exchange.

Taking into account that tricyclohexylphosphine ligand is also a bulky and basic ligand the related rhodium-quinolinate-hydride complex of formula [RhClH(κ^2-O,N-C_9H_6NO)(PCy_3)(CH_3CN)] was studied. It catalyzes the H/D exchange of styrene but with lower activity because their substituents are disposed in a conical fashion pointing out of the equatorial plane of the coordination sphere, whilst IPr adopts an umbrella type disposition with the isopropylphenyl substituents pointing towards the equatorial plane. Thus. the different selectivity is due to the different steric hindrance exerted by the two ligands. NHC ligand has a higher electron releasing capacity than PCy_3 (Figure 3).

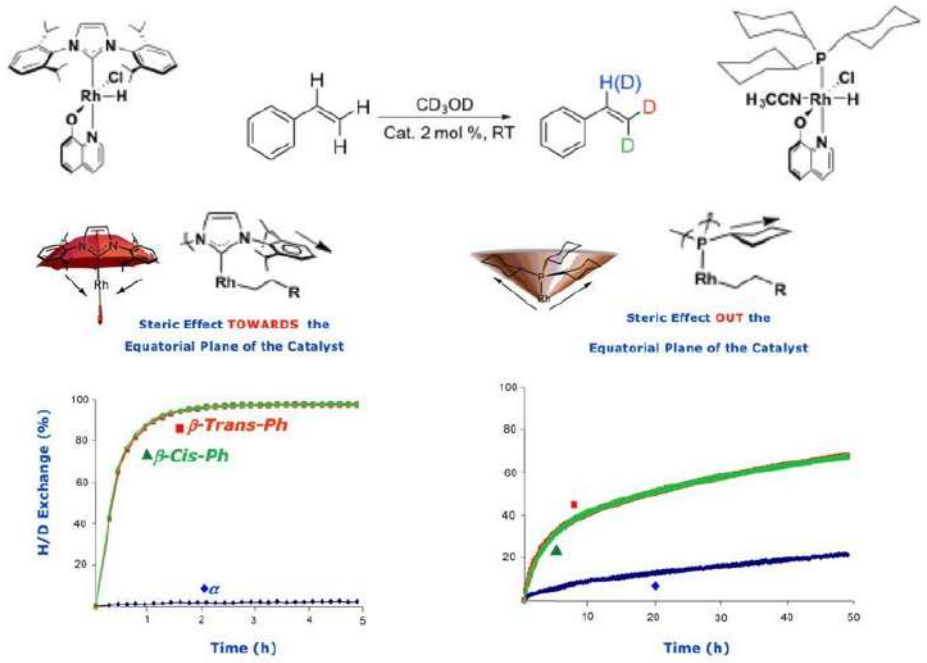

Figure 3. Comparative H/D exchange in styrene at 25 ºC.

These studies[5] contribute to the understanding of the catalytic mechanism of H/D exchange reactions, allowing for the design of better performing catalysts.

Concerning iridium catalysts, we have been particularly interested on hydrosilylation and silylation reactions.[6] In this line, hoping to shed some light on the effect of heterotopic ligands of hemilabile character in the generation of latent coordination sites, we envisaged a 14-electron bis-NHC iridium(III) fragment stabilised by two hemilabile side arms, which would allow ready accessible coordination sites and concomitant protection of the active catalyst for selective catalyzed hydrosilylation of terminal alkynes to vinylsilanes (Figure 4).

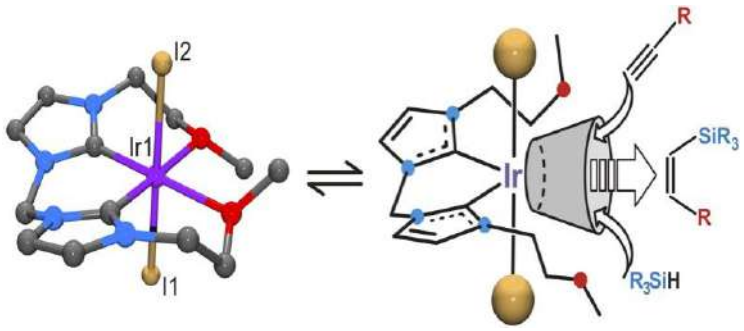

Figure 4. The cation $[Ir(I)_2\{\kappa\text{-C,C,O,O-bis(NHC)}\}]^+$

Interestingly, the $[Ir(I)_2\{\kappa$-C,C,O,O-bis(NHC)$\}]BF_4$ (bis-NHC = methylenebis(N-2-methoxyethyl)imidazole-2-ylidene)) complex shows to be very effective for the hydrosilylation of a range of terminal alkynes, employing different silanes. The reactions proceed with excellent yields and selectivities to their corresponding β–(Z)-vinylsilanes, but only when acetone was used as solvent. The specificity of acetone for the success of the hydrosilylation reaction is based on Si-O interactions between the silane and the acetone solvent, favouring a metal-ligand bifunctional outer-sphere mechanism.[7]

The proposed stepwise outer-sphere mechanism is based on the initial heterolytic splitting of the silane molecule by the metal centre in such way that the acetone molecule facilitate the transfer of the R_3Si^+ moiety from the silane to the terminal alkyne by means of an oxocarbenium ion. In the next step the resulting oxocarbenium ion ($[R_3Si–O(CH_3)_2]^+$) reacts with the corresponding alkyne to give the silylation product ($[R_3Si–CH=C–R]^+$), followed by the selective nucleophilic attack of the hydrido ligand over $[R_3Si–CH=C–R]^+$. The excellent β–(*Z*)-selectivity of the reaction could be explained as a consequence of the higher steric interaction resulting from the geometry of the approach that leads to β–(*E*)-vinylsilanes (Figure 5).[7a]

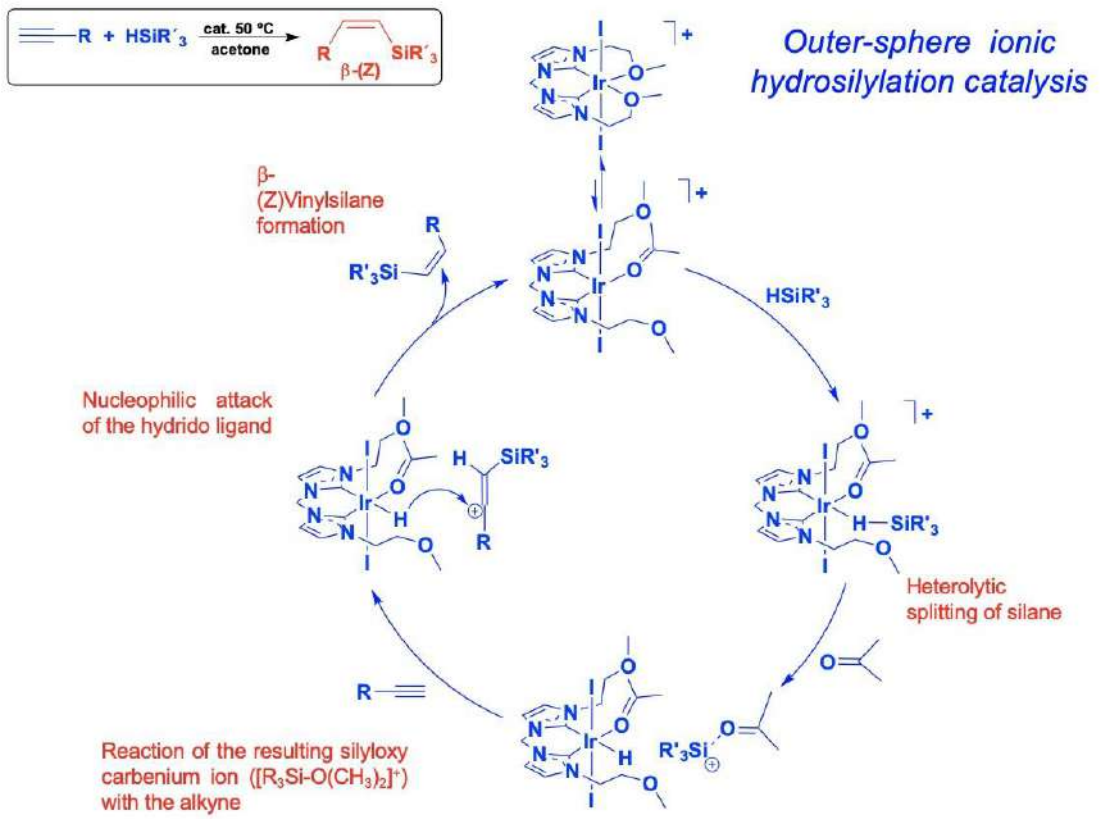

Figure 5. Outer-sphere ionic hydrosilylation catalysis

The mechanism proposal represents the first example of an outer-sphere mechanism for the hydrosilylation of terminal alkynes, in which the acetone acts as a silane shuttle transferring the silyl moiety from the silane to the alkyne. It is noteworthy to mention that while the presence of ionic and concerted outer-sphere mechanisms is well established in hydrogenation catalysis,[8] the development of new hydrosilylation catalysts that operate by ionic or concerted outer-sphere mechanism should be expected.[7b]

References

1 Rhodium Catalysis, in Topics on Organometal Chemistry, Vol. 61, ed. C. Claver, Springer Verlag (2018).

2 (*a*) *Iridium Catalysis*, in Topics on Organometal Chemistry, Vol. 34, ed. P. G. Andersson, Springer-Verlag (2011); (*b*) *Iridium Complexes in Organic Synthesis*, ed. L. A. Oro and C. Claver, Wiley-VCH Verlag GmbH & Co, Weinheim (2008).

3 (*a*) E. Peris. Smart N-Heterocyclic Carbene Ligands in Catalysis. *Chem. Rev.* 2018, **118**, 9988-10031; (*b*) M. Iglesias and L.A. Oro. A Leap Forward in Iridium-NHC Catalysis: New Horizons and Mechanistic Insights. *Chem. Soc. Rev.*, 2018, **47**, 2772-2808.

4 A. Di Giuseppe, R. Castarlenas and L. A. Oro. Mechanistic Considerations on Catalytic H/D Exchange Mediated by Organometallic Transition Metal Complexes. *C.R. Chimie*, 2015, **18**, 713-741.

5 (*a*) A. Di Giuseppe, R. Castarlenas, J. J. Pérez-Torrente, F. J. Lahoz and L. A. Oro. Rhodium(III) Hydride Complexes Bearing NHC Ligands as Catalysts in the Selective H/D Exchange Reaction of α-Olefins: A Structure-Activity Study. *Chem. Eur. J.*, 2014, **20**, 8391-8403; (*b*) A. Di Giuseppe, R. Castarlenas, J. J. Pérez-Torrente, F. J. Lahoz, V. Polo, and L. A. Oro. Mild and Selective H/D Exchange at the β-Position of Aromatic α-Olefins by N-Heterocyclic Carbene-Hydride-Rhodium Catalysts. *Angew. Chem. Int. Ed.*, 2011, **50**, 3938-3942.

6 (*a*) M. Iglesias, F. J. Fernández-Alvarez and L. A. Oro. Non-classical hydrosilane mediated reductions promoted by transition metal complexes. *Coord. Chem. Rev.*, 2019, **386**, 240-266; (*b*) L. Rubio-Pérez, M. Iglesias, J. Munárriz, V. Polo, V. Passarelli, J. J. Pérez-Torrente and L. A. Oro. A well-defined NHC–Ir(III) catalyst for the silylation of aromatic C–H bonds: substrate survey and mechanistic insights. *Chem. Sci.*, 2017, **8**, 4811-4822.

7 (*a*) M. Iglesias, P. J. Sanz Miguel, V. Polo, F. J. Fernández-Alvarez, J. J. Pérez-Torrente and L. A. Oro. An Alternative Mechanistic Paradigm for the sym-Z Hydrosilylation of Terminal Alkynes: The Role of Acetone as a Silane Shuttle. *Chem. Eur. J.*, 2013, **19**, 17559-17566; (*b*) M. Iglesias, F. J. Fernández-Alvarez and L. A. Oro. Outer-Sphere Ionic Hydrosilylation Catalysis. *ChemCatChem*, 2014, **6**, 2486-2489.

8 O. Eisenstein and R.H. Crabtree. Outer sphere hydrogenation catalysis. *New J. Chem.*, 2013, 37, 21-27

SELECTED METAL CATALYSTS SPANNED OVER THE PERIODIC TABLE TOWARDS ALKANE FUNCTIONALIZATION

Armando J. L. Pombeiro

Centro de Química Estrutural, Instituto Superior Técnico, Universidade de Lisboa, Av. Rovisco Pais, 1049-001 Lisboa, Portugal

Armando J. L. Pombeiro is Full Professor Jubilado at Instituto Superior Técnico (Universidade de Lisboa), Full Member of the Academy of Sciences of Lisbon (former Secretary-General and Vice-President of its Class of Sciences) and Fellow of the European Academy of Sciences. Founding President of the College of Chemistry of the Universidade de Lisboa, former Coordinator of Centro de Química Estrutural (CQE) and of its thematic line "Synthesis and Catalysis", founding Director of the FCT PhD Program on "Catalysis and Sustainability" (CATSUS), co-founder of the Portuguese Electrochemical Society and of the Iberoamerican Society of Electrochemistry (SIBAE). He chaired various major international conferences. His research group ("Coordination Chemistry and Catalysis") at CQE investigates the activation of small molecules with industrial, environmental or biological significance, including metal-mediated synthesis and catalysis (*e.g.*, functionalization of alkanes), crystal engineering of coordination compounds, design and self-assembly of polynuclear and supramolecular structures, non-covalent interactions, molecular electrochemistry and theoretical studies.

He authored 1 book, edited 6 books, (co-)authored *ca.* 900 research publications (including *ca.* 120 book chapters and reviews) and *ca.* 40 patents, and presented *ca.* 120 invited plenary and keynote lectures at international conferences. His work has received over 24,000 citations (9,700 citing articles), *h*-index = 69 (Web of Science), 70 (Scopus). Among his honors, he was awarded Honorary Professorship by the St. Petersburg State University (Institute of Chemistry), Invited Chair Professorship by the National Taiwan University of Science & Technology, the "Franco-Portugais Prix" of the French Chemical Society, the Madinabeitia-Lourenço Prize of the Spanish Royal Chemical Society, the Prizes of the Portuguese Chemical and Electrochemical Societies, and the Scientific Prizes of the Universidade Técnica de Lisboa and of the Universidade de Lisboa.Special issues of *Coord. Chem. Rev.* and *J. Organomet. Chem.* were published in his honor. https://fenix.tecnico.ulisboa.pt/homepage/ist10897

1. Introduction

Alkanes are the main components of natural gas and oil, constituting a huge reserve of carbon. They are often burnt as energy source or simply flared off (mainly methane) in oil fields, what **depletes the Earth from carbon** and boosts carbon dioxide

emissions with harmful ecological effects, contributing also to the exhaust of those **non-renewable fossil fuels**.

A sustainable use of alkanes can be envisioned by redirecting their application to **carbon feedstocks for synthesis** of valuable functionalized organic compounds (**alkane functionalization**) for which the alkanes provide the carbon frameworks to bear the desired functional groups, as a blooming tree branch with its blossoms [1] [Fig.1(a)]. This topic has been reviewed recently in a book we have edited [1,2] and constitutes one of the greatest challenges to modern Chemistry in view of alkane inertness which, however, can be overcome by the use of a **catalyst** [Fig.1(b)]. This presentation addresses approaches that have been pursued by the author's Group towards achieving direct and **sustainable routes of alkane functionalization** (Scheme 1) which would provide much easier synthetic methods for the derived organic products that are prepared industrially via multi-stage, complex and energy costly processes.

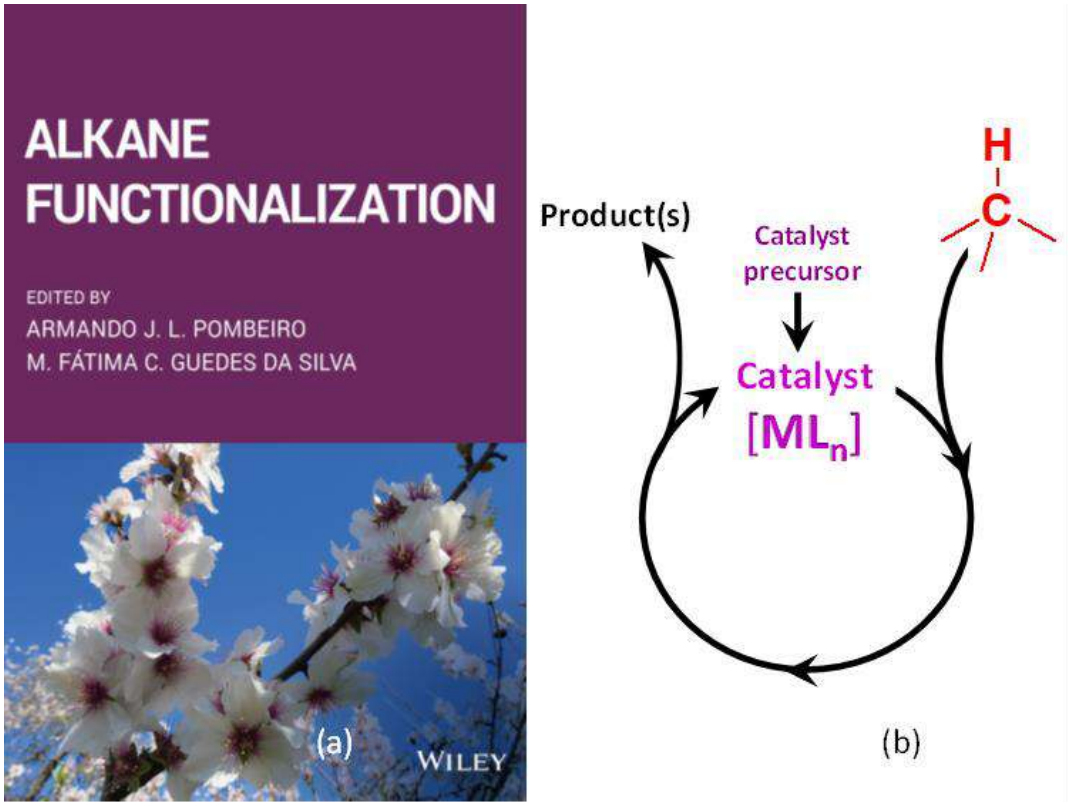

Figure 1. (a) "Alkane Functionalization" book cover [1]. (b) Overall catalytic cycle for the conversion of an alkane into a functionalyzed product. [ML_n] = metal complex catalyst.

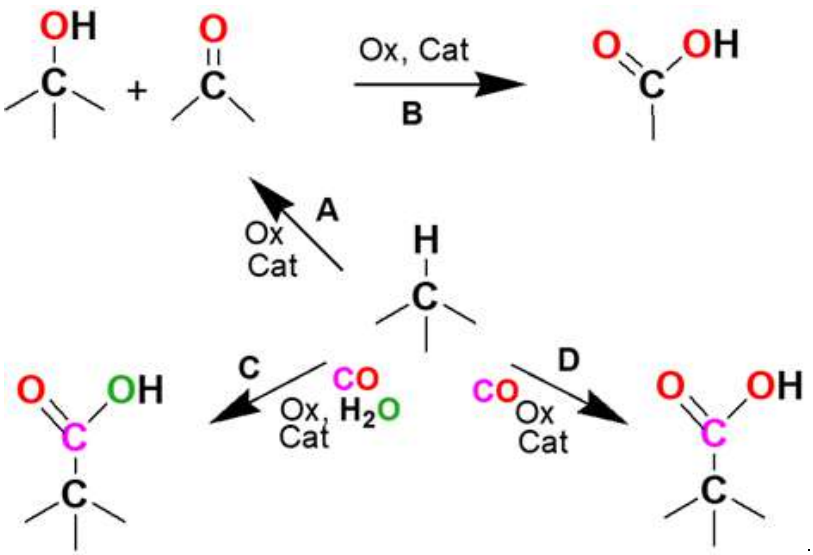

Scheme 1. Alkane functionalizations to alcohols, ketones (**A**) and carboxylic acids (**B**, **C**, **D**). Ox = Oxidant: aqueous H_2O_2 or ROOH (**A**), O_3 (ozone) (**B**) or $K_2S_2O_7$ (**C**, **D**). Solvent: acetonitrile or ionic liquid (IL) (**A**), acetonitrile or IL/water mixture (**C**) or trifluoroacetic acid (TFA) (**D**). Cat = catalyst.

Almost all groups of the **Periodic Table** are represented (Fig. 2), accounting for the main roles played by their elements: groups 1 and 2 (mainly structural role); groups 13-17 (as ligands or their components); groups from 3 (including lanthanum) until 12 (except group 4) (active catalytic role).

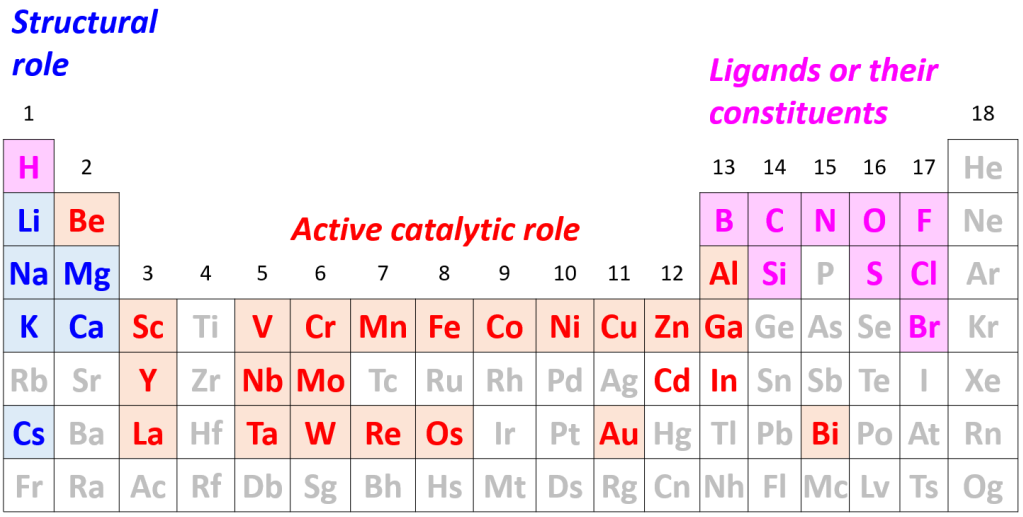

Figure 2. Elements (distributed along the Periodic Table) in catalysts for alkane functionalization which have been applied by the author´s research Group ("Coordination Chemistry and Catalysis"), with assignment of their main roles. Red: active catalytic role; Blue: structural role; Violet: as ligands or their components.

Concerning the catalytically active elements, we have focused our interest mainly on 1st row transition metals (V, Cr, Mn, Fe, Co, Ni, Cu and Zn) which are abundant, cheap and usually without a negative environmental impact, although other metals have also been addressed (see below).

To promote sustainability, the use of **water** would be recommended, although it is challenging in view of the insolubility of the alkanes and usually of the catalysts. The latter difficulty can be surpassed by applying hydrosoluble ligands which would impart water solubility to their complexes (catalysts). They include aminopolyalcohols, N-hydroxyiminocarboxylates, benzene polycarboxylates, azo derivatives of β-diketones, tris(pyrazolyl)methane derivatives, etc. [2-8].

2. Alkane oxidations to alcohols and ketones

Model reaction and catalysts types

The alkane functionalization is mainly oxidative to form an alcohol and a ketone (Scheme 1, route **A**), typically the industrially significant conversion the cyclohexane into cyclohexanol and cyclohexanone, used as a model reaction (Scheme 2, route **A**). Further oxidation, *i.e.*, to adipic acid (Scheme 1, route **B**; Scheme 2, route **B**) is described in the next section. These products are intermediates for the industrial production of Nylon 6,6.

The reactions are usually performed in acetonitrile, with aqueous hydrogen peroxide as oxidant, at ambient temperature (or closeby), leading selectively to those products in good yields, in contrast to the industrial processes which operate under severe conditions and/or with noxious environmental effects.

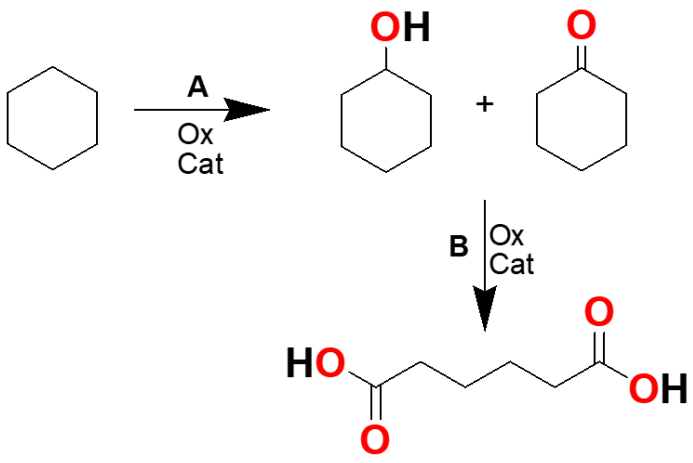

Scheme 2. Oxidation of cyclohexane to cyclohexanol and cyclohexanone (route **A**) as a model reaction for alkane oxidations, and further oxidation to adipic acid (route **B**). Ox = oxidant. Cat = catalyst.

The catalysts can be **mono- or dinuclear** complexes with the above types of ligands, and those with tris(pyrazolyl)methane derivatives (C-scorpions or C-scorpionates) are particularly active conceivably on account of the hemilabile character of these ligands which can coordinate the metal in a bi- or tridentate mode; their trivial name ("scorpionates" for the boron-based analogues), proposed by Trofimenko, was inspired on the similarity to a scorpion grabbing its prey (Scheme 3). Vanadium, iron and copper are among the most active metals in these catalysts [7-9].

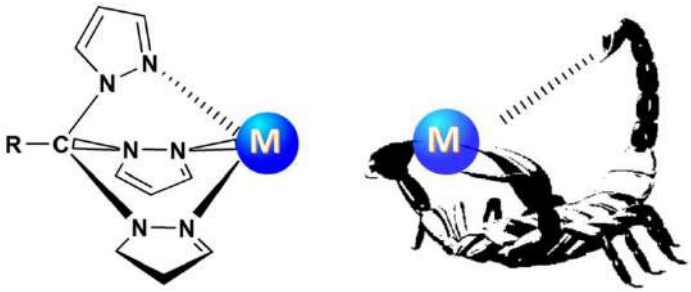

Scheme 3. Hemilabile tri- or bidentate tris(pyrazolyl)methane ("C-scorpion" or "C-scorpionate") ligand resembling a scorpion grabbing its pray. M = VO_2, $VOCl_2$, VCl_3, $FeCl_2$, $NiCl_2$, $CuCl_2$, $AuCl_2$, etc. (isolated with the tridentate coordination). R = H, CH_2OH, SO_3^-, etc.

Self-assembled discrete polynuclear catalysts can also be quite effective, such as the tetracopper-μ-oxido-triethanolaminato complex $[OCu_4(tea)_4(BOH)_4][BF_4]_2$ [10] and other multi-copper compounds [10-12], and **heterometallic** complexes obtained by direct self-assembly from metal powder and aminoalcohols [3,4,13], *e.g.* the heterodimetallic hexanuclear salicylidene-2-ethanolaminate complex $[Co_4Fe_2O(Sae)_8]$ which, in the cyclohexane peroxidative oxidation, allows to achieve a high 46% products yield and a high turnover number (TON, number of moles of product per mole of catalyst) of 3.6×10^3 (corresponding to a turnover frequency, TOF, of 1.1×10^4 h^{-1}) [13].

These multinuclear complexes are more effective, on a weight basis, than the multicopper enzyme particulate methanemonooxygenase (pMMO) which catalyzes the oxidation of light alkanes to alcohols.

High nuclearity metallasilsesquioxanes can also provide good catalysts, such as that with the cluster cage Cu_9Na_6 (work in collaboration with G. Shul'pin and A. Bilyachenko, Moscow) [14].

Moreover, we discovered that **self-assembled metal-organic frameworks (MOFs)** or **coordination polymers** can also be quite active, as illustrated by water soluble heterometallic dioxido-vanadium(V)/alkali metal (Na, K, Cs) polymers with an azine fragment ligand (oxaloyldihydrazone). The catalytic activity (increasing from Na to Cs) parallels their complexity (1-, 2- or 3-dimensional, respectively), *i.e*, a periodic trend appears to be followed [15].

Avoidance of an organic solvent, and catalyst recycling

The volatile organic solvent (acetonitrile) can be avoided by replacing it with an **ionic liquid** (IL), *e.g.,* 1-butyl-3-methylimidazolium dicyanamide ([bmim][$N(CN)_2$]) in the microwave-assisted neat oxidation of cyclohexane catalyzed by [$FeCl_2${$HC(pz)_3$}] [16]. Another advantage of the use of the IL concerns the possibility of catalyst recovery and recycling without leaching, what is explained by theoretical DFT calculations that indicate the IL anion coordination to the metal catalyst [16].

Another way to achieve catalyst recycling consists in its **heterogenization** upon anchoring to a solid matrix. Carbon materials (with the collaboration of S. Carabineiro and J. Figueiredo, University of Porto), specially multiwalled carbon nanotubes (MWCNT) after adequate treatment, were disclosed to be appropriate ones, *e.g.* for [Cl_2Au{$HC(pz)_3$}]Cl [17] and related Fe, V and Cu catalysts in the peroxidative oxidation of cyclohexane.

The use as catalysts of recyclable **magnetic** nanoparticles, *i.e*, first-row-transition-metal silica coated magnetite nanoparticles, $Fe_3O_4@SiO_2$-M^{2+} (M = Mn, Co, Cu or Zn), is also convenient in the same reaction assisted by microwave, without any added solvent, allowing an easy magnetic separation of the catalyst and its recycling [18].

Metal cooperation effects

On the basis of radical trap experiments, selectivity and kinetic studies (with the collaboration of Prof. G. Shul'pin), as well as DFT calculations, the peroxidative alkane oxidation in our systems is believed to involve the metal-promoted formation of O- and C-based radicals, such as the hydroxyl radical $HO^{\bullet}$ derived from H_2O_2, and the alkyl and

peroxyl radicals ($R^{\bullet}$ and $ROO^{\bullet}$, respectively) from the alkane RH (Scheme 4, route **A**) [3-5].

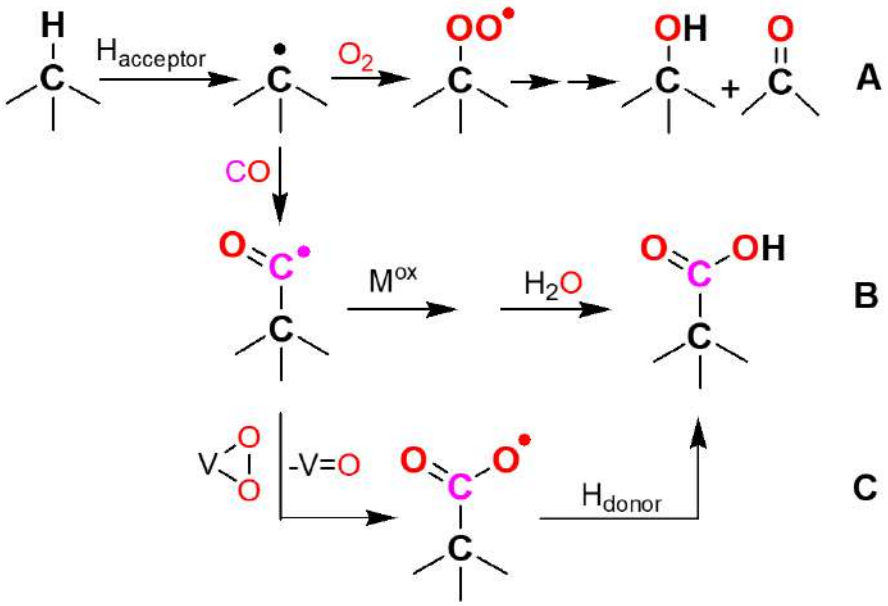

Scheme 4. Overall metal-catalyzed radical mechanisms for the peroxidative oxidation (route **A**), hydrocarboxylation (route **B**) and carboxylation (route **C**) of an alkane. $H_{acceptor}$ (hydrogen atom abstractor) = $HO^{\bullet}$ or $HSO_4^{\bullet}$; H_{donor} (hydrogen atom donor) = RH or CF_3COOH; M^{ox} = metal catalyst as oxidant; V(OO) = peroxido-vanadium(V) catalyst.

The catalytic activity is often promoted by acid (generation of metal coordinative unsaturation upon protonation of an hemilabile basic N,O ligand) and, in some cases, by **water** and by the metal **dinuclear** character in oxido-divanadium catalysts. The latter unexpected behaviours are rationalized by DFT calculations which unveil various types of metal cooperation effects.

In the metal-assisted generation of the hydroxyl radical from H_2O_2, **water** promotes proton-shift steps that are involved therein by forming stabilized 6-membered metal transition states [Scheme 5(a)] [19,20]. In the case of the **oxido-divanadium** catalysts, the bridging oxido ligand also cooperates with the metals, allowing the formation of a stabilized 6-membered di-vanadium transition state without requiring water [Scheme 5(b)] [21].

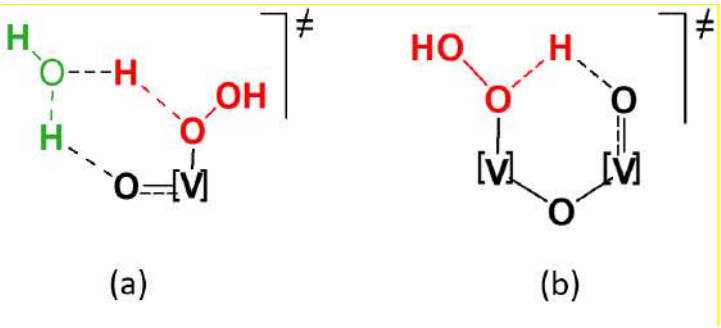

Scheme 5. Stabilized 6-membered transition states in water-assisted (a) and oxido-divanadium-assisted (b) proton-shift steps towards the formation of hydroxyl radical from H_2O_2

Another type of metal-ligand cooperation involves a non-innocent **redox active ligand** in the catalyst, which can perform the role typically assumed by the metal in the redox steps, allowing the latter to preserve its more favourable oxidation state under the reaction conditions.

We firstly proposed [22] this type of interpretation, based on DFT calculations, for the aluminium catalysed oxidation of cycloalkanes, and then extended it [23-25] to other metals of the same periodic group (13: gallium and indium) and of the periodic groups 2 (berillium), 3 (scandium, yttrium and lanthanum), 12 (zinc and cadmium) and 15 (bismuth). These elements form aqua complexes $[M(H_2O)_n]^{m+}$ that act as catalysts for the alkane oxidation with H_2O_2. The key step concerns the reduction of a H_2O_2 ligand by a deprotonated **hydrogen peroxide** co-ligand (HOO^-) to form the hydroxyl radical $HO^{\bullet}$ without requiring the change of the stable metal oxidation state [25].

A quite different type of redox active ligand concerns **hydrazones** with the active azine moiety C=N-N=C. We recognized this effect in some highly active di(oxido-vanadium) catalysts which, in the presence of pyrazinecarboxylic acid additive, can lead to a TON of $4.4x10^4$, with an initial TOF of $3.3x10^3$ h^{-1} in the oxidation of cyclohexane with H_2O_2 [26]. We disclosed other examples not only among vanadium catalysts [27-28], but also in other metal catalysts such as some octaazamacrocyclic(15- and 14-membered) nickel(II) complexes studied in collaboration with V. Arion (University of Vienna) [29]. Quinolinato ligands at vanadium complexes can also play a similar function [30].

3. Alkane Carboxylations and Oxidation to Carboxylic Acids

We discovered [31-33] that alkanes can undergo single-pot hydrocarboxylation with water and CO, proxydisulfate acting as oxidant, in water/acetonitrile medium, to afford the corresponding carboxylic acids in high yields, at low temperature (30-60 °C), according to a radical mechanism in which (as proved by ^{18}O labeled water studies) water behaves as the hydroxide source (Scheme 1, route **C**; Scheme 6). The reaction proceeds via the acyl radical ($RCO^{\bullet}$ formed upon reaction of CO with the alkyl radical $R^{\bullet}$) which, upon oxidation and nucleophilic attack of water, forms the carboxylic acid (Scheme 4, route **B**). The process can occur even in the absence of a metal catalyst, although less effectively.

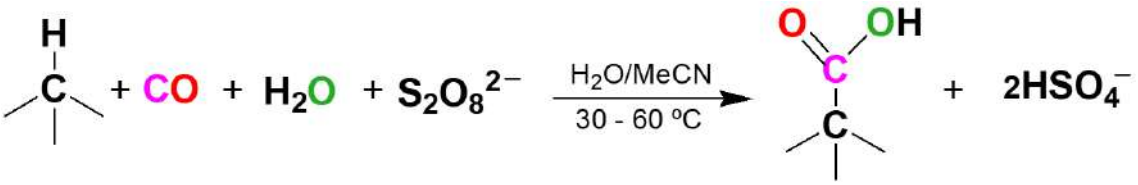

Scheme 6. Alkane hydrocarboxylation in water/acetonitrile

The use of an organic solvent can be eliminated by replacing it (acetonitrile) by an ionic liquid, with the advantages of catalyst recycling and higher selectivity, features of "green" significance, as disclosed for a copper MOF with a bridging (terpyridinyl)benzyloxy benzoate linker [34].

This hydrocarboxylation reaction constitutes a development of a process of carboxylation of alkanes which we had developed earlier in trifluoroacetic acid (TFA), a less convenient solvent than water/acetonitrile, according to a method pioneered by Y. Fujiwara (Fukuoka, Japan).

In fact, we found [35-37] extremely active catalysts operating via a different mechanism (radical instead of electrophilic), namely *Amavadin*, an intriguing natural vanadium complex present in some *Amanita* toadstools, and its models or related vanadium species (Scheme 7). Yields above 90% and TONs over 10^4 could be achieved for methane or ethane carboxylation at the typical temperature of 80 °C.

Oxides of transition metals in the periodic groups 5-7 also act as carboxylation catalysts and the diagonal metals commonly provide the most active oxides in the order V > Re > Mo [38].

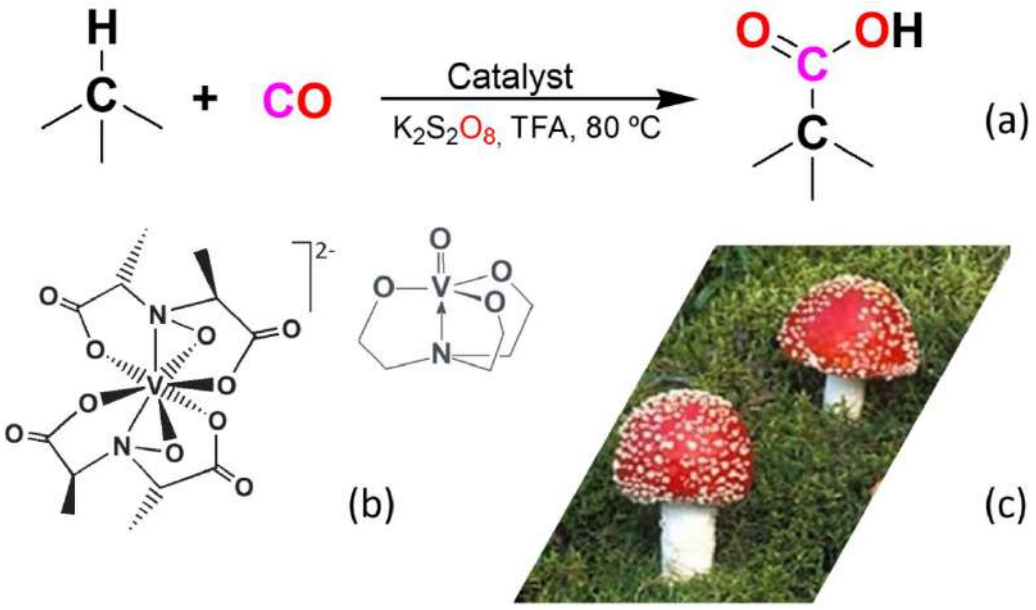

Scheme 7. Alkane carboxylation in trifluoracetic acid: (a) general reaction; (b) typical catalysts (*Amavadin* and vanadatrane); (c) *Amanita* toadstoods.

The reaction mechanism (Scheme 4, route **C**) involves the acyl radical ($RCO^{\bullet}$) as in the above hydrocarboxylation, but now the acyl is converted to the corresponding carboxylate radical ($RCOO^{\bullet}$) by a peroxide-vanadium catalyst [36, 37]. In the absence of CO gas, the reaction also occurs, although much less effectively, where the TFA solvent behaves as the carbonylating agent.

These single-pot alkane hydrocarboxylation and carboxylation reactions to yield carboxylic acids are much simpler and milder than the current industrial processes for the production of those products. However, they require peroxydisulfate as oxidizing agent and efforts to replace it by a "greener" oxidant have been pursued. We noticed [39] that ozone (a non-polluting oxidant), in the presence of the iron catalyst $[FeCl_2\{HC(pz)_3\}]$, can oxidize, in a single-pot, cyclohexane to adipic acid, $HOOC(CH_2)_4COOH$ (Scheme 1, route **B;** Scheme 2, route **B**), which is at a higher oxidation level than cyclohexanol or cyclohexanone (see above).

This one-pot oxidation of cyclohexane to adipic acid, a key intermediate for the production of Nylon-6,6, is also much simpler and sustainable than the industrial processes which usually require the oxidation of cyclohexanol/cyclohexanone with nitric acid leading to the emission of large amounts of the greenhouse nitrous oxide gas (N_2O) by-product.

4. Final Comments

Following our first report (in 2000) on alkane functionalization (when we found that the natural vanadium complex *Amavadin* can act as a catalyst for alkane hydroxylation, oxygenation and halogenation [40]), our work has extended to the design and application in this field, under mild conditions, of a **diversity** of catalysts with metals playing a key catalytic role. They spread over most of the groups of the **Periodic Table** (12 in a total of 18 periodic groups). Elements of almost all the other periodic groups have also been used in the composition of the catalysts, namely with a structural role in their ligands.

The metal catalysts can be hydrosoluble, based on either a transition (almost all periodic groups from 3 to 12) or a non-transition redox inactive metal (in periodic groups 2, 13 and 15), and bioinspired. They can act as homogeneous catalysts in solution or supported on a matrix such as a suitable carbon material.

Routes towards **sustainable** alkane functionalization reactions (*e.g.*, simple, environmentally benign and with a low energy consumption) have already been followed, namely in terms of (i) metal catalysts design and mild operation conditions, (ii) "green" oxidants, (ii) avoidance of organic solvents, and (iii) use of water as solvent, reagent and catalyst. Moreover, applications of other unconventional conditions are growing, namely the use of supercritical carbon dioxide as solvent, of microwave heating or mechanochemical assistance [41].

The reaction **mechanisms** in our systems are of a radical nature and relevant **cooperative metal-ligand** effects have been disclosed.

Oxygenated and carboxylated products with an added value have already been obtained in good yields and under considerably mild conditions, thus demonstrating the potential use of inert alkanes as feedstocks. Can the onset of an Alkane Area for organic synthesis be foreseen?

Acknowledgments

Thanks are due to all the co-authors cited in the references. Prof. M. Fátima Guedes da Silva (Instituto Superior Técnico) is further acknowledged for her assistance

in the preparation of the schemes. The work has been partially supported by the Fundação para a Ciência e Tecnologia (FCT), Portugal, namely through the project UIDB/00100/2020 of the Centro de Química Estrutural.

References

[1] "Alkane Functionalization", A.J.L. Pombeiro (ed.), M.F.C. Guedes da Silva (co-ed.), J. Wiley & Sons, Hoboken, NJ, USA, 2019 (ISBN: 9781119378808). http://dx.doi.org/10.1002/9781119379256

[2] A.J.L.Pombeiro, "Alkane Functionalization: Introduction and Overview", in Ref. [1], Chapter 1, pp.1-15. https://dx.doi.org/10.1002/9781119379256.ch1

[3] D.S. Nesterov, O.V. Nesterova, A.J.L. Pombeiro, "Alkane Oxidation with Multinuclear Heterometallic Catalysts", in Ref. [1], Chapter 7, pp.125-140. https://dx.doi.org/10.1002/9781119379256.ch7

[4] D.S. Nesterov, O.V. Nesterova, A.J.L. Pombeiro, "Homo- and heterometallic polynuclear transition metal catalysts for alkane C-H bonds oxidative functionalization: Recent advances", *Coord. Chem. Rev.* 2018, *355* 199-222. https://doi.org/10.1016/j.ccr.2017.08.009

[5] M. Sutradhar, L.M.D.R.S. Martins, M.F.C. Guedes da Silva, A.J.L. Pombeiro, "Alkane Oxidation with Vanadium and Copper Catalysts", in Ref. [1], Chapter 16, pp.319-336. https://dx.doi.org/10.1002/9781119379256.ch16

[6] M. Sutradhar, L.M.D.R.S. Martins, M.F.C. Guedes da Silva, A.J.L. Pombeiro, "Vanadium complexes: Recent progress in oxidation catalysis", *Coord. Chem. Rev.*, 2015, *301-302*, 200-239. http://dx.doi.org/10.1016/j.ccr.2015.01.020

[7] L.M.D.R.S. Martins, A.J.L. Pombeiro, "Tris(pyrazol-1-yl)methane Metal Complexes for Catalytic Mild Oxidative Functionalizations of Alkanes, Alkenes and Ketones", *Coord. Chem. Rev.*, 2014, *265*, 74-88. http://dx.doi.org/10.1016/j.ccr.2014.01.013

[8] L.M.D.R.S. Martins, A.J.L. Pombeiro, "Water-Soluble C-Scorpionate Complexes – Catalytic and Biological Applications ", *Eur. J. Inorg. Chem.*, 2016, 2236-2252. http://dx.doi.org/10.1002/ejic.201600053

[9] T.F.S. Silva, E.C.B.A. Alegria, L.M.D.R.S. Martins, A.J.L. Pombeiro, "Half-sandwich Scorpionate Vanadium, Iron and Copper Complexes: Synthesis and Application in the Catalytic Peroxidative Oxidation of Cyclohexane under Mild Conditions", *Adv. Synth. Cat.*, 2008, *350*, 706-716. http://dx.doi.org/10.1002/adsc.200700529

[10] A.M. Kirillov, M.N. Kopylovich, M.V. Kirillova, M. Haukka, M.F.C. Guedes da Silva, A.J.L. Pombeiro, "Multinuclear Copper Triethanolamine Complexes as Selective Catalysts for the Peroxidative Oxidation of Alkanes under Mild Conditions", *Angew. Chem., Int. Ed.*, 2005, *44*, 4345-4349. http://dx.doi.org/10.1002/anie.200500585

[11] A.M. Kirillov, M.V. Kirillova, A.J.L. Pombeiro, "Self-assembled Multicopper Complexes and Coordination Polymers for Oxidation and Hydrocarboxylation of Alkanes", *in* "Advances in Organometallic Chemistry and Catalysis" (The Silver/Gold Jubilee ICOMC Celebratory Book), A.J.L. Pombeiro (ed.), J. Wiley & Sons, 2014, Chapter 3, pp. 27–38.

[12] A.M. Kirillov, M.V. Kirillova, A.J.L. Pombeiro, "Homogeneous multicoppercatalysts for oxidation and hydrocarboxylation of alkanes", *Adv. Inorg. Chem.*,2013, *65*, 1−31. http://dx.doi.org/10.1016/B978-0-12-404582-8.00001-8

[13] D.S. Nesterov, E.N. Chygorin,V.N. Kokozay, V.V. Bon, R. Boča, Y.N. Kozlov, L.S. Shul'pina, J. Jezierska, A. Ozarowski, A.J.L. Pombeiro, G.B. Shul'pin, "Heterometallic $Co^{III}_4Fe^{III}_2$ Schiff Base Complex: Structure, Electron Paramagnetic Resonance, and Alkane Oxidation Catalytic Activity", *Inorg.Chem.*, 2012, *51*, 9110-9122. http://dx.doi.org/10.1021/ic301460q

[14] G.S. Astakhov, A.N. Bilyachenko, A.A. Korlyukov, M.M. Levitsky, L.S. Shul'pina, X. Bantreil, F. Lamaty, A.V. Vologzhanina, E.S. Shubina, P.V. Dorovatovskii, D.S. Nesterov, A.J.L. Pombeiro, G.B. Shul´pin, "High-Cluster (Cu-9) Cage Silsesquioxanes: Synthesis, Structure, and Catalytic Activity", *Inorg. Chem.*, 2018, *57*, 11524-11529. https://doi.org/10.1021/acs.inorgchem.8b01496

[15] S. Gupta, M. Kirillova, M.F.C. Guedes da Silva, A.J.L. Pombeiro, A. Kirillov, "Alkali Metal Directed Assembly of Heterometallic V/M (M = Na, K, Cs) Coordination Polymers: Structures, Topological Analysis, and Oxidation Catalytic Properties", *Inorg. Chem.*, 2013, *52*, 8601-8611. http://dx.doi.org/10.1021/ic400743h

[16] A.P.C. Ribeiro, L.M.D.R.S. Martins, M.L. Kuznetsov, A.J.L. Pombeiro, "Tuning Cyclohexane Oxidation: Combination of Microwave Irradiation and Ionic Liquid with the C-Scorpionate $[FeCl_2(Tpm)]$ Catalyst", *Organometallics*, 2017,*36*, 192-198. http://dx.doi.org/10.1021/acs.organomet.6b00620

[17] M. Peixoto de Almeida, L.M.D.R.S. Martins, S.A.C. Carabineiro, T. Lauterbach, F. Rominger, A.S.K. Hashmi, A.J.L. Pombeiro, J.L. Figueiredo, "Homogeneous and Heterogenised New Gold C-scorpionate Complexes as Catalysts for Cyclohexane Oxidation", *Catal. Sci. Technol*., 2013, *3*, 3056-3069. http://dx.doi.org/10.1039/c3cy00552f

[18] N.M.R. Martins, A.J.L. Pombeiro, L.M.D.R.S. Martins, "Green oxidation of cyclohexane catalyzed by recyclable magnetic transition-metal silica coated nanoparticles", *Catal. Commun.*, 2019, *125*, 15-20. https://doi.org/10.1016/j.catcom.2019.03.015

[19] M. Kuznetsov, A.J.L. Pombeiro, "Radical Formation in the $[MeReO_3]$ (MTO) Catalyzed Aqueous Peroxidative Oxidation of Alkanes: a Theoretical Mechanistic Study", *Inorg. Chem.*, 2009, *48*, 307-318. http://dx.doi.org/10.1021/ic801753t

[20] M.V. Kirillova, M.L. Kuznetsov, V. B. Romakh, L..S. Shul'pina, J.J.R. Fraústo da Silva, A.J.L. Pombeiro, G.B. Shul'pin, "Mechanism of H_2O_2Oxidations Catalyzed by Vanadate Anion or Oxovanadium(V) triethanolaminate (Vanadatrane) in Combination with Pyrazine-2-carboxylic acid (PCA): Kinetic and DFT studies", *J. Cat.*, 2009, *267*, 140-157. http://dx.doi.org/10.1016/j.jcat.2009.08.006

[21] M.V. Kirillova, M.L. Kuznetsov, Y.N. Kozlov, L.S. Shul'pina, A. Kitaygorodskiy, A.J.L. Pombeiro, G.B. Shul'pin, "Participation of Oligavanadates in Alkane Oxidation with H_2O_2 Catalysed by Vanadate-anion in Acidified Acetonitrile: Kinetic and DFT Studies", *ACS Catalysis*, 2011, *1*, 1511-1520. http://dx.doi.org/10.1021/cs200237m

[22] M. L. Kuznetsov, Y. N. Kozlov, D. Mandelli, A. J. L. Pombeiro, G. B. Shul´pin, "Mechanism of Al^{3+} -Catalyzed Oxidations of Hydrocarbons: Dramatic Activation of H_2O_2 toward O-O Homolysis in Complex $[Al(H_2O)_4(OOH)(H_2O_2)]^{2+}$ Explains the Formation of $HO^{\cdot}$ Radicals", *Inorg. Chem.*, 2011, *50*, 3996-4005. http://dx.doi.org/10.1021/ic102476x

[23] M.L. Kuznetsov, “Nontransition Metal Catalyzed Oxidation of Alkanes with Peroxides”, in Ref [1], Chapter 22, pp.485-501. https://dx.doi.org/10.1002/9781119379256.ch22

[24] M.L. Kuznetsov, F.A. Teixeira, N.A. Bokach, A.J.L. Pombeiro, G.B. Shul´pin, ”Radical decomposition of hydrogen peroxide catalyzed by aqua complexes $[M(H_2O)_n]^{2+}$ (M = Be, Zn, Cd)”, *J. Cat*., 2014, *313*, 135-148. http://dx.doi.org/10.1016/j.jcat.2014.03.010

[25] B.G.M. Rocha, M.L. Kuznetsov, Y.N. Kozlov A.J.L. Pombeiro, G.B. Shul'pin, “Simple soluble Bi(III) salts as efficient catalysts for the oxidation of alkanes with H_2O_2”, *Cat. Sci. Technol*., 2015, *5*, 2174-2187. http://dx.doi.org/10.1039/C4CY01651C

[26] M. Sutradhar, N. V. Shvydkiy, M.F.C. Guedes da Silva, M.V. Kirillova, Y.N. Kozlov, A.J.L. Pombeiro, G.B. Shul’pin, “ New binuclear Oxovanadium(V) Complex as a Catalyst in Combination with Pyrazinecarboxylic acid (PCA) for Efficient Alkane Oxygenation by H_2O_2”, *Dalton Trans*., 2013, *42*, 11791-11803. http://dx.doi.org/10.1039/c3dt50584g

[27] M. Sutradhar, L.M.D.R.S. Martins, T.R. Barman, M.L. Kuznetsov, M.F.C. Guedes da Silva, A.J.L. Pombeiro, “Vanadium complexes of different nuclearities in the catalytic oxidation of cyclohexane and cyclohexanol - An experimental and theoretical investigation”, *New J. Chem*., 2019, *43*, 17557-17570. http://dx.doi.org/10.1039/c9nj00348g

[28] D. Dragancea, N. Talmaci, S. Shova, G. Novitchi, D. Darvasiová, P. Rapta, M Breza, M Galanski, J. Kožıšek, N.M. R. Martins, L.M.D.R.S. Martins, A.J.L. Pombeiro, V.B. Arion, “Vanadium(V) Complexes with Substituted 1,5-bis(2-hydroxybenzaldehyde)carbohydrazones and Their Use As Catalyst Precursors in Oxidation of Cyclohexane”, *Inorg. Chem.* 2016, *55*, 9187-9203. http://dx.doi.org/10.1021/acs.inorgchem.6b01011

[29] A. Dobrov, D. Darvasiová, M. Zalibera, L. Bučinský, I. Puškárová, P. Rapta, L.M.D.R.S. Martins, A.J.L. Pombeiro, V.B. Arion, “Nickel(II) complexes with redox noninnocent octaazamacrocycles as catalysts in oxidation reactions”, *Inorg. Chem.,* 2019, *58*, 11133-11145. http://dx.doi.org/10.1021/acs.inorgchem.9b01700

[30] I. Gryca, K. Czerwinska, B. Machura, A. Chrobok, L.S. Shul'pina, M.L. Kuznetsov, D.S. Nesterov, Y.N. Kozlov, A.J.L. Pombeiro, I.A. Varyan, G.B. Shul'pin, “High Catalytic Activity of Vanadium Complexes in Alkane Oxidations with Hydrogen Peroxide: An Effect of 8-Hydroxyquinoline Derivatives as Noninnocent Ligands”, *Inorg. Chem.,* 2018, *57*, 1824-1839. https://doi.org/10.1021/acs.inorgchem.7b02684

[31] M.V. Kirillova, A.M. Kirillov, M.L. Kuznetsov, J.A.L. Silva, J.J.R. Fraústo da Silva, A.J.L. Pombeiro, ”Alkanes to Carboxylic Acids in Aqueous Medium: Metal-free and Metal-promoted Highly Efficient and Mild Conversions”, *Chem. Commun.*,2009, 2353-2355. http://dx.doi.org/10.1039/b900853e

[32] A.M. Kirillov, Y.Y. Karabach, M.V. Kirillova, M. Haukka, A.J.L. Pombeiro, “Topologically Unique 2D Heterometallic Cu^{II}/Mg Coordination Polymer: Synthesis, Structural Features, and Catalytic Use in Alkane Hydrocarboxylation”, *Cryst. Growth Des.*, 2012, *12* (3), 1069-1074. http://dx.doi.org/10.1021/cg201459k

[33] A.M.F. Phillips, A.J.L. Pombeiro, “Alkane Carbonylation and Carbene Insertion Reactions”, in Ref. [1], Chapter 18, pp.371-426. https://dx.doi.org/10.1002/9781119379256.ch18

[34] A. Paul, A.P.C. Ribeiro, A. Karmakar, M.F.C. Guedes da Silva, A.J.L. Pombeiro, “A Cu(II) MOF with a flexible bifunctionalised terpyridine as an efficient catalyst for the single-pot

hydrocarboxylation of cyclohexane to carboxylic acid in water/ionic liquid medium", *Dalton Trans.*, 2016, *45*, 12779-12789. http://dx.doi.org/10.1039/C6DT01852A

[35] P.M. Reis, J.A.L. Silva, A.F. Palavra, J.J.R. Fraústo da Silva, T. Kitamura, Y.Fujiwara, A.J.L. Pombeiro, "Single-pot Conversion of Methane into Acetic Acid, in the Absence of CO and with Vanadium Catalysts Such as Amavadine", *Angew. Chem.*, 2003, *115*, 845-847 (*Intern. Ed.*: 2003, *42*, 821-823). http://dx.doi.org/10.1002/anie.200390219

[36] M.V. Kirillova, M.L. Kuznetsov, P.M. Reis, J.A.L. Silva, J.J.R. Fraústo da Silva, A.J.L. Pombeiro, "Direct and Remarkably Efficient Conversion of Methane into Acetic Acid Catalyzed by Amavadine and Related Vanadium Complexes. A Synthetic and a Theoretical DFT Mechanistic Study", *J. Am. Chem. Soc.*, 2007, *129*, 10531-10545. http://dx.doi.org/10.1021/ja072531u

[37] M.V. Kirillova, M.L. Kuznetsov, J.A.L. Silva, M.F.C. Guedes da Silva, J.J.R. Fraústo da Silva, A. J.L. Pombeiro, "Amavadin and Other Vanadium Complexes as Remarkable Efficient Catalysts for the Single-Pot Conversion of Ethane into Propionic and Acetic Acids", *Chem. Eur. J.*, 2008, *14*, 1828-1842. http://dx.doi.org/10.1002/chem.200700980

[38] M.V. Kirillova, A.M. Kirillov, P.M. Reis, J.A.L. Silva, J.J.R. Fraústo da Silva, A.J.L. Pombeiro, "Group 5-7 Transition Metal Oxides as Efficient Catalysts for Oxidative Functionalization of Alkanes under Mild Conditions", *J. Cat.*, 2007, *248*, 130-136. http://dx.doi.org/10.1016/j.jcat.2007.02.025

[39] A.P.C. Ribeiro, L.M.D.R.S. Martins, A.J.L. Pombeiro, "N_2O-Free single-pot conversion of cyclohexane to adipic acid catalysed by an iron(II) scorpionate complex", *Green Chem.*, 2017,*19*, 1499-1501. http://dx.doi.org/10.1039/C6GC03208G

[40] P.M. Reis, J.A.L. Silva, J.J.R. Fraústo da Silva, A.J.L. Pombeiro, "Amavadine as a Catalyst for the Peroxidative Halogenation, Hydroxylation and Oxygenation of Alkanes and Benzene", *J. Chem. Soc., Chem. Commun.*, 2000, 1845-1846. http://dx.doi.org/10.1039/b005513l

[41] A.P.C. Ribeiro, E.C.B.A. Alegria, A. Palavra, A.J.L. Pombeiro, "Alkane Functionalization under Unconventional Conditions: in Ionic Liquid, in Supercritical CO_2 and Microwave Assisted", in Ref. [1], Chapter 24, pp.523-537. https://dx.doi.org/10.1002/9781119379256.ch24

B — Metal Centres in Supramolecular and Biological Structures

NANOPOROUS MATERIALS: FUNCTIONAL SILICATES AND METAL ORGANIC FRAMEWORKS

João Rocha

University of Aveiro, Department of Chemistry, CICECO-Aveiro Institute of Materials, Portugal, rocha@ua.pt

João Rocha (b. 1962) is Full Professor of Chemistry and Director of the University of Aveiro Institute of Materials (CICECO, ca. 480 people), largest and best rated Materials Science Institute in Portugal, he has created in 2002.

He got his Ph.D. in 1990 from the Department of Chemistry, University of Cambridge. This was followed by a post-doc in the same group. He obtained his 'Agregação' (Habilitation) in 1997 in the University of Aveiro, Portugal.

Rocha is member and 'officer' of the Chemistry Division of the European Academy of Sciences (EURASC). He is a member of the Lisbon Academy of Sciences since 2006. He is also Fellow of both the Royal Society of Chemistry and Chemistry Europe. In 2012-2014, he was advisor for the Prime Minister of Portugal, as a member of the National Science and Technology Council. He has received the prize Ferreira da Silva (highest distinction bestowed by the Portuguese Chemical Society), and the Madinabeitia-Lourenço award from the Real Sociedad Española de Química. In 2005, he received the prize for Scientific Excellence from the Portuguese Science Foundation, and in 1990 a prize from Emmanuel College, Cambridge.

Rocha is one of the most cited Portuguese scientists, having published over 500 SCI papers and 25 book chapters, with ca. 22,000 citations and Google Scholar h-index 74 (Scopus: over 18,500 citations, h=64), and 5 patent applications, and gave over 250 invited talks at conferences (mostly international). He has mentored 40 post-docs and 28 Ph.D. students, coordinated over two-dozen projects (6 European, as national PI), and consulted widely for industry.

His present research interests encompass microporous transition metal and lanthanide (Ln) silicates, photoluminescent Ln-bearing materials, and Metal Organic Frameworks for sensing applications, including nanothermometry; nanosystems for multimodal (magnetic resonance, optical and thermometry) imaging and small molecules drug delivery; solid-state NMR and X-ray diffraction.

For decades, there has been much interest for crystalline materials with frameworks exhibiting channels and cavities ('pores') of small-molecule dimensions. For historical reasons, these nanoporous solids are known as microporous materials. Zeolites, the archetypal microporous solids, are crystalline hydrated aluminosilicates with open

framework structures assembled from $[SiO_4]^{4-}$ and $[AlO_4]^{5-}$ tetrahedral units interconnected to each other by sharing all the oxygen atoms. The negative charge of the frameworks is balanced by extra-framework, exchangeable, cations. Zeolites have found real-world applications, particularly in catalysis, gas sorption and separation, and ion-exchange. Other zeolitic materials comprise aluminophosphates dubbed AlPOs, or when doped with silicon or transition metals, respectively, SAPOs or MeAPOS. Pure AlPOs are built up of alternating corner-sharing $[AlO_4]^{5-}$ and $[PO_4]^{3-}$ tetrahedra and, thus, their frameworks have no net charge, no cation-exchange properties, and little catalytic potential.

An outstanding feature of zeolites, AlPOs, and related materials is that their frameworks are all based on tetrahedral (Si, Al, and P) building units. However, microporous silicate solids built from heteropolyhedra such as tetrahedra, pentahedra, and octahedra are also known, even if they are, comparatively, much less studied and commercially explored [1]. Typically, these (so-called OPT) materials contain transition metals, in particular titanium and zirconium, or lanthanides and, in addition to the conventional zeolite properties, exhibit new features, such as magnetism and light emission, that enable a range of new applications. This talk presents selected examples of OPT materials with applications in the treatment of a medical condition, hyperkalemia (excess K^+ in serum), and in light emission (photoluminescence).

Metal Organic Frameworks (MOFs) are crystalline organic–inorganic hybrid materials with nanoporous frameworks built by linking polyatomic metal clusters entirely by strong covalent interactions. While zeolite-like silicates are highly (thermally and chemically) robust systems, allowing applications in relatively harsh conditions, it is very challenging to synthesise the desired architectures and to modify them post-synthesis. In contrast, MOFs operate in milder conditions and often lack robustness, but they are much more amenable to 'rational synthesis' and post-synthetic modification using the conventional methods of organic synthesis. Concerning applications, zeolitic materials and MOFs, thus, complement each other. In this talk I shall present some examples of my groups' research on MOFs. For example, I show that calcium bisphosphonate MOFs are promising for treating bone diseases MIL-125, a Ti-MOF, supported on textile fibres exhibits excellent anti-mosquito activity. Moreover, lanthanide-bearing MOFs for sensing temperature via light emission will also be highlighted. On a different note, MOFs

post-synthetic modification allows engineering optical centres and tuning materials' light emission. A case study will be provided.

1. Health-Related Applications

Hyperkalemia Treatment

Hyperkalemia is a serious medical condition characterised by elevated levels (>5 mmol/L) of potassium in the blood. It is a common electrolyte disorder associated with substantial morbidity. The risk of developing hyperkalemia is increased in patients with chronic kidney disease, diabetes, or heart failure, and in those receiving RAAS inhibitors. A modification of a microporous zirconium silicate developed in my laboratory (AV-13) [2] was eventually explored by the US company ZS Pharma, now part of AstraZeneca, to treat hyperkalemia [3]. The new drug Lokelma (oral intake) has been approved by FDA and the EMA and is already on the market. Lokelma binds K^+ in the gastrointestinal tract, decreasing the serum levels within one hour, following 10 g drug intake. The other drug on the market to treat hyperkalemia is a nonspecific organic ion exchange polymer resin, sodium polystyrene sulfonate, poorly tolerated by the patients. In contrast, Lokelma has a nine-fold larger K^+ binding capacity and is much more (125 times) selective than polymer resins for K^+ over Ca^{2+}, being also well tolerated.

To understand these properties, the general features of the crystal structure of AV-13, ($Na_{2.27}ZrSi_3O_9Cl_{0.27} \cdot 2.5H_2O$) are now described (Figure 1). The framework consists of corner-sharing ZrO_6 octahedra and SiO_4 tetrahedra. The latter form six-membered $[Si_6O_{18}]^{12-}$ rings interconnected by ZrO_6 octahedra. In a given layer, successive distorted-cube Zr_8 cages contain extra-framework $[Na_{6-x}(H_2O)_x](H_2O,Cl^-)$ octahedra and framework cyclohexasilicate units. The cages are accessed via seven-membered $[Zr_3Si_4O_{27}]^{26-}$ windows, with free aperture ca. 2.3×3.2 Å, one per each pseudo-cube face. The latter windows account for the high affinity and selectivity of the material (and also of Lokelma) for K^+ over, say H_3O^+, Ca^{2+} or Mg^{2+}: the former, with an unhydrated ionic diameter of 2.98 Å fits well this window while the other ions do not (respectively, 2.30, 2.00 and 1.44 Å). Because AV-13 contains considerable amounts of exchangeable Na^+ and Cl^- ions, an inconvenient feature for a drug, Lokelma was formulated to avoid this

issue as $Na_{1.5}H_{0.5}ZrSi_3O_9 \cdot 2H_2O$. It is interesting to note that this discrimination mechanism is reminiscent of the potassium ion channel in cells [4].

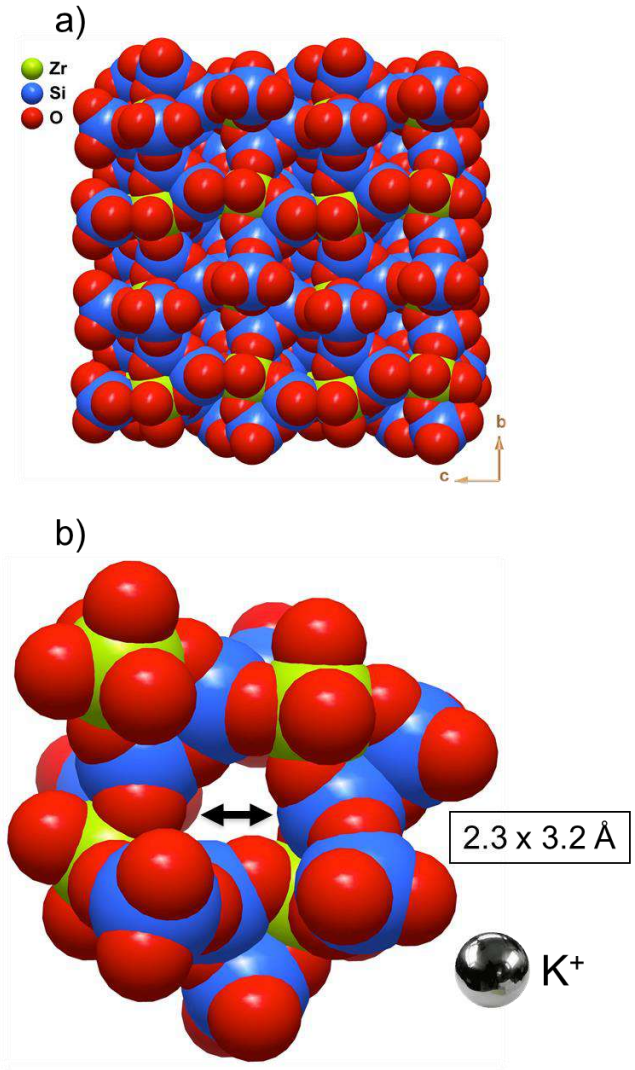

Figure 1 – a) Crystal structure of nanoporous zirconium silicate AV-13. b) Cut away showing the seven-membered $[Zr_3Si_4O_{27}]^{26-}$ windows with free aperture ca. 2.3×3.2 Å. K^+ with an unhydrated ionic diameter of 2.98 Å fit well these windows.

Bone Tissue Disorders Treatment

Bisphosphonates are primary drugs against osteoclast-mediated bone loss due to osteoporosis, Paget's disease of bone, metastasis to the bone, and malignancy-associated hypercalcemia. They were introduced to clinical practice four decades ago. Although the maintenance of an adequate calcium (and vitamin D) intake is crucial for patients

receiving bisphosphonate therapy, this is frequently overlooked. We have, thus, prepared bioactive MOFs comprising Ca^{2+} and a bisphosphonate molecule, rather than supplying calcium and bisphosphonate separately [5]. One such material is [$Ca(H_2O)_3$(p-xylylenebisphosphonate)], in which the organic ligand coordinates to four Ca atoms (Figure 2). The sevenfold Ca atoms are coordinated by four O atoms from four symmetry-related organic ligands and three water molecules. The phosphonate ligands act as pillars linking neighbouring Ca atoms, forming a framework enclosing one-dimensional inorganic chains.

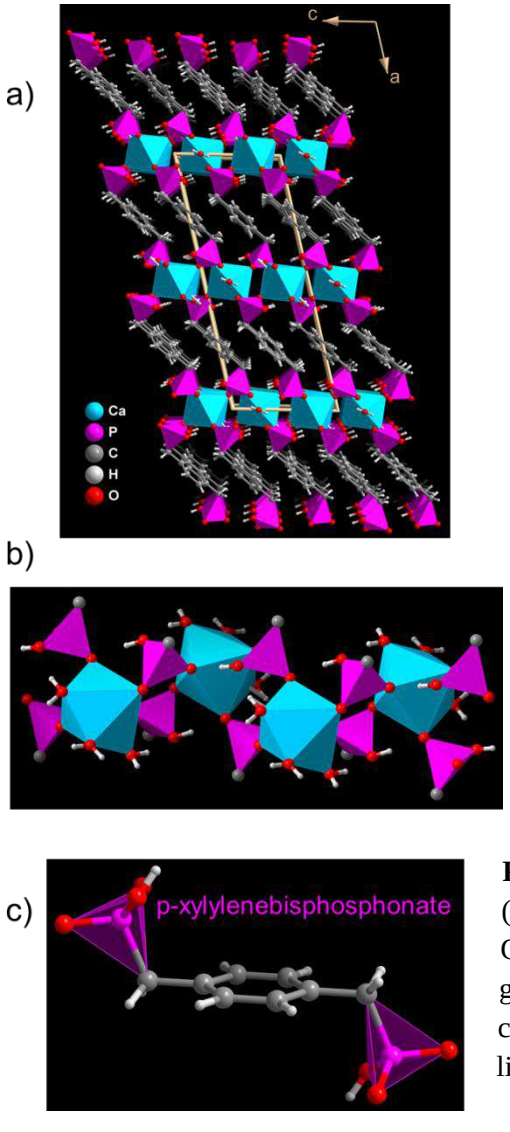

Figure 2 – a) Unit cell of [$Ca(H_2O)_3$ (p-xylylenebisphosphonate)] viewed along b axis. b) Ca^{2+} ions are interconnected via double phosphonate groups forming an infinite inorganic chain.
c) The p-xylylenebisphosphonate ligands act as pillars linking neighbouring Ca^{2+}.

Immersion of pressed pellets of this material in a simulated body fluid (Kokubo's) solution for 3-14 days evidenced the precipitation of bone-precursor phases on the surfaces, octacalcium phosphate and hydroxyapatite (Figure 3). Studies with MG63

osteoblast-like cells indicate that CaP1 is not toxic and stimulates bone mineralization and, thus, holds considerable potential for treating bone diseases, such as osteoporosis.

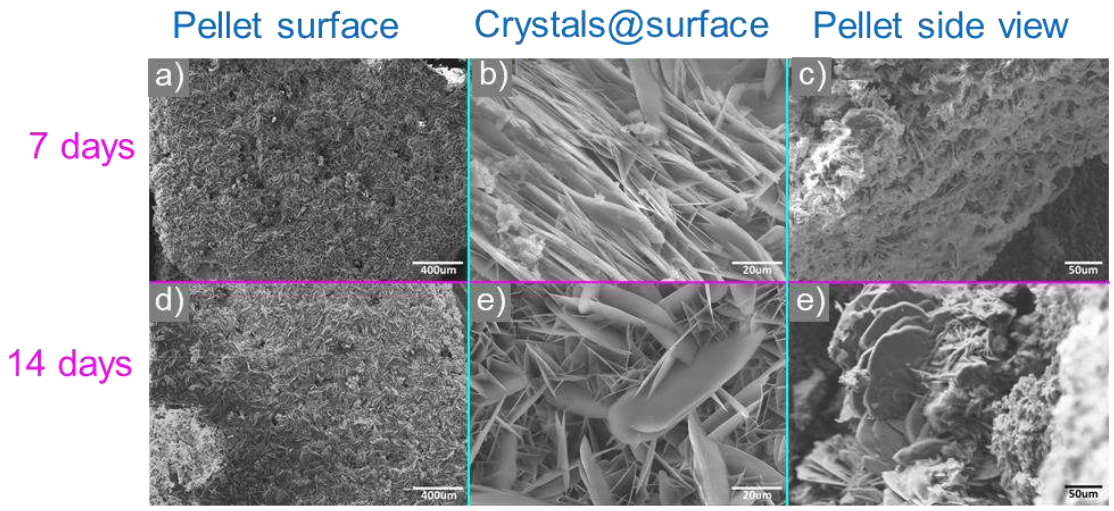

Figure 3 – SEM images of [Ca(H_2O)$_3$(p-xylylenebisphosphonate)] pellet surface after soaking in simulated body fluid for 7 and 14 days exhibiting a clear surface modification with lamellar calcium phosphate crystals: a) overview of the pellet surface;(b) high magnification showing lamellar crystal particles on the surface; c) side view of the pellet; d) overview of the pellet surface; e) high magnification showing lamellar crystal particles on the surface; f) side view of the pellet.

Antimosquito Nets Protection

Mosquitoes are the main vectors of diseases like dengue fever, yellow fever, malaria, lymphatic filariasis, and Japanese encephalitis. Fabrics offer mosquito protection, being deployed in nets, curtains, military uniforms, garments, etc., loaded with insecticides or repellents. These methods have limited efficacy due to lack of durability of the finished fabrics, as insecticide and repellents are removed during washing. Trying to overcome these caveats, we have devised [6] composites of the traditional natural fibers' cotton, viscose, and linen and a Ti-bearing metal−organic framework, NH_2-MIL-125 (Figure 4 [7]), that are very effective against mosquitoes, in the absence of any conventional insecticides. To ensure a good adhesion of the MOFs crystals to the fibers' surface, prior to coating, the fabrics were modified with 3-glycidyloxypropyltrimethoxysilane.

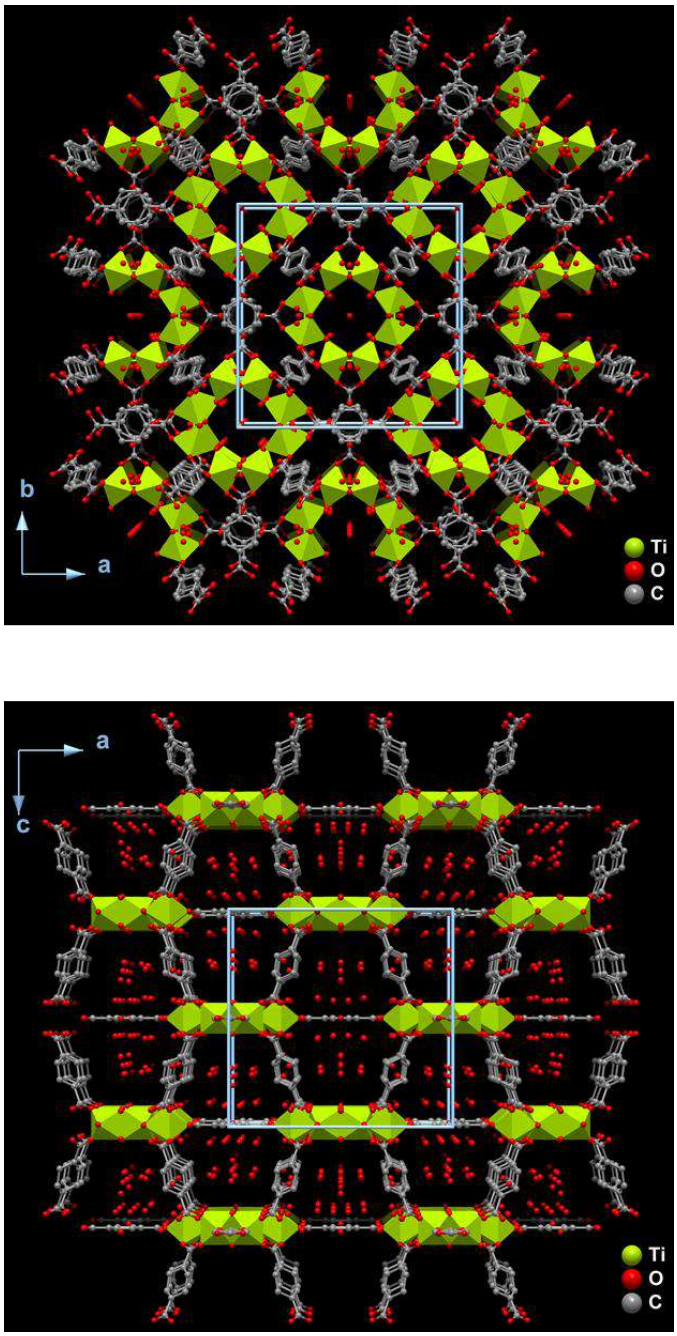

Figure 4 – Crystal structure of MOF NH_2-MIL-125 viewed along the c axis (top) and b axis (bottom).

NH_2-MIL-125 is an efficient photocalyst that decomposes modified urea resin usually present on the surface of cotton fabrics and certain volatile organics in the air, producing CO_2 that attracts mosquitoes. For, as yet, unknown reasons, the MOF kills the landing mosquitoes (Figure 5). Modified fabrics show good washing resistance, surviving more than five washing cycles.

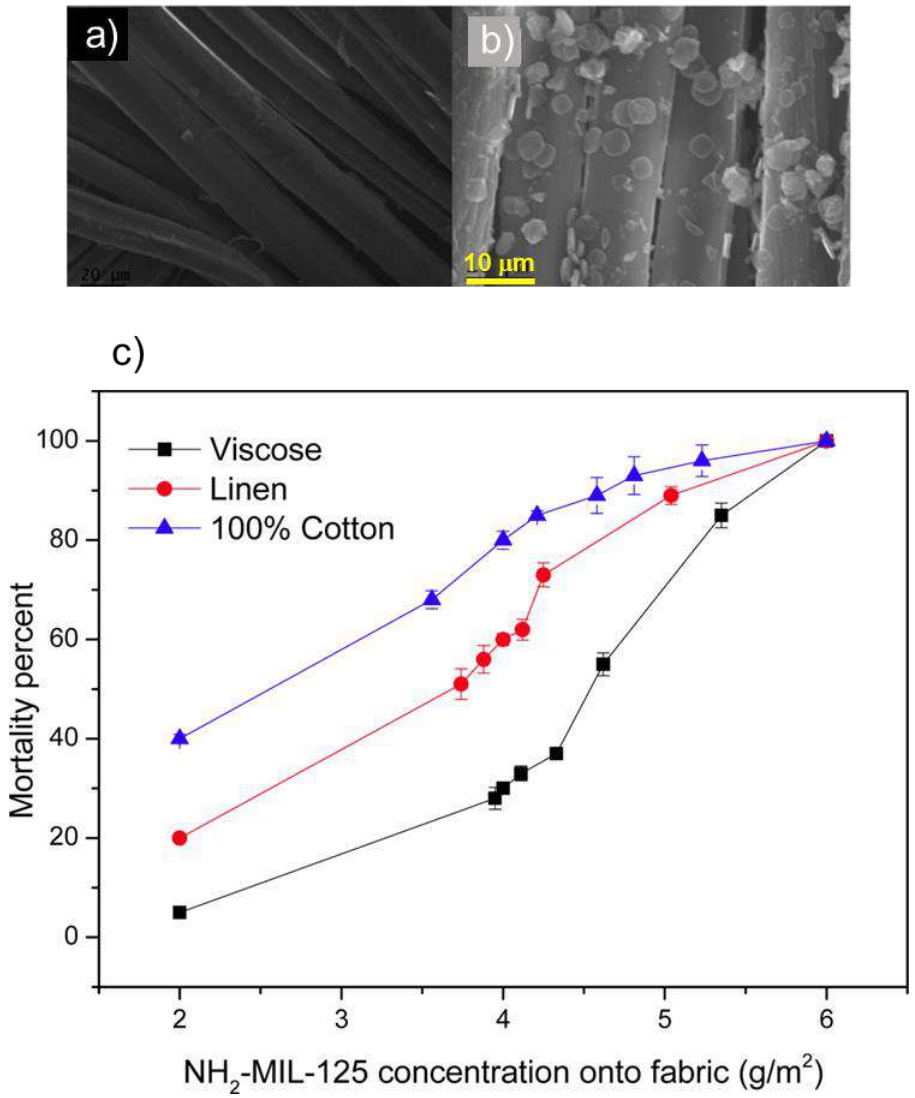

Figure 5 – SEM images of a) silica modified 100% cotton; b) NH_2-MIL-125 modified 100% cotton, showing the fabrics surface coated with small MOFs crystals. c) Relation between NH_2-MIL-125 amounts in treated fabrics and mosquito mortality, after 24 h exposed to light. In the dark, the mortality for the highest dose, 6 gm^{-2}, is 11.0% (viscose), 15.0% (linen), and 18.0% (100% cotton).

2. Light Emission-Related Applications

Light Emission by Lanthanide Silicates

In reference 1, I have reviewed the foundations of this field. The trivalent ions of the lanthanide series are characterized by a gradual filling of the 4f orbitals, from $4f^0$ (La^{3+}) to $4f^{14}$ (Lu^{3+}) with the general electronic configuration [Xe]$4f^n$. Several lanthanide ions exhibit luminescence in the visible or near-infrared (NIR) spectral regions upon irradiation with UV light. The spectroscopic features of the trivalent ions arise from

intraconfigurational f–f transitions inside their partially filled 4f shell, which is shielded by the outer filled 5s and 5p shells. My group has prepared dozens of microporous and layered lanthanide silicates and studied their luminescence properties. A case in point is the system $Na_4K_2X_2Si_{16}O_{38}{\cdot}10H_2O$, X = Eu, Tb, which illustrates the possibility of combining in a given silicate microporosity and optical activity [8]. The Tb-rich material is the first example of a microporous X-ray scintillator, *i.e.*, it exhibits X-ray (CuKα) induced luminescence (60% of the integrated intensity of Gd_2O_2S:Tb, one of the most efficient X-ray phosphors used in imaging detectors, Figure 6) [9]. The Er-rich material, in turn, is a C-band (1.54 □m**)** infrared emitter, particularly in the dehydrated form (Figure 7) [9].

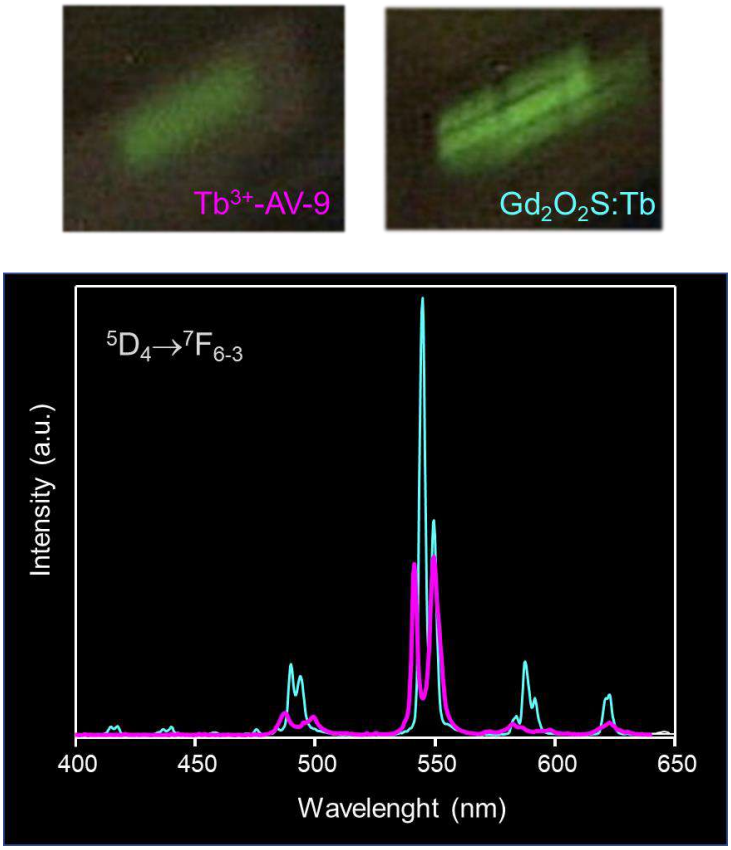

Figure 6 – Luminescence spectra of microporous $Na_4K_2Tb_2Si_{16}O_{38}{\cdot}10H_2O$ (pink line) and standard Gd_2O_2S:Tb (blue line) excited by 8.050 keV X-rays (bottom). The top panels show photographs of the emissions acquired under identical experimental conditions.

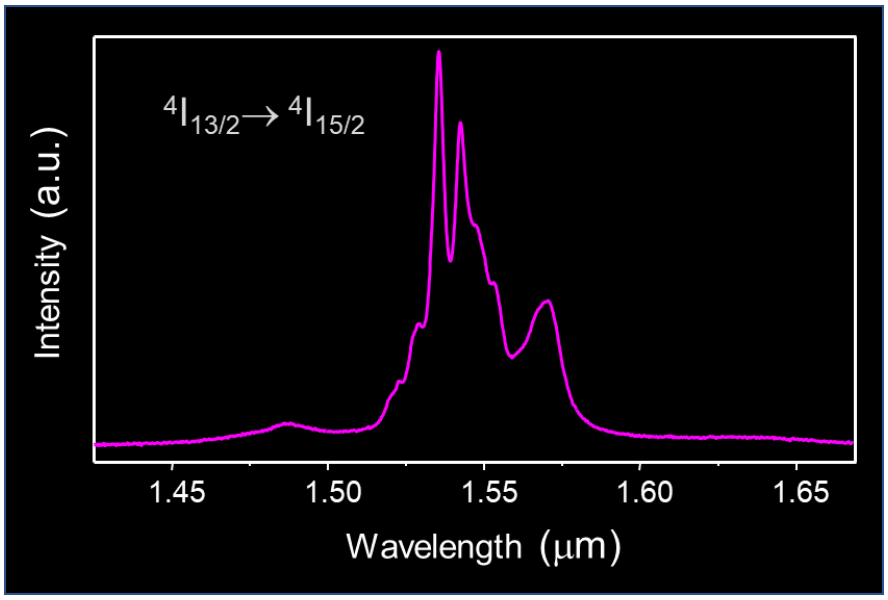

Figure 7 – Infrared emission spectra of dehydrated $Na_4K_2Er_2Si_{16}O_{38}$ recorded at 300K and excited at 514.5 nm.

Luminescent Thermometry

MOFs thermometers ascertain the absolute temperature via the intensities of two transitions of distinct emitting centres (so-called dual-centre thermometers): a ligand (linker) and a Ln^{3+} ion (Eu^{3+} or Tb^{3+}), two Ln^{3+} ions (usually Eu^{3+} and Tb^{3+}), or a dye hosted in the MOFs nanopores and a Ln^{3+} ion [10]. Most MOFs thermometers use the intensity ratio of the $^5D_4 \rightarrow {}^7F_5$ (Tb^{3+}) and the $^5D_0 \rightarrow {}^7F_2$ (Eu^{3+}) transitions as the thermometric parameter. The temperature dependence of the emission intensities is, mainly, governed by the thermally-activated energy transfer between the ligand and the metal ion (and by back transfer).

As an example, in this talk we show that spray-drying prepared MOF nanoparticles of $[(Tb_{0.914}\ Eu_{0.086})_2\ (PDA)_3(H_2O)]\cdot 2H_2O$ (PDA = 1,4-phenylenediacetic acid) (Figure 8) may be used as ratiometric luminescent nanothermometers operative over a wide range of temperatures, in particular, in the cryogenic range (<100 K), combining high sensitivity (up to 5.96 ± 0.04% K^{-1} at 25 K), reproducibility (in excess of 99%), and low-temperature uncertainty (0.02 K at 25 K) [11]. We have also reported luminescent thermometers based on OPT and other materials [12,13].

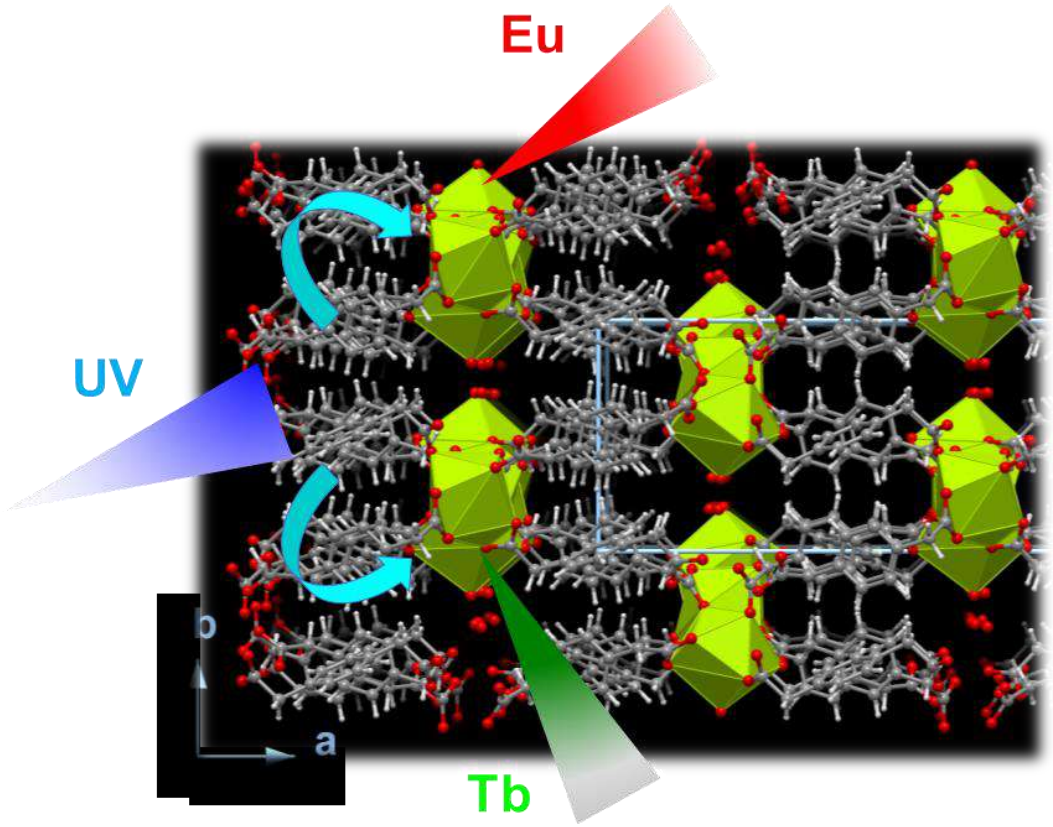

Figure 8 – Schematic ('pedagogical') representation of the emission process of $[(Tb_{0.914}Eu_{0.086})_2(PDA)_3(H_2O)]\cdot 2H_2O$ used in luminescent thermometry. The PDA ligand works an antenna capturing the incoming ultraviolet light and transferring energy to Eu^{3+} and Tb^{3+}, thus boosting their emission.

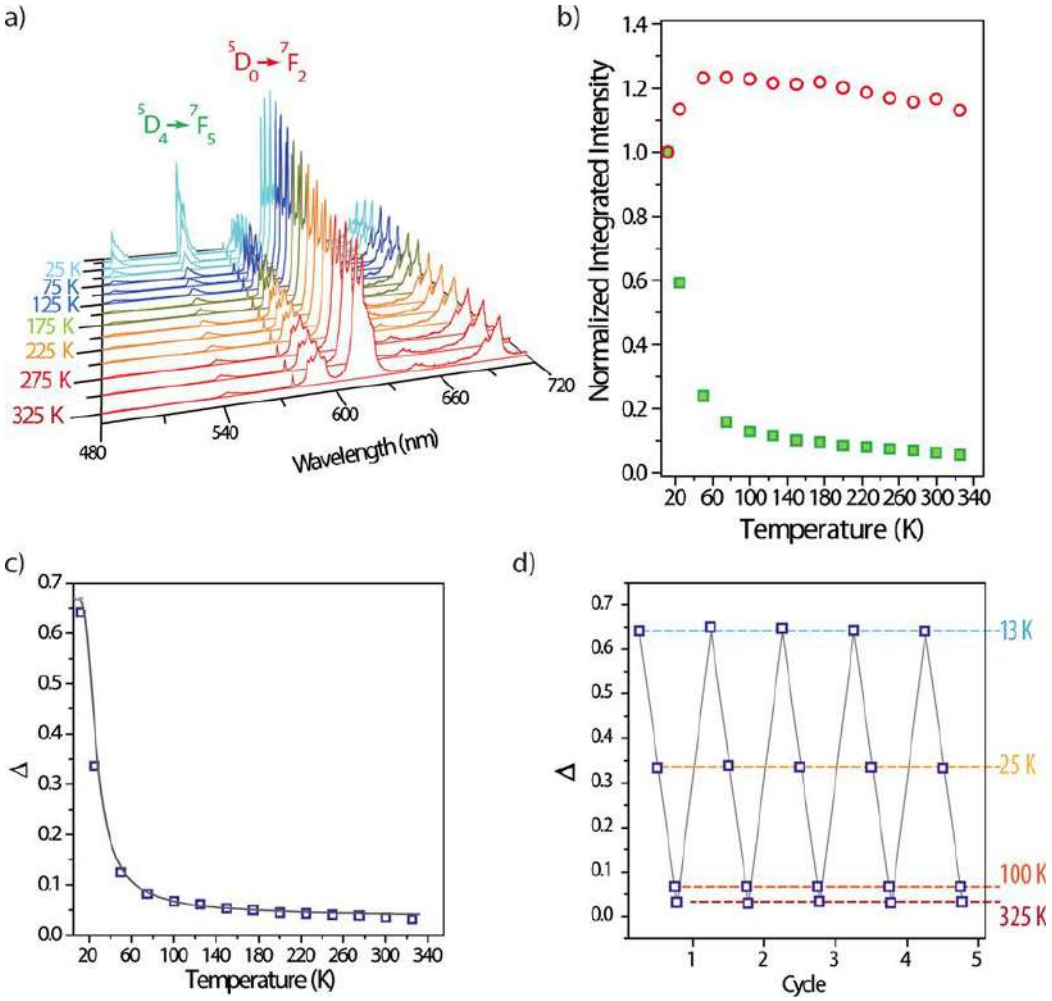

Figure 9 – a) Emission spectra (excited at 377 nm, 10–325 K) of $[(Tb_{0.914}\ Eu_{0.086})_2(PDA)_3(H_2O)]\cdot 2H_2O$; b) I_1 (green) and I_2 (red) integrated areas; c) calibration curve. The open points depict the experimental Δ parameter (I_1/I_2) and the solid line is the best fit to the experimental points; d) temperature cycling between 13 and 325 K reveals reproducibility better than 99%.

MOFs Post-synthetic Modification

An attractive feature of MOFs is the possibility of post-synthetic modification (PSM), particularly the reaction of the linkers with organic reagents, to produce materials with new functionalities. This is, in general, not possible with OPT materials. In a case in point, PSM of IRMOF-3 amino group with ethyl oxalyl monochloride and ethyl acetoacetate followed by the chelation of trivalent lanthanide ions (Figure 10) afforded efficient near infrared (Nd^{3+}) (Figure 11) and visible (Eu^{3+} and Tb^{3+}) light emitters [14].

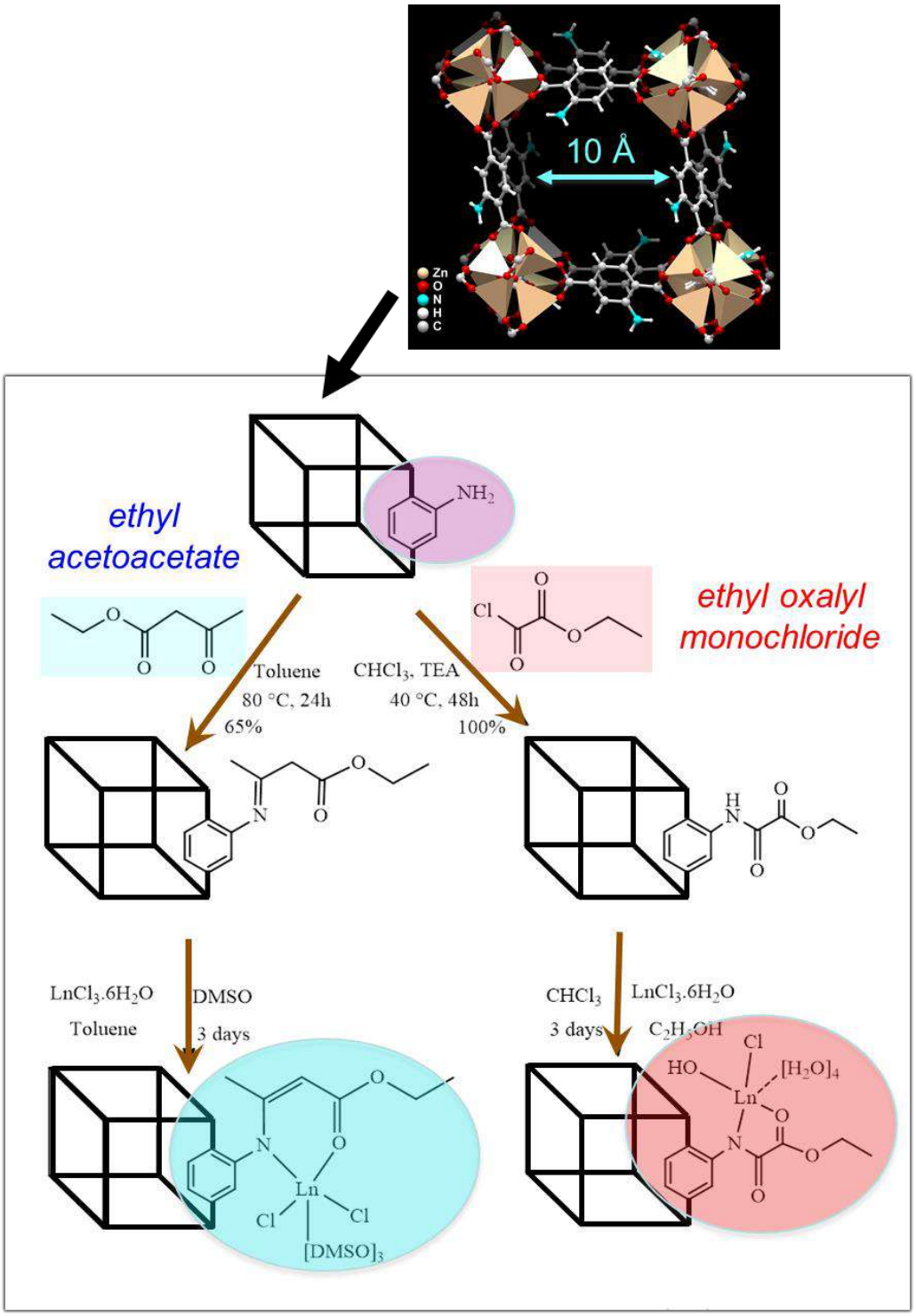

Figure 10 – Post-synthetic covalent modification of IRMOF-3 with ethyl oxalyl monochloride and ethyl acetoacetate and subsequent Nd^{3+} coordination.

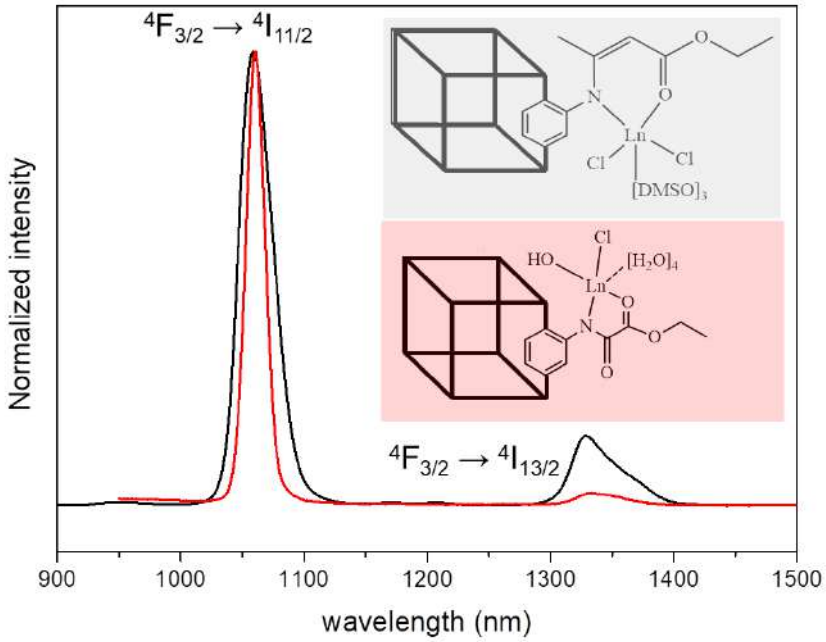

Figure 11 – Room-temperature near-infrared emission of Nd-IRMOF-3-(ethyl acetoacetate) (black line) excited at 400 nm, and Nd-IRMOF-3-(ethyl oxalyl monochloride) (red) excited at 525 nm.

Acknowledgements

"This work was developed within the scope of the project CICECO-Aveiro Institute of Materials, UIDB/50011/2020 & UIDP/50011/2020, financed by national funds through the FCT/MEC and when appropriate co-financed by FEDER under the PT2020 Partnership Agreement"

References

[1] J. Rocha, D. Ananias, F.A.A. Paz, "4.05 - Photoluminescent Zeolite-Type Lanthanide Silicates", *Comprehensive Inorganic Chemistry II (Second Edition), From Elements to Applications, Vol. 4: Solid-State Materials, Including Ceramics and Minerals",* Editors-in-Chief: Jan Reedijk and Kenneth Poeppelmeier, Elsevier, Amsterdam, 2013, pp. 87-110 (http://dx.doi.org/10.1016/B978-0-08-097774-4.00406-X).

[2] Z. Lin, A. Ferreira, M. R., Soares and J. Rocha, "Ab initio structure determination of novel small-pore metal-silicates: knots-and-crosses structures", *Inorg. Chim Acta,* 2013, **356**, 19.

[3] F. Stravos, A. Yang, A. Leon, M. Nuttall and H. S. Rasmussen, "Characterization of structure and function of ZS-9, a K^+ selective ion trap", *PLoS ONE,* 2014, **9**: e114686.

[4] W. Kopec, B. S. Rothberg and B. L. de Groot, “Molecular mechanism of a potassium channel gating through activation gate-selectivity filter coupling”, *Nature Commun.,* 2019, **10**, 5366.

[5] F.-N. Shi, J. C. Almeida, L. A. Helguero, M. H. V. Fernandes, J. C. Knowles and J. Rocha, “Calcium phosphonate frameworks for treating bone tissue disorders”, *Inorg Chem.,* 2015, **54**, 9929.

[6] R. M. Abdelhameed, O. M. H. M. Kamel, A. Amr, J. Rocha and A. M. S. Silva, “Antimosquito activity of a titanium−organic framework supported on fabrics”, *ACS Appl. Mater. Interfaces*, 2017, **9**, 22112.

[7] R. M. Abdelhameed, M. M. Q. Simões, A. M. S. Silva and João Rocha, “Enhanced photocatalytic activity of MIL-125 by post-synthetic modification with Cr^{III} and Ag nanoparticles”, *Chem. Eur. J.,* 2015, **21**, 11072.

[8] D. Ananias, A. Ferreira, J. Rocha, P. Ferreira, J. P. Rainho, C. Morais and L. D. Carlos, “Novel microporous europium and terbium silicates”, *J. Am. Chem. Soc.,* 2001, **123**, 5735.

[9] D. Ananias, J. P. Rainho, A. Ferreira, J. Rocha and L. D. Carlos, “The first examples of X-ray phosphors, and C-band infrared emitters based on microporous lanthanide silicates”, *J. Alloys Compounds,* 2004, **374**, 219.

[10] J. Rocha, C. D. S. Brites and L. D. Carlos, “Lanthanide Organic Framework luminescent thermometers”, *Chem. Eur. J.,* 2016, **22**, 14782.

[11] Z. Wang, D. Ananias, A. Carné-Sánchez, C.D.S. Brites, I. Imaz, D. Maspoch, J. Rocha and L.D. Carlos, “Lanthanide–organic framework nanothermometers prepared by spray-drying”, *Adv. Funct. Mater.,* 2015, **25**, 2824.

[12] D. Ananias, F.A. Almeida Paz, D.S. Yufit, L.D. Carlos and J. Rocha, “Photoluminescent Thermometer Based on a Phase-Transition Lanthanide Silicate with Unusual Structural Disorder”, *J. Am. Chem. Soc.,* 2015, **137**, 3051.

[13] C. D. S. Brites, X. Xie, M. L. Debasu, X. Qin, J. Rocha, X. Liu, X. and L. D. Carlos, *Nature Nanotech,* 2016, **11**, 851.

[14] R. M. Abdelhameed, L. D. Carlos, P. Rabu, S. M. Santos, A. M. S. Silva and J. Rocha, “Designing near-infrared and visible light emitters by post-synthetic modification of Ln^{+3}-IRMOF-3”, *Eur. J. Inorg. Chem.,* 2014, 5285.

DESIGN OF ARTIFICIAL ENZYMES USING THE METALS OF THE PERIODIC TABLE

José J. G. Moura

LAQV-REQUIMTE, DQ, FCT NOVA, Portugal. email: jose.moura@fct.unl.pt

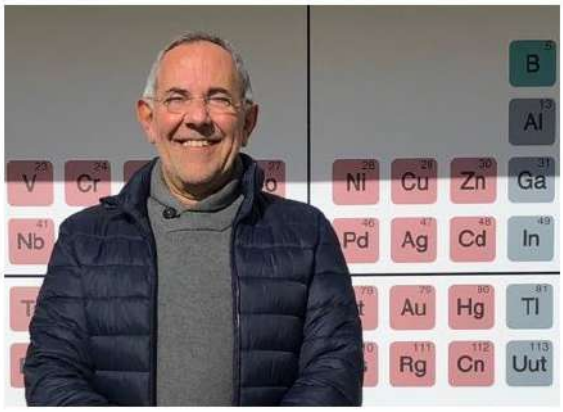

José J. G. Moura has a degree in Chemical Engineering and a PhD in Chemistry and is Full Professor of Chemistry at the Department of Chemistry, Faculdade de Ciências e Tecnologia, Universidade Nova de Lisboa (FCT NOVA). The main field of research is Bioinorganic Chemistry and the role of Metals in Biology. He published more than 400 articles indexed in ISI Web of Knowledge, with an H-index of 60 and oriented 30 PhD Thesis. For extended periods Research Specialist at University of Minnesota (US) and Adjunct Professor at University of Georgia, Athens (US). Past President of Chemistry Department and President of Scientific Council at FCT NOVA, Portuguese Delegate to COST and INTAS, a member of Scientific Panel in the Calouste Gulbenkian Foundation and FCT-MCTES, NST (US) Specialized Panel, and of several scientific editorial boards. In 2006, he was elected Member of Academia das Ciências de Lisboa and in 2010, elected President of the Society of Biological Inorganic Chemistry, for 2 years. Scientific Award MCTES.
Scientific keywords: Bioinorganic, Biophysics, Biocatalysis, Energy Bioconversion (Hydrogen), Role of metals in Biology (heme and non-heme iron, molybdenum, tungsten, nickel, copper, vanadium and cobalt), Inorganic systems as models for biocatalysis, Spectroscopy (NMR, EPR and Mössbauer), (Bio)Electrochemistry, Protein-Protein interactions.
Other interests: Director of the Campus FCT Library and of the Department of Documentation and Culture, promoting Culture/Scientific interfaces, coordinating multidisciplinary curator activities (Art and Science).
http://sites.fct.unl.pt/biologicalchemistryatfctunl
http://docentes.fct.unl.pt/jjgm

UNESCO celebrated, in 2019, the "International Year of the Periodic Table of Chemical Elements" and the 150th anniversary of its creation by Dmitry Mendeleev. Metalloproteins and metal-containing enzymes are well known to be essential to life. The elucidation of structural and functional aspects of metal sites in enzymes has been a goal of model studies putting together Inorganic Chemistry and Synthetic Biochemistry. In particular, synthetic peptides and small proteins involving rich sulfur coordination sites have been extensively used, such as Rubredoxins (Rds) and analogues. The four-Cysteine

metal coordination motif, available in Rds, has the possibility of coordinating a wide variety of metal ions, with particular interest in aiming to model complex metalloproteins.

Artificial Enzymes

Enzymes are complex molecules that may or not contain metals at the catalytic site, where chemical transformations occur with amazing selectivity and at high rates. Of the known enzymes, one third contain metals, coordinated by the side chains of amino acids of the polypeptide chain and/or cofactors. In this case, the substrate is activated at the metal site.

Due to the chemical complexity of the system (large molecular masses, multiple sub-unit composition and intricated architectural structures involving metals) the study of model compounds, retaining functional, structural (or both) characteristics has the advantage of working with a smaller size problem, more suitable for biophysical studies enabling an inorganic chemistry approach for revealing the metal active site properties. Metalloenzymes use a wide range of metals in a variety of structural arrangements and geometries, most with parallel with inorganic compounds, but others still a challenge for synthetic chemistry. Iron contained in iron-sulfur centers and in hemes are the most ubiquitous, but several other transition metals have specific roles, such as Ni, Mo, Cu, Zn and others. Modelling efforts also represent an opportunity for further exploring new applications and functionalities.

The chemical design of models for metalloprotein active sites can be based in small inorganic compounds, and now extend to peptides, protein-based synthetic analogues and simple proteins that are used as templates (or scaffolds) [1-4].

In this extended report of the lecture given at Academy of Sciences of Lisbon, at the Periodic Table celebratory sessions, we address metal substituted Rubredoxins as a scaffold for the construction of models of native metalloenzymes.

Why Rubredoxins?

Rubredoxins (Rds) are small iron containing proteins (approx. 5-6 KDa), which structural and function have been most explored, we could say, by any spectroscopic and structural tool available. Rds provide 4S containing ligands (Cysteines-Cys) in a very

well-defined metal coordinating site. Rds are easy to over-express and enable easy amino acid site direct mutagenesis. It is feasible to accomplish the total chemical synthesis of such a small polypeptide chain and quite facile to replace native iron site, by a wide range of metal.

Artificial Enzymes for Metal-Sulphur rich Coordination Sphere

Important biochemical functions are performed by metalloproteins active sites with transition metals contained in sulphur-rich environments. Several studies had probed the chemistry of thiolates and transition metals, with very relevant accomplishments [4]. Many examples of nickel, copper, zinc and molybdenum (tungsten) in coordination spheres dominated by sulphur atoms are found in key enzymes.

The Fe-site in Rd is stabilized by the native folded polypeptide structure that provides four cysteinyl residues as ligands to the metal, in a tetrahedral arrangement. Due to the interplay between side chain amino-acid residues and metals, derivatives can be envisaged in two ways:

— site specific direct mutagenesis of crucial amino acids at the active site (specially coordinating ones)
— substitution of native metal (iron) by a wide range of metals (^{57}Fe(II), Co(II), Ni(II), Cu(I), Zn(II), Cd(II), Hg(II), Ga(III), In(III), Ge(IV), Hg(II) and Mo(VI,V,IV)) with different objectives, as detailed above [5-15].

The apo Rd is a scaffold and the replacement of native iron by other metals is simples, following a simple process of metal reconstitution/substitution, a simple chemical procedure.

The design of metal substituted Rds aims two main proposes [3]

— to be used as spectroscopic probes for the elucidate the structure/function aspects, and
— to synthetize simple (bio)models of active site of metalloenzymes.

Under this context, the metal substituted Rds, so far prepared, have precise applications:

— replacements by ^{57}Fe, Zn, Co, Cd, Ga, In, and Hg originate specific structural probes for unrevealing structural details and properties of the metal site *per se*, and
— metals such Zn, Ni, Cu, as well as Mo (and recently, W) in sulphur-rich coordination sites are promising models for metal centres in metalloenzymes.

Figure 1 compiles examples of three different enzymes that contain metals in a Sulphur rich environment, most relevant in Energy, Health and Agriculture/Environment. The 3D structures are shown as well as detailed structures of the Sulphur rich coordination found around the metals. [15-18]

Hydrogenase is a Ni-Fe enzyme involved in hydrogen consumption and evolution, relevant for the development of projects on clean fuels - Hydrogen). Xanthine oxidase is a member of mononuclear Mo containing enzymes relevant for health-related problems (i.e. Gout) whose structure drive to the design of pharmaceutical drugs. The nitrogen fixation process, a part of the N-cycle is responsible for the production of di-nitrogen in a assimilative form of nitrogen (ammonia) of primordial importance in agriculture, and contains Mo at the active site in a complex Mo-Fe structure.

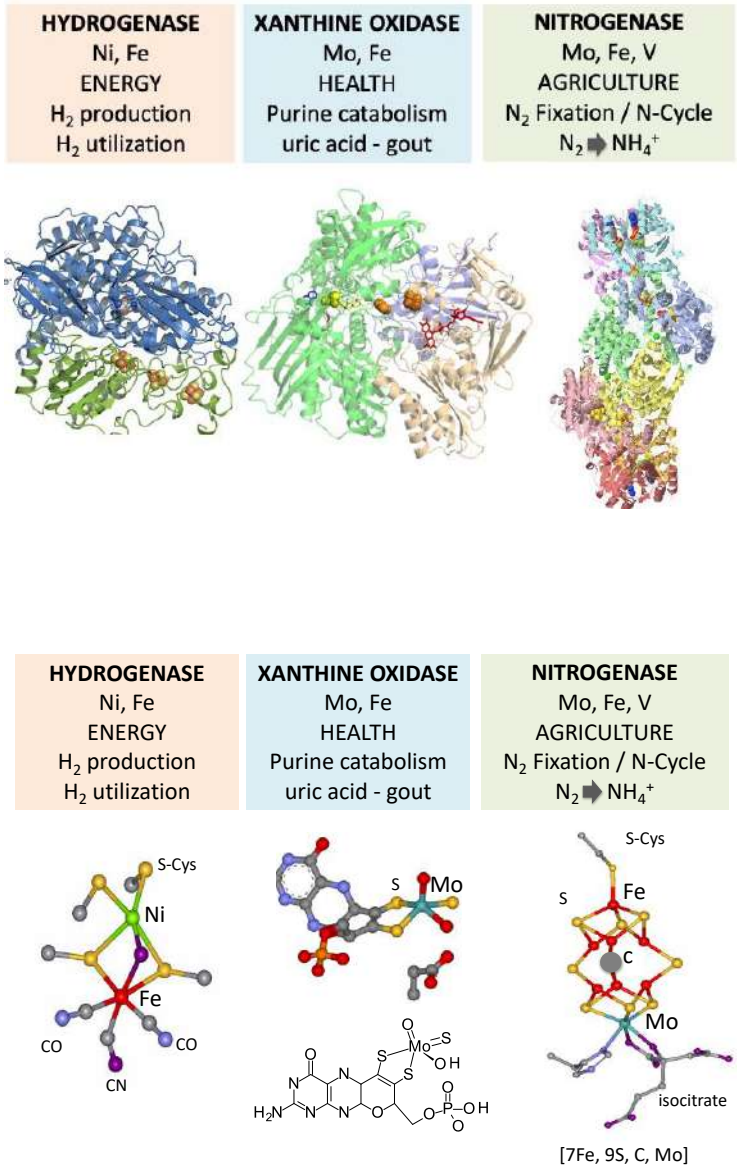

Figure 1

PANEL A - Complex enzymes with sulphur-rich-metal active sites. Examples relevant for Biology (Energy, Health and Environment)

PANEL B - Visualization of the metal-sulfur-rich active centers (the polypeptide was removed).

Ni-Substituted Rubredoxin

There are three classes of bacterial Hydrogenases: [NiFe,] [FeFe] and [Fe only] [18]. The active site of [NiFe] Hydrogenases (as seen in Figure 1) [15, 18,19] is rich in sulfur and the Ni moiety is coordinated by four sulfur atoms (two from Cysteine residues and two sulfur atoms from the chemical bridge established between Ni and Fe, in a

distorted tetrahedral geometry) [15,18]. The substitution of Fe by Ni in Rds is a plausible structural and functional model of the Ni moiety in the [NiFe] cluster in hydrogenase [21]. The Ni(S4) site in *Desulfovibrio* Rds was probed by different spectroscopic tools including UV-vis, NMR, and low temperature MCD [7,9,10,11,12,20]. The resolution of the 3D structure of Rd-Ni isolated from *C. pasteurianum* corroborates with four coordinating S-Cysteine binding to Ni(II) in a tetrahedral arrangement, matching the one depicted for the Ni moiety of bacterial hydrogenases [15-18].

Functional aspects were probed with this model in order to mimic the functional aspects of nickel-containing hydrogenases: hydrogen production, deuterium-proton exchange, and inhibition by carbon monoxide [21]. Ni(II) derivatives built in Rds from *D. vulgaris* Hildenborough and P. *furiosus* can be oxidized and are EPR active with spectral parameters very closeto those observed in Ni-C signal of Hydrogenases, assigned to a Ni(III) oxidation state [7,21]. Electro-catalysis (Hydrogen production) was reported to be promote by Ni-Rd [22].

Mo- Substituted Rubredoxin

Molybdenum (and tungsten) is found in complex enzymes such as Nitrogenase include in a complex metal site Mo-7Fe-9S-C or in mononuclear Mo(W) enzymes, whose active site is coordinated to one or two pyranopterin molecules, and (or not) to side chain amino acids from the polypeptide chains (Figure 1). In this last case, the pyranopterins and Cysteines provide a rich sulfur environment to the metal Mononuclear Mo(W)-containing enzymes [23,24] comprehends a large group of enzymes classified in different families (Xanthine oxidase, DMSO reductase and Sulfite oxidase) and carry out atom transfer reactions between other Mo(W) gain a special relevance in Bioinorganic Chemistry, being recognized as essential metals to life and the heaviest elements used by biology.

Therefore, Rds replaced by molybdenum, synthesized from the apo form of *D. gigas*, are potential models for the catalytic site of mononuclear Mo-enzymes, where four Cys residues mimics a pyranopterin ligation [xx], and additional ligands containing O or S atoms may complete de coordination environment. The Mo-Rd compound was obtained replacing Fe in Rd isolated from Desulfobrio gigas [25].

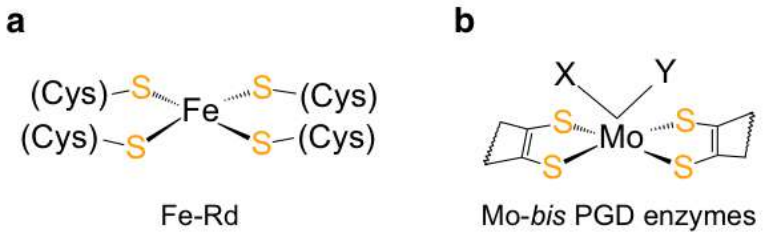

Figure 2. Schematic representations of structures of a) [Fe(S-Cys)4] in Rd and (b) mononuclear molybdenum enzymes (Mo-*bis*-pyranopterin), where X,Y are coordination sites with a large versatility (X,Y=O, S, Se, Asp, Ser, S-Cys, Se-Cys). The Mo-Rd compound was synthesized from the apo form of *D. gigas* Rd [23,25].

Apo-Rd does not provide enough coordination sites to satisfy the higher coordinated numbers required by Molybdenum. The four S-Cysteine residues ligate Mo, being complemented by other exogenous ligands, such as oxygen and thiol, forming a Mo(VI)-(S-Cys)$_4$(O)(X) complex, where X represents –OH or –SR. The Rd-Mo centre is prepared in a Mo(VI) oxidation state, and can attained other oxidation states: Mo(IV) via Mo(V). Mo(V) species (EPR active) observed in reduced reconstituted Mo-Rd, are most relevant for the study of catalytic mechanism (Figure 3).

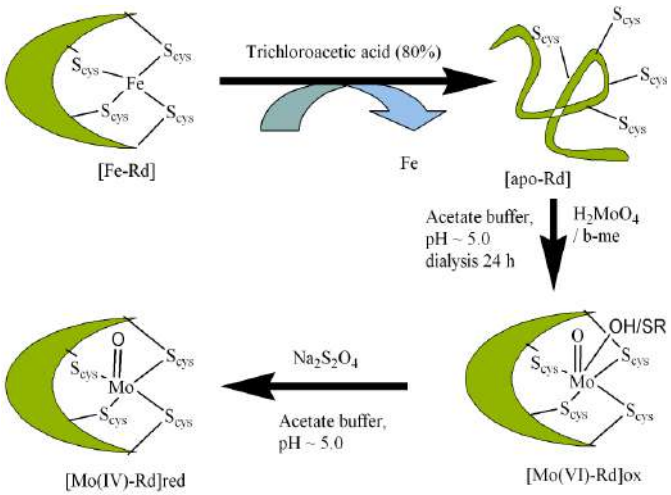

Figure 3. Schematic representation of reconstitution apo-Rd with molybdenum. The figure also indicates coordination modes and oxidation states of molybdenum-substituted-Rd (Mo-Rd). (from [3])

Rd-Mo model provides a simple complex for the study of spectroscopic properties of resting and reduced forms for the DMSO family of mononuclear Mo-*bis* pyranopterin-containing enzymes. The molybdenum site built in Rds was shown to be able to promote oxo-transfer reactions, one of the typical reactions performed by mononuclear Molybdenum enzymes [23,24].

An extension to other biological relevant metals can be consulted in an compreensive review article (3), that was a guide line to this lecture.

Acknowledgements:

This work was supported by the Associate Laboratory for Green Chemistry-LAQV, which is financed by national funds from Fundação para a Ciência e a Tecnologia, MCTES (FCT/MCTES; UID/QUI/50006/2019). Thanks are given to many relevant contributions from Isabel Moura, Marta S. Carepo, Luísa B. Maia, Sofia R. Pauleta, Biplad K. Maiti, Maddalena Elia and Vincent Pecoraro.

8. References

1 Xing G., DeRose V.J. Curr. Opin. Chem. Biol. 5 (2001) 196-200.

2 Kennedy M.L., Gibney B.R. Curr. Opin. Struct. Biol. 11 (2001) 485-490.

3 Maiti B.K., Almeida R.M., Moura I., Moura J.J.G. Coor. Chem Rev. (2017) 352, 379

4 Mathieu E., Tolbert A.E., Koebke K.J., Tard C., Iranzo O., Penner-Hahn J.E., Policar C., Pecoraro Chemistry (2020) 26, 249-258.

5 Rao P.V., R.H. Holm R.H. Chem. Rev. 2004) 104, 527-560.

6 Henkel G., Krebs B., Chem. Rev. (2004) 104,801-824.

7 Parkin G. Chem. Rev. (2004) 104, 699-768.

8 Kowal A.T., Zambrano I.C., Moura I., Moura J.J.G., LeGall J., Johnson M.K., Inorg. Chem. (1988) 1162-1166.

9 Petillot Y., Forest E., Mathieu I., Meyer J., Moulis J.M., Biochem. J. (1993) 296, 657-661.

10 Mahe M., Cross M., Wilce M.C.J., Guss J.M., Wedd A.G. Acta Crystallogr. Section D 60 (2004) 298-303.

11 Goodfellow B.J., Duarte I.C.N., Macedo A.L., Volkmann B.F., Nunes S.G., I. Moura I., Markley J.L., Moura J.J.G., J. Biol. Inorg. Chem.15 (2010) 409-420.

12 LeMaster D.M., J.S. Anderson J.S., G. Hernandez G., *Biochemistry*, 45 (2006) 9956- 9963.

13 Thapper A., A.C. Rizzi A.C., Brondino C.D., Wedd A.G., Pais R.J., Maiti B.K., Moura I., Pauleta S.R., Moura J.J.G. J. Inorg. Biochem.127 (2013) 232-237.

14 Maiti B.K., Maia L.B., Silveira C.M., Todorovic S., Carreira C., Carepo M.S., Grazina R., Moura I., Pauleta S.R., JMoura J.J.G. J. Biol. Inorg. Chem.20 (2015) 821-829.

15 Volbeda A., Charon M.H., Piras C., E.C. Hatchikian E.C., M. Frey M., Fontecilla- Camps J.C. Nature, (1995) 373, 580-587.

16 Enroth C., Eger B.T., Okamoto K., Nishino T., Nishino T., Pai E.F. Proc. Natl. Acad. Sci USA. (2000) 97, 10723-8.

17 Einsle O., Tezcan F.A., Andrade S.L., Schmid B., Yoshida M., Howard J.B., Rees DC. Science (2002) 297, 1696-700.

18 Hu Y., Ribbe M.W. J. Biol. Inorg. Chem. (2015) 20, 435-45.

19 Ogata H., Lubitz W., Higuchi Y. J. Biochem. (2016) 160, 251-258.

19 Garcin E, Montet Y, Volbeda A, Hatchikian C, Frey M, Fontecilla-Camps JC. Biochem. Soc. Trans. (1998) 26, 396-401.

20. Moura J.J.G., M. Teixeira M., I. Moura I. Pure and App. Chem. 61 (1989) 915-921.

21 P. Saint-Martin P., P.A. Lespinat P.A., G. Fauque G., Y. Berlier Y., J. LeGall J., I. Moura I., M. Teixeira M., A.V. Xavier A.V., J.J.G. Moura J.J.G. Proc. Natl. Acad. Sci. USA. 85 (1988) 9378- 9380.

22 Slater J.W., Shafaat H.S. J. Phys. Chem. Lett. 6 (2015) 3731-3736.

23 Maia, L.B., Moura I, and Moura J.J.G. Molybdenum and Tungsten Enzymes: Biochemistry (2017) RSC Metallobiology Series No. 5 p.1-80.

24 Hille R., Hall J., Basu P. Chem Rev. (2014) 114, 3963-4038.

25 Maiti, L.B. Maia, C.M. Silveira, Todorovic S., Carreira C., Carepo M.C., R. Grazina R., Moura I., Pauleta S.R., Moura J.J.G. Biol. Inorg. Chem. 20 (2015) 821-829.

C — Carbon:
an Essential Element

THE VERSATILITY OF CARBON: CUSTOM-MADE NANOSTRUCTURES

José Luís Figueiredo

Laboratório Associado LSRE-LCM, Faculdade de Engenharia, Universidade do Porto
jlfig@fe.up.pt

José Luís Figueiredo (PhD, Imperial College, London, UK, 1975) is Professor Emeritus at the Chemical Engineering Department, Faculty of Engineering, University of Porto, Portugal, and Director of the Laboratory of Catalysis and Materials (LCM), a research unit incorporated into the Associate Laboratory LSRE-LCM. Most of his work has been focused in the areas of Carbon Materials and Heterogeneous Catalysis. Published 8 books and more than 300 papers in scientific journals.

He was distinguished with several scientific awards, namely: FISOCAT Senior Award (2018), Ibero-American Federation of Catalysis Societies (FISOCAT); Prize Ferreira da Silva (2014), Portuguese Chemical Society, SPQ; Lee Hsun Research Award on Materials Science (2014), Institute of Metal Research, Chinese Academy of Sciences; Award for Scientific Excellence (2011), Fac. Engineering, Univ. Porto (FEUP); Stimulus for Scientific Excellence (2004), Ministry for Science and Higher Education, Portugal; Scientific Research Award APDF (2004), Portuguese Association of PhD Students in France.

Member of the Editorial Boards of the journals CARBON and Fuel Processing Technology (Elsevier), Periodica Polytechnica – Chemical Engineering (Budapest University of Technology and Economics), and Catalysts (MDPI).

Corresponding Member of the Academy of Sciences of Lisbon since 2014. Honorary Member of the Portuguese Chemical Society (SPQ) since 2017.

Abstract

In spite of being one of the simplest elements in the Periodic Table, carbon can form an enormous variety of stable structures. In fact, there is a whole branch of Chemistry dedicated to its compounds. On the other hand, there is also a branch of Materials Science dedicated to the multiple forms of the element as a material. Diamond (sp^3 hybridization) and graphite (sp^2 hybridization) are the two ordered carbon allotropes known since ancient times. The discovery of the fullerenes in 1985, followed by the observation of carbon nanotubes in the early 1990s', marks the beginning of the new era of carbon nanomaterials. These include both *nanosized* carbons, as well as *nanostructured* carbons, most of them exhibiting the graphitic structure. The edges of the

graphene layers and structural defects provide reactive sites where various types of surface functional groups can be formed. *Doping* is also possible, when carbon atoms in the graphite lattice are replaced by heteroatoms, such as nitrogen or boron. Thus, in addition to controlling the texture and structure of these materials, we are also able to tune their surface chemical properties, allowing the design of *custom-made* carbons for specific applications. The methodologies used for the synthesis of these carbon nanomaterials will be reviewed, and selected applications will be discussed.

1. From carbon atoms to carbon materials

Carbon is the element number 6 in the Periodic Table, and its corresponding ground state electronic configuration is 1 s^2 $2s^2$ $2p^2$. All four orbitals of the outer shell (one s- and three p- orbitals) are involved in bonding, as they form hybrid orbitals: either two sp- and two p- orbitals; three sp^2- and one p- orbitals; or four sp^3- orbitals. The hybrid orbitals are involved in σ-bonds, while the p-orbitals are involved in π-bonds [1].

The four sp^3- orbitals are oriented in a tetrahedral arrangement, forming angles of 109.5º. This is the type of hybridization found in C compounds involving only single bonds, such as CH_4. Covalent bonding between carbon atoms with this configuration leads to the diamond structure.

The three sp^2- orbitals form angles of 120º in a planar trigonal arrangement. This type of hybridization is found in carbon compounds with double bonds, and in carbon materials with the graphitic structure. Graphite consists of stacked layers of carbon atoms covalently bonded in a hexagonal lattice (graphene layers), the layers being held together by weak van der Waals forces.

The two sp- orbitals are opposed (angle of 180º) leading to a linear molecular geometry, as found in compounds with triple bonds, such as acetylene. The corresponding carbon allotrope (carbyne) would consist of an infinite linear chain of carbon atoms, either with alternating single and triple bonds, -C≡C-C≡C- (polyyne structure), or with only double bonds, =C=C=C=C= (cumulene structure). These structures are the subject of intense research, but they are highly reactive and unstable, and do not exist in nature (at least in pure form).

Diamonds may be "*a girl's best friend*" (Marilyn Monroe dixit), but it is the graphitic structure that dominates the industrial applications of carbon materials. The most important carbon products, in terms of their global consumption and market value,

are listed in Table 1, together with their main applications. These carbon products represent a global market value in excess of 250 x 10^9 US dollars per year.

Table 1 – The most important products of the carbon industry

Product	Consumption (Mt/y)	Market value (10^9 $/y)	Main application
Metallurgical coke	> 350	> 200	Production of iron in the blast furnace
Prebaked anodes	> 30	> 10	Aluminium smelting
Carbon black	> 15	> 15	Filler for rubber (tires)
Graphite electrodes	> 1	> 15	Steelmaking in the electric arc furnace
Activated carbon	> 3	> 5	Adsorbent
Carbon fibers	> 0.3	> 6	Composite materials

2. The dawn of carbon nanomaterials

The discovery of C_{60} (Buckminsterfullerene) by Harold Kroto, Robert Curl and Richard Smalley[1], in 1985 [2], triggered an intense research activity in the area of carbon nanostructures. In fact, C_{60} is one member of a whole family of fullerenes, ranging up to giant molecules such as C_{540}. Fullerenes are molecular solids, consisting of covalently bonded carbon atoms, forming polyhedra with hexagonal and pentagonal faces. In 1991, while synthesizing fullerenes by arc discharge, S. Iijima reported the formation of tubular structures consisting of several concentric graphene layers (multiwalled carbon nanotubes, MWCNTs) [3]; two years later, the observation of single-walled carbon nanotubes (SWCNTs) was reported almost simultaneously by two independent teams [4,5]. These findings are usually highlighted as marking the birth of carbon nanomaterials, but this is really not true. Indeed, there are several reports dating back to the 1950's showing carbon structures that can be unmistakably identified as MWCNTs, although they were not called "nanotubes" at the time [6,7]. Such materials were then described as carbon (or graphite) filaments, sometimes as carbon "whiskers". This area

[1] These three scientists received the 1996 Nobel Prize in Chemistry for the discovery of the fullerenes.

of research became very active in the 1970's, when various groups attempted to understand the mechanisms of carbon formation from hydrocarbons on metal surfaces and catalysts. Considerable insight into the subject was achieved when it became possible to follow the reaction continuously. L.S. Lobo used a microbalance to study carbon formation on different metals, and found that only Ni, Fe and Co were active catalysts; moreover, he observed that they were not deactivated during the process. Based on accurate kinetic measurements, Lobo proposed a mechanism that involved the diffusion of carbon through the metal, driven by a concentration gradient; thus, carbon would precipitate at the back of the metal crystallites, which would therefore be carried on top of the growing deposit, keeping their surface available for reaction and explaining the constant rates of carbon formation observed [8,9]. At about the same time, R.T.K. Baker developed a controlled atmosphere electron microscopy (CAEM) technique that allowed to observe the catalyst *in-situ* under reaction conditions. While studying the Ni catalyzed decomposition of acetylene, he recorded the growth of carbon filaments carrying the metal particles on top. He proposed basically the same mechanism as Lobo, but invoked a temperature gradient (from the exothermic acetylene decomposition) as the driving force for carbon diffusion through the metal particles [10]. This assumption is obviously wrong: a temperature gradient drives heat transfer, not mass transfer; similar growth of carbon filaments is observed when the hydrocarbon decomposition is endothermic (e.g., in the case of methane); moreover, it violates the causality principle [11].

In general, the carbon filaments observed and reported by Baker on a variety of metals and alloys are not tubular, and can be classified as fishbone (or herringbone), platelet and ribbon, according to the orientation of the graphene layers with respect to the filament axis. In the most frequent configuration (fishbone), the graphene layers are at an angle, being neither parallel nor perpendicular to the axis [12]. In its "*Recommended terminology for the description of carbon as a solid*", IUPAC proposed the designation of "filamentous carbon" for such materials [13], but they are currently known as "carbon nanofibers" (CNFs), a designation that was introduced by Nelly Rodríguez [14].

Both CNFs and MWCNTs can be considered as different types of filamentous carbon, as they can be obtained by similar procedures from the decomposition of hydrocarbons in the presence of metal catalysts, a process known as Catalytic Chemical Vapor Deposition, CCVD [15]. Their common features were addressed in a dedicated NATO Advanced Study Institute that took place in Budapest, in June 2000 [16].

In addition, such structures can act as templates for the growth of so-called Vapor-Grown Carbon Fibers (VGCFs): in the first stage, a filament grows by CCVD; then, at higher temperatures, the filaments cease to grow and start thickening as a result of pyrolytic carbon deposition [17,18]. Figure 1 shows three different carbon materials obtained from methane by CCVD in our Laboratory. Temperature is the most important parameter determining the type of structure formed.

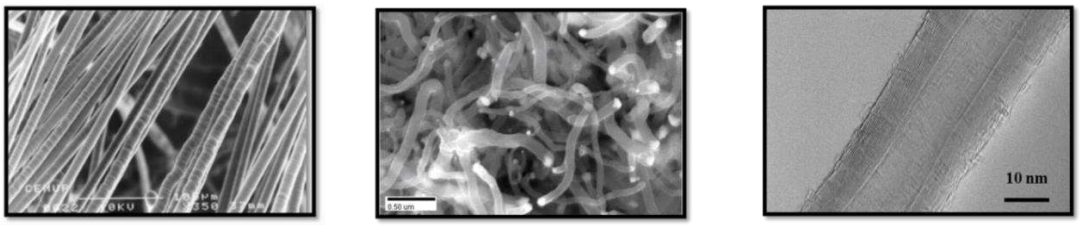

Figure 1 — Carbon materials obtained from methane by CCVD. From left to right: MWCNTs (diameter ≈ 25 nm); CNFs (diameter ≈ 100 nm); VGCFs (diameter ≈ 10 μm).

From the discussion above, it may be concluded that research on carbon nanostructures started some 40 years before the advent of fullerenes and nanotubes. A different terminology was used at the time, which may explain why these earlier reports are frequently overlooked in the recent literature.

3. Nanosized carbon materials

After the discovery of fullerenes and carbon nanotubes, several other morphologies of nanometer-sized carbon materials have been described, such as nano-onions [19], nano-cones [20], and nano-horns [21]. A major breakthrough occurred in 2004, when Geim and Novoselov[2] were able to isolate graphene [22], which quickly became a hot topic of research with many promising technological applications. More recently, some hybrid structures were also reported, such as “nano-buds”, consisting of SWCNTs with covalently attached fullerenes [23], and N-doped graphene/SWCNT hybrids [24]. These nanocarbons are schematically shown in Figure 2.

[2] Andre Geim and Konstantin Novoselov were awarded the Nobel Prize in Physics in 2010 "*for groundbreaking experiments regarding the two-dimensional material graphene*."

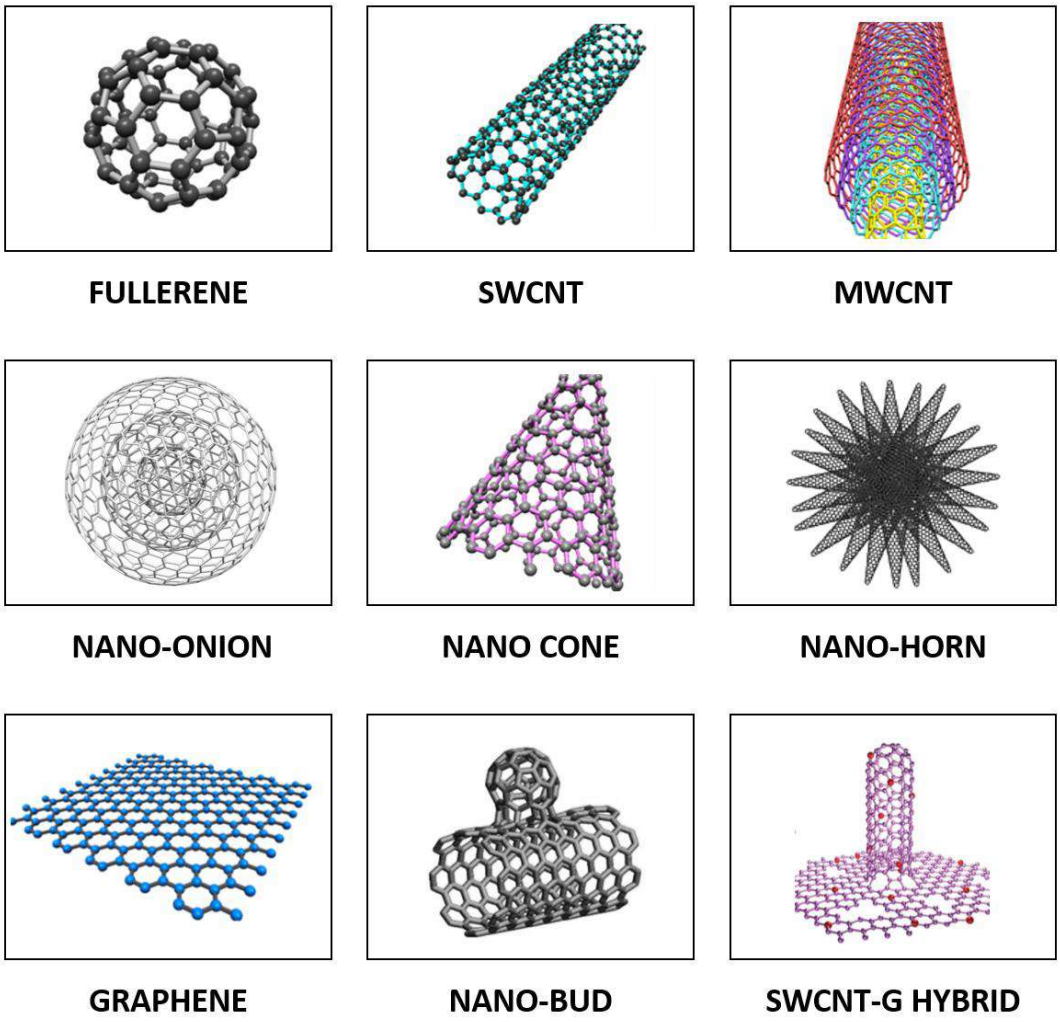

Figure 2 — Schematic illustration of some nanosized carbons.
Adapted from references [19-25].

All carbons shown in Figure 2 share the graphitic structure. But there are also nanosized carbon materials with sp^3- hybridization, namely nanodiamonds, which are produced by detonation of explosives in the absence of oxygen, a process that was discovered in 1963 [26]. The materials obtained in this way consist of a diamond core coated with a graphene shell [27], a feature that is useful for functionalization, as will be described subsequently. And, quite recently, researchers succeeded in synthesizing a "donut"-shaped sp-hybridized molecular carbon allotrope, namely cyclo[18]carbon, a ring of 18 carbon atoms with alternating single and triple bonds [28].

The global carbon nanotubes market reached 4×10^9 US dollars in 2017, a value that is expected to double by 2023 [29].

4. Nanostructured carbon materials

Porous carbon materials with their structure and texture controlled at the nanometer scale are included in the broad definition of nanocarbons (or carbon nanomaterials) proposed by Inagaki and Radovic [30]. These nanostructured carbons can be synthesized either by sol-gel or by templating procedures, as recently reviewed [31].

Carbon gels are obtained by carbonization of organic gels prepared by polycondensation of hydroxybenzenes with aldehydes, as first described by Pekala [32]. Figure 3 shows the steps involved in the synthesis of a carbon gel from resorcinol and formaldehyde under alkaline conditions. According to the drying method used, the materials obtained are called aerogels (supercritical drying), xerogels (conventional drying) or cryogels (freeze drying). They consist of microporous nodules which are aggregated into a network, the voids between nodule chains being the large pores (meso/macropores).

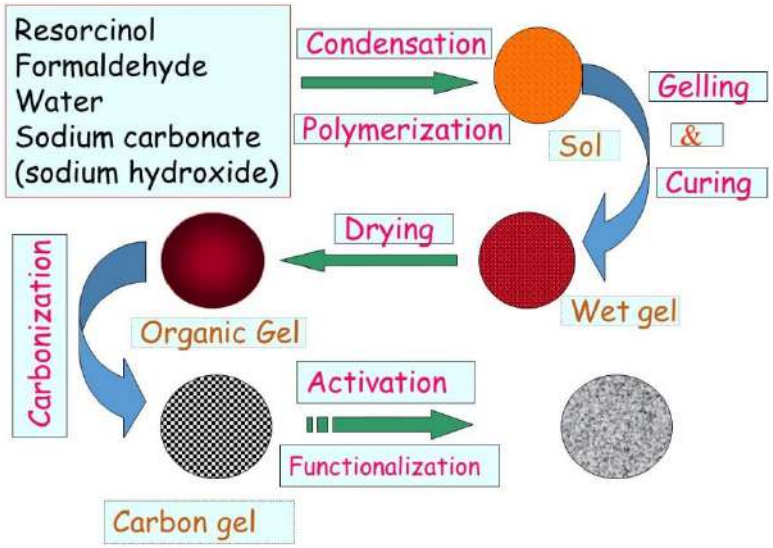

Figure 3 — Steps in the synthesis of carbon gels.

The textural properties of carbon gels can be controlled by adjusting the synthesis conditions, such as the pH and the dilution ratio (molar ratio between solvents and reactants) [33,34]. Thus, it is possible to prepare customized carbon gels, ranging from purely microporous materials to micro-mesoporous materials with well-defined mesopore sizes, and to micro-macroporous materials.

The templating methods go a step further, as they offer the possibility to control both the pore size and the tridimensional structure, yielding materials with ordered and uniform pores. In *exotemplating* (also known as *nanocasting* or *hard templating*) a porous solid is used as a mould, which is impregnated with the carbon precursor. In the case of *endotemplating* (or *soft templating*) the carbon precursors aggregate by self-assembly around the template, which consists of supramolecular structures such as micelles. In both cases, ordered mesoporous carbons (OMCs) are obtained after carbonization and removal of the template [31]. Ordered mesoporous silicas (such as MCM-48 and SBA-15) are often used as templates for nanocasting, originating mesoporous carbons with cubic or hexagonal structures, high specific surface areas and large pore volumes, their pore sizes being determined by the pore size of the template [35]. A more versatile route is provided by soft templating. As in the case of carbon gels, hydroxybenzenes and aldehydes are used as carbon precursors, while triblock copolymers (such as Pluronic® F127) are the preferred structure-directing agents [36]. The textural properties of the OMCs obtained by this method are determined by the synthesis conditions, in particular by the hydroxybenzene/template ratio [31].

Carbohydrates can be easily converted into carbon materials by hydrothermal carbonization (HTC), but additional procedures are generally required to develop the porosity and to improve the textural properties. A recently devised strategy towards this goal consists in using nanocarbons (carbon nanotubes or graphene oxide) as condensation/polymerization promoters, simultaneously providing a scaffold for the growth of carbon gels derived from glucose [37,38].

Figure 4 shows different types of nanostructured carbons obtained in our Laboratory.

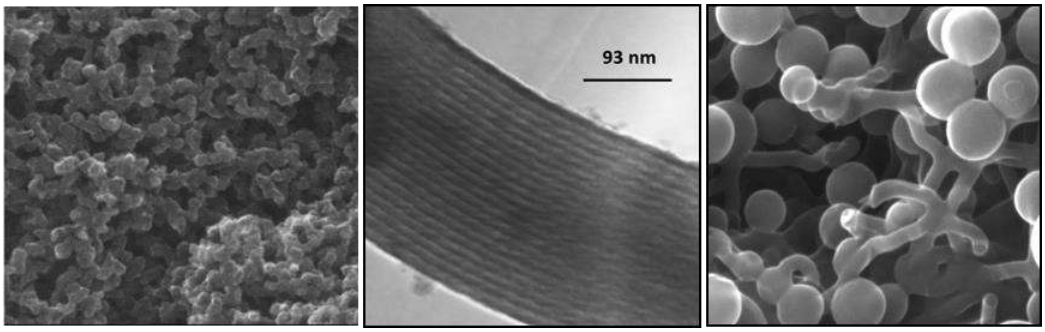

Figure 4 — SEM micrograph of a carbon xerogel (left); TEM micrograph of an OMC obtained by nanocasting with an SBA-15 template (center); and SEM micrograph of a carbon gel obtained by hydrothermal carbonization of a glucose/MWCNT hybrid (right).

5. Tuning the surface chemistry

Most of the carbon nanomaterials described above are based on the graphitic structure; thus, surface functionalization is possible at the unsaturated carbon atoms at the edges of the graphene layers, and at defects of the basal planes. Oxygen functional groups are the most important; they can form spontaneously by exposure to the atmosphere, or they can be incorporated by reaction with oxidizing agents in gaseous or liquid phase. Most of these groups are acidic (carboxylic acids and anhydrides, lactone and phenol groups); ether and carbonyl groups are neutral or can form basic structures, such as quinone and pyrone groups [39].

Nitrogen-containing groups include pyridinic (N6), pyrrolic (N5), and oxidised nitrogen (NX) at the edges, and quaternary nitrogen (NQ) incorporated into the graphene structure (replacing carbon atoms). These groups increase the carbon basicity, in particular the pyridinic nitrogen [40]. Functionalization with nitrogen can be achieved by treatment with ammonia in the gas phase, by hydrothermal treatment with urea solutions, or during synthesis, by adding a suitable nitrogen precursor. A new mechanothermal method consists in ball-milling a mixture of carbon nanotubes [41] or graphene oxide [42] with a nitrogen precursor (urea or melamine), followed by thermal treatment under inert atmosphere.

Quantitative determination of the functional groups can be obtained by deconvolution of temperature-programmed desorption (TPD) profiles or X-ray photoelectron spectra (XPS), as described in detail elsewhere [39,43]. Since the different groups are stable in different temperature ranges, fine tuning of the surface chemistry can be achieved by thermal treatments at different temperatures, as shown in Figure 5 for oxygen groups, or at a given temperature for different periods of time. In this way, some undesired groups can be selectively removed, or samples can be prepared with different amounts of the required groups without significant textural changes [43,44].

Functionalization with sulfur, phosphorus and boron may also be relevant for specific applications. The subject has been addressed in recent reviews [45,46].

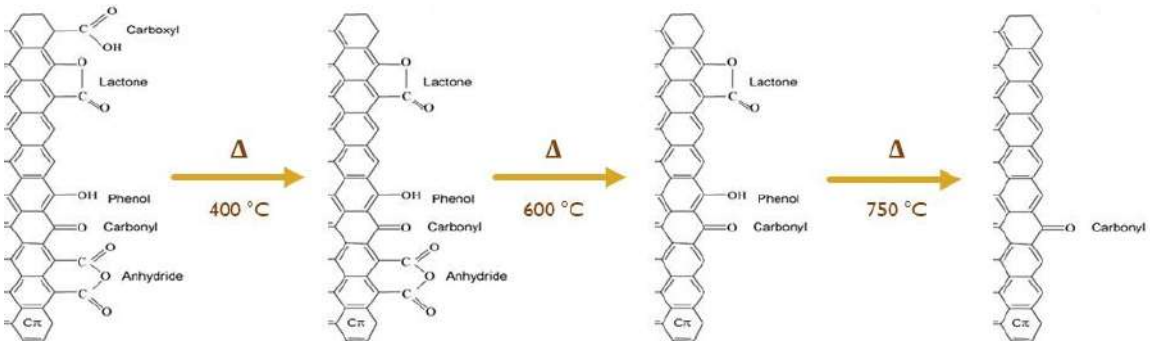

Figure 5 — Schematic illustration of the changes in the surface chemistry of oxidized MWCNTs upon thermal treatments under inert atmosphere.

6. Applications in energy conversion and storage

The applications of carbon nanomaterials in catalysis were the subject of recent comprehensive reviews [25,47]. In the present communication, we will focus more specifically on the use of nanostructured carbons in electrochemical devices for energy conversion (fuel cells) and storage (supercapacitors).

The carbon electrodes for supercapacitors (or electrochemical double layer capacitors, EDLCs), should have large surface areas, hierarchical porosity, and high electrical conductivity [48,49]. Activated carbons are the standard carbon materials for this purpose. They have large micropore volumes responsible for their high adsorption capacities (micropores are defined as having width < 2 nm), which can be accessed through larger pores (mesopores with widths between 2 and 50 nm, and macropores, with width > 50 nm). These pores are organized hierarchically, larger pores subdividing into smaller ones, in a tree-like arrangement [50]. This hierarchical pattern (in series) is quite different from those of carbon gels and OMCs, where there is a parallel network of mesopores, the micropores being present in the primary nodules of carbon gels or in the mesopore walls of OMCs, as shown in Figure 6. This arrangement of the nanostructured carbons is more advantageous, facilitating the access to the micropores [51].

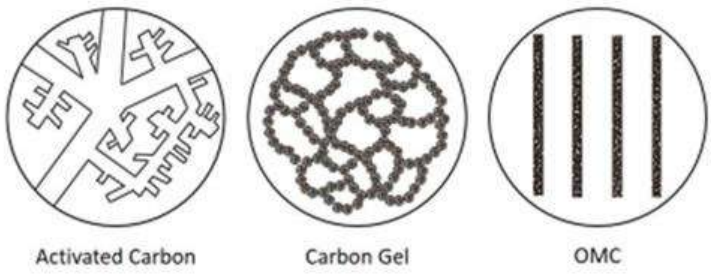

Figure 6 – Comparison of the hierarchical pore systems of activated carbons, carbon gels and ordered mesoporous carbons (OMC). Adapted from references [50,51].

In addition to adequate textural properties, the surface chemistry of the carbon electrodes can also be tuned in order to enhance the capacitance, as a result of Faradaic redox reactions involving some of the oxygen and nitrogen surface functional groups (pseudo-capacitance). The presence of such groups also improves the wettability of the carbon surface [48,49].

Suitable electrodes for EDLCs were prepared by hydrothermal carbonization of glucose in the presence of MWCNTs, followed by chemical activation with KOH. The addition of MWCNTs was found to improve the performance of these hybrid carbons, particularly the capacitance retention, as shown in Figure 7. The best results were obtained by adding just 2 wt.% of MWCNTs, the corresponding electrode (AG_2%CNT_KOH) yielding 206 F g^{-1} and 78% of capacitance retention up to 0.8 V and 20 A g^{-1}, as well as high rate cyclability (97% after 5000 cycles). This performance is much better than that of the reference activated carbon (DLC Supra 50), with a capacitance of only 150 F g^{-1} which drastically decreases above a current density of 2 A g^{-1} [38].

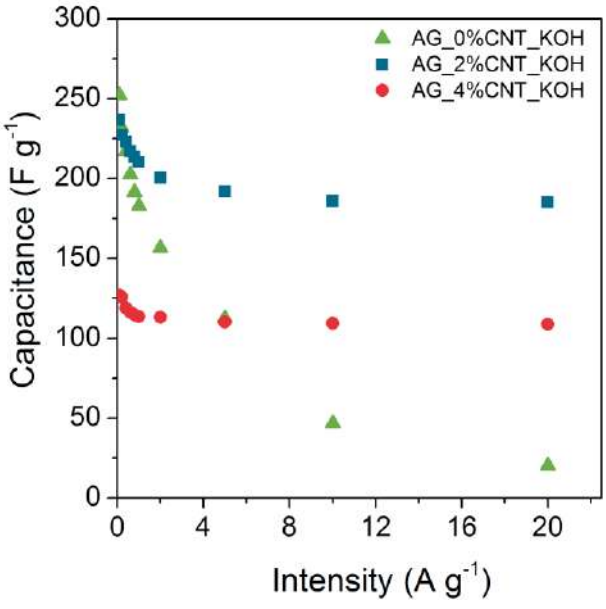

Figure 7 - Capacitance retention of chemically activated glucose-MWCNT hybrid carbons with different proportions of MWCNTs (0, 2 and 4 wt.%), measured within a voltage window of 0.8 V. Adapted from reference [38].

Another set of materials was prepared following a similar procedure, but H_3PO_4 was used as a chemical activation agent instead of KOH. The carbons obtained in this way contained a large amount of both oxygen and phosphorus functional groups. The oxygen groups anchored directly to the carbon surface provided a significant contribution to the pseudocapacitance, while the phosphorus groups enhanced the electrostatic charge. The capacitance was found to increase significantly with the amount of P incorporated; moreover, higher P contents allowed to increase the current density applied. The best electrode material showed a capacitance of 110 F g^{-1} and a capacitance retention of 93% after 10 000 cycles at 10 A g^{-1}, exceeding the performance of commercial activated carbon electrodes at high current densities [52].

The situation is more complicated in the case of fuel cells (FCs). These devices generate electricity by oxidizing a fuel (e.g., hydrogen) at the anode and reducing oxygen at the cathode, the electrode surfaces being covered with a thin layer of an electrocatalyst. The currently available catalysts for the anode and cathode reactions are based on platinum supported on carbon black. The high price of Pt, its scarcity, and its sensitivity to poisons are the major hurdles that hinder the widespread application of FCs. In the quest for alternative electrocatalysts, particularly for the slow oxygen reduction reaction (ORR), two promising strategies have recently emerged, based on the use of either transition metal N_4-macrocycle compounds, or N-containing metal-free materials, such as nitrogen-doped carbons and graphitic-carbon nitride (g-C_3N_4)-based hybrids [53,54].

The high electrocatalytic activity of nitrogen-doped carbon nanotubes for the ORR in alkaline media was first reported in 2009 [55]. Since then, there has been an intense activity in this area of research. In addition to carbon nanotubes, other nanosized materials have shown excellent performances. For instance, the ORR activity of the N-doped graphene/SWCNT hybrid shown in Figure 2 was found to be comparable to that of the commercial Pt catalyst [24].

Lately, we have been focusing on nanostructured carbons, in particular materials prepared by hydrothermal carbonization of glucose, since their textural and chemical properties can be tailored to enhance their electrochemical performance towards the ORR. We found that the increase of microporosity improves the limiting current density, while the incorporation of nitrogen improves the onset potential and shifts the mechanism towards a four-electron pathway. However, the type of N-groups is more important than the total amount of nitrogen. Thus, we observed that a higher N6/NQ ratio favors the

onset potential, while a lower NQ/N5 ratio favors the number of electrons exchanged during ORR [56]. The addition of MWCNTs during the hydrothermal polymerization of glucose leads to further improvements in the performance of the carbon material towards the ORR, in particular as a result of higher electrical conductivity [57]. However, these materials could not match the performance of the reference Pt electrocatalyst, in spite of significant improvements.

Better results were achieved with a micro-macroporous activated carbon xerogel doped with nitrogen and iron [58], demonstrating the importance of tuning both the textural and surface chemical properties of the carbon material in order to optimize its electrochemical performance. The organic gel was synthesized by microwave heating, and the synthesis parameters were selected in order to obtain macropores of about 100 nm. A carbon gel was then obtained by physical activation with carbon dioxide at 1000 ºC (sample AX-1000). The activation procedure yielded a material with large surface area (1460 m^2 g^{-1}) and micropore volume (0.5 cm^3 g^{-1}); moreover, the high activation temperature allowed to reach an adequate electrical conductivity (140 S m^{-1}). This sample was then functionalized with nitrogen (AX-1000N). A third sample was prepared by impregnating AX-1000N with iron(II) phthalocyanine (AX-1000NFe). Figure 8 shows the electrochemical performance of these samples, in comparison to a commercial ORR electrocatalyst (20 wt% Pt on carbon black, Pt/C). The wide macropores facilitate the access of the reactants to the micropores, where the catalytic sites are mainly located, and nitrogen-doping shifts the reaction mechanism to the four electron pathway (direct route), as shown in Fig. 8b. Further improvements were achieved after incorporation of iron, the performance of sample AX-1000NFe being comparable to that of the commercial platinum electrocatalyst [58].

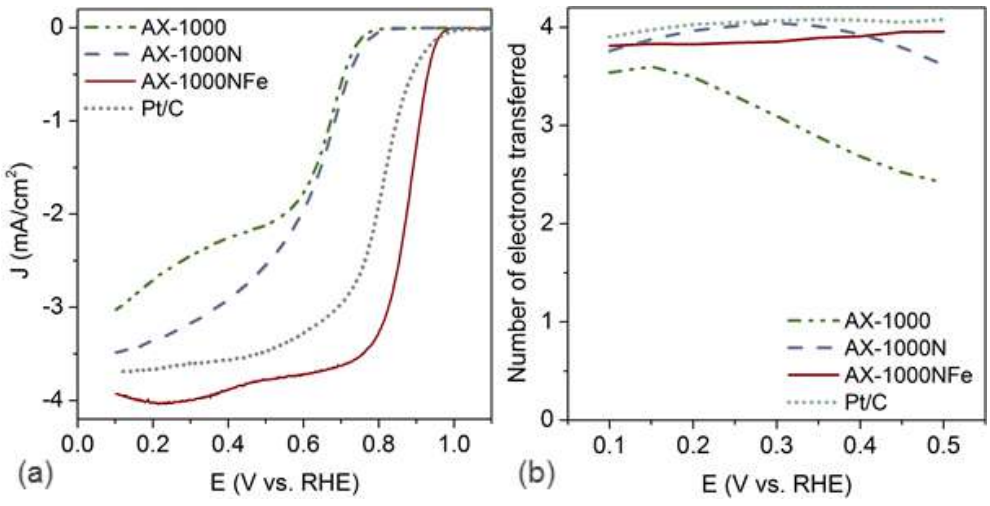

Figure 8 – Effect of nitrogen and iron doping on the electrocatalytic performance of a micro-macroporous carbon xerogel: Linear sweep voltammograms (a) and number of electrons transferred during the ORR (b). The performance of a commercial Pt/C catalyst is included for comparison. Adapted from reference [58].

7. Summary and outlook

The versatility of carbon is unmatched in the periodic table. Carbon is present in a huge variety of compounds, some of them essential to all living organisms; this is the realm of Organic Chemistry. Moreover, carbon also plays a key role in several other equally important areas. In his essay "*The four worlds of carbon*", S.H. Friedman refers the role of carbon in converting iron into steel, in making polymers, and in providing most of the energy used by mankind (fossil fuels) [59]. But the industrial dimension of carbon must also be recognized, as the products of the carbon industry account for a sizeable market share (cf. Table 1). Carbon nanomaterials appeared only in the 1990's, but there is already a considerable industrial production, especially in the case of MWCNTs, which are mainly used for the manufacture of polymer matrix composites. Nanostructured carbons with hierarchical porosity, obtained by sol-gel and templating procedures and functionalized or doped with heteroatoms, offer the possibility of fine-tuning their texture and surface chemistry, allowing the design of *custom-made* materials for the envisioned applications. Some examples were discussed in the field of energy conversion and storage, which is currently the focus of a considerable research effort and where major breakthroughs are foreseeable in the short term.

Acknowledgements - Base Funding - UIDB/50020/2020 of the Associate Laboratory LSRE-LCM - funded by national funds through FCT/MCTES (PIDDAC).

References

[1] H. Marsh, Introduction to Carbon Science. Butterworths, London, 1989.

[2] H.W. Kroto, J.R. Heath, S.C. O'Brien, R.F. Curl, R.E. Smalley, Nature, 318 (1985) 162-163.

[3] S. Iijima, Nature 354 (1991) 56–58.

[4] S. Iijima, T. Ichihashi, Nature 363 (1993) 603–605.

[5] D.S. Bethune, C.H. Kiang, M.S. De Vries, G. Gorman, R. Savoy, J. Vazquez, R. Beyers, Nature 363 (1993) 605–607.

[6] H.P. Boehm, Carbon 35 (1997) 581-584.

[7] M. Monthioux, V.L. Kuznetsov, Carbon 44 (2006) 1621-1623.

[8] L.S. Lobo, Ph.D. Thesis, Univ. London, 1971.

[9] L.S. Lobo, D.L. Trimm, J.L. Figueiredo, in: *Proc. 5th International Congress of Catalysis, Miami Beach, Florida, 1972*, (J.W. Hightower, Ed.) vol. 2, North Holland, Amsterdam, 1973, pp. 1125–1135.

[10] R.T.K. Baker, M.A. Barber, P.S. Harris, F.S. Feates, R.J. Waite, J. Catal. 26 (1972) 51–62.

[11] L.S. Lobo; J.L. Figueiredo; C.A. Bernardo, Catal. Today, 178 (2011) 110-116.

[12] R.T.K. Baker, P.S. Harris, in: *Chemistry and Physics of Carbon* (P.L. Walker, Jr., P.A. Thrower, Eds.) vol.14, Marcel Dekker, New York, 1978, pp. 83-165.

[13] E. Fitzer, K.-H. Kochling, H.P. Boehm, H. Marsh, Pure & Appl. Chem. 67 (1995) 473-506.

[14] N.M. Rodríguez, J. Mater. Res. 8 (1993) 3233-3250.

[15] P. Serp, in: *Carbon Materials for Catalysis* (P. Serp, J.L. Figueiredo, Eds.) John Wiley & Sons, Hoboken, NJ, 2009, pp. 309–372.

[16] L.P. Biró, C.A. Bernardo, G.G. Tibbetts, Ph. Lambin (Eds.), Carbon Filaments and Nanotubes: Common Origins, Differing Applications? Kluwer Academic Publishers, Dordrecht, 2001.

[17] M. Endo, K. Takeuchi, K. Kobori, K. Takahashi, H.W. Kroto, A. Sarkar, Carbon 33 (1995) 873–881.

[18] Ph. Serp, J.L. Figueiredo, Carbon 34 (1996) 1452-1454.

[19] D. Ugarte, Nature 359 (1992) 707–709.

[20] M. Ge, K. Sattler, Chem. Phys. Lett. 220 (1994) 192–196.

[21] S. Iijima, M. Yudasaka, R. Yamada, S. Bandow, K. Suenaga, F. Kokai, K. Takahashi, Chem. Phys. Lett. 309 (1999) 165-170.

[22] K.S. Novoselov, A.K. Geim, S.V. Morozov, D. Jiang, Y. Zhang, S.V. Dubonos, I.V. Grigorieva, A.A. Firsov, Science. 306 (2004) 666–669.

[23] A.G. Nasibulin, A.S. Anisimov, P.V. Pikhitsa, H. Jiang, D.P. Brown, M. Choi, E.I. Kauppinen, Chem. Phys. Lett. 446 (2007) 109-114.

[24] G.-L. Tian, M.-Q. Zhao, D. Yu, X.-Y. Kong, J.-Q. Huang, Q. Zhang, F. Wei, Small 10 (2014) 2251-2259.

[25] D.S. Su, S. Perathoner, G. Centi, Chem. Rev. 113 (2013) 5782-5816.

[26] V.V. Danilenko, Phys. Solid State 46 (2004) 595–599.

[27] E.M. Baitinger, E.A. Belenkov, M.M. Brzhezinskaya, V.A. Greshnyakov, Phys. Solid State, 54 (2012) 1715–1722.

[28] K. Kaiser, L.M. Scriven, F. Schulz, P. Gawel, L. Gross, H.L. Anderson, Science 365 (2019) 1299–1301.

[29] Carbon Nanotubes (CNT) Market, https://www.marketsandmarkets.com/Market-Reports/carbon-nanotubes-139.html (accessed on March 11, 2020).

[30] M. Inagaki, L.R. Radovic, Carbon 40 (2002) 2279-2282.

[31] M. Enterría, J.L. Figueiredo, Carbon 108 (2016) 79–102.

[32] R.W. Pekala, J. Mater. Sci. 24 (1989) 3221-3227.

[33] N. Job, R. Pirard, J. Marien, J.P. Pirard, Carbon 42 (2004) 619–628.

[34] N. Rey-Raap, J.A. Menéndez, A. Arenillas, Microporous Mesoporous Mater. 223 (2016) 89–93.

[35] R. Ryoo, S.H. Joo, M. Kruk, M. Jaroniec, Adv. Mater. 13 (2001) 677-681.

[36] C. Liang, S. Dai, J. Am. Chem. Soc. 128 (2006) 5316–5317.

[37] F.J. Martín-Jimeno, F. Suárez-García, J.I. Paredes, A. Martínez-Alonso, J.M.D. Tascón, Carbon 81 (2015) 137-147.

[38] N. Rey-Raap, M. Enterría, J.I. Martins, M.F.R. Pereira, J.L. Figueiredo, ACS Appl. Mater. Interf. 11 (2019) 6066-6077.

[39] J.L. Figueiredo. J. Mater. Chem. A, 1 (2013) 9351–9364.

[40] H.P. Boehm, in: *Carbon Materials for Catalysis* (P. Serp, J.L. Figueiredo, Eds.) John Wiley & Sons, Hoboken, NJ, 2009, pp. 219–265.

[41] O.S.G.P. Soares, R. P. Rocha, A.G. Gonçalves, J.L. Figueiredo, J.J.M. Órfão, M.F.R. Pereira, Carbon, 91 (2015) 114-121.

[42] R.P. Rocha, A.G. Gonçalves, L.M. Pastrana-Martínez, B.C. Bordoni, O.S.G.P. Soares, J.J.M. Órfão, J.L. Faria, J.L. Figueiredo, M.F.R. Pereira, A.M.T. Silva, Catalysis Today, 249 (2015) 192–198.

[43] J.L. Figueiredo, M.F.R. Pereira, M.M.A. Freitas, J.J.M. Órfão, Carbon 37 (1999) 1379-1389.

[44] R.P. Rocha, A.M.T. Silva, S.M.M. Romero, M.F.R. Pereira, J.L. Figueiredo, Appl. Catal. B: Environ.147 (2014) 314-321.

[45] R.P. Rocha, O.S.G.P. Soares, J.L. Figueiredo, M.F.R. Pereira, C 2 (2016) 17 (18 pp).

[46] O.S.G.P. Soares, R.P. Rocha, J.J.M. Órfão, M.F.R. Pereira, J.L. Figueiredo, C 5 (2019) 30 (14 pp.).

[47] J.L. Figueiredo, in: *Nanotechnology in Catalysis: Applications in the Chemical Industry, Energy Development, and Environment Protection* (M. Van de Voorde, B.F. Sels, Eds.) vol. 1, Wiley-VCH Verlag GmbH & Co. KGaA, 2017, pp. 37-55.

[48] E. Frackowiak, F. Béguin, Carbon, 39 (2001) 937-950.

[49] E. Frackowiak, Phys. Chem. Chem. Phys., 9 (2007) 1774–1785.

[50] F. Rodríguez-Reinoso, A. Linares-Solano, in: *Chemistry and Physics of Carbon* (P.A. Thrower, Ed.) vol. 21, Marcel Dekker, New York, 1989, pp. 1–146.

[51] J.L. Figueiredo, Surface & Coatings Technology, 350 (2018) 307-312.

[52] N. Rey-Raap, M.A.C. Granja, M.F.R. Pereira, J.L. Figueiredo, Electrochimica Acta, submitted.

[53] Y. Zheng, Y. Jiao, M. Jaroniec, Y. Jin, S.Z. Qiao, Small, 8 (2012) 3550–3566.

[54] L. Yang, J. Shui, L. Du, Y. Shao, J. Liu, L. Dai, Z. Hu, Adv. Mater., 31 (2019) 1804799 (20 pp.).

[55] K. Gong, F. Du, Z. Xia, M. Durstock, L. Dai, Science, 323 (2009) 760-764.

[56] R.G. Morais, N. Rey-Raap, J.L. Figueiredo, M.F.R. Pereira, Beilstein J. Nanotech., 10 (2019) 1089-1102.

[57] R.G. Morais, N. Rey-Raap, R.S. Costa, C. Pereira, A. Guedes, J.L. Figueiredo, M.F.R. Pereira, J. Compos. Sci. 4 (2020) 20 (14 pp.).

[58] M. Canal-Rodríguez, N. Rey-Raap, J.A. Menéndez, M.A. Montes-Morán, J.L. Figueiredo, M.F.R. Pereira, A. Arenillas, Microporous and Mesoporous Materials 293 (2020) 109811.

[59] S.H. Friedman, Nature Chem. 4 (2012) 426.

CARBON AS A NATURAL ELEMENT, CHEMISTRY AND LIFE

José A. S. Cavaleiro

University of Aveiro, Department of Chemistry, 3810-193 Aveiro, Portugal

José A.S. Cavaleiro got his B.Sc. degree at the University of Coimbra, Portugal and his Ph.D. degree at the Robert Robinson Laboratories, University of Liverpool, U.K (supervision of Profs. George W. Kenner and Kevin M. Smith). His academic career as a staff member started at Coimbra University and later continued at Lourenço Marques (Mozambique) and Aveiro (Portugal) Universities. Since 1986 he has been Professor of Chemistry at the Aveiro University. He was the supervisor of B.Sc., M.Sc. and Ph.D. students as well as of postdoctoral researchers. He is the recipient of several prizes (e.g., Parke--Davis prize, Liverpool University, 1973; Ferreira da Silva prize, Portuguese Chemical Society, 2004; Spanish-Portuguese prize Madinaveitia--Lourenço, Royal Spanish Chemical Society, 2010). His research interests are centered on the synthesis, reactivity, and applications (medicinal, catalytic, and others) of porphyrins and related compounds; also he has been engaged on studies on natural compounds, mainly terpenoids and flavonoids. He has been acting as referee of many organic chemistry publication sources and also as an evaluation member of colleagues CVs on request from Universities, academies and societies abroad. He is the author of 540 scientific publications in major journals of organic chemistry.

Abstract

Life would not be taking place or it would be totally different if carbon, the number 6 element of the Periodic Table, would not exist. Carbon compounds are present in vital functions. As an example, the detoxification of xenobiotics is played by the enzymes of the Cytochromes P450 group. The mimicking of such processes might lead to significant biological information. That is illustrated with mimicking studies on the oxidative transformation of six carbon compounds which are potential drugs.

1. Introduction

Carbon is an element known since prehistoric times. It is the element with atomic number 6 in the Periodic Table put forward by Dmitri Ivanovich Mendeleyev. It was in 1869 that the first version of the Table was proposed, bringing a desired order to the chaos which was taking place at the time in the chemical science involving the known elements. As Krebs stated, the Periodical Table proposed was “the most elegant organizational chart

ever devised". Although dealing with 63 elements known at the time, the table already predicted the place for future elements which could be discovered, and that gracefully has happened [1,2].

Carbon is the 15th most abundant element in the crust of our planet and the 2nd one by mass in the human body after the oxygen. Carbon is a vital element to all kinds of life. Without carbon our life would be different if not impossible. However, the number of carbon atoms is not at all so abundant; in our body for each 200 atoms group of H,O,C the number of carbon atoms is just 19! Carbon is the one which is able to make links with several other different atoms and with itself. From simple to very complex and robust structures, with linear, branched and cyclic shapes are made having carbon as the significant atom connection element. Proteins, DNA / RNA, carbohydrates, fats, are examples of such biomolecules.

2. Carbon compounds. Natural and synthetic derivatives. Vital functions.

Nature is a "fantastic chemist" in our everyday life with the biosynthesis, mode of action and catabolism of many carbon compounds; a wide range of them are responsible for the bioprocesses which rule the life on earth. Many other carbon compounds, related or not related with the natural ones, have been obtained by chemists in their studies about new synthetic methodologies and potential applications for the new compounds. In such way it can be stated that millions of carbon compounds do exist and that is due to the way played by Nature or to the synthetic studies carried out by chemists. In many cases chemists aim to understand Nature and such target implies to carry out studies on the mimicking of the natural processes. Once more such chemical/biochemical world is due to the fantastic properties of carbon as the element present in all those compounds.

Vital functions played by Nature rule the way life is happening on earth and almost all involve carbon molecules. One of them is the xenobiotics' detoxification. This is usually an oxidative process catalyzed by a class of metalloenzymes, known as the Cytochrome P450-dependent monooxygenases (CyP450). Such enzymes have protoporphyrin-IX [(**1**), Fig. 1] in the form of Iron(III) complexes containing cysteine groups as axial ligands.

It should be mentioned at this stage that protoporphyrin-IX is also a common precursor to the natural derivatives of such porphyrin which are involved in the

respiratory and photosynthetic processes. In fact, respiration, photosynthesis and detoxification processes make a fantastic interconnection between the living species worlds.

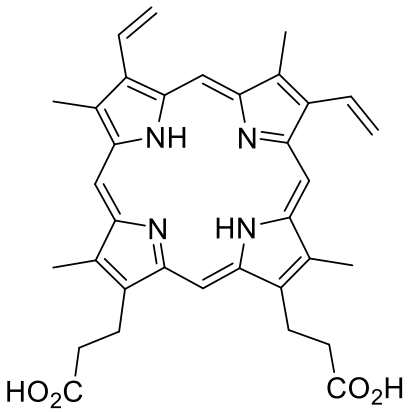

(**1**)

Fig. 1 – Structure of Protoporphyrin-IX (**1**)

The Cytochrome P450 enzymes can be found in almost all forms of life. A wide range of (regio, stereo) selective catalyzed monooxygenations by O_2 takes place. Living organisms on earth have had along many thousands (perhaps millions) of years an adaptation to their life conditions at each moment. That has included the constant metabolism of drugs and other xenobiotics in their environmental living space. It is Nature involving carbon compounds (CyP450) against other carbon derivatives, with an implicit target of better life.

The mechanism of the Cytochrome P450-catalyzed oxidative processes is shown in Fig. 2, and the overall transformation can be represented by the following equation, where RH is the substrate and H_2D the nicotinamide adenine dinucleotide phosphate, [NAD(P)H], the reductant cofactor species.

$$RH + O_2 + H_2D \xrightarrow{P450} ROH + D + H_2O$$

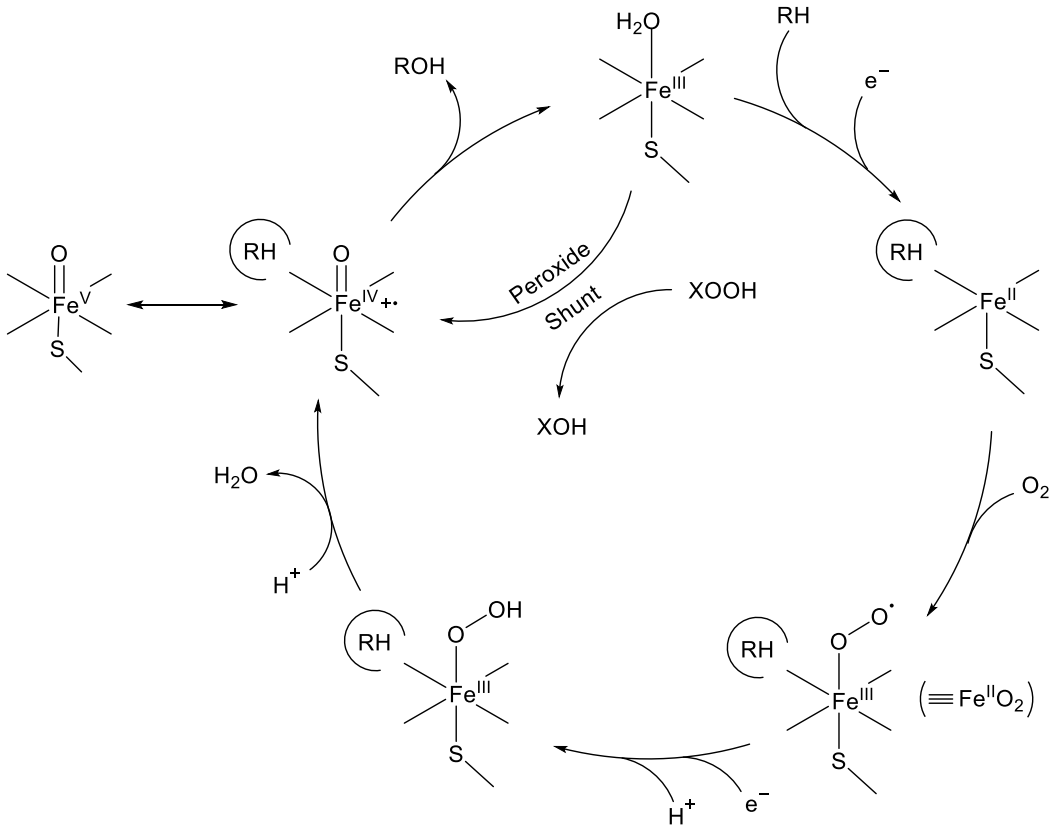

Fig. 2 – Possible CyP450 catalytic cycle

Presumably the substrate interacts with the hydrophobic CyP450 site (near the porphyrin iron center) and that is followed by a NAD(P)H electron transfer which is followed by the 0_2 binding. After that, a second electron transfer takes place leading to the formation of a hydroperoxoiron(III) species which by an heterolytic cleavage gives rise to the Iron(IV) oxoporphyrin radical cation. This is a powerful oxidant species and its interaction with the substrate gives rise to a significant variety of oxidized products [3,4].

Several types of natural oxidative transformations take place (Scheme 1). As significant examples it can be mentioned those involving epoxidations, hydroxylations, N-oxides, sulfoxides, C=O, etc.

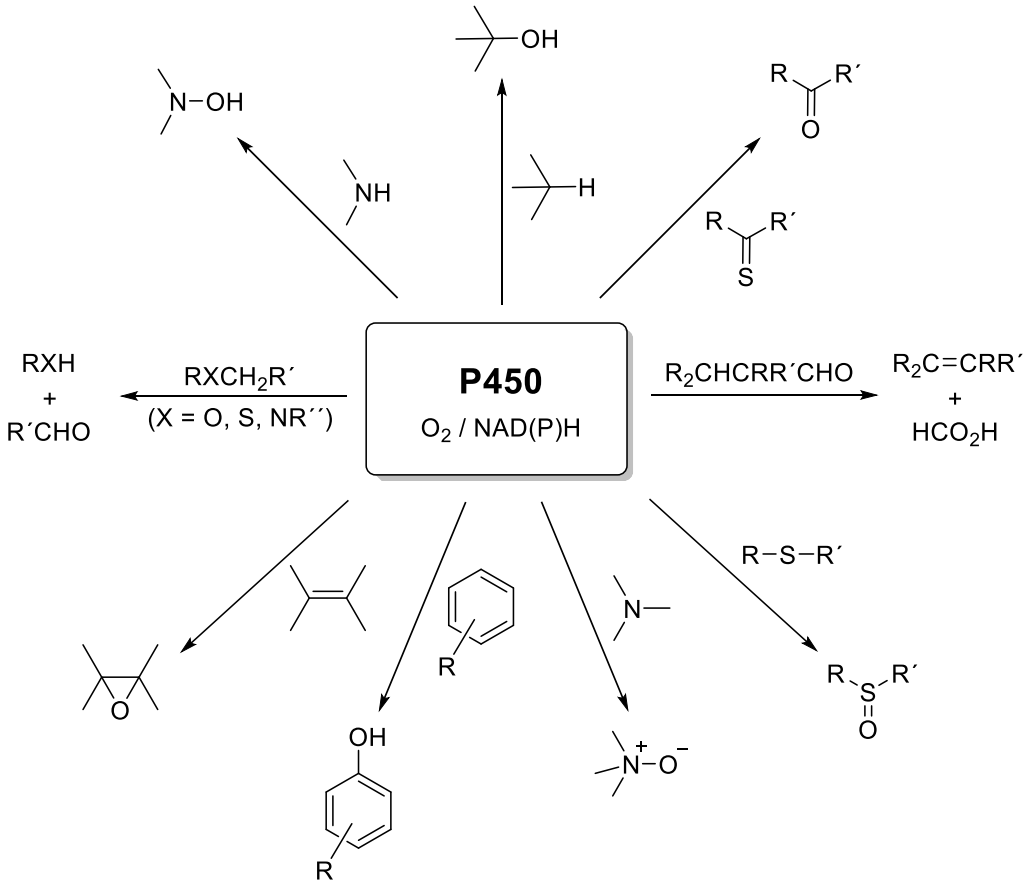

Scheme 1 – Examples of oxidation transformations catalyzed by P450 monooxygenases

An interesting feature of the CyP450 action was found in the 1970s. It was demonstrated that in the presence of oxygen donors (H_2O_2, RO_2H, periodate, iodosylbenzene) isolated liver CyP450 samples catalyzed the hydroxylation of hydrocarbons. Such transformation pointed to new synthetic procedures and applications; it is known as the peroxide shunt pathway (Fig. 2).

3. Metalloporphyrins and Cytochrome P450 mimicking processes

3.1. Metalloporphyrins as P450 mimicking catalysts

A significant amount of information can be found in the literature about the understanding of the Cytochrome P450 natural processes. The mimics of such processes allow to preview the action and metabolism of new drugs and also to apply such procedure in fine chemistry. It will be possible to transform a cheap substrate into another value-added one. The natural compounds' field is highly open to this possibility.

Metalloporphyrins have been used as catalysts in biomimetic studies. The most used macrocycles have been Fe, Mn, Cr, Ru complexes of *meso*-tetraphenylporphyrin derivatives. Pioneering studies on the epoxidation of alkenes and the hydroxylation of alkanes were reported by Groves and collaborators using the Fe(III) complex of *meso*-tetraphenylporphyrin and PhIO as the oxygen donor. However, that porphyrin macrocycle is not be very stable under the oxidizing reaction conditions. Certain derivatives of such macrocycle containing electron-withdrawing groups at the *meso*-phenyl groups or at the b-peripheral positions have been considered to be more robust porphyrins and have been widely used in further studies.

3.2. Aveiro studies using Hydrogen Peroxide

The Aveiro group has studied the oxidation of several acyclic and cyclic substrates, many of them being natural compounds (e.g., mono- and diterpenoids). The metalloporphyrins used have been Fe(III) and Mn(III) complexes of *meso*-tetraaryl-substituted porphyrin derivatives considered to be more robust than those from meso-tetraphenylporphyrin. The transformations have been studied mainly under homogeneous conditions, at room temperature, and the oxygen donor has been hydrogen peroxide, an environmentally safe oxidant [6,7]. The porphyrin catalysts have been the Mn(III) and Fe(III) complexes of robust porphyin derivatives already mentioned.

This communication will consider the studies carried out with six compounds which have demonstrated significant medicinal applications and can be used as drugs. Such compounds are shown in (Fig. 3). The porphyrin catalyst used was the Mn(III) complex of *meso*-tetra-2,6-dichlorophenylporphyrin [Mn(TDCPP)Cl] since its use was common to the studies initially carried out with the six substrates.

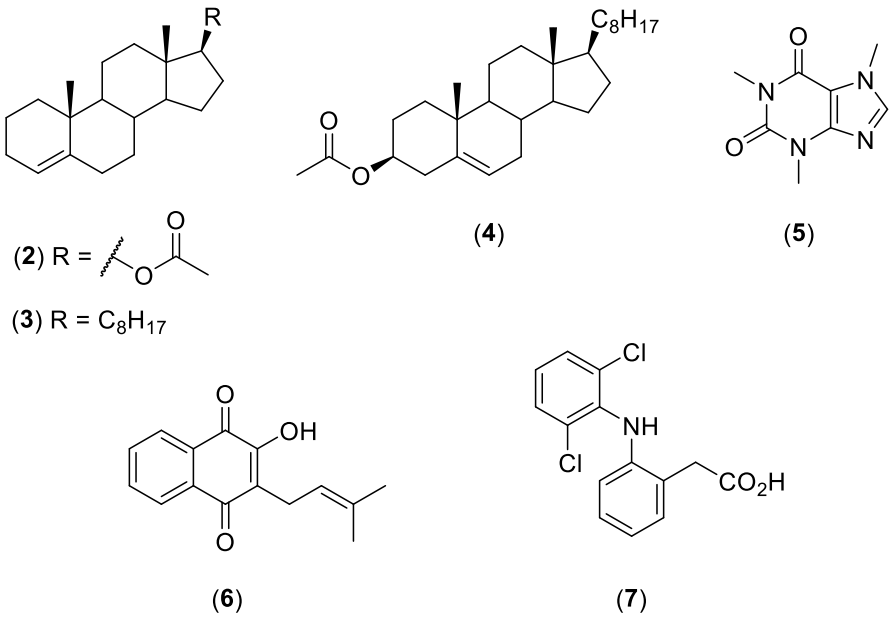

Fig. 1 – Structures of substrates used in this work

3.2.1 Steroids

Certain steroid derivatives have excellent medicinal applications, being used against several diseases and particularly in the treatment of breast cancer. Such compounds act by blocking the estrogen biosynthesis thus giving rise to the tumors regression. Since the functionalization at positions 4 and 6 of the steroid backbone have been considered to be synthetic targets, three compounds were chosen for these stereoselective studies. Those substrates were 17β-acetoxy-4-androstene (**2**), 4-cholestene (**3**) and 3b-acetoxy-5-cholestene (**4**), having in mind that the goal targets were to study the epoxidation procedures of such Δ^4- and Δ^5-steroids.

It has been known since several decades that the direct epoxidation of such type of steroids with peroxy acids leads mainly to the formation of α-epoxides. But in our work different experimental conditions were being used. The oxygen donor was an aqueous solution of hydrogen peroxide and the catalyst and co-catalyst have been [Mn(TDCPP)Cl] and ammonium acetate. The use of the classical oxidant *m*-chloroperbenzoic acid (*m*-CPBA) was also carried out for comparative purposes.

The oxidation of the two Δ^4--steroid substrates (**2**) and (**3**) is a selective epoxidation with a β/β+α ratio of 70% in a 1h reaction with 90% conversion. The main products are the two β (**2a**,**3a**) and the two α (**2b**,**3b**) epoxides (Fig. 4). Other products at trace levels were obtained from allylic oxidation.

The oxidation of the Δ^5-steroid (**4**) under similar experimental conditions was 100% chemoselective for epoxidation. Conversion of 80% and β/β+αselectivity ratio of 90% were obtained for the two epoxides (**4a**, **4b**) (Fig. 5).

The reactions of (**2**), or (**3**), or (**4**) with *m*-CPBA and in the absence of the porphyrin catalyst is chemoselective in the formation of the epoxides, but with epoxidation selectivity values β/β+α of 40% with 100% conversions in 1 h reactions time.

It is considered that the oxidation with H_2O_2 / Mn(TDCPP)Cl / NH_4OAc follows the CyP450 shunt pathway (Fig. 2), with the formation of the high-valent oxo species, which might be the final oxidant species. Considering the substrates stereo-hindrance the oxidant species should approach the double bond from the *cis* side, and in such way the β-epoxides are preferentially formed.

It can be stated that Δ^4- and Δ^5-steroids can be successfully transformed into the corresponding epoxides. And with the new environmentally safe conditions the major product is the b-epoxide derivative. These are then available for further reactions involving the epoxide moieties and a significant number of new steroids derivatives can be obtained.

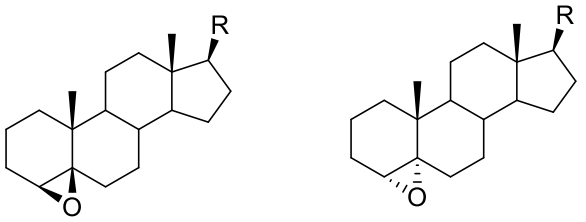

(**2a**) R = OAc (**2b**) R = OAc

(**3a**) R = C_8H_{17} (**3b**) R = C_8H_{17}

Fig. 2 – β- and α-epoxides, respectively (**2a**),(**3a**) and (**2b**),(**3b**), obtained from androstene (**2**) / cholestene (**3**) and H_2O_2 / Mn(TDCPP)Cl / NH_4OAc

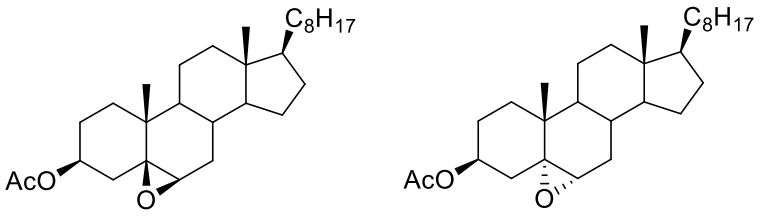

(**4a**) (**4b**)

Fig. 3 – β- and α-epoxides obtained from cholestene (**4**) and H_2O_2 / Mn(TDCPP)Cl / NH_4OAc

3.2.2. Caffeine

Caffeine (**5**) is usually taken as beverages constituent or combined with analgesics. It can be considered as a legal drug and so its oxidative transformation has been studied. It has been shown that *in vivo* its oxidation involves the 3-*N*-demethylation. Several studies have been carried out in laboratories using ozone. The major product obtained has been dimethylparabanic acid (**5a**). We have carried out the oxidation studies of caffeine using H_2O_2 /Mn(TDCPP)Cl / NH_4OAc. The reaction took place with 90% conversion being (**5a**), (**5b**) and (**5c**) the most abundant products of which (**5c**), a new spiro-derivative was always the major one, Figure 6. It was also shown that the formation of **(5b)** was due to a secondary reaction of **(5a)** with ammonium acetate and the formation of **(5c)** could be explained by epoxidation at the double bond linking the two heterocyclic moieties of caffeine, followed by C–N bond cleavage, hydrolysis and lactonization. This is a new racemic spiro-derivative of caffeine [9].

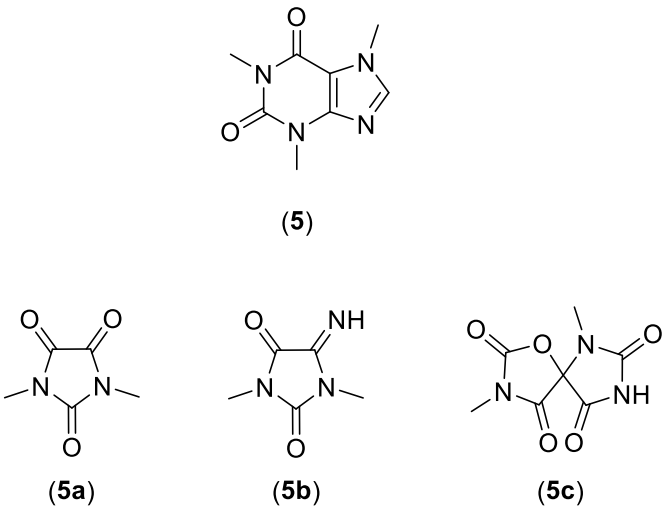

Fig. 4 – Structures of caffeine (**5**) and of its products obtained in the reaction with Mn(TDCPP)Cl/H_2O_2/NH_4OAc.

3.2.3. Lapachol

Lapachol **(6)** is a natural naphthoquinone present in the heartwood of several trees. It is known that lapachol as well some of its derivatives have demonstrated an important set of biological activities (anti-inflammatory, anti-tumor, antibacterial, fungicidal and others). Lapachol has been the subject of a wide range of synthetic studies involving structural modifications for the synthesis of eventually more active derivatives. The

identification of its *in vivo* metabolites, mainly those coming from the CyP450 acting enzymes, is another target of great significance.

Several studies on the oxidation of lapachol have been reported on literature. But such procedures have had no environmental concern. In the present work the already described environmentally safer conditions [Mn(TDCPP)Cl, H_2O_2, NH_4OAc] were used. A comparative study using *m*-CPBA, the classical procedure, was also carried out [10].

The products obtained in one of the two mentioned procedures are different from those obtained in the other one. And the oxidation reaction times with *m*-CPBA are much longer than those with the porphyrin catalyst and H_2O_2. In the *m*-CPBA procedure the two already known *ortho*-naphthoquinones **(6a)** and **(6b)** were obtained; the other procedure involving the porphyrin catalyst and H_2O_2 gave rise to two new *para*-naphthoquinones **(6c)** and **(6d)** and to a new lactone **(6e)**, Figure 7.

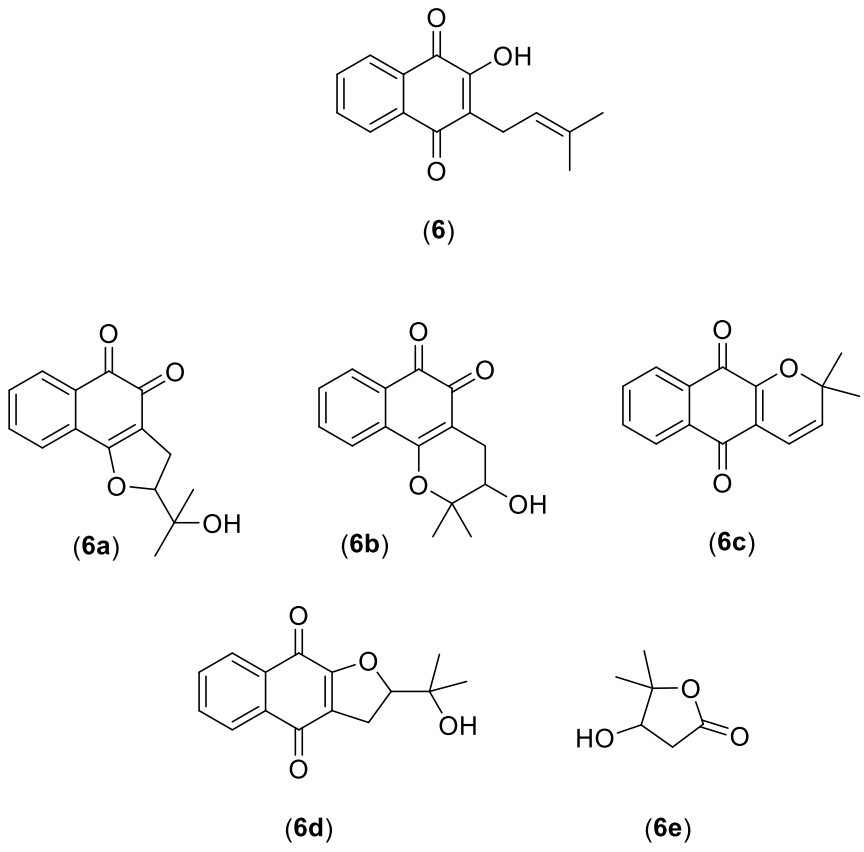

Fig. 5 – Structures of lapachol (**6**) and of the *m*-CPBA and Mn(TDCPP)Cl/H_2O_2/NH_4OAc oxidized products, respectively [(**6a**),(**6b**)] and [(**6c**),(**6d**),(**6e**)].

It is then clear that the system [Mn(TDCPP)Cl, H_2O_2, NH_4OAc] when applied to the lapachol oxidation gives rise to *para*-naphthoquinones and to a lactone. There is epoxidation not only at the lapachol side chain double bond but also at the double bond present in the quinone ring, which brings the possibility of the molecule cleavage. A possible mechanism for the formation of lactone **(6e)** is shown in Scheme 2.

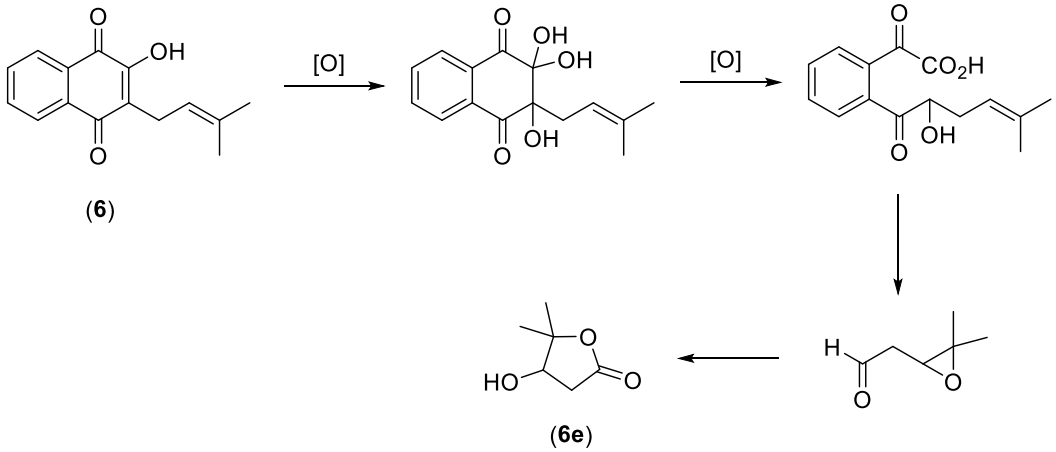

Scheme 1 – Possible formation of lactone (**6e**).

3.2.4. Diclofenac

Diclofenac **(7)** is an anti-inflammatory drug now having a frequent humans' use. Metabolites containing hydroxyl groups in the phenyl rings and other decarboxylated derivatives have been isolated from the CyP450 oxidative action. Literature data reveals that diclofenac and its derivatives have been isolated from environmental samples and oxidative methods have been considered for their removal. Biomimetic models might give an important contribution for such situation even with the possibility of showing potential unstable in vivo metabolites.

The oxidation of diclofenac was undertaken by using the environmentally safe conditions already reported for the previous compounds and involving the [Mn(TDCPP)Cl, H_2O_2, NH_4OAc] system. The products' mixture was not simple and seven compounds were obtained, chromatographically purified and identified by the usual spectroscopic techniques and for a few of them by using X-ray crystallography, (Fig. 8). Mechanistic proposals for the *in vitro* formation of such products have been put forward. The oxidation process might involve oxidative decarboxylation, followed by formation of alcohol, ester and aldehyde derivatives [11].

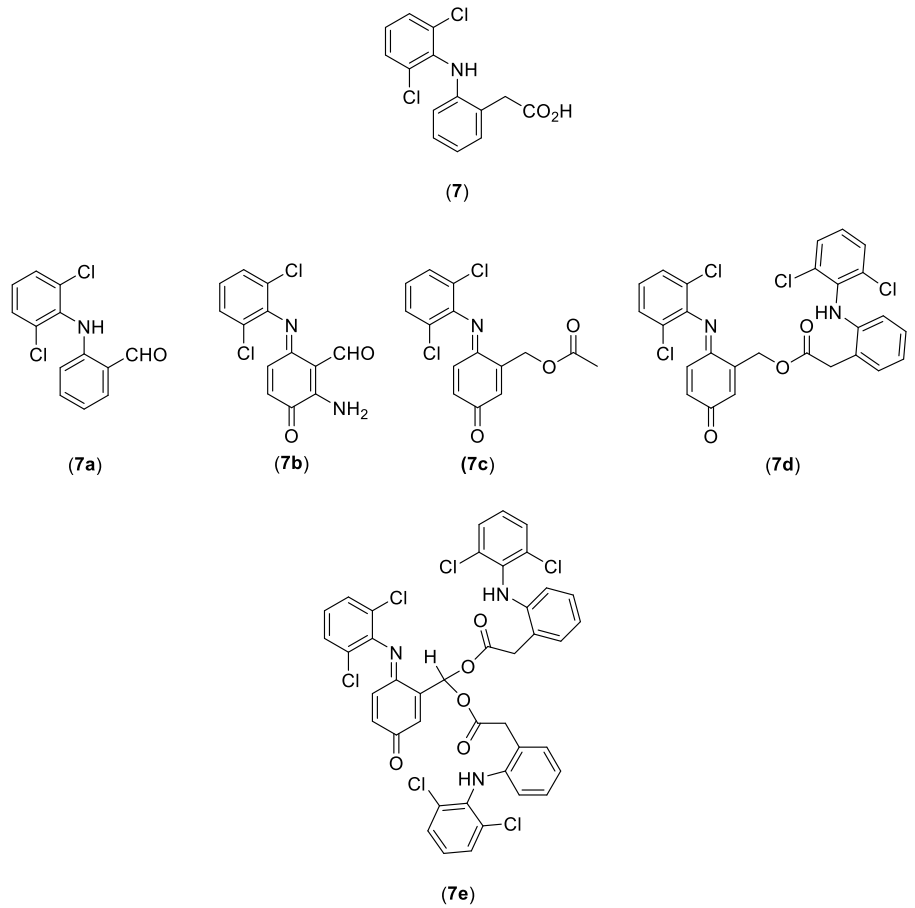

Fig. 6 – Structures of diclofenac (**7**) and derivatives (**7a**)-(**7e**) obtained.

Final remarks

Carbon compounds are present in vital functions. The mimicking of such transformations give rise to a better understanding of their action and to develop new chemical procedures leading to new useful carbon derivatives. A mimicking of the natural detoxification process was chemically applied to each substrate; new products can be considered as possible metabolites occurring from the natural use of each potential drug.

Acknowledgements

Thanks are due to the University of Aveiro and FCT—QOPNA for funding. Thanks are also due to all colleagues and students as co-authors of the work mentioned in references 6—11 and also to Dr. Nuno Moura for the help to set up the manuscript final version.

References

1. R. E. Krebs, The History and Use of our Earth's Chemical Elements, Westport, Conn.: Greenwood, 1998, p. 25
2. B. Bryson, A Short History of Nearly Everything, Transworld Publishers, London, 2003, p. 309
3. D. Mansuy, A Brief History of the Contribution of Metalloporphyrin Models to Cytochrome P450 Chemistry and Oxidation Catalysis, C. R. Chimie, 2007, 10, 392—413
4. R. A. Sheldon, Oxidation Catalysis by Metalloporphyrins, A Historical Perspective, In: Metalloporphyrins in Catalytical Oxidations, R. A. Sheldon, Ed., Marcel Dekker, p. 1—27, 1994, New York
5. J.T. Groves, T. E. Nemo and R. S. Myers, Hydroxylation and Epoxidation Catalyzed by Iron-porphine Complexes. Oxygen Transfer from Iodosylbenzene, J. Am. Chem. Soc., 1979, 101, 1032-1033
6. M. M. Q. Simões, S. M. G. Pires, M. G. P. M. S. Neves and J. A. S. Cavaleiro, Oxidative Transformations of Organic Compounds Mediated by Metalloporphyrins as Catalysts, In: Handbook of Porphyrin Science, K. M. Kadish, K. M. Smith and R. Guilard eds., vol 44, chapter 214, p. 197--306, 2016, World Scientific, Singapore
7. M. M. Q. Simões, C. M. B. Neves, S. M. G. Pires, M. G. P. M. S. Neves and J. A. S. Cavaleiro, Mimicking P450 Processes and the Use of Metalloporphyrins, Pure Appl. Chem., 2013, 85, 1671--1681
8. S. L. H. Rebelo, M. M. Q. Simões, M.G.P. M. S. Neves, A. M. S. Silva, J. A. S. Cavaleiro, A. F. Peixoto, M. M. Pereira, M. R. Silva, J. A. Paixão and A. M. Beja, Oxidation of Δ^4- and Δ^5-Steroids with Hydrogen Peroxide Catalyzed by Porphyrin Complexes of Mn(III) and Fe(III), Eur. J. Org. Chem., 2004, 4778-4787
9. C. M. B. Neves, M. M. Q. Simões, I. C. M. S. Santos, F. M. J. Domingues, M. G. P. M. S. Neves, F. A. A. Paz, A. M. S. Silva and J. A. S. Cavaleiro, Oxidation of Caffeine with Hydrogen Peroxide Catalyzed by Metalloporphyrins, Tetrahedron Lett., 2011, 52, 2898-2902
10. S. M. G. Pires, R. De Paula, M. M. Q. Simões, A. M. S. Silva, M. R. M. Domingues, I. C. M. S. Santos, M. D. Vargas, V. F. Ferreira, M. G. P. M. S. Neves and J. A. S. Cavaleiro, Novel Biomimetic Oxidation of Lapachol with H_2O_2 Catalyzed by a Manganese(III) Porphyrin Complex, RSC Adv., 2011, 1, 1195-1199
11. C. M. B. Neves, M. M. Q. Simões, M. R. M. Domingues, I. C. M. S. Santos, M. G. P. M. S. Neves, F. A. A. Paz, A. M. S. Silva and J. A. S. Cavaleiro, Oxidation of Diclofenac Catalyzed by Manganese Porphyrins: Synthesis of novel Diclofenac Derivatives, RSC Adv., 2012, 2, 7427-7438

AB INITIO POTENTIALS: FROM CBS EXTRAPOLATION TO GLOBALNESS TO RIDDLES IN THE CHEMISTRY OF SMALL CARBON CLUSTERS

A.J.C. Varandas

Department of Physics, Qufu Normal University, China
Department of Physics, Universidade Federal do Espírito Santo, 29075-910 Vitória, Brazil and
Department of Chemistry, and Chemistry Centre, University of Coimbra, 3004-535 Coimbra, Portugal

António J. C. Varandas obtained a degree in Chemical Engineering from University of Porto (1971), and a Ph.D. in Theoretical Chemistry from University of Sussex (1976). After graduation, he joined the Department of Chemistry of Universidade de Coimbra, where he is Full Professor since 1988. Distinguished Professor at the Department of Physics of Qufu Normal University (China), he is also Professor at the Department of Physics of Universidade Federal do Espírito Santo (Brazil). With an impact factor of h=56 (Google Scholar), he published more than 430 papers, co-authored the first monograph in Molecular Potential Energy Functions (Wiley 1984), and wrote 2 other books in portuguese. He received awards: Prize Artur Malheiros for Physics and Chemistry of Lisbon Academy of Sciences (1985), Prize Ferreira da Silva of Portuguese Chemical Society (2001), and Prize Stimulus to Excellence of Portuguese Ministry of Science, Innovation and High Studies (2004). He serves amongst others the editorial board of Journal of Theoretical and Computational Chemistry where recurrently acts as Editor. He received honorific recognitions abroad, the most recent in China where he has been awarded in 2018 the title of Shandong Provincial Distinguished Foreign Expert. He is corresponding member of the Academia de Ciências de Lisboa since 2006, and member of the EU Academy of Sciences since 2014

The importance of *ab initio* electronic structure calculations in quantum molecular science has prompted this short overview with emphasis on carbon compounds at the Periodic Table celebratory sessions in the Academy of Sciences of Lisbon. Aiming at accuracy, the issue of extrapolating the calculated raw energies to the complete one-electron basis-set (CBS) limit is first examined. For brevity, only the electron correlation contribution to the total energy is considered since it is the most difficult to converge. With the uniform-singlet-and-triplet-extrapolation scheme at the focal point, the emphasis is on recent updates. Still, rather than an even survey, the discussion centers on applications to pure carbon clusters and related carbon-hydrogen compounds, with references given here and there to other material that is left uncovered. Aiming at spectroscopic and reaction dynamics studies, the representation of global potential energy surfaces is then briefly addressed by concentrating on methods developed over the years in the author's Group. Because the purist route to the calculation and modeling of global

potentials for large-sized clusters from first-principles appears unaffordable at present, a predictive scheme is suggested to prompt first guesses for more complete *ab initio* work ahead. Prospects for future work conclude the overview.

I. Introduction

Approximations are unavoidable in molecular physics, with that due to Born and Oppenheimer[1] (BO) being most fundamental. Owing to the mass disparity of nuclei and electrons (the former are at least 1837 times heavier than the latter), BO proposed that their motions could be treated separately. In fact, an even smaller mass ratio may justify such an approximation: by considering four equally charged fermions, two positive and two negative, we have shown[2,3] that a mass ratio between the heavier (assumed the positive ones) and lighter (negative) fermions of 200 was enough to validate the separability of their motions up to $\simeq 80\,\%$. As a result, the electronuclear Schrödinger equation splits into two: one for the electrons moving at a fixed arrangement of the nuclei (electronic Schrödinger equation, eSE), the other for the nuclei moving on the potential energy surface (PES or potential) created by the electrons (nSE). The nuclei are said to move adiabatically governed by the PES. Only the eSE is of concern in the present work, leaving aside the nSE which is key in reaction dynamics[4] and where classical[5] (and references therein) approaches are often validated due to the large masses of the nuclei.

Two major difficulties (explosions) arise in computational quantum chemistry based solely in first principles (*ab initio*):[6] a) the $\mathcal{X}^{3N-6}$ explosion signals the number of times that the eSE needs to be solved pointwise to map the PES of a N-atom species ($\mathcal{X}$ is a typical number required per dimension); b) the $\mathcal{X}^{12}$ explosion which indicates how the cost per point raises with the cardinality of the basis (X is its cardinal number).[7] Added to such explosions is the need for PESs with chemical accuracy (≤ 1 kcal mol^{-1}) in reaction dynamics, and spectroscopic accuracy (≤ 1 cm^{-1}) if rovibrational calculations are at stake. Both essentially imply that the PES is at least calculated at the one-electron complete basis set (CBS) limit. Extrapolation is then required, which may use purely mathematical methods or be based on a physically motivated asymptotic theory as is the case here.

The utility of CBS extrapolation gets enhanced when combined with fragment-based methods in which a large molecule is made tractable by explicitly considering all

parts into which it can be fragmented, thence as a many-body expansion[8] (MBE) development. If the eSE eigenenergies are first split into HF- and correlation-type contributions, as usually done in modern *ab initio* theory, the approach is known as double-MBE[9,10] (DMBE).

Appearing in the second row of the periodic table, the carbon atom has four bonding electrons in its valence shell, and hence it can form four bonds with other atoms. In particular, C atoms can bond together forming C-clusters. Given the flexibility of carbon to form bonds with most elements, we focus on applications to clusters and elementary reactions where it is involved, in particular with hydrogen. Naturally, the focus will be on relatively small clusters and molecules, since they are key to underpin the properties of larger ones.

Following common practice in the literature, bond lengths are given in bohr (a_0=0.529 × 10^{-10} m, and energies in hartree, kcal mol^{-1} or kJ mol^{-1}; 1 Eh = 627.510 kcal mol^{-1} = 2625.5 kJ mol^{-1}).

II. Electronic structure methods: A synopsis

Methods for solving the eSE are of utmost importance in computational molecular science.[11] The simplest is Hartree-Fock (HF), a mean-field theory where electron correlation is ignored. The error due to its disregard is significant, and hence more sophisticated single-reference (SR) MO-based ones emerged variational (configuration interaction, CI), perturbative Møller-Plesset (many-body perturbation theory like MP2), and couple-cluster (CC). Of these, the CC singles and doubles with perturbative triples method, CCSD(T), is commonly viewed as the golden rule of quantum chemists.

Because the electron-electron repulsion operator has a singularity at r_{12} = 0, the exact wave function must have a discontinuous derivative as implied by Kato's[12] cusp condition. Because the conventional methods fail to satisfy it, this largely explains their very slow convergence. An enormous progress has recently been done toward the solution of this problem through the development of so-called explicitly correlated (R12 and F12) electron correlation methods since they allow to accelerate the basis set convergence of the wavefunction.[13-15] In fact, studies of thermochemistry,[16-19] noncovalent interactions,[20-24] and vibrational frequencies[25,26] have reported gains of at least two[27] angular momentum increments on their conventional counterparts. Yet, such

methods involve approximations: benchmark runs with the CCSD-F12a variant of CCSD show a slight overestimation of correlation, while the CCSD-F12b variant favours a slight underestimation. Moreover, their convergence to CBS limit is often nonmonotonic. Because integration of the eSE with accuracy at demand is expensive, mostly unreachable, the alternative is to systematize the error of conventional methods and extrapolate to predict the inherent error.

Two ways stand therefore to obtain accurate energies: solution of the eSE after explicit introduction of correlation in the wave function,[15]and exploitation of the convergence of hierarchized correlation consistent basis sets toward the CBS limit. Despite a fast convergence (often reported $\propto X^{-7}$), explicitly correlated (R12-type) methods appear to perform inefficiently with small basis sets[15]. Additionally, conventional and R12 methods are known to converge to the same asymptotic energy, with CBS extrapolation even outperforming in overcoming noncompleteness of the one-electron basis set, a merit recognized[28] by the number of CBS schemes vying the R12 techniques (see elsewhere[29] for an extrapolation calculator developed for some popular schemes).

Suffice it to add at this point that the HF energy converges exponentially, while being computationally less demanding.[30] The focal point here will then be at the correlation energy,[6,31] with the reader addressed elsewhere[32,33] for HF/CBS or CASSCF/CBS [the latter involves only static (nondynamical) correlation; see later] extrapolation schemes.

Since SR methods still miss the nondynamical correlation, this must be recovered at the multireference (MR) level, typically with complete-active-space-self-consistent-field (CASSCF; particularly popular is the so-called full-valence CASSCF or FVCAS variant) and MRCI wave functions, the latter accounting for the dynamical correlation by inclusion of singles and doubles excitations (MRCISD), often also with inclusion of Davidson's correction for quadruple excitations, MRCI+Q. In this case too, extrapolation to the one-electron CBS limit plays an extremely useful role.[32] Although extrapolation to the $\mathcal{N}$-electron basis set limit has been investigated,[34] its application has been less common in the literature.[35-37]

Another popular a priori electronic structure approach is density functional theory (DFT). By far the leading method used in computing the electronic structure properties

of medium and large-sized molecules, the Kohn-Sham[38] (KS) DFT variant is its mainstream. It is an exact formulation of quantum mechanical electronic structure theory but relies on approximate exchange-correlation functionals.[39] As a result, there is a proliferation of DFT functionals, with the best for one application being often not the best for another.[40] Recently,[41,42] we have shown that second-order Møller-Plesset perturbation theoretic results extrapolated from the first steps of the hierarchical staircase[6,31,43] to the CBS limit can rival DFT/M06-2X[39] (and references therein) both on time and accuracy. Such a performance actually extends to other popular DFT functionals.[41,42]

The surge of DFT methods in fields like cluster chemistry and organometallic catalysis to find the many existing stationary points and even reaction pathways comes therefore as no surprise given its cost-effectiveness. In fact, although chemical intuition and comparison with similar reactions can help on the endeavour, the number of such topographical features makes it a formidable task which, most importantly, remains prone to overlooks. To overcome drawbacks, the development of automated procedures to find intermediate species is pivotal.[44-50] Some of these techniques combine geometrical approaches to identify the stationary point with dynamics simulations, with the minima obtained by tracing the intrinsic reaction coordinate paths from the transition states.

III. CBS extrapolation: electron correlation

From a partial-wave expansion for two-electron atoms, it has been established that:[51] a) for natural-parity singlet states, the leading contribution to the energy at second-order of perturbation theory is $\propto (\ell + 1/2)^{-4}$ with no odd-terms either $\propto (\ell + 1/2)^{-5}$ or $\propto (\ell + 1/2)^{-7}$; b) for triplet states, the leading term is or $\propto (\ell + 1/2)^{-6}$; These findings remain essentially unaltered for atoms with any number of electrons.[51,52] If $\Delta E_l \propto \sum_{m=4} a_m (l + 1/2)^{-m}$, the convergence error when $\ell \geq L$ assumes then the form:

$$\Delta E = \sum_{m=4} A_{m-1} (L + 1)^{-m+1} \qquad (1)$$

with A_3 and A_5 being the first two leading coefficients; considering just the first can be accuracy-limiting.[52]

Largely motivated by the possibility of CBS extrapolation, modern basis sets are commonly built according to a principal expansion. Among them are the popular Gaussian-type orbital (GTO) correlation-consistent basis sets[53-55] (cc-pV*X*Z or V*X*Z),

diffuse augmented ones (aug-cc-pVXZ or AVXZ), etc., where the cardinal number X (= 2: D, 3: T, 4: Q…) is identifiable with n and $L + 1$.[56,57] The above slow convergence must be compounded with further scalings[58] at MP2, CCSD, and CCSD(T) calculation levels, namely $N^5N_b^4$, $N^6N_b^4$, and $N^7N_b^4$, where N_b is the number of basis functions per atom; $N_b \simeq X^3$ for a VXZ basis.[7,57] Because correlated calculations beyond QZ are often unaffordable for many interesting systems, the raw energies may then be left too far for a safe extrapolation by some popular schemes.

A. The USTE scheme: update survey

CBS extrapolation of conventional electronic energies is best performed by extrapolating separately its HF and correlation components. The latter, the only of concern in the present work, scales $\propto X^{-3}$ for opposite spin electron pairs and $\propto X^{-5}$ for pairs with the same spin. The USTE[59] scheme accounts for both as

$$E_X^{\text{corr}} = E_\infty^{\text{corr}} + \frac{A_3}{(X+\alpha)^3}\left[1 + \frac{\tau_{53}}{(X+\alpha)^2}\right] \tag{2}$$

where $\tau_{53} = (A_5^{\text{o}}/A_3) + cA_3^{m-1}$; α, A_5^{o}, and c are universal *ab-initio*-based parameters. Empirical-free and showing the correct asymptotic behavior,[6] it is dual-level giving a prediction as accurate as one possibly can get when extrapolating from raw energies for the two highest affordable X values. Yet, use of (D, T) at most is key for larger systems. This is the goal of GUSTE,[60] where τ_{53} has been suggested to be treated as invariant over configuration space once determined for one geometry with $X \geq Q$ raw data. However, even this is there out of reach.

Eq. (2) may be rewritten[61] as $E_X^{\text{corr}} = E_\infty^{\text{corr}} + Ax^{-3}$ where the hierarchical number $x \equiv \widetilde{X}$ is defined by

$$\widetilde{X} = (X+\alpha)\left[1 + \frac{A_5/A_3}{(X+\alpha)^2}\right]^{-1/3} \tag{3}$$

The novel concept is that the basis is educated to account for deficiencies on its composition according to the recovered correlation energy. Stated differently, a hierarchical staircase as straight as possible in X^{-3} is envisaged to enhance reliability when

extrapolating from any two steps.[61] Although more than one possibility exists for reassignment,[61] we suggested[43] to obtain the new hierarchical numbers (x) as statistical averages of the values obtained from the condition that the $X \leq 6$ values fall on the straight line obtained by fitting USTE(5,6) correlation energies.[59] The method kept the original acronym[43] but specifies the hierarchical number-pair used for the extrapolation: USTE(x_1, x_2). The novel hierarchical numbers $x = d, t, q, p, h, \ldots,$ are real positive but still universal as they apply to any correlation-consistent-type basis sets.[62] Since the correspondence for sub-minimal [sM, thence smaller than *D*Z, which are minimal (M); larger ones are extended (E)] basis sets may not be obvious,[63] the basis may alternatively be indicated.

The most recent version of USTE assumes the form:[63]

$$E_X^{\text{corr}} = \eta\, E_\infty^{\text{corr}} + \frac{A_3}{x^3} \tag{4}$$

where η is a tolerance factor, and

$$x = X - p_0 - \frac{1}{2}\tanh\left(\frac{X-X_0}{p_1}\right) \tag{5}$$

where X_0, p_1 and p_2 are universal parameters. Named USTE$_a$(x-1, x), where *a* stands for analytic, this protocol[63] yields high quality results while allowing to extrapolate from any pair of x values, thence any basis sets. Its reliability has actually been checked against the best available estimates which have also been employed as reference to scrutinize raw energies obtained from MP2-F12 and CCSD(T)-F12 calculations.[64] To enhance agreement and delve into subchemical accuracy (<1 kcal mol^{-1}), a tiny scaling (fixed at $\eta \simeq 1 \pm 0.001$) has been allowed. This tiny scaling helps to level off the effect of having used CBS(V*5*Z, V*6*Z) energies as reference, and the fact that the calculations were not at optimized geometries but at all-electron CCSD(T)/CVTZ ones.[43] Indeed, it enhances agreement of the USTE$_a$ predictions with the reference raw F12 energies:[64] rmsd of 0.180 and 0.086 kcal mol^{-1} for MP2/CBS and CCSD(T)/CBS, respectively. To go beyond this (*i.e.*, to attain spectroscopic accuracy) would imply including other corrections such as core and core-valence effects, perturbative contributions for connected quadruple excitations, and relativistic effects that lie outside the scope of the model.

Given its high reliability, USTE$_a$(x-1, x) may also be used to assign a cardinal number to any arbitrary basis.[63] With it, basis sets from subminimal Pople's STO-nG and Huzinaga's MINI ones to the most advanced extended VXZ-F12 anstazes have been ranked from their ability to recover the correlation energy.

USTE has also been extensively applied, and much of the work recently reviewed.[6] Most recently, it has been used[41] to assess how correlated MO calculations perform versus Kohn-Sham DFT by testing the performance of both methods on the calculation of 38 hydrogen transfer barrier heights and 38 non-hydrogen transfer barrier heights/isomerizations extracted from extensive databases, in addition to four 2p isomerization reactions and six others for large organic molecules.[39] All KS DFT calculations employed the popular M06-2X functional, while the correlated MO-based ones used MP2 and CCSD(T) with the raw MO energies subsequently CBS(d, t) extrapolated. MP2/CBS(d, t) was found[41] to be as cost effective as DFT/M06-2X while showing a satisfactory accuracy when compared with the reference data. A similar performance was observed for even-numbered carbon clusters.[65]

Another illustration that is claimed by the paper's title involves an organic molecule with as many as 45 isomers, since such molecules are known to pose a challenging problem to DFT.[66-69] Specifically considered is C_8H_8 since accurate isomerization energies are available[70] for comparison from *ab initio* calculations and the W1-F12 thermochemical protocol.[71] Moreover, a whole range of hydrocarbon functional groups [these include (linear and cyclic) polyacetylene, polyyne, and cumulene moieties, as well as aromatic, anti-aromatic, and highly-strained rings] is involved, while results are available also from composite semiempirical procedures and a panoply of DFT functionals.[70]

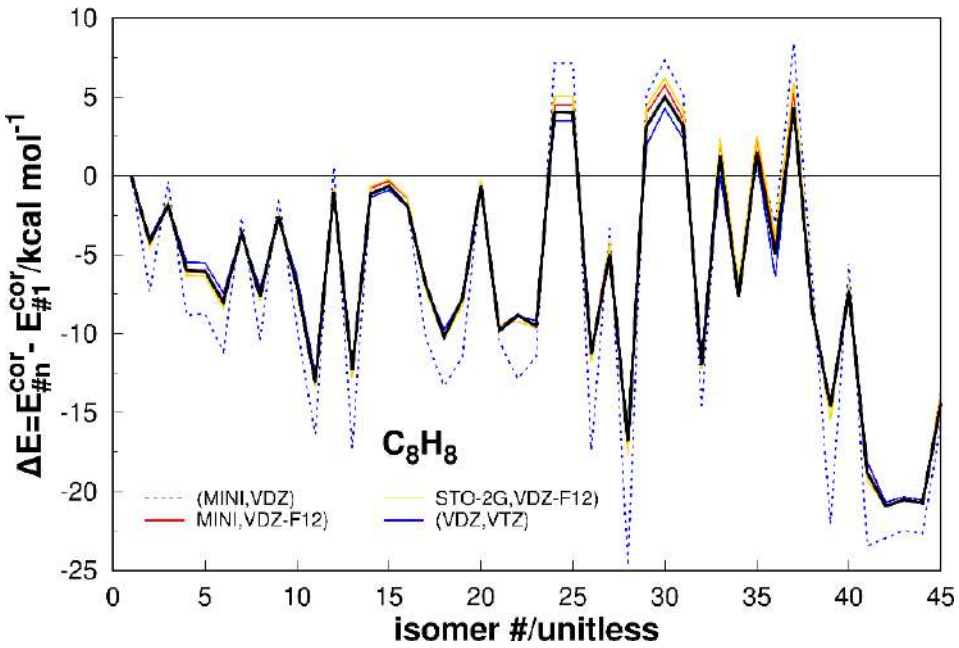

Figure 1 — Energy separations of the C_8H_8 isomers at CCSD(T) level of theory; see elsewhere[70] for their names and B3LYP geometries. Shown[70] in solid black is CBS(V*D*Z-F12,V*T*Z-F12). Adapted from Ref. 63.

Figure 1 compares the CCSD(T)/CBS correlation energies for C_8H_8 with the best available results.[63] Suffice here to note that the trends observed with MP2 are similar but at a drastically smaller cost.[63] Indeed, the MP2/CBS energetics may be enhanced at zero-cost to approximate couple-cluster quality via spin scaling[72] using variable-scaling opposite spin[73] (VOS) theory. The following results are highlighted:[63] a) use of a (sM, M) basis-set pair is enough to mimic the CCSD(T) reference data[71] with high accuracy [rmsd of 3.01, 0.42, and 0.64 kcal mol^{-1} from (MINI, VDZ), (MINI, VDZ-F12), and (STO-2G, VDZ-F12), respectively], which compares with 0.49 kcal mol^{-1} from our recently[41] recommended CBS(*d, t*) scheme; b) the wall-times are generally much smaller than the references,[70] and up to a fiftyfold factor than CCSD(T)/CBS(V*D*Z-F12, V*T*Z-F12) for the cheapest extrapolation pair; c) the above results outperform DFT/M06-2X by up to 2.8 kcal mol^{-1}, which performs itself similar to MP2/CBS(MINI, VDZ-F12); d) CBS(sM, M) schemes are pseudo single-level;[6,74] e) CBS(sM, sM) extrapolations show somewhat modest performances, but at drastically smaller costs while occasionally performing at an accuracy comparable to some DFT functionals. Reasons for such a performance were advanced based on the so-called closeness criterion.[63] In summary, while giving a reliable prediction of the ups and downs in the evolution of the

isomerization energy, such educated predictions contrast with the mismatched pattern observed at raw ab initio level with sM bases, an ordering also difficult to get with DFT.[70]

IV. A further glimpse on carbon compounds

Continuing on carbon compounds, suffice it to note that much of their diversity and complexity stems from the capacity of C atoms to bond with one another in various chain and ring structures and 3*D* conformations, as well as for linking with other atoms. Indeed, they are probably as many as the different types of living organisms, thus justifying the specialized field of organic chemistry. Although organic molecules may contain other elements, it is the carbon-hydrogen bond that defines them as organic and organic chemistry as chemistry of life. Having addressed some intricacies of C_3H_8 in section IIIA, we turn in this section to pure carbon clusters and C_3H, an akin carbon-hydrogen compound.

A. Small pure carbon clusters

Carbon clusters have long attracted both chemists and physicists alike. The small ones are key in the chemistry of carbon rich stars, comets and interstellar molecular clouds, while acting as building blocks in the formation of complex C-containing species. Besides the panoply of astrophysical significance, they are important in the formation of fullerenes, nanotubes, and carbon-rich thin films, while predominant in terrestrial shooting flames.[75-83] All this due to the exceptional properties of C in forming single, double, and triple (eventually quadruple in the dimer[84]) bonds. Clearly, the elucidation of possible mechanisms leading to formation and growth of such C-clusters requires that the properties of small ones are understood.[80] It turns out that distinct but nearly isoenergetic isomers can be formed in a high-density of low-lying singlet and triplet states, which makes their study most challenging.[81,83] In fact, C-clusters in the small size range have been described in a variety of mass spectrometric observations,[65,75-77,93-99] while both spin states have been extensively studied with *ab initio* and DFT[100,101] calculations.

Although KS DFT has been vastly used in studying C-clusters, we have recently[41] shown that MP2/CBS(*d, t*) energies[6,31,43] rival DFT calculations with the popular M06-2X functional[39] (and references therein) both in time and accuracy. Such a performance extends to other functionals: MP2/CBS(*d, t*) outperforms DFT/B3LYP-

D3[102] for the same V*D*Z basis set by showing energy errors at least twice smaller for the same test set. Suffice to add that the MP2/CBS(*d*, *t*) energetics could be enhanced at zero-cost to approximate couple-cluster quality by using variable-scaling opposite spin[73] (VOS) theory.

Carbon clusters also offer a fertile ground to test methods for automated location of the many stationary points occurring on their potentials, and even full reaction pathways. Even if no claim is made of a fully elaborated tool,[65] we have suggested a simple scheme based solely on *ab initio* calculations that may be used to locate their most relevant intermediates. The approach consists of inducing an adiabatic breakup of a bond (preferably at a minimum), which is then stimulated to follow until dissociation using *ab initio* techniques. Because it is essentially a generalization of our own optimized reaction coordinate[61,103] (ORC) method, it was named ORC for stimulated evolution (ORCSE[65]) where all but the inactive degrees of freedom (DOF) are optimized. Briefly, the following three-point premise is accepted in ORCSE: (1) all intermediates are well approximated at MP2/CBS(*d*, *t*) level of theory; (2) all are accessible through a reaction coordinate that involves the stretch of a bond, a twist, or even any specially designed combination of stretches and twists, once all other DOF are fully optimized; (3) given the limitations of the optimization process, alternative paths may potentially be induced in unveiling other (unknown) stationary points. Although full optimization of all DOF but the inactive coordinate warrants in principle completeness, this cannot be ensured due to difficulties in covering the full configuration space and the fact that most algorithms converge to the closest stationary point.

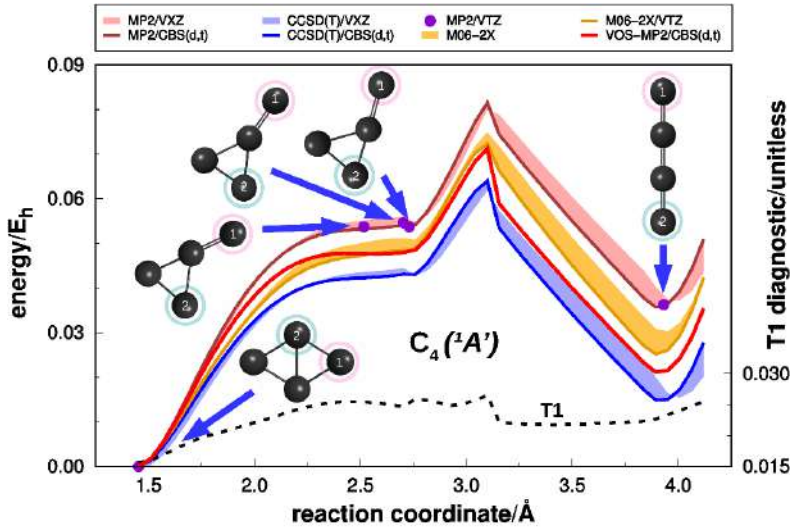

Figure 2: ORCSE path showing all structural isomers of $C_4(^1A')$ obtained by varying the distance between atoms 1 (circled in pink) and 2 (cyan). With R_{12} the inactive coordinate, all other DOF have been fully optimized, and the energies taken relative to the starting geometry. The shaded areas indicate the range of energies covered from *DZ* to CBS(*d*, *t*), with the latter indicated by the solid colored line. A similar procedure is adopted for DFT, except for the line that refers now to M06-2X/V*TZ*. The dots indicate fully optimized MP2/V*TZ* energies, and the black dashed line the T1 diagnostic[106] for validity of single-reference methods. For illustration, two other structures (not necessarily stationary points up to a tight convergence) before and after the C_{2v} TS, are also shown. Adapted from Ref. 65.

In the following, we illustrate ORCSE for singlet C_4 (see elsewhere[65] for other clusters), which aimed originally at validation of the approach since it had already been studied at high levels of *ab initio* theory.[83] In fact, linear triplet C_4 has also been studied spectroscopically, although cyclic ^1A_g eluded identification thus far. Being a small cluster, the V*TZ* basis set could be utilized,[104,105] with all raw energies subsequently CBS extrapolated from the two lowest steps of the hierarchical staircase for correlation consistent basis sets, $x = d$ and t. Figure 2 shows the ORCSE path[65] for $C_4(^1A')$. The overall evolution process is seen to occur stepwise in a plane: starting from the ^1A_g global minimum (rhombic), the system attains a C_s monocyclic ring form (distorted kite) via a ring-opening process in which a single peripheral bond is broken, crosses the C_{2v} transition state (TS), visits the other equivalent kite structure, and finally attains linearity after passing a peak of high energy associated with a *L*-shaped structure. Along such a path, single-point MP2/V*DZ*, VOS-MP2/V*XZ*, and CCSD(T)/V*XZ* (*X*=*D*, *T*) calculations were next performed, and subsequently CBS(*d*, *t*) extrapolated.[65] Notably, the height of the C_{2v} transition state in C_4 shows good agreement with our own CASDC/CBS(*T*,*Q*)

estimate[83] of 29.73 kcal mol^{-1} using AV*X*Z basis sets (see elsewhere[107] for the CASDC method). The corresponding result with DFT/M06-2X and a V*D*Z basis is 33.1 kcal mol^{-1}, thence similar to MP2/CBS(*d, t*) value of 33.9 kcal mol^{-1}. No comparison has been possible for the V*T*Z basis since M06-2X does not predict such a saddle point, apparently not an uncommon finding.[108] Of course, the very good agreement[50] observed may have been somewhat accidental as the CASDC/CBS(*T, Q*) estimate[83] for the relative stability of the cyclic *vs* linear forms places the latter 6.14 kcal mol^{-1} above the former, which is nearly 50 % smaller than VOS-MP2/CBS(*d, t*) but yet a fourfold factor smaller than with DFT/M06-2X.[108]

Of crucial interest for reaction dynamics is the availability of a global PES, preferably in analytical form. Among the most reliable approaches, the MBE[8,109] and DMBE[9,110,11] methods play a prominent role having acquired popularity. By developing the total interaction energy as an expansion of the energies of all involved atomic subclusters,[8] such methods provide an accurate description of valence interactions while accounting for the correct asymptotic behavior of all *n*-body terms in the series. In fact, all dissociation limits (as well as long- range interactions in DMBE) are naturally warranted. In fact, once the potentials of all fragments have been obtained, a truncated series may even be used to predict an approximate version of the PES for the target polyatomic[8,109] (see later). A word of caution is mandatory though: even if converging rapidly, chemical accuracy is generally attainable only when including up to the highest-order non-pairwise-additive terms.[8,9]

Regarding *l*-$C_4(^3\Sigma_g^-)$, the Wigner-Witmer spin-spatial correlation rules[112,113] show that it dissociates adiabatically as follows:

$$l\text{-}C_4(^3\Sigma_g^-) \rightarrow C_2(a\,^3\Pi_u) + C_2(a\,^3\Pi_u) \quad (6)$$

$$\rightarrow l\text{-}C_3(\tilde{X}\,^1\Sigma_g^+) + C(^3P) \quad (7)$$

$$\rightarrow C_2(a\,^3\Pi_u) + 2C(^3P) \quad (8)$$

$$\rightarrow 4C(^3P) \quad (9)$$

So, like $C_3(\widetilde{X}\,^1\Sigma_g^+)$,[8,114-116] *l*-$C_4(^3\Sigma_g^-)$ does not dissociate to ground-state C_2 fragments. Indeed, channel (6) lies[117] 17.2 kJ mol^{-1} above $C_2(X\,^1\Sigma_g^+) + C_2(X\,^1\Sigma_g^+)$ which is spin-forbidden for *l*-$C_4(^3\Sigma_g^-)$; it correlates[118] with *l*-$C_4(^1\Sigma_g^+)$. Dissociation into $C_2(a\,^3\Pi_u)$ fragments is also found to occur with an endothermicity of 607.0 kJ mol^{-1}, while dissociation into C_3 and C fragments gives both in their ground states; for the energetics, see left panel of Figure 3. The above collinear reaction path is actually the lowest for formation of *l*-$C_4(^3\Sigma_g^-)$ being exothermic by 503.7 kJ mol^{-1}. In fact, the first excited asymptotic channel $C_3(\tilde{a}\,^3\Pi_u)$+$C(^3P)$ lies[119,120] 202.8 kJ mol^{-1} above the asymptote in Eq. (7), thus correlating with higher excited states like *l*-$C_4(^3\Pi_u)$[121] and *l*-$C_4(^1\Sigma_g^+)$. Atomization occurs via dissociation of $C_3(\widetilde{X}\,^1\Sigma_g^+)$ into $C_2(a\,^3\Pi_u)$ + $C(^3P)$, followed by fragmentation of the diatomic into $C(^3P)$+$C(^3P)$.[116]

Using the above, the DMBE[9,110,111] PES of C_4 truncated at three-body terms assumes the form

$$V_{C_4}^{(2+3)}(\mathbf{R}) = V_{C_aC_b}^{(2)}(R_1)+V_{C_aC_c}^{(2)}(R_2)+V_{C_aC_d}^{(2)}(R_3)+V_{C_cC_d}^{(2)}(R_4)+V_{C_bC_d}^{(2)}(R_5)+V_{C_bC_c}^{(2)}(R_6)$$
$$+V_{C_aC_bC_c}^{(3)}(R_1,R_2,R_6)+V_{C_aC_cC_d}^{(3)}(R_2,R_3,R_4)+V_{C_aC_bC_d}^{(3)}(R_1,R_3,R_5)+V_{C_bC_cC_d}^{(3)}(R_4,R_5,R_6), \quad (10)$$

where $\mathbf{R}=\{R_i\}$ is a collective variable of all interparticle distances. According to the DMBE[9,110,111] formalism, each *n*-body term is then partitioned into its extended Hartree-Fock (EHF) and dynamical correlation (dc) contributions; see elsewhere[116,122] for details. Suffice to add that all the fragments dissociate into ground-state C atoms, hence one-body terms are not required as they are set as reference.

Regarding the potential functions used for two- and three-body terms, they have been taken from *ab initio* potentials previously reported. For enhanced reliability, some have been fine-tuned from available spectroscopic data. Specifically, for the trimers, a simplified version of the multiple energy switching (ES) rovibrational energies up to about 4000 cm^{-1} above zero-point energy (ZPE); see the original publications for details.

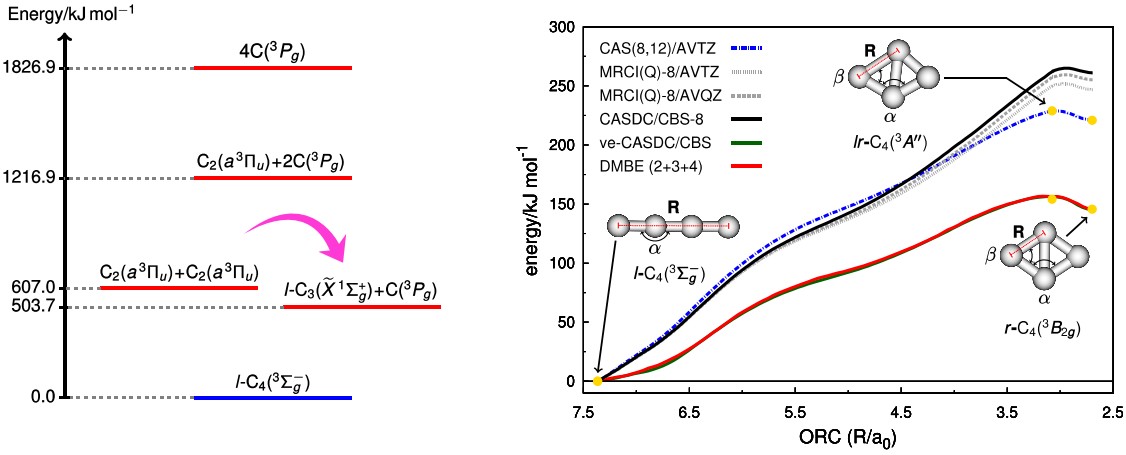

Figure 3: Left: Energetics of the various asymptotic channels of l-$C_4(^3\Sigma_g^-)$; the arrow signals the $C_2 + C_2 \rightarrow C_3 + C$ exothermic reaction, not studied thus far. Right: Optimized reaction path for interconversion between l-$C_4(^3\Sigma_g^-)$, and r-$C_4(^3B_{2g})$, via *lr*-$C_4(^3A'')$. The inactive coordinate corresponds to the peripheral bond length of the r-$C_4(^3B_{2g})$ structure (R), with all remaining DOF optimized at each grid point. Stationary structures obtained at CAS(8,12)/AVTZ, CASDC/CBS and CASDC/CBS//CAS(8,12)/AVTZ levels are symbolized by circles, diamonds and triangles, respectively. Energies are relative to *l*-$C_4(^3\Sigma_g^-)$. See also text. Adapted from Ref. 83.

Even if repeatedly noted, high accuracy can only be expected when adding up to the highest-order terms in the MBE, and hence a four-body term is needed. To enhance the PES accuracy, an approximate four-body term has therefore been added to DMBE(2+3), which is denoted DMBE/ES-SS-(2+3) in Ref. 83. For this, the *n*-body distributed polynomial method[125] was employed but with Gaussian functions centered at convenient geometries. It assumes the form[83]

$$V_{C_4}^{(4)}(\mathbf{R}) = \sum_{i=1}^{7} P_i^{(4)}(\mathbf{\Gamma}) G_i(\mathbf{\Gamma}), \tag{11}$$

scheme[123,124] has been employed, with the functions so obtained showing rmsds of some cm^{-1} for where $P_i^{(4)}(\mathbf{\Gamma})$ are cubic polynomials,

$$P_i^{(4)} = (c_0 + c_1\Gamma_1 + c_2\Gamma_1^2 + c_3\Gamma_2 + c_4\Gamma_3 + c_5\Gamma_1^3 + c_6\Gamma_1\Gamma_2 + c_7\Gamma_1\Gamma_3 + c_8\Gamma_4 + c_9\Gamma_5 + c_{10}\Gamma_6) \tag{12}$$

and

$$G_i(\mathbf{\Gamma}) = \exp[-\gamma_i(\Gamma_1)^2] \tag{13}$$

are range-determining factors. In turn, Γ_i (i=1-6) are totally coordinates[8,126]

$$\Gamma_1 = Q_1 \tag{14}$$
$$\Gamma_2 = Q_2^2 + Q_3^2 + Q_4^2 \tag{15}$$
$$\Gamma_3 = Q_5^2 + Q_6^2 \tag{16}$$
$$\Gamma_4 = Q_2 Q_3 Q_4 \tag{17}$$
$$\Gamma_5 = Q_6^3 - 3Q_6 Q_5^2 \tag{18}$$
$$\Gamma_6 = Q_6(2Q_2^2 - Q_3^2 - Q_4^2) + \sqrt{3}Q_5(Q_3^2 - Q_4^2) \tag{19}$$

where Q_i (i=1-6) are symmetrized displacements from a T_d reference of bond length R_0:[8,126]

$$\begin{pmatrix} Q_1 \\ Q_2 \\ Q_3 \\ Q_4 \\ Q_5 \\ Q_6 \end{pmatrix} = \begin{pmatrix} \sqrt{1/6} & \sqrt{1/6} & \sqrt{1/6} & \sqrt{1/6} & \sqrt{1/6} & \sqrt{1/6} \\ \sqrt{1/2} & 0 & 0 & -\sqrt{1/2} & 0 & 0 \\ 0 & \sqrt{1/2} & 0 & 0 & -\sqrt{1/2} & 0 \\ 0 & 0 & \sqrt{1/2} & 0 & 0 & -\sqrt{1/2} \\ 0 & 1/2 & -1/2 & 0 & 1/2 & -1/2 \\ \sqrt{1/3} & -\sqrt{1/12} & -\sqrt{1/12} & \sqrt{1/3} & -\sqrt{1/12} & -\sqrt{1/12} \end{pmatrix} \begin{pmatrix} R_1-R_0 \\ R_2-R_0 \\ R_3-R_0 \\ R_4-R_0 \\ R_5-R_0 \\ R_6-R_0 \end{pmatrix}. \tag{20}$$

Thence, in the T_d symmetry point group, Q_1 transforms as A_1, (Q_2, Q_3, Q_4) as the triply-degenerate T_2 irreducible representation and (Q_5, Q_6) as the double-denegerate E mode.

To calibrate the above four-body term, 663 *ab initio* points have been calculated for C_4. Of them, 53 refer to constrained optimized geometries for collinear approximations of $C_3 + C$ and $C_2 + C_2$ at CASDC/CBS level, using C_{2v} and D_{2h} symmetries, respectively. The four-body interaction energies were then obtained from the requirement that they should vanish at all dissociation limits once subtracting DMBE(2+3) from the total interaction energies. Additionally, 76 arrangements related to the ORC path in Figure 3 have been included. To acquire CASDC/CBS quality, the actually computed MRCI(Q)-8/AV*T*Z energies were finally scaled to reproduce the CASDC/CBS splitting between the *l*-$C_4(^3\Sigma_g^-)$ and *r*-$C_4(^3B_{2g})$ forms (ΔE_{lr} = 0.0555 E_h) using

$$\mathcal{F} = \frac{[E_3^{\text{MRCI(Q)-8}}(\mathbf{R}_r) - E_3^{\text{MRCI(Q)-8}}(\mathbf{R}_l)]}{\Delta E_{lr}}, \tag{21}$$

where $E_3^{\text{MRCI(Q)-8}}(\mathbf{R}_r)$ and $E_3^{\text{MRCI(Q)-8}}(\mathbf{R}_l)$ denote MRCI(Q)-8/AV*T*Z energies of the rhombic and linear isomers at FVCAS/AV*T*Z optimized geometries, yielding $\mathcal{F}$=1.7010. From Eq. (21), the total interaction energy of any arbitrary structure x with respect to *l*-$C_4(^3\Sigma_g^-)$ was then obtained as

$$E_x(\mathbf{R}) = \frac{[E_3^{\text{MRCI(Q)-8}}(\mathbf{R}_x) - E_3^{\text{MRCI(Q)-8}}(\mathbf{R}_l)]}{\mathcal{F}} + E_l(\mathbf{R}), \tag{22}$$

where $E_l(\mathbf{R})$ = -0.7127 E_h is the total interaction energy of the linear global minima (with respect to the infinitely separated atoms) predicted from CASDC/CBS calculations, a result in excellent agreement with the experimental estimate of -0.6958 E_h.[98,116,127]

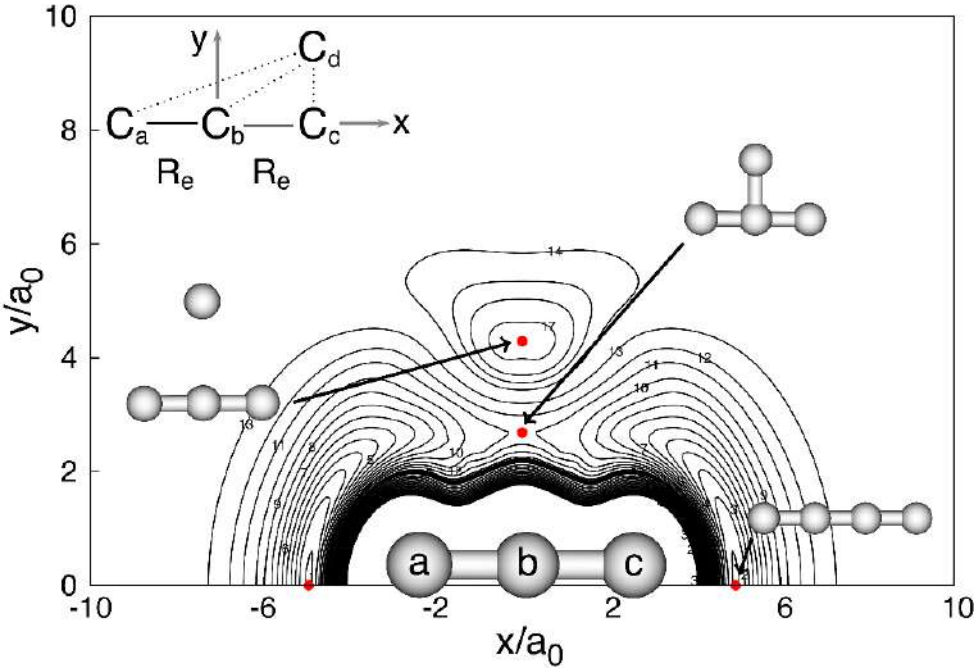

Figure 4: Partially relaxed contour plot of DMBE(2+3+4) PES [DMBE/ES-SS-(2+3+4) in the original work] for C moving around C_3 which lies along the x axis with the origin fixed at the central carbon atom. Contours are equally spaced by 0.015 E_h, starting at -0.7312 E_h. Adapted from Ref. 83.

Figures 4 and 5 illustrate salient attributes of the final DMBE(2+3+4) PES so obtained for ground-state triplet C_4.[83] Specifically, Figure 4 shows a contour plot for C moving around C_3. The notable feature is the T-shaped structure at (x, y)=(0.00, 2.69) a_0, which resembles the top of a barrier connecting the two symmetry equivalent l-$C_4(^3\Sigma_g^-)$ structures. It turns out not to be a true transition state in the 6D configuration space of C_4 but a saddle point of index 3, as actually predicted from the MRCI(Q) calculations. Another feature is the T-shaped long-range structure at (x, y) = (0.00, 4.02) a_0 where C_4 assumes an equilateral triangular form with D_{3h} symmetry possibly a symmetry-imposed conical intersection due to the involved C_3 fragments where such a topological feature is present. It turns out that preliminary CAS(8,12)/AV*T*Z calculations and the sign-reversal property of the wave-function[128] have not confirmed such a prediction but revealed the presence of a high-density of close-in-energy states in that region. Note that C-clusters

are fertile ground for the appearance of such topological features, with the interested reader referred elsewhere[83,129,130] (and references therein) for details on the underlying theory. The in-plane attack of C_2 by another C_2 is shown in Figure 5.[83] A notable feature is a C_{2v} structure at $(x, y) = (0.00, 4.05)\ a_0$. Apparently a minimum, it is actually a saddle point in 6*D*. Related to the degenerate isomerization of symmetrically equivalent *l*-$C_4(^3\Sigma_g^-)$ structures, such a feature has been confirmed both at MRCI(Q)-8/AV*T*Z and CCSD(T)/AV*T*Z levels of theory.[83] Instead, such a C_3-monocyclic form is found to be a minimum in DFT calculations.[108,131] Also visible are two additional extrema on the DMBE potential: a distorted C_2 capped triangle at $(x, y) = (4.58, 2.64)\ a_0$ and a quasi-rhomboedric form at $(x, y) = (5.08, 0.67)\ a_0$. Although predicted as minimum and transition state (respectively) in 2*D*, their rigorous assignment could not be done as it would require high-level FVCAS/MRCI frequency calculations, a task unaffordable at present.

B. A key carbon-hydrogen molecule: C_3H

Ubiquitous in the interstellar medium (ISM),[132] small carbon-bearing species like C_n and C_nH(n = 1-3) are conspicuous in driving C-chemistry[133] in cold dense clouds[134-136] and circumstellar envelopes of evolved C-rich stars.[137-139] In ISM,[140] C_3H is believed to play a major role, reaching high fractional abundances ($\approx 10^{-9}$) when compared to H_2.[133,141] Both its cyclic[142] (*c*-CH_3, cyclopropynylidyne) and linear[143] (ℓ-C_3H; propynylidyne) isomers are deemed as formed there either via dissociative electron recombination of[144] *c*,ℓ-$C_3H_2^+/C_3H_3^+$ or through the $C+C_2H_2$ neutral pathway[144-147] which is key in the formation of C-chains in space.[145-147] This prompted further surmises[148] on the role of *c*-C_3H as intermediate (via *c*-C_3H_2 formation) in the synthesis of interstellar polycyclic aromatic hydrocarbons which are recognized as potential carriers of unidentified IR bands.[149] The following summarizes the current status of the title radical with emphasis on the work done at the author's Group.[150]

Starting with ℓ-C_3H, it has a $^2\Pi$ ground-state and two bending modes, ν_4 (C-C-H) and ν_5 (C-C-C), which are perturbed by Renner-Teller (RT) and spin-orbit effects.[143] Discovered by Gottlieb *et al.*[151] who measured its microwave spectra in both $^2\Pi_{1/2}$ and $^2\Pi_{3/2}$ (ground) vibronic states, it was further studied by Yamamoto[152] and Kanada *et al.*[153] who recorded pure rotational lines in $\nu_4(^2\Sigma^u)$ while finding ℓ-C_3H to have

an extremely low vibrationally excited state ($\approx 27\ cm^{-1}$ above $^2\Pi_{1/2}$) due to strong RT effects in ν_4.[152] Subsequent work focused on improving[154] the spectroscopic constants of $^2\Pi_r$ and $v_4(^2\Sigma^\mu)$ and extending the range of rotational transitions in the $^2\Sigma$ vibrationally excited manifold.[155] IR vibrational band centers for stretching modes v_1, v_2 and v_3 were provided both in Ar matrices,[156] and gas phase.[157]

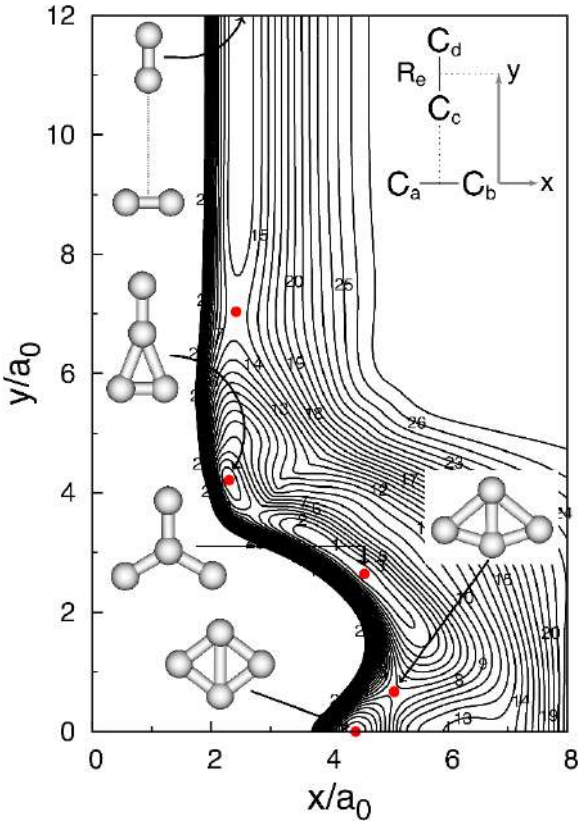

Figure 5: Partially relaxed contour plot for C_{2v} insertion of C_2 into another C_2 obtained from the DMBE(2+3+4) [ES-SS-(2+3+4) in the original work] PES. Contours are equally spaced by 0.015 E_h, starting at -0.6770 E_h. Adapted from Ref. 83.

Regarding *c*-C_3H, it has a $^2B_2$[142] ground electronic state as first detected by Yamamoto *et al.*[142,158] using microwave spectroscopy. Based on the predicted rotational constants, they reported the molecular structure of *c*-C_3H, while confirming its C_{2v} symmetry.[158]

Theoretically, a wealth of *ab initio* calculations were reported for C_3H. Early ones[142,153,156,159-164] were mainly devoted to elucidate discrepancies between the predicted

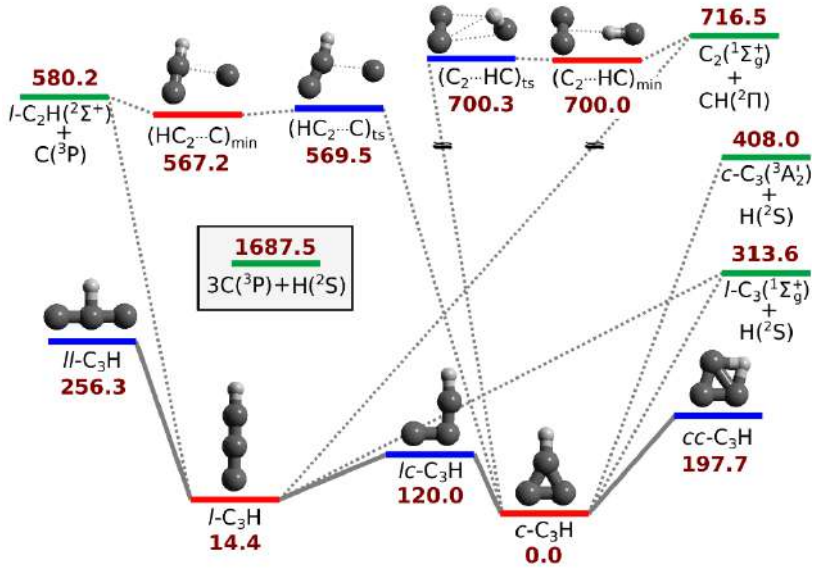

Figure 6: Pathways connecting the stationary points in CHIPR PES. Energies (in kJ mol^{-1}) refer to the global c-C3H minimum. Dotted lines connect dissociative channels (in green), while solid ones connect isomeric structures (red for minima, blue for transition states). Adapted from Ref. 150.

symmetries of the ℓ- and c-C_3H forms and those inferred from microwave spectroscopy,[153,158] with the best estimate[164] placing c-$C_3H \approx 14$ kJ mol^{-1} more stable than ℓ-C_3H. Such studies suggest that the calculated optimum structures may be transition states and that a slightly distorted C_s form may prevail. Such a symmetry breaking issue was first considered for the cyclic isomer by Stanton and coworkers.[165,166] Using the equation-of-motion CCSD method for ionized states, they emphasized the basis set role on the proper determination of its C_{2v} symmetry and increase of $X\ ^2B_2 \rightarrow A\ ^2A_1$ excitation energy. They further noted that the pseudo-Jahn-Teller effect between such states (previously considered[158] as responsible for its C_s equilibrium structure) is weakened when the size of the one-electron basis set is enhanced and CBS extrapolation done. Similar conclusions (regarding also the N-electron basis) were drawn at the MRCI+Q/VXZ ($X = D$ - Q) level of theory,[104,167] with Halvick[168] noting that the stiffness of the PES along the C-C asymmetric w_4 increases with correlation enhancement. In turn, Bassett and Fortenberry[169] reported a quartic force field (QFF) for c-C_3H from a composite scheme based on accurate CBS extrapolated CCSD(T)/AVXZ ($X = T$-5) energies that were additively corrected for core correlation and scalar relativistic effects.[169] From a QFF local form so obtained and using second-order vibrational perturbation theory, the authors further reported[169] rotational constants, structural parameters and anharmonic vibrational frequencies for the ground-state ($X\ ^2B_2$) that are

likely the highest-level *ab initio* estimates thus far. Most recently, Bennedjai *et al.*[170] performed a spectroscopic characterization of the C_3H isomers at CCSD(T)-F12/AV*T*Z level of theory. Yet, the most comprehensive theoretical study to date on ℓ-C_3H was carried out by Perić *et al.*[171] who provided local MRCI+Q/V*T*Z forms (including relativistic effects) for both ^{2}A' and ^{2}A" electronic states correlating with the $^2\Pi$ term. They further employed their PESs to compute the vibronic and spin-orbit structure of the ℓ-C_3H spectrum using a variational approach.[171] Moreover, they noted the extremely flat nature of the CCC-H bending potential curve (^{2}A') and, like others,[153,162] did not rule out the possibility of its quasilinearity. Despite the fact that their local forms assume $C_{\infty v}$ equilibrium geometries, the various spectroscopic parameters have shown excellent agreement with the experimental results. Indeed, Ding *et al.*[172] have shown that the minimum structure of ℓ-C_3H tends to move with basis set size enhancement (from AV*T*Z to AV*Q*Z) from a bent to a linear geometry at both CASSCF and CCSD(T) levels of theory. In turn, from CCSD(T)/6-311+G(3df,2p) calculations on the ground-state C_3H, Mebel and Kaiser[173] pointed out that the ℓ- and *c*-forms forms rearrange into each other through a ring-opening step via an asymmetric transition state (ℓc-C_3H) with a barrier of about 115 kJ mol^{-1}. They further note that besides $C(^3P_j)+C_2H_2(X^1\Sigma_g^+)$, the barrierless reactions $CH(X\,^2\Pi) + C_2(X\,^1\Sigma_g^+)$ and $C(^3P) + C_2H(X\,^2\Sigma^+)$ may be facile neutral-neutral exothermic pathways to yield carbon trimer in cold interstellar environments. Figure 6 underpins[150] most prominent features of the C_3H PES, clearly making it a unique and challenging species both from the chemical and astrophysical viewpoints.

Despite the prevalence of C_3H in ISM and its relevance in C-chain formation having stimulated considerable experimental[142,151-158,172] and theoretical[159-166,168-171,173,174] work to understand its intricate chemistry, most studies focused on energetics, symmetry and spectroscopy of its isomeric forms, and hence on local potential functions. Most recently, we have reported[150] the first global PES for ground state C_3H based on the CHIPR[175-177] method. It correlates with the $^2\Pi$ state at linear geometries and $^2B_2$ at cyclic ones, while describing correctly all fragmentation channels (see Figure 6). Indeed, it has already been successfully employed to carry out the first dynamics study of the $H + C_3$ reaction.[150] The analytical form is based on the matrix

$$\mathcal{H}_e = \begin{pmatrix} \mathcal{V}_{11}^{(2+3)}(\mathbf{R}) & \epsilon(\mathbf{R}) \\ \epsilon(\mathbf{R}) & \mathcal{V}_{22}^{(2+3)}(\mathbf{R}) \end{pmatrix} \tag{23}$$

where

$$\mathcal{V}_{11}^{(2+3)}(\mathbf{R}) = \sum_{i=1}^{3} V^{(2)}_{\mathrm{CH}(^2\Pi)}(R_i) + \sum_{i=4}^{6} V^{(2)}_{\mathrm{C_2}(^3\Pi_u)}(R_i) + V^{(3)}_{\mathrm{C_2H}(^2\mathrm{A}')}(R_2,R_3,R_6) + V^{(3)}_{\mathrm{C_2H}(^2\mathrm{A}')}(R_1,R_3,R_5) + V^{(3)}_{\mathrm{C_2H}(^2\mathrm{A}')}(R_2,R_3,R_6) + V^{(3)}_{\mathrm{C_3}(^1\mathrm{A}')}(R_4,R_5,R_6) \tag{24}$$

$$\mathcal{V}_{22}^{(2+3)}(\mathbf{R}) = \sum_{i=1}^{3} V^{(2)}_{\mathrm{CH}(^2\Pi)}(R_i) + \sum_{i=4}^{6} V^{(2)}_{\mathrm{C_2}(^1\Sigma_g^+)}(R_i) + V^{(3)}_{\mathrm{C_2H}(^2\mathrm{A}')}(R_2,R_3,R_6) + V^{(3)}_{\mathrm{C_2H}(^2\mathrm{A}')}(R_1,R_3,R_5) + V^{(3)}_{\mathrm{C_2H}(^2\mathrm{A}')}(R_2,R_3,R_6) + V^{(3)}_{\mathrm{C_3}(^3\mathrm{A}')}(R_4,R_5,R_6) \tag{25}$$

Because CHIPR assumes the MBE[8] form, with the reference being the infinitely separated ground-state C and H atoms, only a few remarks are required on its two-body and three-body terms. Following Ref. 178, $V^{(2+3)}(\mathbf{R})$ has been first defined as the lowest PES arising from diagonalization of a 2×2 pseudo-diabatic matrix, with the diagonal terms constructed from previously reported two- and three-body (ground-state) potentials for $C_2H(^2A')$,[179] $C_3(^1A')$[180] and $C_3(^3A')$[178] (see the original work[178-180] for details). In turn,

$$\epsilon^{(4)}(\mathbf{R}) = E^{\mathrm{CC/CBS}(d,\,t)}(\mathbf{R}) - V^{(2+3)}(\mathbf{R}) \tag{26}$$

is a coupling term chosen to warrant that the eigenvalues of $\mathcal{H}_e$ are continuous everywhere. The energetics of the various dissociation channels predicted from $V^{(2+3)}(\mathbf{R})$ compare well[150] with CC/CBS(d, t) calculations as well as experiment.[127,179,180] In fact, the agreement is quite good, with just a slight discrepancy for ℓ-$C_3(^1\Sigma_g^+)$ + $H(^2S)$, which is attributed to the more attractive nature of the ℓ-$C_3(^1\Sigma_g^+)$ three-body term. Note that this channel has the largest experimental uncertainty, while an accurate estimate of the ℓ-C_3 atomization energy still awaits determination. Because four-body energies vanish at all asymptotic channels, the dissociation energies in $V^{(2+3+4)}(\mathbf{R})$ remain as in $V^{(2+3)}(\mathbf{R})$.

An effective four-body term $V^{(4)}(\mathbf{R})$ must next be added,[150] namely

$$V^{(4)}(\mathbf{R}) = \sum_{i,j,k,l,m,n=0}^{L} C_{i,j,k,l,m,n} \left[\sum_{g \in G}^{} \mathcal{P}_g^{(i,j,k,l,m,n)} (y_1^i y_2^j y_3^k y_4^l y_5^m y_6^n) \right] \quad (27)$$

In fact, according to the CHIPR formalism the interaction energy, $\epsilon^{(4)}(\mathbf{R})$ can be conveniently modelled[175,176] using a L^{th}-degree polynomial ($i + j + k + l + m + n \leq L$), where $C_{i,j,k,l,m,n}$ are expansion coefficients and y_p ($p = 1, 2, \ldots, 6$) are transformed coordinates (see below). Note that only C coefficients referring to excitations of at least four modes (thence $i \leq j \leq k \leq l \leq m \leq n$) can be included, thus satisfying the constraints that avoid inclusion of two- or three-body contributions. Note further that the second summation runs over all permutation elements $g \in G$, where G is a subgroup of the $\mathcal{S}_4$ symmetric group.[182] For an AB_3-type molecule like the title one, $\mathcal{P}_g^{(i,j,k,l,m,n)}$ operators that reflect the action of the particle permutations[182] of $\mathcal{S}_4$ onto the exponent set $\{i, j, k, l, m, n\}$ brought by the first summation in Eq. (27). They will generate the required symmetrized sums of monomials that make $V^{(4)}(\mathbf{R})$ invariant to all permutations of identical atoms.[175-177]

Being a key point in CHIPR, every y_p is then expanded as a distributed-origin contracted basis[175-177]

$$y_p = \sum_{\alpha=1}^{M} c_\alpha \phi_{p,\alpha}, \quad (28)$$

with $\phi_{p,\alpha}$ expressed either as

$$\phi_{p,\alpha}^{[1]} = \text{sech}^{\eta}(\gamma_{p,\alpha} \rho_{p,\alpha}) \quad (29)$$

or

$$\phi_{p,\alpha}^{[2]} = \left[\frac{\tanh(\beta R_p)}{R_p} \right]^{\sigma} \text{sech}^{\eta} \left(\gamma_{p,\alpha} \rho_{p,\alpha} \right) \quad (30)$$

where $\rho_{p,\alpha} = R_p - R_{p,\alpha}^{\text{ref}}$ defines the displacement coordinate from the origin of the α^{th} primitive, $R_{p,\alpha}^{\text{ref}}$, $\gamma_{p,\alpha}$ are non-linear parameters, and $\eta = 1$, $\sigma = 6$ and $\beta = 1/5$ are constants.[175-177] As usual,[10] both $\phi_{p,\alpha}^{[1]}$ and $\phi_{p,\alpha}^{[2]}$ are employed,[150] with the latter appearing only once as the last term in the summation. Additionally, all distributed origins are related by[175-177]

$$R_{p,\alpha}^{\text{ref}} = \zeta (R_p^{\text{ref}})^{\alpha-1} \tag{31}$$

where ζ and R_p^{ref} are adjustable parameters.

Multiple cuts on the 6*D* configurational space of the CHIPR form have shown that it to reproduces reliably all its major topographical attributes.[150] For example, the left panel of Figure 7 illustrates the isomerization of the symmetry-equivalent *c*-C_3H structures which occurs via the C_{2v} transition state *cc*-C_3H, yet unreported at the date of our publication.[150] Located 197.7 kJ mol^{-1} above *c*-C_3H, it shows an imaginary frequency of 1693.9 cm^{-1} for the H wagging motion through the *c*-C_3 center-of-mass. In turn, classical barrier heights calculated[178] from CC/CBS(*d*, *t*) and MRCI+Q/CBS(*D*, *T*) protocols have shown good agreement with the CHIPR predictions, namely 194.2 and 188.8 kJ mol^{-1}, in the same order. Indeed, a close look at inset (b) shows that the CHIPR form reproduces accurately the entire minimum energy path (MEP) calculated at the CC/CBS(*d*, *t*) level of theory.

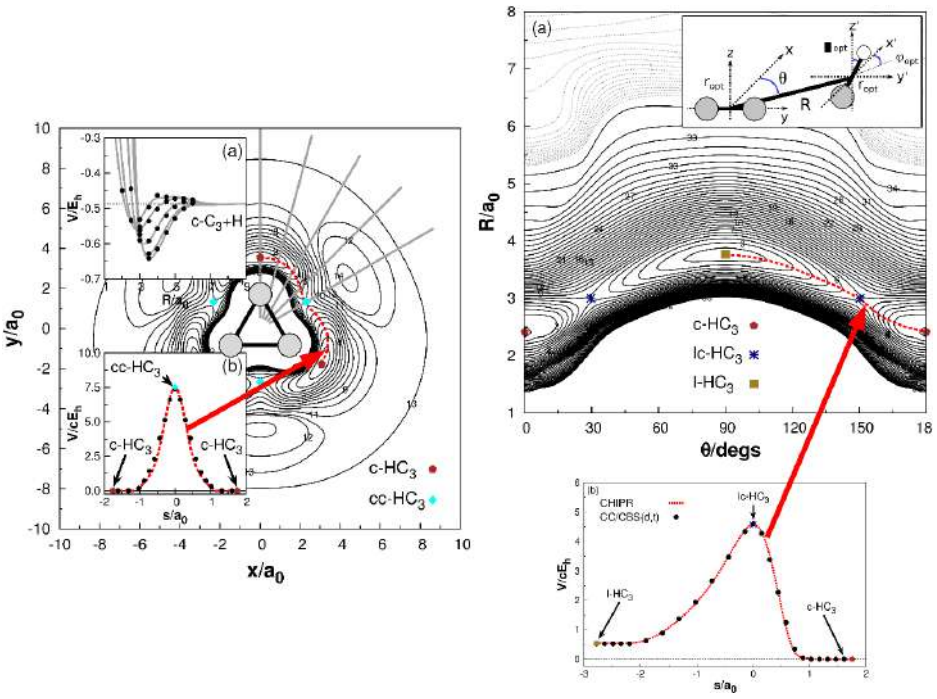

Figure 7: Left: contours for H atom moving around partially relaxed *c*-C_3 with center-of-mass fixed at the origin. Contours are equally spaced by 0.0135 E_h starting at -0:65 E_h. The reference energy is that of the infinitely separated atoms. Insets: (a) optimized 1*D* cuts; (b) minimum energy path for isomerization process (*s* is the reaction coordinate, with the reference energy being that of *c*-C_3H). Solid dots indicate *ab initio* CC/CBS(*d*, *t*) points while the dotted lines represent the dissociation predicted from $V^{(2+3)}$(**R**). Right: (a) contours for CH moving around a C_2 diatomic with center-of-mass fixed at the origin. All DOF but *R* and θ are partially relaxed. Black solid and gray dotted contours are equally spaced by 0.0075 and 0.00075Eh starting at -0.65 and -0.385 E_h. (b). MEP (s is the reaction coordinate in mass-scaled atomic units) for the isomerization *c*-

$C_3H \leftrightharpoons \ell$-$C_3H$ via transition state ℓc-C_3H. In both contour plots, the zero of energy refers to the infinitely separated atoms while for the right hand side (b) plot it corresponds to *c*-C_3H. Adapted from Ref. 150.

Besides *c*-C_3H the CHIPR form[150] predicts a linear ℓ-C_3H isomer which shows as a minimum 14.4 kJ mol^{-1} above the cyclic form. For comparison, the corresponding energy differences predicted at CC/CBS(*d, t*), CC-F12/AV*T*Z,[170] and MRCI+Q/CBS(*D, T*) levels of theory are 11.8, 15.4 and 5.3 kJ mol^{-1}, respectively. Regarding ℓ-C_3H, the structural parameters predicted from the CHIPR form[150] also agree well with the experimental (vibrationally averaged) r_0 values,[153] with CHIPR placing ℓ-$C_3H \sim 14.5$ kJ mol^{-1} above *c*-C_3H. However, discrepancies may be expected in the description of C-C-H and C-C-C degenerate bending modes whose vibrational angular momenta is known[153,154] to couple with the $^2\Pi$ (total) electronic angular momentum. Recall[153,171] that the strong RT effect makes the lowest ^{2}A' PES very flat along w_4, with appearance of a quasi-linear C_3H molecule. Yet, in accordance with recent CC-F12 calculations[170] and Ref. 172, CBS extrapolations tend to favor the highest symmetry $C_{\infty v}$ species. Suffice to add that the predicted structural parameters and harmonic frequencies for ℓ-C_3H are close to those predicted from the PES from the Perić *et al.*[171].

To conclude this section, the right hand side panel of Figure 7 shows a contour plot for CH moving around C_2. Clearly visible is the presence of a T-shaped (C_2v) transition state, $\ell\ell$-C_3H, which is responsible for the degenerate isomerization of the symmetry-equivalent ℓ-C_3H structures. Its calculated imaginary frequency amounts to 1111.7 cm^{-1} and points toward the H wagging motion through the ℓ-C_3 center-of-mass. Such a feature, firstly reported in our work,[150] lies about 241.9 and 256.3 kJ mol^{-1} above the ℓ-C_3H and *c*-C_3H (respectively), with the corresponding isomerization barriers predicted from CC/CBS(*d, t*) and MRCI+Q/CBS(*D, T*) being 246.3 and 245.8 kJ mol^{-1}. Moreover, the bottom right-hand-side panel of Figure 8 evinces the reliability of the CHIPR form in reproducing the CC/CBS(*d, t*) MEP for this process. Note that the isomerization between *c*-C_3H and ℓ-C_3H occurs via the ℓc-C_3H transition state[144,173] whose imaginary frequency (796.1 cm^{-1}) points along the C-C bond breaking/forming process. Indeed, its classical barrier height of 120.0 kJ mol^{-1} relative to *c*-C_3H compares well with both CC/CBS(*d, t*) and MRCI+Q/CBS(*D, T*) estimates of 122.1 and 123.8 kJ mol^{-1}, respectively.

C. Large-size carbon clusters: are global potentials affordable?

Although a clear yes might be the expected answer, some remarks are in order. First, to recall that all reactions take place on a PES, although in a very large molecule (always assumed along the paper to be in vacuum) where thousands of coordinates may be involved (a well known case is protein folding,[183] even if in vacuum) there will be a difference relative to a simple chemical reaction: the conformational freedom is much larger than in the case of a small molecule, and hence the possibility arises that entropy is more important than in most small-molecule reactions. Because the point here is to discuss PESs rather than free-energy surfaces, there is the need to impose a limiting size to what is meant by large molecule: it must be such that reaction is expected to be governed by the potential energy (rather than the free energy) but still big enough for stimulating the posed query and some helpful analysis.

As a second remark, the terms full-dimensionality and globalness (often used in the literature as equivalent) deserve clarification. A local (versus global) potential function may be full-dimensional when involving all (3*N*-6) DOF, but a global potential must be full-dimensional, while implying that all possible channels associated to the involved *N*-atom molecule are in principle assessable. Thence, the latter should in principle be applicable in any dynamics study, from intramolecular to scattering, non-reactive or reactive.

Now, if global, the PES may be obtained by numerical interpolation [although the literature is vast[184] (and references therein), the most traditional approach – not implying cost-effectiveness or feasibility – employs cubic splines[185]] or by least-squares fitting of some functional form. While a truly global numerical potential is hardly conceivable (suffice it to recall the fact that the eSE may not have a converged solution at some regions of configuration space), analytical forms are commonly cheaper to use but suffer from being hard to formulate in hugely dimensional configuration spaces. All this without having in mind the computational cost of such a numerical potential, an issue already raised in the Introduction. Entering the realm of C-clusters, one should now recall that all intricacies encountered in the PESs of small clusters (and even more subtle ones that are likely to arise with increasing cluster size) will be present in the hugely dimensional configuration spaces of large clusters (174*D* for C_{60}).

From the above paragraphs, it is plausible to conclude that obtaining an accurate *ab initio*-based global PES for such large C-clusters is currently little less than unaffordable. Approximate methods are therefore at stake, with the problem demanding approximations both in the selection of the *ab initio* method for solution of the eSE and approach in fitting the myriad of points that must be calculated.

Rather than focusing on the purist approach of solving the eSE and fitting of the calculated points in a blind manner, we survey a recent suggestion to predict the structures and energetics of such C-clusters[186] by employing a truncated MBE[8] or its DMBE congener.[9,110,111] Accordingly, the PES of the large cluster is first approximated through a MBE development in terms of the potentials of the involved subclusters up to four-body ones.[8] This will not only warrant a correct description of the asymptotic behavior of every *n*-body term in the MBE, but also the involved dissociation limits (as well as long-range interactions in the case of using the DMBE method) are naturally described. Once such building-blocks are obtained, the truncated MBE or DMBE so obtained will enable a first prediction of the PES for the target polyatomic.[8,109] Of course, and emphasizing the point once more, high accuracy is only attainable when including up to the highest-order (in the limit, all non-pairwise-additive) terms.[8,9] Still, a major advantage over popular semiempirical valence-bond theories such as the DIM method[187-189] is that simpler and more flexible functional forms can be employed to fit *ab initio* and/or experimental information, and hence obtain reliable high-dimensional global potentials.

Regarding C-clusters, we follow Pitzer and Clementi[190] who first recognized the ℓ-C_x forms as low energy isomeric structures on their corresponding PESs. Thence, odd- and even-numbered chains (for $x > 2$) are assumed to correlate with their $^1\Sigma_g^+$ and $^3\Sigma_g^-$ ground electronic states, respectively. This is to say that all comparisons with the predictions to be made follow such an assumption.

Indeed, despite the fact *ab initio* calculations tend to support that monocyclic (singlet) isomers are nearly isoenergetic or even more stable than linear (triplet) arrangements,[191] the current predictions seem to indicate (in absence of cyclic global minima) that the fragments on which the corresponding $V^{(2+3+4)}$ DMBE forms are built correlate with triplet states of the C_x (x = 4, 6, 8, 10) clusters. This is rationalized from the fact that the PESs of ℓ-$C_3(\widetilde{X}\,^1\Sigma_g^+)$ and ℓ-$C_4(^3\Sigma_g^-)$ dissociate as follows:

$$\ell\text{-}C_3(\tilde{X}\,^1\Sigma_g^+) \rightarrow \quad C_2(a\,^3\Pi_u)+C(^3P) \tag{32}$$

$$\rightarrow \quad 3C(^3P), \tag{33}$$

and

$$\ell\text{-}C_4(\,^3\Sigma_g^-) \rightarrow \quad C_2(a\,^3\Pi_u)+C_2(a\,^3\Pi_u) \tag{34}$$

$$\rightarrow \quad \ell\text{-}C_3(\tilde{X}\,^1\Sigma_g^+) + C(^3P) \tag{35}$$

$$\rightarrow \quad C_2(a\,^3\Pi_u)+2C(^3P) \tag{36}$$

$$\rightarrow \quad 4C(^3P), \tag{37}$$

thus restricting any dissociation of the C_x (x = 5-10) PESs to occur according to the above.

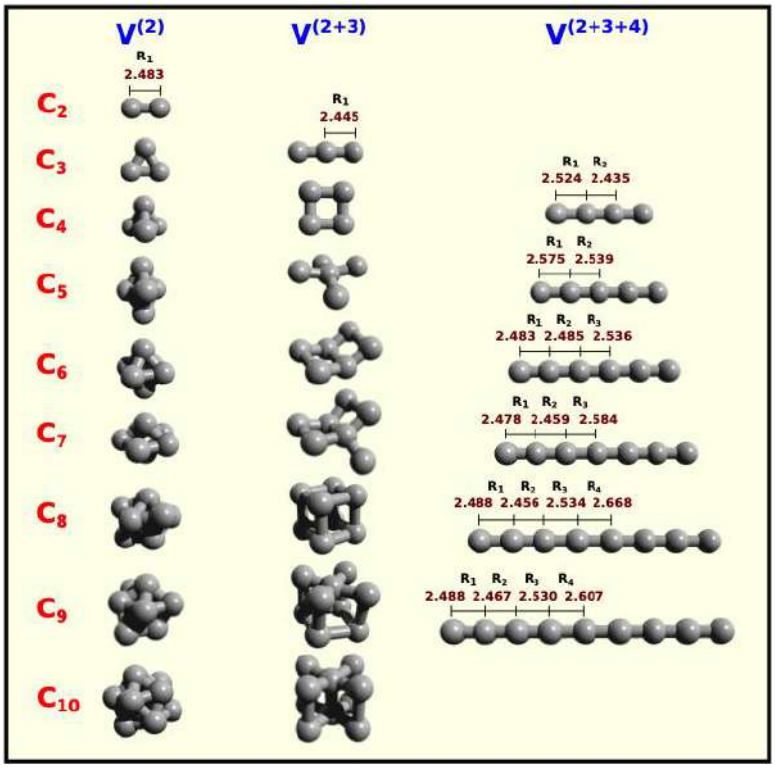

Figure 8: C_x (x=2-9) global minima as predicted from a truncated $V^{(2+3+4)}$ DMBE expansion. Also shown are structures obtained when PESs with only two- [$V^{(2)}$] or two- plus three-body potentials [$V^{(2+3)}$] are employed to get structural parameters, harmonic vibrational frequencies and dissociation energies for the ℓ-C_x clusters. Adapted from Ref. 186.

We next survey some virtues of the approach[186] by examining the first estimates of global DMBE PESs for C_x (x = 5-10) clusters obtained from the reported potentials for C_2, C_3, C_4.[83,116] First, Figure 9 illustrates the predictive capability of $V^{(2+3+4)}$ in providing estimates of global minima and their associated thermochemical properties.[186] Clearly, the good quality of the results give important insights into the structure-determining nature of the (2+3+4)-body terms. Indeed, they allow to judge the methodology as providing at least satisfactory first guesses of the true C_x potentials. Furthermore, it opens the way to construction of global reliable forms for large C-clusters (and possibly even other atomic clusters). Of course, the present approach may be open to improvement, *e.g.* by employing simple functional forms for higher-order terms (say, n=5 or 6) while assuming that the MBE/DMBE approximately converges beyond them. Unfortunately, this is difficult to judge since such terms may be minor but are numerous, *e.g.* for C_{10} there are 210 and 120 six- and seven-body terms, respectively. Still, for large clusters, it is fair to say that a large number of such terms approximately vanish since many of the atoms are far from the others.

Figure 9 shows contour plots for the collinear reactions ℓ-$C_{(x-2)} + C_2 \rightarrow \ell$-$C_{(x-1)} + C$, thence for the lowest-energy path yielding ℓ-C_x as predicted from the truncated DMBE forms.[186] Clearly, the predictive nature and cost-effectiveness of the method suggest that such truncated DMBE potentials may even be employed in evaluating gradients and hessians for large species, which may then be used as first guesses for stationary point searches in actual electronic structure calculations. Indeed, the approach has proven useful for C_4.[83]

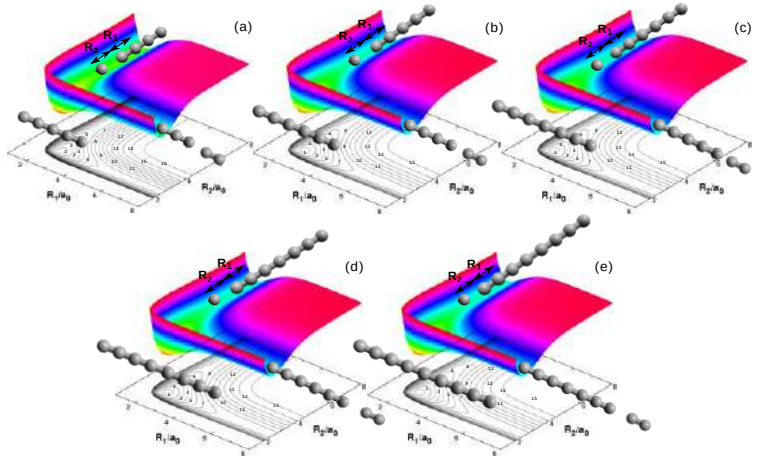

Figure 9: Partially relaxed contour plots for the collinear reactions (a) ℓ-C_3 + C_2 → ℓ-C_4 + C. Contours are equally spaced by 0.02 E_h, starting at -1.1 E_h; (b) ℓ-C4 + C2 → ℓ-C_5 + C. Contours are equally spaced by 0.03 E_h, starting at -1.3 E_h; (c) ℓ-C_5+C_2 → ℓ-C_6+C. Contours are equally spaced by 0.02 E_h, starting at -1.1 E_h; (d) ℓ-C_6 + C_2 → ℓ-C_7 + C. Contours are equally spaced by 0.02 E_h, starting at -1.1 E_h; (e) ℓ-C_7 + C_2 → ℓ-C_8 + C. Contours are equally spaced by 0.02 E_h, starting at -1.1 E_h. Adapted from Ref. 186.

V. Concluding remarks

Saturating a basis in electronic structure calculations is key but mostly unaffordable for medium- and large-sized molecules. CBS extrapolation offers a cost-effective and reliable way out, and we have shown[6,63] how to obtain highly accurate correlation energies from various methods and basis sets by CBS extrapolating the raw energies with the USTE scheme. The method is applicable to any basis set family even if not of the correlation consistent type, which we have shown how to hierarchize from the recovered correlation energy. Because the joint use of a SM and an E basis sets costs as much as a single-point calculation just with the latter, its USTE$_a$ variant has become, as efficient and perhaps even more reliable than any genuine single-level scheme.[6] Indeed, due to the low-cost and reliability of MP2/CBS(sM, M) and MP2/CBS(M, M) methods *vs* KS DFT, a wealth of topics are open to revisitation, ranging from CBS extrapolations in large systems to explicitly correlated calculations and on-the-fly dynamics. Left unreviewed in this work was progress on optimal basis sets[192,193] for direct extrapolation of the correlation energy. Specifically built for CBS extrapolating the correlation energy at the same cost as Dunning's V*X*Z and AV*X*Z ansatzes from which they have been derived, the novel optimized basis sets typically outperform the latter by factors of three- to fivefold. Although extrapolation of the HF energy is also key when accuracy is at demand, the topic could not be discussed for brevity, with the reader being addressed elsewhere.[6,31]

Using MRCI or CCSD(T) calculations, we have also shown how to model the global potential energy surfaces of any triatomic or even tetratomic systems in their full dimensionality by using the DMBE expansion and CHIPR methods. Indeed, a general computer code has recently been made available to generate triatomic CHIPR forms, while another of the same family will soon be reported for any tetratomic molecule jointly with an option for refining CHIPR two-body *ab initio* curves to spectroscopic accuracy from a fit to available vibrational levels. Both DMBE and CHIPR methods have

also been illustrated by considering ground-state C_4 and the akin C_3H radical. It is hoped that this work may stimulate further theoretical and experimental studies on such species which are of utmost relevance in carbon chemistry both in terrestrial and interstellar media, just to mention a few areas.

Acknowledgments

I wish to thank all my coworkers for their valuable contributions to the topics covered in the present work. The support from Fundação para a Ciência e a Tecnologia and Coimbra Chemistry Centre, Portugal, through the project UI0313/QUI/2013, co-funded by FEDER/COMPETE 2020-EU, and from China's Shandong Province "Double-Hundred Talent Plan" (2018) is also gratefully acknowledged.

References

1. M. Born and J. R. Oppenheimer, Ann. Phys. **84**, 457 (1927).

2. A. J. C. Varandas, J. P. da Providência, M. Brajczewska, and J. da Providência, Chem. Phys. Lett. **610**, 167 (2014).

3. A. J. C. Varandas, J. da Providência, and J. P. da Providência, Can. J. Phys. **98**, 379 (2020).

4. S. Ghosh, R. Sharma, S. Adhikari, and A. J. C. Varandas, Phys Chem Chem Phys **21**, 20166 (2019).

5. A. J. C. Varandas, Chem. Phys. Lett. **439**, 386 (2007)

6. A. J. C. Varandas, Ann. Rev. Phys. Chem. **69**, 177 (2018).

7. A. J. C. Varandas, J. Chem. Phys. **113**, 8880 (2000).

8. J. N. Murrell, S. Carter, S. C. Farantos, P. Huxley, and A. J. C. Varandas, *Molecular Potential Energy Functions* (Wiley, Chichester, 1984).

9. A. J. C. Varandas, Adv. Chem. Phys. **74**, 255 (1988).

10. A. J. C. Varandas, in *Reaction Rate Constant Computations: Theories and Applications*, edited by K. Han and T. Chu (The Royal Society of Chemistry, 2013), chap. 17, pp. 408–445.

11. T. Helgaker, P. Jørgensen, and J. Olsen, *Molecular Electronic-Structure Theory* (Wiley, Chichester, 2000).

12. T. Kato, Commun. Pure Appl. Math. **10**, 151 (1957).

13. S. Ten-no and J. Noga, WIREs Comput Mol Sci **2**, 114–125 (2012).

14. L. Kong, F. A. Bischoff, and E. F. Valeev, Chem. Rev. **112**, 75 (2012).

15. C. Hättig, W. Klopper, A. Köhn, and D. P. Tew, Chem. Rev. **112**, 4 (2012).

16. D. Vogiatzis, R. Haunschild, and W. Klopper, Theor Chem Acc **133**, 1446 (2014).

17. W. Klopper, B. Ruscic, D. P. Tew, F. A. Bischoff, and S. Wolfsegger, Chem. Phys. **356**, 14–24 (2009).

18. N. Sylvetsky, K. A. Peterson, A. Karton, and J. M. L. Martin, J. Chem. Phys. **144**, 214101 (2016).

19. M. K. Kesharwani, N. Sylvetsky, A. Köhn, D. P. Tew, and J. M. L. Martin, J. Chem. Phys. **149**, 154109 (2018).

20. L. A. Burns, M. S. Marshall, and C. D. Sherrilla, J. Chem. Phys. **141**, 234111 (2014).

21. D. A. Sirianni, L. A. Burns, and C. D. Sherrill, J. Chem. Theory Comput. **13**, 86-99 (2017).

22. M. K. Kesharwani, A. Karton, and J. M. L. Martin, J. Chem. Theory Comput. **12**, 444-454 (2016).

23. B. Brauer, M. K. Kesharwani, S. Kozuch, and J. M. L. Martin, Phys. Chem. Chem. Phys. **18**, 20905 (2016).

24. D. Manna, M. K. Kesharwani, N. Sylvetsky, and J. M. L. Martin, J. Chem. Theory Comput. **13**, 3136 (2017).

25. D. P. Tew, W. Klopper, M. Heckert, and J. Gauss, J. Phys. Chem. A **111**, 11242 (2007).

26. J. M. L. Martin and M. K. Kesharwani, J. Chem. Theory Comput. **10**, 2085 (2014).

27. D. P. Tew, W. Klopper, C. Neissb, and C. Hättig, Phys. Chem. Chem. Phys. **9**, 1921–1930 (2007).

28. D. Feller, K. A. Peterson, and T. D. Crawford, J. Chem. Phys. **124**, 054107 (2006).

29. V. Vasilyev, Computational and Theoretical Chemistry **1115**, 1 (2017).

30. W. Kutzelnigg, Int. J. Quantum Chem. **51**, 447 (1994).

31. F. N. N. Pansini, A. C. Neto, and A. J. C. Varandas, Theor. Chem. Acc. **135**, 261 (2016).

32. A. J. C. Varandas, J. Chem. Phys. **126**, 244105 (2007).

33. A. J. C. Varandas, Phys. Chem. Chem. Phys. **21**, 8022 (2019).

34. L. Bytautas and K. Ruedenberg, J. Chem. Phys. **122**, 154110 (2005).

35. L. Bytautas and K. Ruedenberg, J. Chem. Phys. **128**, 214308 (2008).

36. L. Bytautas and K. Ruedenberg, J. Chem. Phys. **130**, 204101 (2009).

37. L. Bytautas and K. Ruedenberg, J. Chem. Phys. **132**, 074109 (2010).

38. W. Kohn and L. Sham, Phys. Rev. A **140**, 1133 (1965).

39. R. Peverati and D. G. Truhlar, Phil. Trans. R. Soc. A **372**, 20120476 (2014).

40. N. Mardirossian and M. Head-Gordon, J. Chem. Theory Comput. **12**, 4303 (2016).

41. A. J. C. Varandas, M. M. González, L. A. Montero-Cabrera, and J. M. G. de la Vega., Chem. Eur. J. **23**, 9122 (2017).

42. M. M. González, F. G. D. Xavier, J. Li, L. A. Montero-Cabrera, J. M. G. de la Vega, and A. J. C. Varandas, J. Phys. Chem. A **124**, 126 (2020).

43. A. J. C. Varandas and F. N. N. Pansini, J. Chem. Phys. **141**, 224113 (2014).

44. K. Bondensgard and F. Jensen, J. Chem. Phys. **104**, 8025 (1996).

45. W. Quapp, M. Hirsch, O. Imig, and D. Heidrich, J. Comp. Chem. **19**, 1087 (1998).

46. K. Irikura and R. Johnson, J. Phys. Chem. A **104**, 2191 (2000).

47. E. Muller, A. de Meijere, and H. Grubmuller, J. Chem. Phys. **116**, 897 (2002).

48. D. J. Wales and J. P. K. Doye, J. Phys. Chem. A **101**, 5111 (1997).

49. S. Habershon, J. Chem. Theor. Comput. **12**, 1786 (2016).

50. S. Maeda, S. Komagawa, M. Uchiyama, and K. Morokuma, Angew. Chem. Int. Ed. **50**, 644 (2011).

51. W. Kutzelnigg and J. D. Morgan, J. Chem. Phys. **96**, 4484 (1992).

52. J. R. Flores, R. Slupski, and K. Jankowski, J. Chem. Phys. **124**, 104107 (2006).

53. T. H. Dunning Jr., K. A. Peterson, and D. E. Woon, in *Encyclopedia of Computational Chemistry*, edited by P. v. R. Schleyer, N. L. Allinger, T. Clark, J. Gasteiger, P. A. Kolman, and H. F. Schaefer III (Wiley, Chichester, 1998), p. 88.

54. T. H. Dunning Jr., J. Phys. Chem. A **104**, 9062 (2000).

55. F. Jensen, Advanced Review p. 1 (WIREs Comput. Mol. Sci.) (2012).

56. T. Helgaker, W. Klopper, H. Koch, and J. Noga, J. Chem. Phys. **106**, 9639 (1997)

57. A. Halkier, T. Helgaker, P. Jørgensen, W. Klopper, H. Koch, J. Olsen, and A. K. Wilson, Chem. Phys. Lett. **286**, 243 (1998).

58. K. Raghavachari and J. B. Anderson, J. Phys. Chem. **100**, 12960 (1996).

59. A. J. C. Varandas, J. Chem. Phys. **126**, 244105 (2007).

60. A. J. C. Varandas, J. Phys. Chem. A **112**, 1841 (2008).

61. A. J. C. Varandas, J. Phys. Chem. A **114**, 8505 (2010).

62. F. N. N. Pansini, A. C. Neto, and A. J. C. Varandas, Chem. Phys. Lett. **641**, 90 (2015).

63. A. J. C. Varandas, Phys. Chem. Chem. Phys. **20**, 22084 (2018).

64. J. G. Hill, K. A. Peterson, G. Knizia, and H.-J. Werner, J. Chem. Phys. **131**, 194105 (2015).

65. A. J. C. Varandas, The European Physical Journal D **72**, 180 (2018).

66. S. Grimme, Angew. Chem. Int. Ed. **45**, 4460 (2006).

67. P. R. Schreiner, A. A. Fokin, R. A. Pascal Jr, and A. de Meijere, Org. Lett. **8**, 3635 (2006).

68. P. R. Schreiner, Angew. Chem. Int. Ed. **46**, 4217 (2007).

69. M. S. S. Grimme and M. Korth, J. Org. Chem. **72**, 2118 (2007).

70. A. Karton and J. M. Martin, Mol. Phys. **110**, 2477 (2012).

71. A. Karton and J. M. L. Martin, J. Chem. Phys. **136**, 124114 (2012).

72. S. Grimme, J. Chem. Phys. **118**, 9095 (2003).

73. A. J. C. Varandas, J. Chem. Phys. **133**, 064104 (2010).

74. F. N. N. Pansini and A. J. C. Varandas, Chem. Phys. Lett. **631-632**, 70 (2015).

75. S. Arulmozhiraja and T. Ohno, J. Chem. Phys. **128**, 114301 (2008).

76. L. Belau, S. E. Wheeler, B. W. Ticknor, M. Ahmed, S. R. Leone, W. D. Allen, H. F. Schaefer III, and M. A. Duncan, J. Am. Chem. Soc. **129** (2007).

77. K. E. Yousaf and P. R. Taylor, Chem. Phys. **349**, 58 (2008).

78. N. Sakai and S. Yamamoto, Chem. Rev. **113**, 8981 (2013).

79. N. L. J. Cox and F. Patat, A&A **565**, A61 (2014).

80. T. W. Yen and S. K. Lai, J. Chem. Phys. **142**, 084313 (2015).

81. C. M. Rocha and A. J. C. Varandas, J. Chem. Phys. **144**, 064309 (2016).

82. S. K. Lai, I. Setiyawati, T. W. Yen, and Y. H. Tang, Theor. Chem. Acc. **136**, 20 (2017).

83. A. J. C. Varandas and C. M. R., Phil. Trans. Roy. Soc. A **376**, 20170145 (2018).

84. S. Shaik, D. Danovich, W. Wu, P. Su, H. S. Rzepa, and P. C. Hiberty, Nat Chem. **4**, 195 (2012).

85. E. A. Rohlfing, D. M. Cox, and A. Kaldor, J. Chem. Phys. **81**, 3322 (1984).

86. H. W. Kroto, J. R. Heath, S. C. O'Brien, R. F. Curl, and R. E. Smalley, Nature **318**, 162 (1985).

87. M. Y. Hahn, E. C. Honea, A. J. Paguia, K. E. Schriver, A. M. Camarena, and R. L. Whetten, Chem. Phys. Lett. **130**, 12 (1986).

88. E. A. Rohlfing, J. Chem. Phys. **93**, 7851 (1990).

89. T. Moriwaki, K. Kobayashi, M. Osaka, M. Ohara, H. Shiromaru, and Y. Achiba, J. Chem. Phys. **107**, 8927 (1997).

90. Y. K. Choi, H. S. Im, and K. K. W. Jung, Int. J. Mass Spectrom. **189**, 115 (1999).

91. M. E. Geusic, M. F. Jarrold, T. J. McIlrath, R. R. Freeman, and W. L. Brown, J. Chem. Phys. **86**, 3862 (1987).

92. C. H. Bae and S. M. Park, J. Chem. Phys. **117**, 5347 (2002).

93. J. D. Watts and R. J. Bartlett, Chem. Phys. Lett. **190**, 19 (1992).

94. J. Hutter and H. P. Lüthi, J. Chem. Phys. **101**, 2213 (1994).

95. J. M. L. Martin and P. R. Taylor, J. Phys. Chem. **100**, 6047 (1996).

96. R. O. Jones, J. Chem. Phys. **110**, 5189 (1999).

97. Y. Shlyakhter, S. Sokolova, A. Lüchow, and J. B. Anderson, J. Chem. Phys. **110**, 10725 (1999).

98. Karton, A. Tarnopolsky, and J. M. Martin, Mol. Phys. **107**, 977 (2009).

99. A. J. C. Varandas, European Physical Journal D **72**, 134 (2018).

100. N. A. Poklonski, S. V. Ratkevich, and S. A. Vyrko, J. Phys. Chem. A **119**, 9133 (2015).

101. C. Mauney, M. B. Nardelli, and D. Lazzati, ApJ **800**, 1 (2015).

102. S. Grimme, J. Comput. Chem. **27**, 1787 (2006).

103. A. J. C. Varandas, Phys. Chem. Chem. Phys. **16**, 16997 (2014).

104. T. H. Dunning Jr., J. Chem. Phys. **90**, 1007 (1989).

105. T. H. Dunning, Jr, K. A. Peterson, and A. K. Wilson, J. Chem. Phys. **114**, 9244 (2001).

106. T. J. Lee, Chem. Phys. Lett. **372**, 362 (2003).

107. A. J. C. Varandas, J. Phys. Chem. A **117**, 7393 (2013b).

108. A.C.Ngandjong, Z.Mezei, J. Mougenot, A.Michau, K.Hassouni, G.Lombardi, M.Seydou, and F.Maurela, Comp. Theor. Chem. **1102**, 105 (2017).

109. A. J. C. Varandas and J. N. Murrell, Faraday Discuss. Chem. Soc. **62**, 92 (1977).

110. A. J. C. Varandas, Mol. Phys. **53**, 1303 (1984).

111. A. J. C. Varandas, J. Mol. Struct. Theochem. **21**, 401 (1985).

112. E. P. Wigner and E. E. Witmer, Z. Physik. **51**, 859 (1928).

113. G. Herzberg, *Molecular Spectra and Molecular Structure. III Electronic Spectra and Electronic Structure of Polyatomic Molecules* (Van Nostrand, New York, 1966).

114. S. Carter, I. M. Mills, and J. N. Murrell, J. Mol. Spectrosc. **81**, 110 (1980).

115. S. Carter, I. M. Mills, and R. N. Dixon, J. Mol. Spectrosc. **106**, 411 (1984).

116. C. M. R. Rocha and A. J. C. Varandas, J. Chem. Phys. **143**, 074302 (2015).

117. M. Martin, J. Photochem. Photobiol. A **66**, 263 (1992)

118. J. P. Ritchie, H. F. King, and W. S. Young, J. Chem. Phys. **85**, 5175 (1986).

119. W. Weltner and D. McLeod, J. Chem. Phys. **40**, 1305 (1964).

120. Y. Sych, P. Bornhauser, G. Knopp, Y. Liu, T. Gerber, R. Marquardt, and P. P. Radi, J. Chem. Phys. **139**, 154203 (2013).

121. V. Wakelam, J.-C. Loison, E. Herbst, D. Talbi, D. Quan, and F. Caralp, A&A **495**, 513 (2009).

122. C. M. R. Rocha and A. J. C. Varandas, J. Chem. Phys. **144**, 064309 (2016).

123. A. J. C. Varandas, J. Chem. Phys. **105**, 3524 (1996).

124. A. J. C. Varandas, J. Chem. Phys. **119**, 2596 (2003).

125. E. Martínez-Núñez and A. J. C. Varandas, J. Phys. Chem. A **105**, 5923 (2001).

126. A. J. C. Varandas and J. N. Murrell, Chem. Phys. Lett. **84**, 440 (1982).

127. K. A. Gingerich, H. C. Finkbeiner, and R. W. Schmude, J. Am. Chem. Soc. **116**, 3884 (1994).

128. A. J. C. Varandas, J. Tennyson, and J. N. Murrell, Chem. Phys. Lett. **61**, 431 (1979).

129. A. J. C. Varandas, Chem. Phys. Lett. **487**, 139 (2010).

130. A. J. C. Varandas and B. Sarkar, Phys. Chem. Chem. Phys. **13**, 8131 (2011).

131. S. J. Blanksby, D. Schroder, S. Dua, J. H. Bowie, and H. Schwarz, J. Am. Chem. Soc. **2000**, 7105 (2000).

132. B. A. McGuire, ApJS **239**, 17 (2018).

133. R. I. Kaiser, Chem. Rev. **102**, 1309 (2002).

134. I. W. M. Smith, E. Herbst, and Q. Chang, MNRAS **350**, 323 (2004).

135. I. W. M. Smith, A. M. Sage, N. M. Donahue, E. Herbst, and D. Quan, Faraday Discuss. **133**, 137 (2006).

136. J.-C. Loison, V. Wakelam, K. M. Hickson, A. Bergeat, and R. Mereau, MNRAS **437**, 930 (2014).

137. T. J. Millar and E. Herbst, A&A **288**, 561 (1994).

138. R. J. Hargreaves, K. Hinkle, and P. F. Bernath, MNRAS **444**, 3721 (2014).

139. M. Agúndez, J. Cernicharo, G. Quintana-Lacaci, A. Castro-Carrizo, L. Velilla Prieto, N. Marcelino, M. Guélin, C. Joblin, J. A. Martín-Gago, C. A. Gottlieb, et al., A&A **601**, A4 (2017).

140. *NIST standard reference database number 101* (2013), release 16a. Editor: Russell D. Johnson III, URL http://cccbdb.nist.gov/.

141. M. Agúndez and V. Wakelam, Chem. Rev. **113**, 8710 (2013).

142. S. Yamamoto, S. Saito, M. Ohishi, H. Suzuki, S.-I. Ishikawa, N. Kaifu, and A. Murakami, ApJ **322**, L55 (1987).

143. P. Thaddeus, C. A. Gottlieb, A. Hjalmarson, L. E. B. Johansson, W. M. Irvine, P. Friberg, and R. A. Linke, ApJ **294**, L49 (1985).

144. J.-C. Loison, M. Agúndez, V. Wakelam, E. Roueff, P. Gratier, N. Marcelino, D. N. Reyes, J. Cernicharo, and M. Gerin, MNRAS **470**, 4075 (2017).

145. K. M. Hickson, J.-C. Loison, and V. Wakelam, Chem. Phys. Lett. **659**, 70 (2016).

146. D. C. Clary, E. Buonomo, I. R. Sims, I. W. M. Smith, W. D. Geppert, C. Naulin, M. Costes, L. Cartechini, and P. Casavecchia, J. Phys. Chem. A **106**, 5541 (2002).

147. R. I. Kaiser, C. Ochsenfeld, M. Head-Gordon, Y. T. Lee, and A. G. Suits, Science **274**, 1508 (1996).

148. T. Furtenbacher, I. Szabó, A. G. Császár, P. F. Bernath, S. N. Yurchenko, and J. Tennyson, ApJS **224**, 44 (2016).

149. A. G. G. M. Tielens, Annu. Rev. Astron. Astrophys. **46**, 289 (2008).

150. C. M. R. Rocha and A. J. C. Varandas, Phys. Chem. Chem. Phys. **21**, 24406 (2019).

151. C. A. Gottlieb, J. M. Vrtilek, E. W. Gottlieb, P. Thaddeus, and A. Hjalmarson, ApJ **294**, L55 (1985).

152. S. Yamamoto, S. Saito, H. Suzuki, S. Deguchi, N. Kaifu, S.-I. Ishikawa, and M. Ohishi, ApJ **348**, 363 (1990).

153. M. Kanada, S. Yamamoto, S. Saito, and Y. Osamura, J. Phys. Chem. **104**, 2192 (1996).

154. M. Caris, T. Giesen, C. Duan, H. Muller, S. Schlemmer, and K. Yamada, J. Mol. Spectrosc. **253**, 99 (2009).

155. M. C. McCarthy, K. N. Crabtree, M.-A. Martin-Drumel, O. Martinez, B. A. McGuire, and C. A. Gottlieb, ApJS **217**, 10 (2015).

156. Q. Jiang, C. M. L. Rittby, and W. R. M. Graham, J. Chem. Phys. **99**, 3194 (1993).

157. S. M. Sheehan, B. F. Parsons, J. Zhou, E. Garand, T. A. Yen, D. T. Moore, and D. M. Neumark, J. Chem. Phys. **128**, 034301 (2008).

158. S. Yamamoto and S. Saito, J. Chem. Phys. **101**, 5484 (1994).

159. H. Yamagishi, H. Taiko, S. Shimogawara, A. Murakami, T. Noro, and K. Tanaka, Chem. Phys. Lett. **250**, 165 (1996).

160. J. Takahashi and K. Yamashita, J. Chem. Phys. **104**, 6613 (1996).

161. K. Aoki, S. Ikuta, and A. Murakami, J. Mol. Struct.: THEOCHEM **365**, 103 (1996).

162. C. Ochsenfeld, R. I. Kaiser, Y. T. Lee, A. G. Suits, and M. Head-Gordon, J. Chem. Phys. **106**, 4141 (1997).

163. R. K. Chaudhuri, S. Majumder, and K. F. Freed, J. Chem. Phys. **112**, 9301 (2000).

164. J. C. Sancho-García and A. J. Pérez-Jiménez, J. Phys. B At. Mol. Opt. **35**, 3689 (2002).

165. J. F. Stanton, Chem. Phys. Lett. **237**, 20 (1995).

166. J. C. Saeh and J. F. Stanton, J. Chem. Phys. **111**, 8275 (1999).

167. R. A. Kendall, T. H. Dunning Jr., and R. J. Harrison, J. Chem. Phys. **96**, 6796 (1992).

168. P. Halvick, Chem. Phys. **340**, 79 (2007).

169. M. K. Bassett and R. C. Fortenberry, J. Chem. Phys. **146**, 224303 (2017).

170. S. C. Bennedjai, D. Hammoutène, and M. L. Senent, ApJ **871**, 255 (2019).

171. M. Perić, M. Mladenović, K. Tomić, and C. M. Marian, J. Chem. Phys. **118**, 4444 (2003)

172. H. Ding, T. Pino, F. Güthe, and J. P. Maier, J. Chem. Phys. **115**, 6913 (2001).

173. A. M. Mebel and R. I. Kaiser, Chem. Phys. Lett. **360**, 139 (2002).

174. Y. Wang, B. J. Braams, and J. M. Bowman, J. Phys. Chem. A **111**, 4056 (2007).

175. A. J. C. Varandas, J. Chem. Phys. **138**, 054120 (2013).

176. A. J. C. Varandas, J. Chem. Phys. **138**, 134117 (2013).

177. A. J. C. Varandas, in *Reaction Rate Constant Computations: Theories and Applications* (The Royal Society of Chemistry, U.K., 2014), vol. 17, chap. Putting together the pieces: global description of valence and long-range forces via combined hyperbolic inverse-power representation of the potential energy surface for use in reaction dynamics, pp. 408–445.

178. C. M. R. Rocha and A. J. C. Varandas, J. Phys. Chem. A **123**, 8154 (2019).

179. S. Joseph and A. J. C. Varandas, J. Phys. Chem. A **114**, 2655 (2010).

180. C. M. R. Rocha and A. J. C. Varandas, Chem. Phys. Lett. **700**, 36 (2018).

181. R. S. Urdahl, Y. Bao, and W. M. Jackson, Chem. Phys. Lett. **178**, 425 (1991).

182. B. E. Sagan, *The Symmetric Group: Representations, Combinatorial Algorithms, and Symmetric Functions* (Springer, New York, 2001).

183. M. Karplus, Folding & Design **2**, S69 (1997).

184. H. Wang and R. P. A. Bettens, Phys. Chem. Chem. Phys. **21**, 4513 (2019).

185. M. Patrício, J. L. Santos, F. Patrício, and A. J. C. Varandas, J. Math. Chem. **51**, 1729 (2013).

186. C. M. Rocha, J. Li, and A. J. C. Varandas, J. Phys. Chem. A **123**, 3121 (2019).

187. F. O. Ellison, J. Am. Chem. Soc. **85**, 3540 (1963).

188. J. C. Tully, Adv. Chem. Phys. **42**, 63 (1980).

189. P. J. Kuntz, in *Atom-Molecule Collision Theory*, edited by R. Bernstein (Plenum, New York, 1979), p. 79.

190. K. S. Pitzer and E. Clementi, J. Am. Chem. Soc. **81**, 4477 (1959).

191. A. Van Orden and R. J. Saykally, Chem. Rev. **98**, 2313 (1998).

192. A. J. C. Varandas and F. N. N. Pansini, J Chem. Phys. **150**, 154106 (2018).

193. A. J. C. Varandas and F. N. N. Pansini, International Journal of Quantum Chemistry **120**, e26135 (2020)

194. C. M. Rocha and A. J. C. Varandas, Comp. Phys. Comm. **247**, 106913 (2020).